Structural Changes and Chain Mobility During Processing of Bloodmeal-Based Thermoplastics

A thesis

submitted in fulfilment

of the requirements for the degree

of

Doctor of Philosophy in Engineering

at

The University of Waikato

by

JAMES MICHAEL BIER

THE UNIVERSITY OF
WAIKATO
Te Whare Wānanga o Waikato

2013

Abstract

The purpose of this study was to use concepts from classical polymer physics to develop a fundamental understanding of the interdependent relationship between structure, properties and processing in Novatein™ Thermoplastic Protein (NTP). NTP is produced from bloodmeal, a by-product of the meat industry which is 95% protein, by extruding with sodium sulphite, urea, sodium dodecyl sulphate, water and tri-ethylene glycol (TEG). Dynamic mechanical thermal analysis (DMA) and differential scanning calorimetry (DSC) were used to investigate thermal transitions and chain relaxation, accompanied by synchrotron based Fourier transform infrared spectroscopy (FT-IR) to investigate chain architecture and structural changes. Extrusion, injection moulding and mechanical testing were used to investigate macroscopic properties, such as processability and mechanical properties.

Material pocket DMA enabled detection of glass transition temperatures not only for moulded NTP test pieces, but also for each processing step: bloodmeal, NTP prior to extrusion, extruded NTP, and conditioned NTP. The pockets increased resolution for injection moulded and conditioned samples, revealing multiple transitions which indicated the presence of more than one phase. Spatially resolved FT-IR experiments were used to characterise the relative content and distribution of protein secondary structures in bloodmeal and NTP after each processing step. Increased chain mobility was observed due to the additives used, and also drastic structural rearrangement consistent with consolidation into a thermoplastic material after extrusion. Viscoelastic phenomena such as creep and stress relaxation further confirmed processed NTP was a consolidated thermoplastic, exhibiting time dependent behaviour characteristic of thermoplastic polymers.

The thermal properties of NTP suggested an underlying semi-crystalline structure, with protein secondary structures such as α-helices and β-sheets constraining motion in the amorphous phase, contributing to a broad glass transition region. These structures do not melt at typical temperatures encountered during extrusion processing, but are dispersed more evenly throughout an amorphous matrix. Other than plasticisation, strong hydrogen bonding interactions stabilising secondary structures were the dominant influence on mechanical properties of the

processed NTP. When TEG was included as a plasticiser, the degree of crystallinity decreased, and the fraction of randomly coiled protein chains was greater at all stages of processing compared to NTP without TEG. TEG competes with protein side groups for hydrogen bonding sites on the protein backbone, reducing secondary structure formation. β-sheets increased when NTP was heated in the absence of shear, displacing TEG and causing it to migrate out of the particles. The short residence time and presence of shear and mixing during extrusion and injection moulding prevented migration during processing, but an overall increase in β-sheet content was still observed after these processing steps.

The relationship between structure, properties and processing of NTP is therefore characterised by its semi crystalline nature, in which additives overcome protein-protein interactions in the amorphous phase enabling β-sheet dispersion throughout the material during processing. Future attempts at modifying properties should be informed by this understanding.

Acknowledgments

First and foremost, I would like to thank and acknowledge my friend, colleague, mentor, coffee companion, running buddy, personal trainer and all round fantastic chief supervisor, Dr. Johan Verbeek. Thank you for your expert supervison, encouragement, mentorship, advice, vision, passion, direction, and most of all, your friendship. Thanks also to Dr. Mark Lay, for being a great second supervisor, friend and colleague. The enthusiasm with which the two of you support and assist your students is inspiring.

There are many other staff members at the University of Waikato that I would also like to thank for their assistance over the past few years: Mary Dalbeth, for administrative help and a friendly welcoming face in the Engineering office; Ass. Prof. Kim Pickering, for encouragement and being another running buddy; Dr. Michael Mucalo, for assistance with Chemistry's FT-IR facilities; Chris Wang and Yuanji Zhang, for technical support in the Large Scale lab; Indar Singh, for assistance with purchasing and with the XRD; Cheryl Ward, for assistance with ordering library books; Dr. Rob Torrens, for providing marking and lab demonstration opportunities to supplement my income; Brett Nichol, for practical suggestions and the loan of some of your teaching equipment; Gwenda Pennington, for fantastic assistance with scholarships, and lastly Prof. Janis Swan, for first meeting with me and suggesting suitable supervisors which led to this project.

A highlight of my PhD. experience was being able to travel to the Australian Synchrotron to conduct experiments on the FT-IR microspectroscopy beamline. I would like to acknowledge the enthusiastic and supportive staff at the Synchrotron and especially thank Dr. Mark Tobin and Dr. Danielle Martin for scientific and technical support, and Fran Westmore for assistance with acquiring the appropriate import permits for our samples. Thanks also to Don Smith at the Royal Society of New Zealand and The New Zealand Synchrotron Group for travel funding support.

I am very grateful for the financial support of the University of Waikato Doctoral Scholarship, Pukehou Poutu Scholarship and Claude McCarthy Fellowship throughout my studies. Without such support, it would not have been practical for

me to pursue this research. I'm also very grateful to Dropbox for providing an online backup when my laptop was stolen just over a week before submission.

I'm not quite ready to abandon bloodmeal just yet, and I'm very thankful for the opportunity to continue research in this area in my new role at Aduro Biopolymers. Thanks to Darren, Johan and Robyn for welcoming me on board.

I have been blessed with being a part of a great research group, and I would like to especially thank the other doctoral students working with bloodmeal-based thermoplastics, Aaron and Rashid, thanks for leading the way and setting a good example to follow. Talia, Marcel, all the best for your continued studies. I would also like to acknowledge some of the short termers, Nick, Velram and Max, for your comradery and help in the lab. A special thanks to De Wet van der Merwe for being my assistant in the Summer of 2011-2012, sitting at the Instron for those long viscoelasticity experiments, and laughing at my Dad jokes.

I would also like to thank the Postgraduate Students Association, especially Carrie Swanson, for helping broaden my horizons and encouraging me interact with other postgraduate students from outside my faculty.

Outside the University there are several people who have helped keep me sane and healthily distracted in the evenings and on weekends. Thanks to Andrew and Ruth Brehaut for your friendship, assistance with Naomi and generally just being amazing. Andrew George and Jo Stringer, thanks for great conversations and guitar sessions. To our supportive Church family at Hillcrest Chapel, thanks for being so wonderful when Naomi came along, for the opportunity to serve musically, and our homegroup especially, for keeping us in your prayers.

Lastly, I would like to thank my family, Mum and Dad Bier, Mum and Dad Wheeler, Peter and Elvina, Miriam, Stephen and Roseanne, for their encouragement, support and love over the years and during my PhD studies. To my wife Joy, thank you for supporting me financially, emotionally and practically through this journey, and for bringing our little Naomi into the world. The two of you are fantastic reasons to come home at the end of the day, and God has truly blessed me.

Contents

1

Introduction

Introduction

New Zealand has a large agricultural sector. The meat industry is worth $4-5 billion dollars in sheep and beef exports per year, producing 350,000 tonnes of lamb and 341,000 tonnes of exported beef products annually [1]. Although less significant in terms of export dollars, the poultry industry produces 165,000 tonnes of meat for the domestic market [2].

Large amounts of blood are also produced as a by-product of the meat industry. Approximately 3-4 % of the live weight of a typical animal is blood, of which approximately 15 % is recoverable solids, 90-95 % of which is protein [3-5]. The high biological oxygen demand of blood means that it cannot be simply discharged into the environment, but must be treated [3]. While blood can be separated to produce plasma and edible fractions, in practice, large proportions are not collected hygienically [4]. Bloodmeal is produced by steam-coagulating this blood, dewatering, milling the dried powder and is sold as fertiliser, and in small quantities as an animal feed.

Bloodmeal is mostly aggregrated haemoglobin and serum albumin with less than 5 % moisture, held together through hydrogen bonding, hydrophobic and ionic interactions and covalent cross-links between protein chains. It is brittle, mostly insoluble and inedible. Due to its relatively low cost and limited applications bloodmeal is a good source of protein for conversion to thermoplastics. Unlike other potential protein sources, it is not fit for consumption by humans or ruminant animals.

Previous work has successfully enabled bloodmeal to be extruded and injection moulded by adding water as a plasticiser, urea to disrupt hydrogen bonding, sodium dodecyl sulphate to reduce hydrophobic interactions and sodium sulphite to break covalent disulphide bonds [6]. This discovery was patented by the University of Waikato [7], and is subject to commercialisation efforts by Waikatolink Ltd and Aduro Biopolymers LP. The material, Novatein™ Thermoplastic Protein (NTP) has the potential to be of economic significance in New Zealand by producing a higher value bio-based, compostable [8] plastic from a renewable resource that is a by-product of our existing agricultural sector.

NTP can be processed on conventional plastics processing equipment, suggesting that it behaves like a thermoplastic However, its underlying structure and how this affects properties and processing is not well understood.

Crucial to this understanding is the concept of chain mobility. Protein extrusion requires proteins to denature, disassociate, unravel and align [9]. This structural rearrangement requires sufficient chain mobility at the elevated temperatures encountered during extrusion and injection moulding. After consolidation into a moulded shape, chain mobility is still important, as molecular mobility, along with the bond strength of interchain interactions, is a key influence in important mechanical properties such as strength, stiffness and toughness.

In bloodmeal, overall chain mobility is insufficient for processing at temperatures that do not cause excessive degradation, which is why additives are required. While water is an efficient plasticiser for processing protein based plastics, it desorbs from the material under ambient conditions causing embrittlement. For this reason, less volatile plasticisers may be also be used. The most important of these for proteins are small diols and polyols, for example glycerol, ethylene glycol and its oligomers and propylene glycol [9]. An unpublished screening study of potential plasticisers for bloodmeal-based thermoplastics conducted at the University of Waikato had identified tri-ethylene glycol (TEG) as one of the most promising. Although a few phenomona had been explored in TEG containing formulations prior to commencment of this thesis, a thorough characterisation of the effects of TEG at different levels had not yet been conducted.

Furthemore, the effect of TEG on protein structures, such as α-helices and β-sheets, was not known. Their presence and distribution among amorphous regions will affect chain mobility when forming a melt and in the processed material. Chain mobility and structure also play an important role in understanding mechanical properties, processability and what types of products can be produced from NTP.

The purpose of this study was to adapt concepts from classical polymer physics to a fundamental understanding of the interdependent relationship between structure, properties and processing of NTP. Dynamic mechanical thermal analysis (DMA)

and differential scanning calorimetry (DSC) were used to investigate thermal transitions and chain relaxation. Synchrotron based Fourier transform infrared spectroscopy (FT-IR) was used to investigate chain architecture and structural changes. Extrusion, injection moulding and mechanical testing were used to investigate macroscopic properties.

More specific objectives of the thesis were:

- Investigate the effect of plasticisation and other additives on mechanical properties and glass transition temperature of NTP.
- Develop a methodology and conditions to detect and analyse thermomechnical transitions of NTP at different processing steps in the production of a moulded plastic article (prior to extrusion, after extrusion, after injection moulding and after conditioning).
- Characterise the structural changes that occur when bloodmeal is transformed into NTP and after each of the processing steps.
- Correlate the above results to determine relationships between structure, processing and dynamic mechanical properties.

These specific objectives were addressed in eight chapters, made up of a published book chapter and seven journal papers, followed by a concluding discussion.

Chapter 2 describes synthesis and characterization of thermoplastics from agro polymers such as starch and proteins. In addition to an overview on producing these materials, this chapter describes thermal analysis and structural analysis techniques used in this thesis and the sorts of conclusions drawn from such techniques by other researchers.

In Chapter 3, the similarities or differences between thermal behaviour of dry native proteins, proteins in solution and protein-based thermoplastic materials are discussed. The structure-property relationship leading to observed properties was also discussed by evaluating expected thermal transitions and their approximate temperature ranges with a focus on proteins relevant to plastic production.

Plasticisation of NTP was investigated in Chapter 4 by assessing changes in mechanical and thermal properties after replacing different amounts of water with TEG. The amounts of other additives were chosen to provide a formulation that embrittled without TEG, so that the effect of TEG could clearly be observed. After exploring the effect of TEG at a constant level of these additives, the roles of these additives at a constant level of TEG were assessed. This was achieved using a factorial experiment with urea, SDS, SS and water content as variables. In the wider context of this thesis, the results served to identify an optimised reference formulation, which could be used as a benchmark for future modifications and which would be directly comparable between different experiments performed in subsequent chapters.

Chapter 5 investigated the use of material pocket DMA to determine transition temperatures in NTP. In particular, the relaxation behaviour of bloodmeal, modified bloodmeal (prior to extrusion) and processed NTP were compared using powdered samples. Analysing bloodmeal and modified bloodmeal required the material pocket as these materials are in powder form. As a comparison, solid bars (i.e. injection moulded thermoplastics) of the resultant product were also analysed. A further objective was assessing the validity of various methods of identifying relaxation temperatures, specifically relating to the material pocket. Different techniques used were the peak in tanδ, onset of drop in storage modulus (E') or peak in loss modulus (E''). In terms of the overall thesis objectives, the research reported in this chapter served to develop a consistent methodology for interpreting DMA results for NTP and provided the first insight into how properties changed after each processing step, and what this may mean for structure.

In Chapter 6, visco-elasticity of NTP was used to assess the effect of sodium sulphite content and injection moulding temperature on the strength of chain interactions. Using a modified four element (MFE) model, experimental results from creep, recovery and stress relaxation were modelled to compare fitted parameters which reflect chain mobility and the strength of chain interactions. In the wider context of the thesis, Chapter 5 further supplemented the understanding of chain mobility, viscoelasticity and relaxation behaviour from dynamic experiments by examining viscoelastic phenomena on a longer time scale than that used in DMA.

The objective of Chapter 7 was to determine if there was spatial variation of protein secondary structures in bloodmeal and NTP. This was explored using FT-IR microspectroscopy at the Australian Synchrotron. Specifically, changes induced by processing were evaluated which should demonstrate consolidation. The multi-phase behaviour implied by dynamic mechanical thermal properties could then be correlated with structural changes. This chapter forms a very significant part of this thesis as it revealed the contribution each processing step (mixing with additives, extrusion, injection moulding and conditioning) had on protein secondary structure composition and distribution, for both samples with and without TEG as a plasticiser. This directly relates to the overall thesis goal of relating protein structure to processing. Furthermore, it served to confirm the hypothesis that NTP behaves as a semi crystalline polymer as suggested by the thermal transitions identified in Chapter 5.

In Chapter 8, the changes in protein secondary structure when heating NTP through its glass transition temperature, and to a typical extrusion temperature were investigated. Observed structural changes were compared with DMA and DSC results over the same temperature range. This chapter provided a link between structural rearrangements and thermal properties of NTP at temperatures relevant for processing, further examining how this is explained in terms of multiphase, semi-crystalline behaviour.

Chapter 9 extended the brief discussion on spatial distribution of TEG in NTP from Chapter 7 to include peaks corresponding to both the alcohol and ether groups of TEG. The objective was to determine how these changed relative to the amide III region on heating pre-extruded powder and after each processing step. How protein/plasticiser interactions varied spatially on the micro-scale and were influenced by heating and thermoplastic processing was examined. This chapter therefore brought the discussion of thermally induced changes in bloodmeal-based thermoplastics relevant to processing back to the context of plasticiser interactions initially discussed in Chapter 4.

The experimental chapters are followed by a concluding discussion in Chapter 10, which presents the fundamental understanding of Novatein^{TM} as a semi-crystalline thermoplastic.

References

1. Ministry of Agriculture and Forestry, *Situation and Outlook for New Zealand Agriculture and Forestry (SONZAF) 2011*. 2011, Ministry of Agriculture and Forestry: Wellington.
2. Poultry Industry Association of New Zealand (PIANZ), *New Zealand Poultry Meat Production Statistics 1997-2011*. 2012.
3. Swan, J.E., *Animal By-Product Processing*, in *Wiley encyclopedia of food science and technology*, F.J. Francis, Editor. 2000, Wiley: New York. p. 4 v. (xxi, 2768).
4. Filstrup, P., *Processes and Equipment for Protein By-products in the Meat Industry*, in *Applied Protein Chemistry*, R.A. Grant, Editor. 1980, Applied Science Publishers Ltd: London. p. 181-222.
5. Fernando, T., *Blood Collection and Processing*, in *Proceedings of a Meat Byproducts Quality Control Workshop held at Hawkesbury Agricultural College, Richmond, NSA. 13th - 17th May, 1984 (online version)*, W.F. Spooncer, CSIRO Meat Reseach Laboratory, and H.A.C. School of Food Sciences, Editors. 1984, School of Food Sciences, Hawkesbury Agricultural College.: Richmond, NSW. p. 114-122.
6. van den Berg, L., *Development of 2nd generation proteinous bioplastics / by Lisa van den Berg.*, in *School of Science and Engineering*. 2009, The University of Waikato, Te Whare Wananga o Waikato Hamilton. p. xiv, 134 leaves : ill. (chiefly col.) ; 30 cm.
7. Verbeek, C.J.R., et al., *NZ551531: Plastics material*, IPONZ, Editor. Granted 2009, Waikatolink Limited: New Zealand Patent.
8. Verbeek, C.J.R., T. Hicks, and A. Langdon, *Biodegradation of Bloodmeal-Based Thermoplastics in Green-Waste Composting.* Journal of Polymers and the Environment, 2012. **20**(1): p. 53-62.
9. Verbeek, C.J.R. and L.E. van den Berg, *Extrusion Processing and Properties of Protein-Based Thermoplastics.* Macromolecular Materials and Engineering., 2010. **295**(1): p. 10-21.

2

Synthesis and Characterization of Thermoplastic Agro-polymers

An invited book chapter

by

C.J.R. VERBEEK AND JAMES M. BIER[1]

Published in

RSC Green Chemistry No. 12. A Handbook of Applied Biopolymer Technology: Synthesis, Degradation and Applications

[1]Although I was not first author of this work, it has been included in this thesis as it provides a useful background for readers unfamiliar with thermoplastic processing of starch or proteins and the properties of the resulting materials. As a co-author, I prepared the first draft of the sections on thermal analysis and structural analysis, and together with Dr. Verbeek revised and edited the entire manuscript into the form submitted for publication.

CHAPTER 7

Synthesis and Characterization of Thermoplastic Agro-polymers

C. J. R. VERBEEK AND J. M. BIER

School of Engineering, University of Waikato, Private Bag 3105,
Hamilton 3240, New Zealand

7.1 Introduction

Petrochemical polymers have become ubiquitous for their excellent properties and durability. Unfortunately, they also create an enormous environmental burden. Motivations behind sustained research in reducing dependence on polymers from petrochemical sources are similar to those in energy research; a decreasing fossil fuel supply with a corresponding price increase and a widespread awareness of sustainability.[1] As a result, finding new uses for agricultural commodities has become an important area of research.

Petroleum-based materials could potentially be replaced with renewable and biodegradable materials such as polysaccharides or proteins.[2] Biodegradable materials are capable of undergoing microbial or enzymatic degradation,[3] although this does not does not necessarily imply renewability, and several petroleum-based biodegradable polymers are commercially available. Biodegradable polymers are generally classified as outlined in Figure 7.1.[3–5] In some cases blends between natural and synthetic polymer are considered a separate class.[6]

The potential use of agro-polymers in the plastics industry has long been recognized. Agro-polymers are extracted from either plants or animals. They could contribute to a reduction of dependence on fossil resources as agricultural resources are generally sustainable. Some of the polymers in this family

RSC Green Chemistry No. 12
A Handbook of Applied Biopolymer Technology: Synthesis, Degradation and Applications
Edited by Sanjay K. Sharma and Ackmez Mudhoo

Published by the Royal Society of Chemistry, www.rsc.org

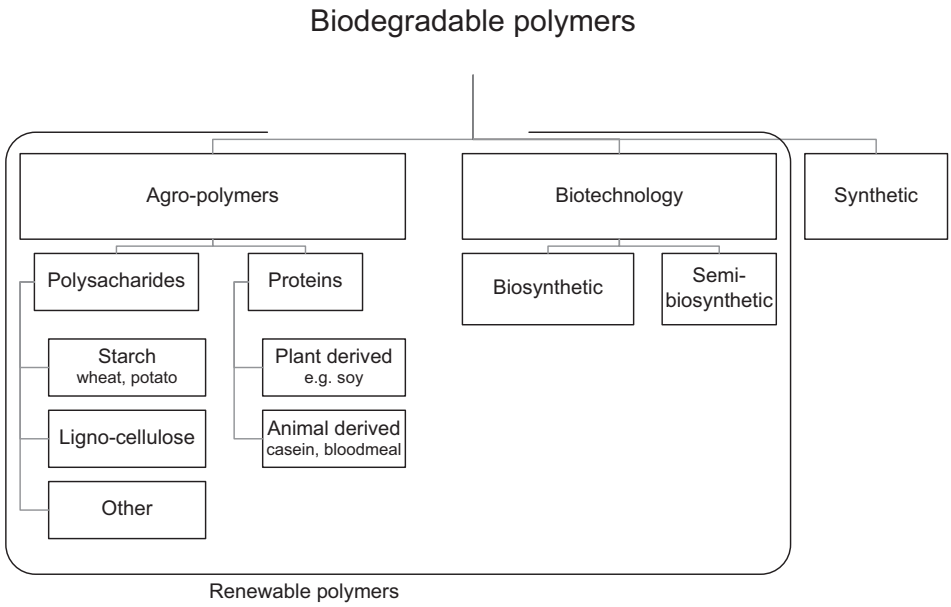

Figure 7.1 Classification of biodegradable polymers.

can be processed directly into thermoplastic materials; however, most require chemical modification. A further benefit is that these polymers are often by-products of other agricultural activities. Common characteristics of agro-polymers are their hydrophilicity, fast degradation rate and sometimes unsatisfactory mechanical properties, particularly in wet environments.[4,5] These polymers can be considered an innovative and sustainable approach to reduce reliance on petrochemical polymers.[3] The main technological challenge is to successfully modify the properties of these materials to account for deficiencies such as brittleness, water sensitivity, and low strength.

7.1.1 Polysaccharides

Polysaccharides are carbohydrate polymers, formed from either mono- or di-saccharides through glycosidic bonds. The most significant polysaccharides of relevance here are cellulose, starch, lignin, pectin and chitin. The structures of some of these polymers are shown in Figure 7.2.

Cellulose is one of the most abundant biopolymers and forms the major constituent of plant cell walls. Currently cellulose is only processed thermoplastically after chemical modification;[2] cellulose acetate would be the most significant product of this nature.

Starch is produced by many plants as a source of stored energy and is found in plant roots, stalks, crop seeds and crops such as rice, corn, wheat, tapioca and potato. It consists of linear amylose and branched amylopectin.[2] Starch is recovered by wet grinding, sieving and drying as native starch.[7]

Lignins are aromatic amorphous polymers and are obtained from almost all types of natural plants, in association with cellulose.[8] Lignins are recovered

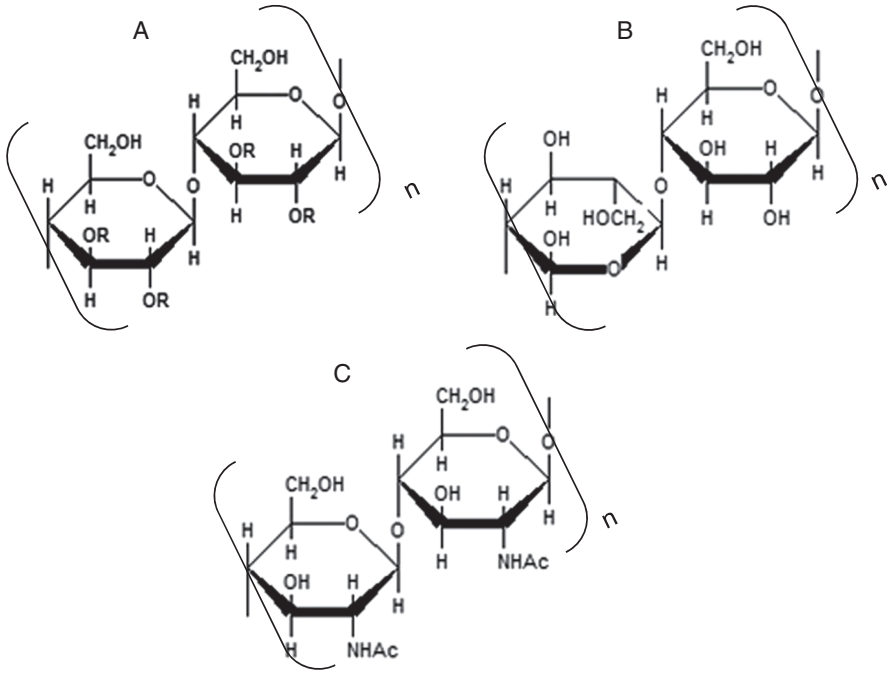

Figure 7.2 Monomers of polysaccharides. A: cellulose (R = H) or cellulose acetate (R = Ac); B: starch; C: chitin.

from cellulose by strong acid/base treatment or by high pressure steam followed by solvent extraction.[8] Modified lignins have been compounded or grafted with thermoplastics. The benefit of the ligneous residues is that they are very polar whilst having a hydrophobic skeleton. As a result, thermoplastic properties are dependent on the presence of a polar plasticizer such as water.[9] Interest in lignin as a polymeric material is mainly because it is readily available, although molecular mass and structure may vary considerably depending on the chemical processes followed during extraction.[1]

Pectins are polysaccharides that contain 1,4-linked α-D-galactosyluronic acid residues. Pectin substances are present in various proportions in plants and act as an intercellular cement. Their gelling properties allow the formation of films which are often used for as fruit or vegetable coating.[9]

Chitin (poly-*N*-acetyl-D-glucosamine, 2-acetamido-2-deoxy-1,4-β-D-glucan) is one of the three most abundant polysaccharides (along with starch and cellulose) and is extracted from shells of crustaceans and cell walls of fungi.[2] Chitosan is produced by deacetylation of chitin and can be spun into fibres, cast into films, or precipitated in a variety of micro-morphologies. Major applications are in biomaterials, pharmaceuticals, cosmetics, metal ion sequestration, agriculture and the food industry.[1,2]

Of the polysaccharide family, starch would be the only substance that is widely used as a thermoplastic without chemical modification and will be discussed in further sections.

7.1.2 Proteins

Proteins are natural polymers which contribute to biological functions within a cell, along with other biological macromolecules such as polysaccharides and nucleic acids. Proteins are classified as condensation polymers because their synthesis involves elimination of water to produce peptide bonds between amino acids. As well as being important for biological systems, proteins are also used in the medicine, food and materials industries. Due to the diverse building blocks of proteins and their unique structure, a large variety of biodegradable materials can be produced offering a wide range of functional properties.[10]

Proteins are readily available as by-products or wastes of the agricultural and horticultural industries. As a result, proteins from plants (wheat gluten, soy, sunflower and corn) and animals (gelatin, keratin, casein, whey and bloodmeal) have been manufactured into plastics. Many studies have been carried out using casting and compression moulding techniques. However, commercial viability of protein-based plastics hinges on utilization of common synthetic processing techniques such as extrusion and injection moulding.[11]

In the next section, synthesis of thermoplastics from starch and proteins is discussed. Only these two polymers are included in the discussion as these form the majority of potential thermoplastics produced from renewable, agricultural sources. Polymers requiring chemical modification of the monomer are specifically excluded as this chapter focuses on direct utilization of natural resources.

7.2 Synthesis

It is well known that polymers can generally be classified as either thermoset, thermoplastic, or rubbery. Most agro-polymers do not behave thermoplastically without some additives and would typically degrade before a flowable melt can be formed. It is therefore necessary to consider the synthesis route to render these materials ready for thermoplastic processing.

Polymer processing is concerned with the mixing and shaping of polymeric materials to form them into useful products. Processing usually involves the application of heat and pressure, with the specific method depending on whether the material is thermoplastic or thermoset.[10] Thermoplastic processing involves melting a polymer, followed by shaping and finally cooling the material in its new form. The softening temperature and atmospheric stability of the polymer, as well as the geometry and size of the finished product, are important. The heat required for melting can be supplied by radiation, conduction, or mechanical work. The most important thermoplastic processing techniques are extrusion, post-die processing, thermo-forming and injection moulding. The largest volume of thermoplastics is probably processed by means of extrusion.[10]

An extruder consists of a heated, fixed metal barrel that contains either one or two screws. The screws act by conveying the material through the heated barrel, inducing shear forces and increasing pressure along the barrel before

leaving the extruder at the die. Process variables include the feed material's composition, screw speed, barrel temperature profile, feed rates and die size and shape. The degree of screw fill, specific mechanical energy input (SME), torque, pressure at the die, residence time and product temperature are influenced by these process variables.[11]

7.2.1 General Considerations

In order to reach a flowable state, amorphous polymer chains need to be above their glass transition and crystalline regions need to be at a temperature above the melting point. Polymer chains are typically linked by a multitude of interactions such as hydrogen bonding, hydrophobic interactions and other weak van der Waal's forces. When sufficient thermal energy is supplied and these interactions are overcome, chains will have the mobility necessary to allow them to move in relation to each other, or flow.[9] Chain entanglements and secondary interactions are what differentiate synthetic polymers from other low molecular mass organic substances. Inter- and intra-molecular bonds, as well as chain entanglements, prevent chain slippage, thus leading to the superior properties of polymers.[10]

It has been found that by heating hydrophilic polymers (such as starch and protein) in closed volumes in the presence of water, homogeneous melts may be formed which can be processed like conventional petrochemical-based thermoplastics.[12] The transformation of agro-polymers into a thermoplastic is often more complex than conventional thermoplastic processing. The diversity of polymer structures and interactions, as well as the dependence of their structure on the extraction technique followed complicates processing. Furthermore, hydrogen bonding is strongly water-sensitive which makes processing this class of polymers even more complex.[9]

7.2.2 The Role of Additives

Thermoplastic properties of agro-polymers depend on the presence of water or other plasticizers. Agro-polymers have relatively low degradation temperatures and the energy required to disrupt intermolecular bonding is close to the energy leading to degradation.[9] Plasticizers improve processability by interposing themselves between the polymer chains and alter the forces holding the chains together. This occurs through two mechanisms, lubrication and increasing free volume. For example, with proteins small molecules are easily incorporated into the protein matrix, shown by the high plasticizing effect of water and glycerol. Water is considered a natural plasticizer of proteins and is used extensively in protein extrusion. When plasticizers are compared based on the mass fraction in a bioplastic, low molecular mass compounds such as water will be present at larger numbers compared to high molecular mass compounds. Every plasticizer molecule can interact with a protein chain, which implies that at equal mass fractions, water is normally more efficient than other plasticizers.[11]

Most agro-polymers contain polar functionalities forming hydrogen bonding with water molecules through hydroxyl groups or amines. Many interactions with water are possible, with variable intensity, and typically define the polymer's water-holding capacity.[9] Water is often considered an essential constituent of agro-polymers and makes processing delicate. It is the interaction with water and between chains that influence structure–property relationships which makes thermal analysis a useful method to assess the role of water in agro-polymers.[5]

The low boiling temperature of water is a serious complication during processing as evaporation typically occurs before adequate processing temperatures for low enough viscosity are reached.[9] Alternatively, hydrophilic compounds such as polyols, carbohydrates and amines may also interact with polar groups in agro-polymers, thereby plasticizing the material. Some examples are glycerol, sorbitol, saccharose, urea, triethylene glycol and polyethylene glycol.[11] These molecules must be polar to ensure compatibility with polymers and small enough to penetrate the macromolecular network. These plasticizers also allow preparation of compounds which can be preserved before further processing because equilibrium moisture content in agro-polymers (with ambient air) is not sufficient to allow a flowable melt.

7.2.3 Starch

One specific thermoplastic agro-polymer of interest here is thermoplastic starch (TPS). Starch can only be converted into a thermoplastic material in the presence of plasticizers using heat and shear.[1,6] The benefit of TPS is its renewability, compostability and relatively low price compared with synthetic thermoplastics.[8] One problem with the use of starch is its high glass transition temperature (T_g). Brittleness also increases with time due to free volume relaxation and retrogradation. In order to increase flexibility and processability, plasticizers such as water, glycol, sorbitol, urea, amide, sugars and quaternary amines have been used in TPS.[6] Dimensional stability and mechanical properties of thermoplastic starch are highly dependent on moisture content.[1] Unfortunately, the excessive hydrophilicity of starch is not significantly reduced by polyol plasticizers.

In its native state, starch is semi-crystalline (about 20–45%) and water insoluble. Native starch granules typically have dimensions ranging from 0.5 to 175 μm and appear in a variety of shapes. It is composed of linear (amylose) and branched (amylopectin) polymers of α-D-glucose. Amylose has a molecular mass of about 10^5–10^6 g mol^{-1}, while amylopectin has a molecular mass in the range 10^7–10^9 g mol^{-1}. Starch rich in amylose is usually preferred for conversion to TPS as the linearity of amylose improves the processability of starch even though it is present as a minor component (between 20 and 30wt%). The ratio of amylose to amylopectin depends on the source and age of the starch, and can also be influenced by the extraction process.[4,9,13,14]

TPS is obtained after disruption and plasticization of native starch's granular structure into a homogeneous amorphous phase by applying thermo-mechanical energy in a continuous extrusion process. Water and glycols are commonly used plasticizers, although urea and formamide have also been explored.[15,16] A chemical agent, such as urea, favours granule destruction by disrupting hydrogen bonding in the crystallites.[9] Thermal processing of TPS involves multiple chemical and physical reactions:[13]

- water diffusion
- granule expansion
- gelatinization
- decomposition/destruction
- melting and crystallization.

Gelatinization is particularly important and it is the basis of thermoplastic synthesis. The destruction of crystalline regions in starch granules is an irreversible process that includes granular swelling, crystalline melting and molecular solubilization.[13] As a consequence of gelatinization, the melting temperature (T_m) and the glass transition (T_g) are reduced. Excess water is generally required to ensure dispersion and a high degree of gelatinization. If using less water in the formulation (<20 wt%), the melting temperature (T_m = 220–240 °C) tends to be close to the degradation temperature. To overcome this, a non-volatile plasticizer (glycerol or other polyols) is added to decrease the glass transition temperature.[8] During extrusion, shear forces physically tear apart starch granules, allowing faster transfer of water into the interior molecules. At low moisture content, small amounts of gelatinized, melted, as well as fragmented starch (due to degradation or decomposition) exist simultaneously.[13]

Starch processing is much more complicated and difficult to control than conventional polymer processing due to its unique phase transitions, high viscosity, water evaporation and fast retrogradation. However, with proper formulation development (plasticizer selection, *etc.*) and suitable processing conditions, many of these challenges can be overcome.[6,13]

One of the challenges of TPS is the result of the structures of amylose and amylopectin. Amylose is considered a linear structure and amylopectin branched. Superior mechanical properties can be obtained if the structure is formed at low water contents and if it is based on the branched component of amylopectin.[12] These macromolecules are able to create short range interactions (van der Waal's and hydrogen bonding) between macromolecules or functional groups (*e.g.* OH). However, chain entanglements develop if chains are long enough to develop long range interactions leading to higher elongation at break values. Neither amylose nor amylopectin develop significant long range interactions; these materials are not cohesive enough. In addition, hydrophilicity also enables the system to partially crystallize (or retrograde) as a function of the water content.[6,15]

Melting and mixing are the two main objectives of compounding or extrusion processing, and process parameters are typically adjusted to minimize chain

degradation. However, fragmentation is unavoidable, with the extent depending on operating conditions, such as screw speed, temperature, moisture content and starch type. Controlling degradation is important since it influences processing properties such as viscosity, but it can also affect the performance of final products.[13]

After processing, TPS shows ageing as evident from an increase in mechanical properties such as tensile modulus. Below the T_g it shows physical ageing accompanied by material densification, while above the T_g, recrystallization is even more pronounced. The re-ordering of gelatinized or thermoplastic starch into crystalline regions is known as retrogradation. The retrogradation kinetics depend on chain mobility, plasticizer type and content.[8]

7.2.4 Proteins

It has been said that in order for proteinaceous bioplastics to be commercially feasible, they need to be processable using equipment currently used for synthetic thermoplastics. Proteinaceous bioplastics are often brittle and water sensitive, and overcoming this is one of the driving forces behind research in this field. Physiochemical properties and processing conditions are often governed by the protein's structural properties, and therefore also final material properties.[17]

A synthetic polymer consists of identical monomers, covalently bonded in a long chain. Unlike synthetic polymers, proteins are complex hetero-polymers, consisting of up to 20 different amino acid repeat units. The amino acid repeat unit contains two carbon atoms as well as nitrogen, differing only in their functional side groups. In its natural environment, a protein will be folded into secondary, tertiary and quaternary structures stabilized through hydrophobic interactions, hydrogen bonding and electrostatic interactions between amino acid functional groups. The folded conformation is a delicate balance of these interactions.[18] Once folded, the structure may be stabilized further with strong covalent cross-links. Due to the diverse building blocks of proteins and their unique structure, a large variety of biodegradable materials can be produced offering a wide range of functional properties.[11]

It is well known that the visco-elastic behaviour of amorphous or semi-crystalline polymers can be divided into five regions; these are the glassy, leathery, rubbery rubbery-flow and viscous states. The transformation from one region to another is dependent on temperature, while the temperature at which each transition occurs is dependent on the polymer structure. Processing can only be done above temperatures corresponding to the rubbery-flow region. Most literature on proteinaceous bioplastics suggests that processing be done above the protein's softening point, which would imply a temperature well above the T_g.

Extrusion and injection moulding of polymers require that a viscous melt be formed by the polymer upon the addition of heat. That implies that interactions

between chains are sufficiently low to allow relative movement of chains, but some interaction is required to impart some degree of melt strength in the material. Synthetic polymers generally satisfy these requirements. In the absence of strong intermolecular forces (hydrogen bonds), chain entanglements and van der Waal's forces are the most important mechanisms that impart a good melt strength.

Small changes in environmental conditions, such as increasing temperature, pressure, change of pH or addition of chemicals, can disrupt a protein's folded conformation and this is called denaturing. Denaturation is a unique property of proteins and can be defined as the modification of secondary, tertiary or quaternary structures of a protein molecule. This is not to be confused with degradation, which is the loss of primary structure, or breaking of covalent peptide bonds. For a protein to behave like a synthetic polymer, the protein chain is required in an extended conformation enabling the formation of sufficient chain entanglement. In order to do this, multiple non-covalent and covalent interactions need to be reduced, allowing chains to unfold and form new interactions and entanglements.[10,11]

Unlike starch, where destructuring leads to an amorphous fluid, denaturation of proteins exposes core structural groups which can be more hydrophobic than surface groups (depending on the environment). In a polar environment the structure forms with polar residues in the surface and hydrophobic ones inside, and vice versa. Furthermore, with an increase in temperature, chains become more mobile but their movement is restricted because of newly formed intermolecular forces. Hydrophobic interaction intensifies due to temperature and denaturation which is followed by coagulation.[9]

Hydrogen bonds, ionic interactions, hydrophobic interactions and covalent disulfide bonds are affected during denaturation, causing an unravelling of protein structure into a random coil conformation. Denaturation can have several important consequences, such as increase in viscosity of protein solutions, decrease of solubility due to exposure of hydrophobic groups, increase of reactivity of side groups, altered sensitivity to enzymatic proteolysis and altered surfactant properties. Denaturing exposes functional groups of the amino acid side chains, thereby introducing new interactions by means of hydrophobic, hydrogen or ionic bonding. Although some of these effects can be seen as negative, denaturation and the consequences thereof are important for protein processing.

Understanding how to process agro-polymers with similar properties to synthetic polymers requires an understanding of how these forces are manifested in proteins. The processability of proteins depends on their transition from the glassy to rubbery and viscous-flow states. These transitions are achieved with judicial application of heat, pressure, shear, chemical additives and plasticizers. Specific amino acid residues (primary protein structure) and initial structure (natural protein state) of the protein will influence each of these factors. Based on the structure of proteins and the requirement for thermoplastic processing, three broadly categorized processing requirements have been identified:[11]

- breaking of intermolecular bonds (non-covalent and covalent) that stabilize proteins in their native form by using chemical or physical means
- arranging and orientating mobile chains in the desired shape
- enabling formation of new intermolecular bonds and interactions to stabilize the three-dimensional structure.

In order to fulfil these requirements, a typical formulation of a proteinaceous bioplastic would include some or all of the following components:

- plasticizers or a combination of plasticizers to promote flowability
- reactive additives to promote cross-link reduction, such as sodium sulfite or sodium bisulfite[19,20]
- additives such as pigments, preservatives (sodium benzoate), foaming agents, bleaching agents (hydrogen peroxide, calcium carbonate, barium peroxide),[21] titanium oxide, sodium bisulfate[22] or anti-foaming agents
- lubricants or extrusion aids such as soybean oil, fatty acids and vegetable oils[23] as well as fused silica and ammonium hydroxide[24]
- extenders such as fibres and clay, to improve mechanical properties
- modifiers to impart water resistance.

The processes occurring during extrusion are considered an equilibrium reaction between temperature-induced polymerization and shear-induced de-polymerization. In this context, polymerization means the formation of intermolecular forces or covalent cross-links while de-polymerization may also imply protein degradation. It was found that high temperatures and high specific mechanical energy (SME) input could induce excessive cross-linking and/or degradation of protein chains. At high temperatures and low moisture or plasticizer content, viscous heat dissipation could increase the likelihood of protein degradation.[11]

Denaturing, cross-linking and plasticization are probably the most important aspects of protein processing. The melt temperature and the temperature dependence of viscosity can be affected by the type and the amount of plasticizer. Generally, increasing the amount of plasticizer will lower the melt temperature and viscosity of the blend.[25] The extruder is particularly suitable for processing proteins which do not aggregate excessively and therefore maintain a lower constant processing torque.

7.3 Characterization

7.3.1 Overview of Characterization

Selecting appropriate biopolymers for commercial use is a complicated task and involves careful consideration of the properties of the polymeric material. In the context of this chapter, the meaning of the term 'Characterization of Agro-polymers' is twofold. Not only are the techniques used for

characterization important, but also how they define the characteristics of agro-polymers. Typically, chemical structure and morphology as well as mechanical and thermal properties are important. In addition to these, aspects that need consideration are the shape and form of raw materials as well as their quality, supply, cost and physical properties.[26] Obtaining optimal material properties in a final product requires appropriate processing which is dependent on structure. Structure, property and processing cannot be considered independently, as illustrated in Figure 7.3.

The structure of polymers is described at multiple levels. Biochemists traditionally refer to the primary, secondary and tertiary structure of native proteins. Similarly for thermoplastics there are multiple levels of structural information, such as chain architecture and crystallinity. All of these contribute to observed material properties and can be manipulated by processing. In Figure 7.4, the general structure of proteins, starch and synthetic polymers are compared. At the monomeric level starch is made up of repeating units of glucose and exists in two forms – branched (amylopectin) or unbranched (amylose). In native starch these are arranged in granules consisting of hard and soft regions.[27] The blockets in the hard shell are made up of crystalline amylopectin surrounded by amorphous amylose. Processing disrupts these ordered regions.[28] Proteins consist of a chain of peptide linkages with various amino acid side groups present. These side groups contribute to a range of interactions which, combined with hydrogen bonding around the polypeptide backbone, lead to different secondary structures.[11] Synthetic plastics include a range of materials with different monomers and linkages. Olefins, or vinyl-like polymers, such as polypropylene are hydrophobic, whereas nylons contain amide linkages similar to the peptide backbone in proteins which are hydrophilic and form hydrogen bonds with water.[29] Vinyl-type polymers form helical conformations similar to α-helices in proteins and many petroleum-derived

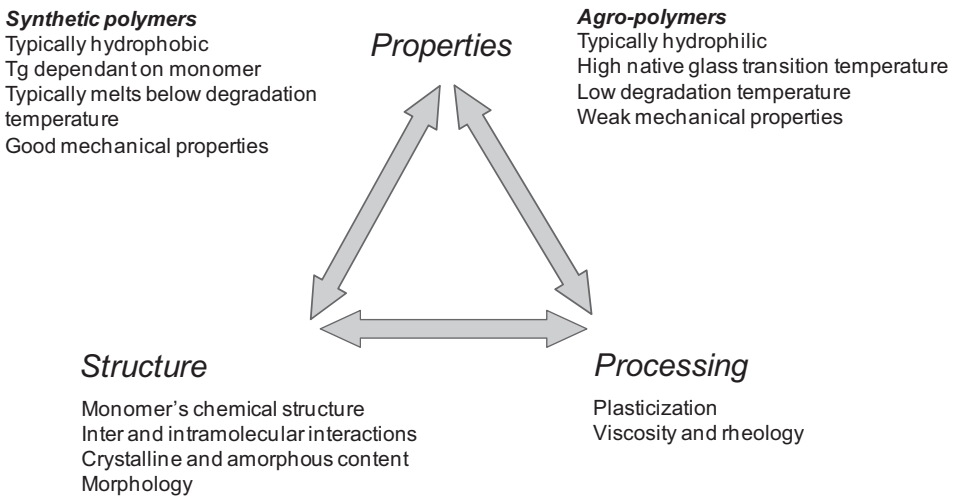

Figure 7.3 Structure–property–processing relationship.

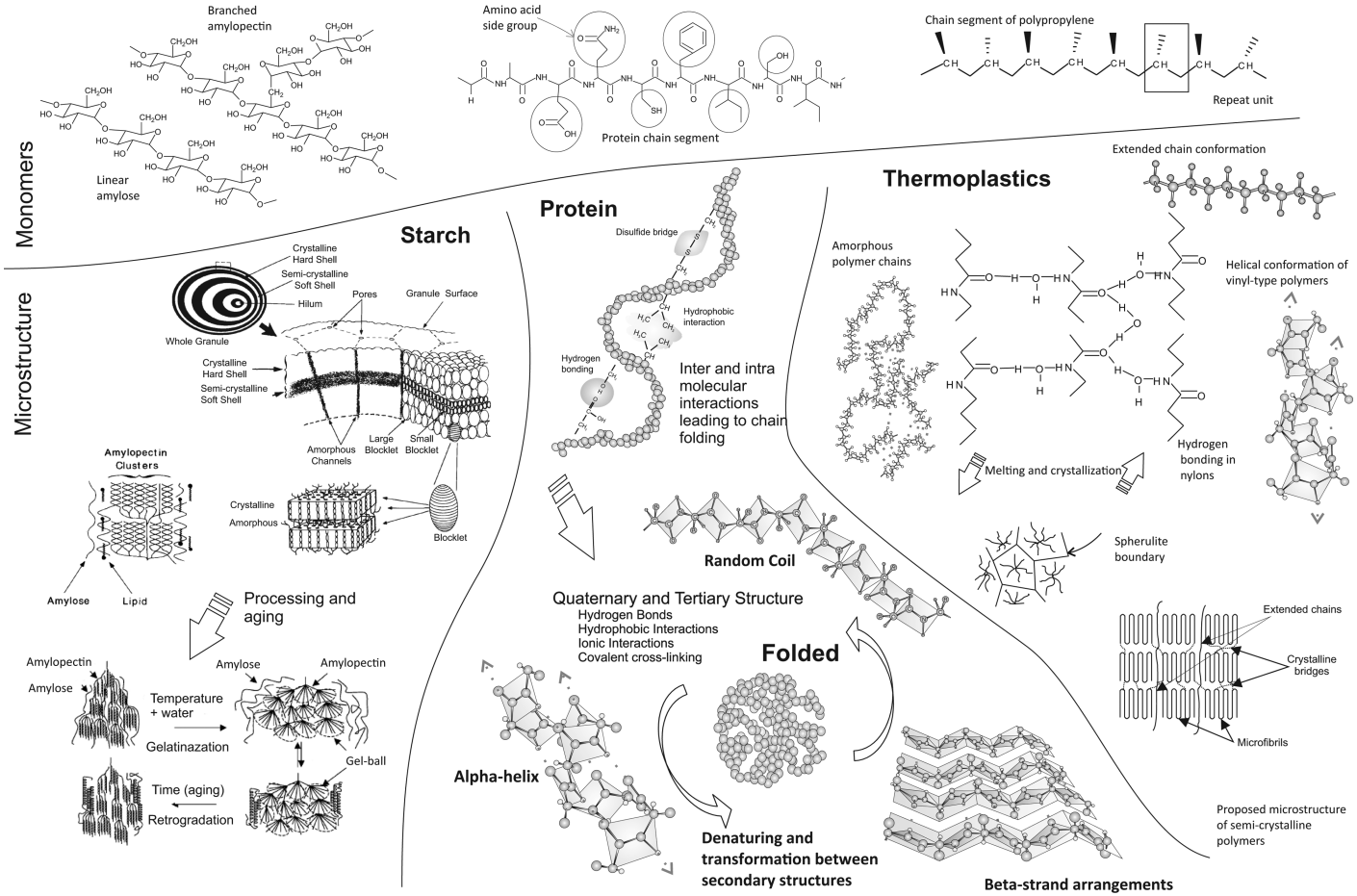

Figure 7.4 Monomers and microstructure of starch, protein and examples of synthetic thermoplastics. Microstructure of starch reprinted from *Carbohydrate Polymers*, **32**(3–4), D. J. Gallant, B. Bouchet, and P. M. Baldwin, Microscopy of starch: Evidence of a new level of granule organization, page No. 188, Copyright (1997), with permission from Elsevier.[27] Gelatinization and retrogradation of starch reprinted with kind permission from Springer Science+Business Media: *Journal of Materials Science Microstructure* and mechanical properties of orientated thermoplastic starches, **40**(1), 2005, 115, L. Yu and G. Christie, figure 4, © 2005 Springer Science + Business Media, Inc.[28]

polymers are semi-crystalline and contain spherulites.[30,31] Within these there are crystalline regions surrounded by an amorphous region with similar morphology to the amylopectin clusters in starch.[29] The techniques discussed in this section are used to assess these structural aspects and how they define the characteristics of thermoplastic starch or proteins.

Techniques such as Fourier transform infrared spectroscopy (FT-IR) and nuclear magnetic resonance (NMR) are used in determining information about the chemical structure of the monomers and the nature of covalent bonds between them. Molecular mass and molecular mass distribution, as well as chemical nature of side groups, determine the interaction between polymer chains. Where interactions between chains lead to ordered regions, crystalline phases are observed, whilst other less ordered regions are said to be amorphous. X-ray diffraction is often used to assess structural information, such as the degree of crystallinity and specific crystal structures while microscopy techniques, such as SEM or TEM, are used to determine morphology.

All these different levels of structure contribute to the quality of the final product, as defined by it mechanical and physical properties. Important mechanical and physical properties are summarized in Table 7.1.[26]

As well as being rate dependent, the mechanical properties of polymers show significant temperature-related effects. Of particular importance for

Table 7.1 Mechanical and physical properties of polymers.[26,32]

Mechanical properties		*Physical properties*	
Tension, compression, torsion and flexural	Yield, modulus, stress at break, Poisson's ratio, elongation at break and toughness	Density	kg/m^3
Hardness	Resistance to permanent deformation by indentation	Melting temperature	Crystalline melting
Fatigue	Susceptibility to failure due to cyclic loading	Glass transition	Amorphous relaxation
Creep	Permanent elongation due to a static load over a long period	Heat deflection temperature	Similar to softening point
Impact	Dynamic loading	Thermal decomposition temperature	Thermally induced degradation
Viscoelasticity	Time-temperature effects under dynamic/cyclic loading	Specific heat, thermal conductivity and thermal expansion	Important process design parameters
		Optical properties	Colour, reflectance and opacity
		Chemical resistance	Resistance to chemical reactions during and after processing
		Water absorption	Measures material-solvent interaction

thermoplastic processing is the glass transition of amorphous regions. At low temperatures polymers exhibit glassy properties, as chains are not particularly mobile, effectively frozen into place amongst the other chains. As temperature increases, the chains become more mobile, and are able to slide past each other more quickly in response to applied forces. The transition from the glassy state to the rubbery state is influenced by chain architecture and micro-structure. Agro-polymers, especially proteins, have severely more complicated structures than synthetic polymers, and relating this relaxation behaviour to structure can be challenging. In addition, starch and proteins are highly hydrophilic and their mechanical and physical properties are highly dependent on moisture content. The rate at which water is absorbed or lost as well as equilibrium moisture content are important characteristics of agro-polymers. Other properties of particular interests for natural polymer thermoplastics include thermal decomposition, thermally induced cross-linking (thermosetting behaviour) and crystallization.

Effective characterization is more than just assessing these properties, but also understanding the effect of processing parameters such as the method used, temperature, conditioning time and additives.

7.3.2 Mechanical Behaviour

Mechanical properties can probably be regarded as the most significant aspect of materials, as adequate mechanical properties are required for any application. This is not to say that other physical properties, such as density and thermal conductivity, can be neglected as these are also vital in materials selection. In understanding the mechanical properties of agro-polymers it is useful to compare their behaviour to that of synthetic polymers.

Mechanical properties are essentially a description of a material's response to an external load and its ability to reversibly or irreversibly deform as a result of it. These properties are generally evaluated by standardized methods. Mechanical properties of natural polymers (or agro-polymers) are not characterized any differently than conventional polymers and important properties include strength, Young's modulus, stress at yield, elongation and toughness (energy to break), *etc*.

Polymers typically behave visco-elastically, that is their mechanical properties are time and temperature dependent. However, the properties mentioned above are measured almost instantaneously and it is assumed that the material behaves elastically, or more importantly linear elastic if a Young's modulus is considered. In Figure 7.5, typical stress–strain diagrams are shown for brittle, plastic and highly elastomeric behaviour, as observed in many synthetic polymers. This behaviour is dependent on temperature as well as the amount of plasticizer (or other additives).[32,33]

Synthetic polymers have an exceptionally broad range of mechanical properties. Highly stiff and brittle behaviour is observed, but also more ductile materials that can show extensions of up to 1000%. Figure 7.6 presents a summary of some commodity polymers' relationship between Young's

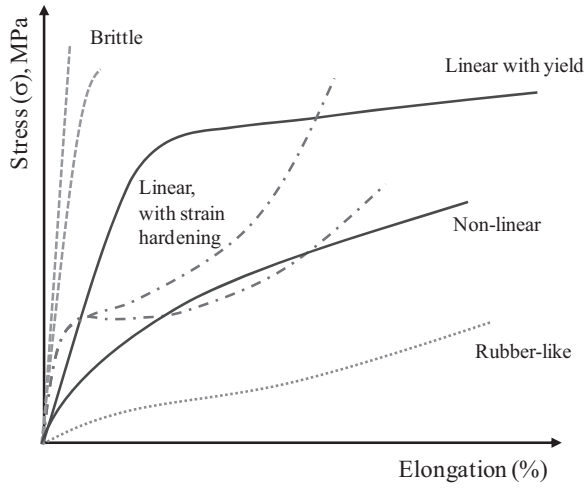

Figure 7.5 Idealized stress strain behaviour of typical agro-polymers.

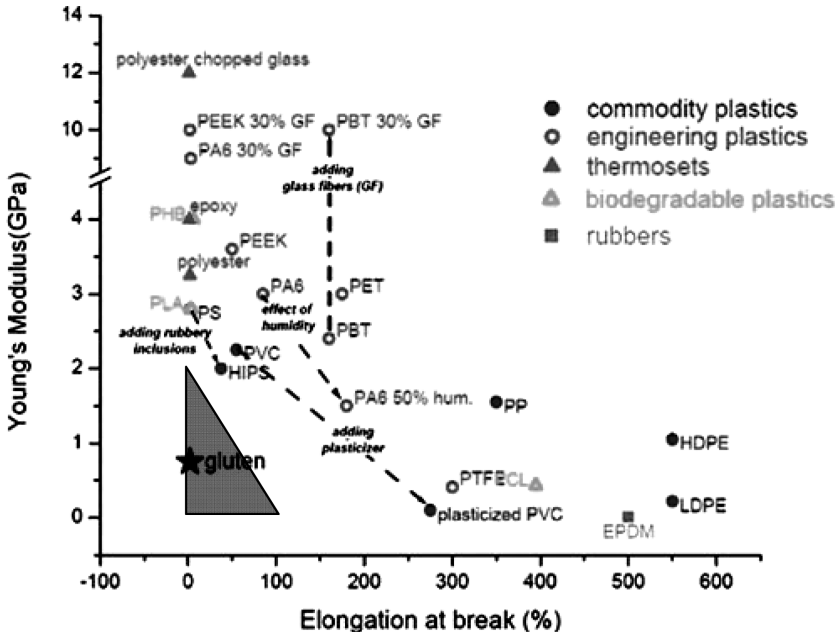

Figure 7.6 Mechanical properties of biomaterials compared to currently available synthetic polymers.[34] Adapted with permission from B. Lagrain, B. Goderis, K. Brijs and J. A. Delcour, *Biomacromolecules*, 2010, **11**, 533–541. Copyright 2010 American Chemical Society. The shadowed triangle shows systems of soy,[35] sunflower isolate,[36,37] starch/zein,[38] soy/corn starch,[39] whey,[40] zein,[41] and wheat protein.[42]

modulus and elongation at break.[34] Also shown in Figure 7.6 is thermoplastic gluten, relative to synthetic polymers.[34] Although gluten is not representative of all agro-polymers, it does fall in the broad region of where agro-polymers could be expected (indicated by shaded triangle).

The mechanical properties of polymers are largely associated with distribution and concentration of inter- and intra-molecular forces. Extrusion and other thermal processing techniques lead to structural rearrangements and new interactions which can be adjusted with the use of plasticizers and chemical additives. In general, true plasticizers will increase the flexibility of a moulded product, imparting greater extensibility. On the other hand, increasing molecular interactions will result in a material with higher tensile strength and stiffness. Furthermore, harsh processing conditions can lead to degradation, adversely effecting mechanical properties.[11]

The mechanical properties of agro-polymers are generally a lot weaker than those of commodity engineering plastics. Their properties are also strongly dependent on moisture content as well as other plasticizers because of their characteristic hydrophilicity. Apart from these, the most prevalent factors affecting the mechanical properties include processing conditions and composition.

Starch and protein agro-polymers show a variety of stress–strain behaviour; from rubber-like to highly brittle. The specific behaviour is determined by the factors mentioned earlier. Idealized stress–strain diagrams for a few selected systems are shown in Figure 7.5. As an example, wheat gluten plasticized with glycerol showed linear behaviour with yield, while cross-linking eliminated the yield point.[43] Zein plastics have been shown to exhibit behaviour that is similar to thermoplastic-rubber blends; that is effectively linear behaviour followed by strain hardening.[44] It has been shown for feathermeal-based plastics that the yield point is associated with breaking secondary interactions, such as hydrophobic interactions. If the load is removed before break, the deformation across the yield point was reversible due to chain refolding.[45] Non-linear behaviour, shown in Figure 7.6, has also been observed for whey protein isolate films[42] and wheat flower polymers.[46] Transition between different behaviour is often observed and depends on moisture content, plasticizer content and additives.

Microscopic techniques including scanning electron microscopy (SEM), transition electron microscopy (TEM) and light microscopy are used to study structure and morphology at higher levels. SEM is used to study fracture morphology after tensile testing.[47–49] SEM is also used to investigate phase morphology and generate emulsification curves in the study of blends, such as thermoplastic starch blended with polyethylene,[50] soy protein blended with polylactide[51] or soy protein and polyester.[52]

When electron microscopy is used to study the morphology of agro-materials, the surface roughness is often taken as an indication of the failure mode. In the example shown (Figure 7.7), soy protein isolate (SPI) was plasticized with stearic acid and glycerol.[53] SPI resin with 30% glycerol (Figure 7.7A) showed lower roughness at the fracture surface than the other two specimens containing 25% stearic acid (Figure 7.7B). The height and contour of the asperities at the fractured surface of the resin containing stearic acid also indicated that the presence of stearic acid resulted in a more ductile failure.

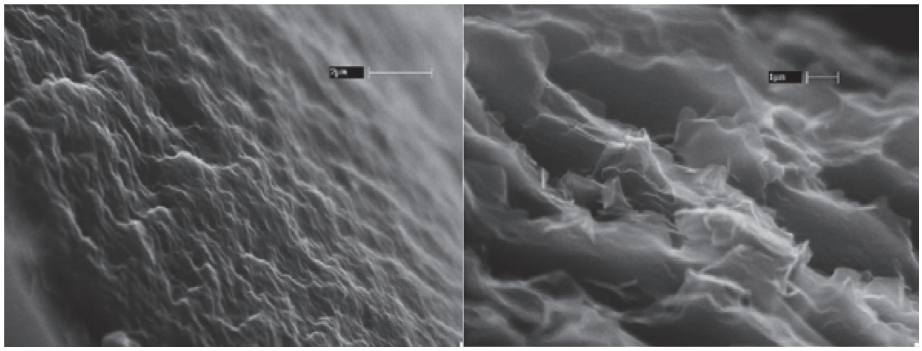

A B

Figure 7.7 Fracture surface of SPI plasticized with glycerol, with (B) and without (A) stearic acid.[53] Reprinted from *Industrial Crops and Products*, **21**(1), P. Lodha and A. N. Netravali, Thermal and mechanical properties of environment-friendly 'green' plastics from stearic acid modified-soy protein isolate, 49–64, Copyright (2005), with permission from Elsevier.

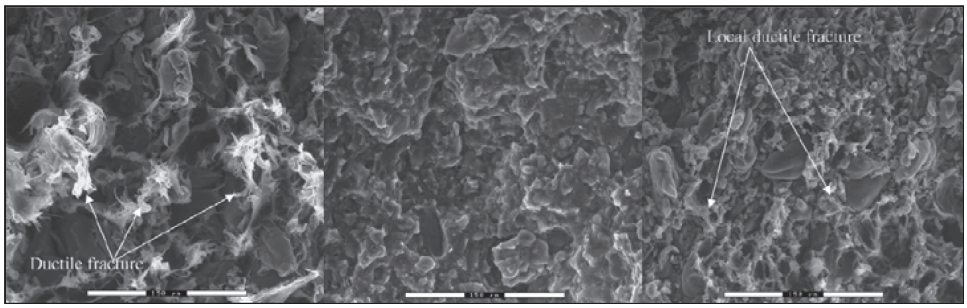

A B C

Figure 7.8 Tensile fracture surfaces of (A) glycerol, (B) sorbitol and (C) polyester amide plasticized soy-based agro-polymers.[48] Reprinted with permission from P. Tummala, W. J. Liu, L. T. Drzal, A. K. Mohanty and M. Misra, *Ind. Eng. Chem. Res.*, 2006, **45**, 7491–7496. Copyright 2006 American Chemical Society.

In a further example, the tensile fracture surfaces for soy protein plasticized by glycerol, sorbitol and polyester amide are shown in Figure 7.8. It can be seen that glycerol plasticized samples showed ductile fracture features with a coarse surface. Sorbitol plasticized samples showed brittle fracture features with relatively smooth surfaces. These samples also had higher strength and stiffness, but lower elongation at break. Using polyester amide as a plasticizer resulted in local ductile fracture features and the samples had moderate mechanical properties.[48]

If soy protein is plasticized with acetamide, it was shown that brittle fracture dominated up to 20% acetamide, as evident from the sharp ridges on the SEM images (Figure 7.9). As plasticizer content increased the surface become

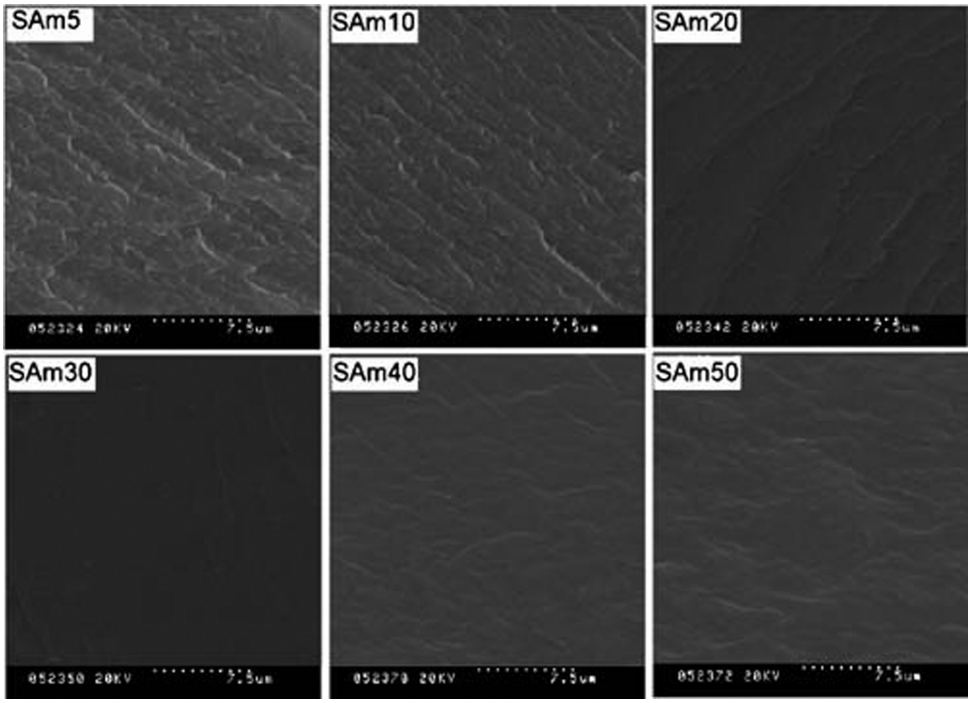

Figure 7.9 SEM images of cross sections of soy plastic sheets plasticized with different amounts of acetamide.[54] Liu, D. and L. Zhang: Structure and properties of soy protein plastics plasticised with acetamide. *Macromolecular Materials and Engineering* 2006, **291**, 820–828. Copyright Wiley-VCH Verlag GmbH & Co. KGaA. Reproduced with permission.

smoother, but above 30% the surface again appeared fluctuant, most likely because of excess plasticizer.[54]

Similar observations have been made for starch plasticized with glycerol, xylitol, sorbitol or maltitol. Fractured surfaces are shown in Figure 7.10 and it was observed that the surface of glycerol plasticized material (A) was rough. This was likely due to glycerol- and amyl pectin-rich domains forming a heterogeneous material. The fractured surface of xylitol plasticized system (B) appeared different with a rough structured surface, while sorbitol (C) and maltitol (D) plasticized surfaces were perfectly smooth.[55]

Unfortunately, overall mechanical property improvements in agro-polymers have been slow. A large range of starch-based plastics have been surveyed in terms of strength at break versus their elongation at break.[15] It has been shown that the mechanical properties follow a master curve that is almost exclusively dependent on the amount of plasticization (Figure 7.11).[15] The situation for protein-based plastics is not much different, and tensile strengths seldom exceed 25 MPa, with elongation at break being less than 140%.[35–38,41,42,56] As with starch-based materials, this behaviour is mostly determined by the amount of plasticizer. Very little research has been successful in developing high strength agro-polymer, with corresponding high elongation.

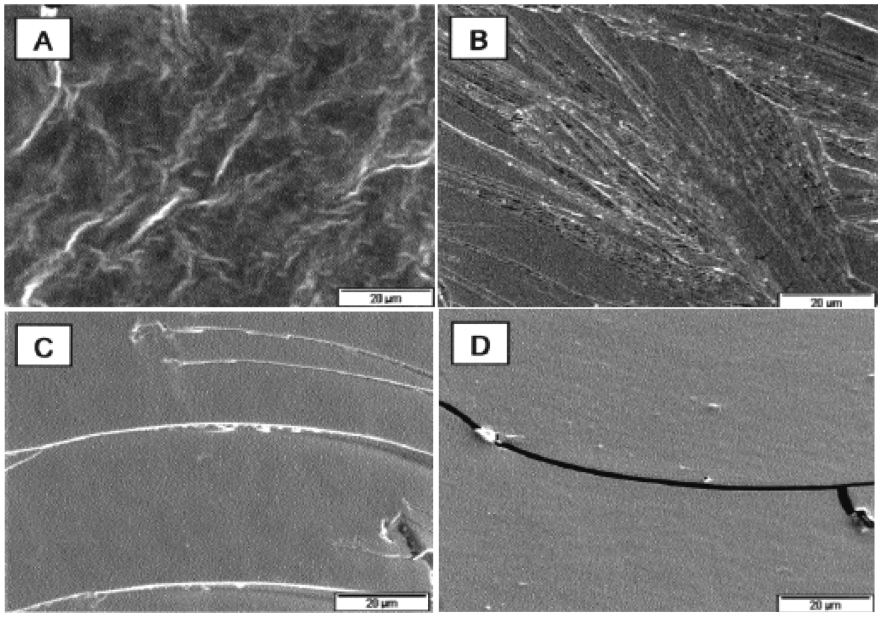

Figure 7.10 Scanning electron micrographs of the fractured surface of (A) glycerol, (B) xylitol, (C) sorbitol and (D) maltitol plasticized starch. Reprinted with permission from A. P. Mathew and A. Dufresne, *Biomacromolecules*, 2002, **3**, 1101–1108. Copyright 2002 American Chemical Society.

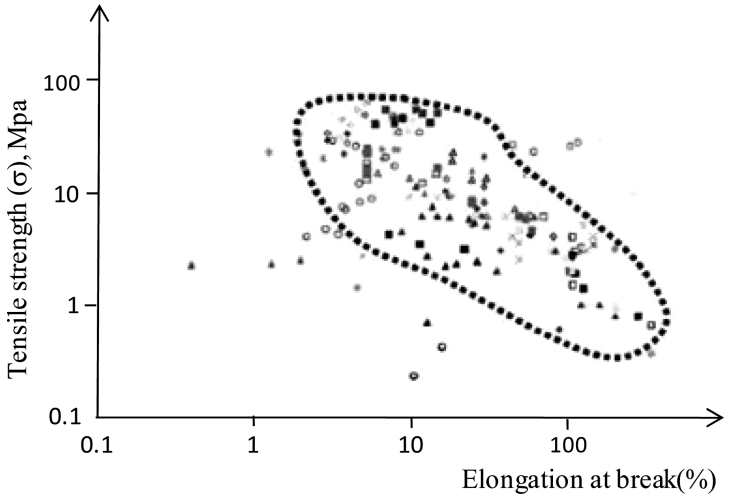

Figure 7.11 Tensile strength versus elongation at break for a variety of starch based agro-polymers.[15] N. Follain, C. Joly, P. Dole and C. Bliard: Mechanical properties of starch-based materials. I. Short review and complementary experimental analysis. *Journal of Applied Polymer Science*, 2005, **97**(5), 1783–1794. Copyright John Wiley and Sons. Reproduced with permission.

7.3.2.1 Factors Affecting Mechanical Properties

Moisture Content. The moisture content or water uptake of agro-polymers is an important topic and just about every research paper dealing with agro-polymers also considers moisture content.[44,55,57–63] Moisture content is important from at least two perspectives. Most importantly, the moisture content directly influences the mechanical properties of the plastic, typically increasing elongation and reducing strength by effectively plasticizing the material.[4,10,11,44] Secondly, in protein-based systems, the ability to absorb water could also be an indication of cross-link density.[10,59]

Water is required in the manufacture of both thermoplastic starch and thermoplastic protein. For starch, it ensures gelatinization and the formation of a continuous thermoplastic phase. In proteins, it lowers the glass transition and denaturing temperature,[10,11] allowing processing. However, dry resin ensures dimensional stability directly after injection moulding and over time.

The equilibrium moisture content of hydrophilic agro-polymers depends on the relative humidity of the environment and is typically described by the Guggenheim-Anderson-de Boer (GAB) and Brunauer-Emmett-Teller (BET) equations.[63,64] Equilibrium moisture content is also influenced by the type and amount of plasticizer in the system. Careful selection of additives and plasticizers could control the equilibrium moisture content of these materials, but only to a limited extent. The equilibrium moisture content of starch as a function of relative humidity and plasticizer type and content has been determined. It was found that the equilibrium moisture content for starch can be as high as 30% at 70% relative humidity, but, by using different plasticizers, this number could be significantly reduced.[55,62] In Figure 7.12, a phase diagram for a water/glycerol/starch system (as a function of plasticizer content) is shown which highlights the importance of the interactions between water, plasticizer and polymer.[65]

Plasticization. Plasticizers are typically high boiling substances and are usually good solvents for the polymer. The mechanism of how plasticizers work is typically described using the free volume theory.[66] Free volume can be increased by increasing the number of chain ends, or by decreasing the molecular mass. Alternatively, flexible side chains also increases free volume. This is called internal plasticization, and the free volume is spatially fixed with regard to the polymer molecule. Changing functional groups on the protein chain is not a common method of altering T_g, although it has been shown that after reacting proteins with aldehydes the processability was improved, but additional plasticizers were still required.[67]

External plasticization is the addition of a small molecule that can increase free volume at any location along the polymer chain and is proportional to the amount of this molecule added. The increased free volume enables more chain movement, by the mechanisms mentioned earlier, thereby decreasing the T_g.

The chemical nature of the plasticizer will strongly influence its efficiency. Aspects such as polarity, hydrogen bonding capability and density will

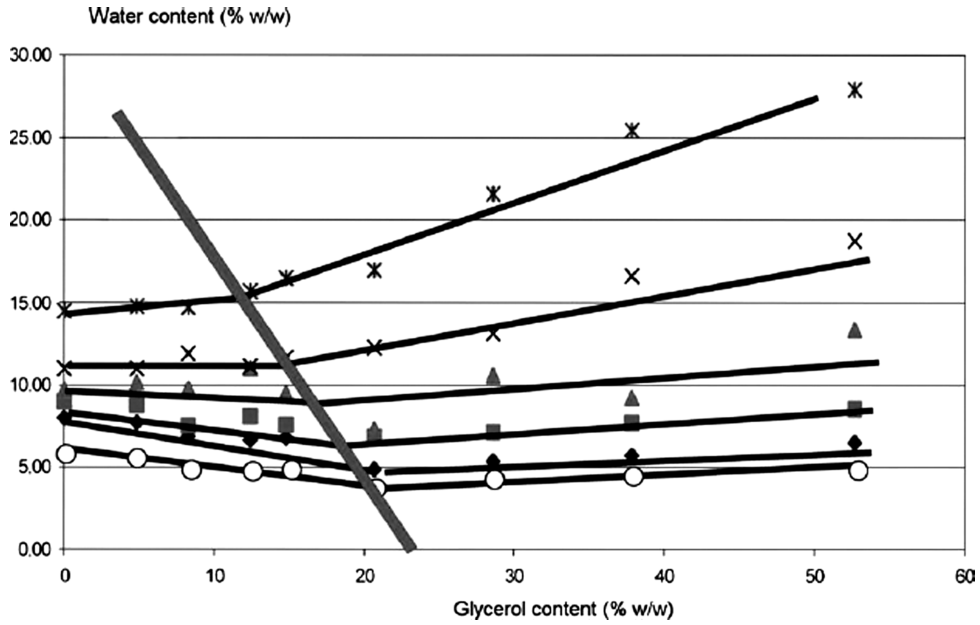

Figure 7.12 Equilibrium moisture content in plasticized starch as a function of plasticizer content at different relative humidity[65] (○ - 11%, ♦ - 33% , ■ - 44%, ▲ - 58%, X - 68%, *- 80%). Reprinted from *Food Chemistry*, **96**(3), L. Godbillot, P. Dole, C. Joly, B. Rogé and M. Mathlouthi, Analysis of water binding in starch plasticized films, 380–386. Copyright (2006), with permission from Elsevier.

determine how it functions as a plasticizer. However, chain flexibility may also permit protein chains to associate tightly with each other, leading to more intermolecular interactions; efficient plasticizers for proteins are therefore those that also disrupt these interactions.[33,66]

The basic rationale of plasticization is that plasticizers in agro-polymers can attract the water molecules around them, reduce the intermolecular interactions between the agro-polymer chains, and then increase the flexibility of the product. The effective working parts or active sites of plasticizers in agro-polymers are believed to be their hydrophilic parts such as hydroxyl groups. Hydroxyl groups are considered to develop hydrogen bonds between polymer–water–plasticizer or polymer–plasticizer, replacing the polymer–polymer interactions in the unplasticized agro-polymer materials.[64]

Ultimately, the amount and type of plasticizer is important in determining the mechanical properties of agro-polymers.[14,40,56,59,61,68–72] Although plasticization is required for processing the net result is a reduction in mechanical properties, as pointed out in Figure 7.11.

Chemical Composition. Along with additives such as plasticizers and moisture content, the chemical structure of the macromolecules used as agro-polymers also affects their mechanical properties. For starch, the amylopectin

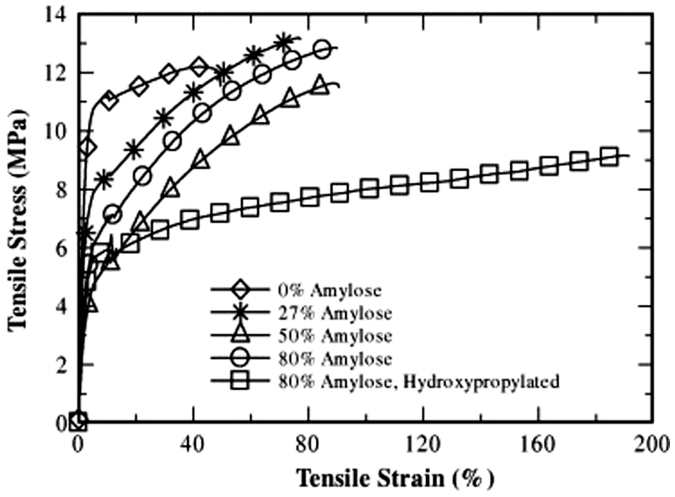

Figure 7.13 TS of thermoplastic starch containing different amounts of amylose.[74] Reprinted from *Carbohydrate Polymers*, **78**(4), A. L. Chaudhary, P. J. Torley, P. J. Halley, N. McCaffery and D. S. Chaudhary, Amylose content and chemical modification effects on thermoplastic starch from maize – Processing and characterisation using conventional polymer equipment, 917–925. Copyright (2009), with permission from Elsevier.

to amylose ratio is important,[15,68,69,73,74] whereas the primary structure or amino acid sequence of proteins are important.[10,11] As an example, the tensile strength of thermoplastic starch with varying amounts of amylose is shown in Figure 7.13. It can be seen that a more ductile material was obtained when the amylose content was higher.

Short range interactions, such as van der Waal's and hydrogen bonding, develop at low distance between functional groups (*e.g.* OH) and if these are strong enough the strength of the material at a low elongation will be high.[15] On the other hand, long-distance interactions are required for a large elongation at break; this is mostly chain entanglement and is dependent on molecular mass. Starch[15] and protein-based thermoplastics often suffer from not being able to develop sufficient chain entanglements and therefore have a low elongation at break.

In protein and starch based polymers, new interactions often form after processing. For starch, ageing or retrogradation causes chain rearrangement, often resulting in embrittlement.[35,68,69,72,74] For proteins the level (intra- and intermolecular) at which cross-links are formed determine the tensile properties of protein based plastics.[11,43,57,75–77] Cross-linking can be a result of the chemical nature of the protein or can be induced to improve mechanical properties.[43]

7.3.3 Thermal Properties

The thermal behaviour of agro-polymers is complicated relative to conventional polymers. As with mechanical properties, the thermal properties of

proteins and starches depend on moisture content, which may change during heating.[73] In addition, the composition of agro-polymers also influences their thermal behaviour. For example, the aforementioned variable ratio of amylose to amylopectin in starch also gives rise to different thermal properties.[14] Proteins are heteropolymers with a combination of hydrophobic, hydrophilic, acidic and basic side chains and have a wide range of different intermolecular interactions compared to synthetic homopolymers.

7.3.3.1 Thermal Analysis Techniques

Thermal analysis refers to a range of techniques were one or more properties of a material is measured as a function of temperature. Common techniques, their abbreviations and their application are listed in Table 7.2. Of these, DSC, DMA and TGA are widely used for characterizing thermal transitions and thermal stability.

DSC. DSC measures the difference in heat flow between a specimen and a reference as a function of temperature. Specimens are placed in a special pan, which can either be sealed or not. The reference is usually an identical, but

Table 7.2 Summary of common thermal analysis techniques.[78,79]

Technique	*Abbreviations*	*Measures*	*Reveals*
Thermogravimetry or thermal gravimetric analysis	TG or TGA	Mass change	Decomposition temperature Oxidation temperature Volatilisation of moisture and plasticiser Moisture content
Differential thermal analysis	DTA	Temperature difference	Exothermic and endothermic thermal events
Differential Scanning Calorimetry	DSC	Heat flow difference	Heat capacity Phase changes (melting etc) Glass transition
Dilatometry	TD	Length or volume change	Creep, thermal expansion
Thermomechanical analysis	TMA	Deformation under constant load	Creep, thermal expansion, heat deflection temperarure
Dynamic mechanical analysis or Dynamic mechanical thermal analysis	DMA or DMTA	Deformation under oscillating load	Viscoelastic properties Glass transition
Dielectric Analysis	DES	Dielectric properties	Glass transition
Simultaneous DSC/TGA or DTA/TGA	SDT	Mass change and heat flow or temperature difference	Causes of mass loss events.

empty pan. In heat flux DSC both pans are heated in the same oven and the temperature difference between them is used to determine heat flow to the sample. Exothermic events cause the sample pan temperature to be higher than the reference, whilst endothermic events cause the sample temperature to be lower at any given point in time. In power compensation DSC the pans are held in separate ovens and the difference in electrical work needed to keep the temperature increasing at the same rate is used to determine the heat flow. Exothermic events cause the sample pan to require less energy input and endothermic events cause it to require more. The main output of a DSC experiment is a curve representing heat flow versus temperature. Depending on the level of analysis required, the first or second derivative may also be useful.

As a polymer is heated through its glass transition, a sudden change in heat capacity occurs. The heat flow measured by the DSC is proportional to the specific heat capacity and hence reveals this transition.[79] Figure 7.14 shows the identification of this region in scans of thermoplastic starch plasticized with glycerol and containing different amounts of citric acid.

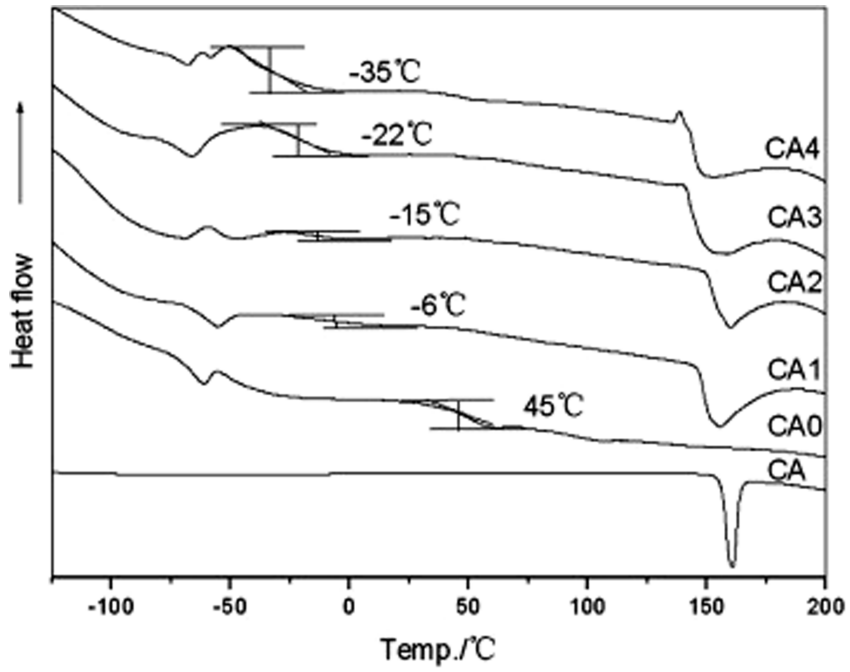

Figure 7.14 Identification of the glass transition as a step change in heat flow, CA = citric acid, CA0 = TPS with 30 pph glycerol, CA1 = TPS with 30 pph glycerol and 10 pph citric acid, CA2 = TPS with 30 pph glycerol and 20 pph citric acid, CA3 = TPS with 30 pph glycerol and 30 pph citric acid, CA4 = TPS with 30 pph glycerol and 40 pph citric acid.[70] Reprinted from *Carbohydrate Polymers*, **69**(4), R. Shi, Z. Z. Zhang, Q. Y. Liu, Y. M. Han, L. Q. Zhang, D. F. Chen and W. Tian, Characterization of citric acid/glycerol co-plasticized thermoplastic starch prepared by melt blending, 248–755. Copyright (2007), with permission from Elsevier.

Table 7.3 Typical DSC responses to thermal events in polymeric samples.[78,79]

Thermal Event	*Effect on plot of heat flow* vs *temperature*
Glass transition	Step change in heat flow
Crystallisation	Exothermic peak
Melting	Endothermic peak
Denaturing (in proteins)	Endothermic peak
Degradation (in inert atmosphere)	Endothermic trend
Oxidation	Exothermic trend

It would be better to measure the glass transition by cooling, but for historical reasons, it is usually measured in heating.[79] The typical DSC responses to this and other thermal events are listed in Table 7.3.

DSC is sensitive to the thermal history of the sample. A common approach is to heat and cool a specimen prior to scanning for thermal events during a second heating cycle. The first heating scan provides information about the thermal history (processing or ageing) of the sample. The cooling and second heating cycle are then performed at known thermal history. Transitions, such as the glass transition, are then determined from the results of the second scan.[80] This may pose a concern for proteins as heating during the first scan may affect protein conformation and hydration. An alternative approach is to use modulated DSC, in which the heating rate oscillates.[81] This allows separation of reversible events (glass transition and melting or fusion) and non-reversible events (oxidation, curing, relaxation and cold crystallization) which is complicated as these may overlap.[78,81] For starch this can be particularly useful for studying the multiple transitions that occur during gelatinization, although the onset and peak temperatures appear lower than those observed in conventional DSC.[82]

One other complication is that results from a DSC experiment depend on the rate of temperature change. For this reason the temperature ramp rate should always be reported with the results. It is also advisable to complement the analysis with other techniques, such as DMA.

DMA. In DMA a specimen is subjected to an oscillating force and the material's response is recorded as a function of temperature or frequency. Different instrument geometries allow testing of fibres, films, bars or even powders. Optimal choice of testing mode and sample size depends on sample stiffness and geometry.[83]

The main outputs of a DMA scan (as a function of temperature) are:

- the elastic (or storage) modulus (E'), representing the elastic component of the material's response, or energy stored by reversible deformation of the material
- the loss modulus (E''), representing the viscous component of the material's response, or energy dissipated as heat by molecular rearrangement

- the damping coefficient (tan δ); this is the tangent of the phase lag between applied force and the sample responding and is equal to E''/E'.

The glass transition region is identified as the region in which the elastic modulus drops rapidly by around two orders of magnitude and there is a local maximum in the loss modulus. These contribute to a clear peak in the plot of tan δ versus temperature.[14,48,80,84–86] The glass transition temperature could also be reported as the peak in the loss modulus or the onset of drop in storage modulus.[47,87]

DMA results for the glass transition are frequency dependent. For this reason the frequency of testing should always be reported. It is also good practice to test at more than one frequency and compare results with those from other techniques, such as DSC. For agro-polymers, the loss of moisture during scanning may also contribute to higher observed glass transition temperatures than those determined using DSC in sealed pans.[58]

Below the T_g, other thermal transitions relating to short range movements within polymer chains are identified as regions of rapid drop in storage modulus, but these are less dramatic than the glass transition. Above the glass transition, protein denaturing has been associated to a minimum in tan δ.[88] Figure 7.15 shows examples of plots of tan δ versus temperature for a thermoplastic protein and a thermoplastic starch. For the soy protein, β transitions can clearly be seen, along with a peak for ice melting at high water contents. The low temperature peak observed for the amylose films is likely due to the glycerol-rich phase, whereas the shifting upper peak will be the glass transition of the plasticized amylose.

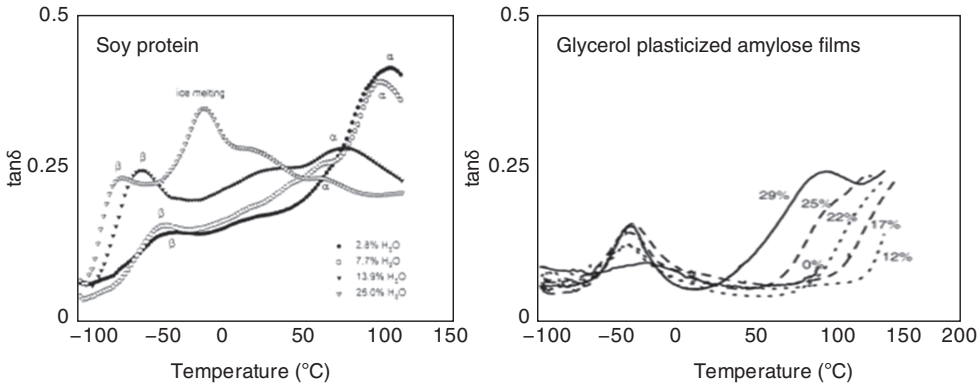

Figure 7.15 Plots of tan δ versus temperature for DMA scans of extruded soy protein sheets at different moisture contents[58] (reprinted from *Polymer*, **42**(6), J. Zhang, P. Mungara and J. Jane, Mechanical and thermal properties of extruded soy protein sheets, 2569–2578. Copyright (2001), with permission from Elsevier) and amylose films plasticized with different glycerol contents[89] (reprinted from *Carbohydrate Polymers*, **22**(3), G. K. Moates, T. R. Noel, R. Parker and S. G. Ring, Dynamic mechanical and dielectric characterisation of amylose-glycerol films, 247–253. Copyright (2001), with permission from Elsevier.)

TGA. In TGA mass loss is measured as a function of temperature. The sample is subjected to both a controlled temperature profile and a controlled atmosphere.[79] This reveals information such as the temperatures where moisture, solvents and plasticizers are volatilized from the material, as well as mass loss due to combustion or pyrolysis. Many instruments offer combined SDT analysis which allows for easier identification of the cause of mass loss events.[78] Additionally, FT-IR analysis can confirm volatilized species and decomposition products associated with mass loss events.[86] One of the most common applications of TGA is determination of thermal stability by heating to high temperatures in an inert atmosphere, usually nitrogen.[79] If a polymer is to be used in air, it is also important to determine its thermo-oxidative stability.[79] An example of the output of a TGA experiment is shown in Figure 7.16 for soy protein isolate with plasticizer made up of different ratios of ε-caprolactone to glycerol in both air and an inert atmosphere. The mass loss is usually presented as a function of temperature, and the first derivative is also plotted against temperature to more clearly determine the onset of thermal events.

For characterization of new materials it is advisable to utilize TGA prior to techniques such as DSC or DMA where thermal decomposition should be avoided.

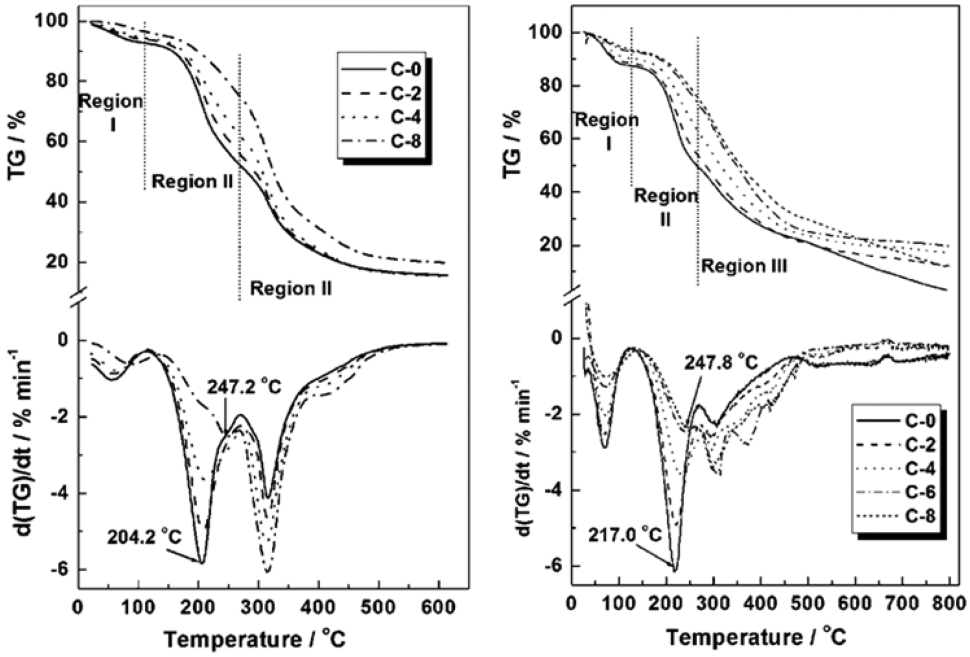

Figure 7.16 Percentage mass loss and first derivative TGA thermograms of SPI with 40 wt% plasticizer containing ε-caprolactone/glycerol ratios of 0:8 (C0), 2:6 (C2), 4:4 (C4), 6:2 (C6) and 8:0 (C8) in N_2 (left) and air (right).[86] Reprinted with permission from P. Chen, H. Tian, L. Zhang and P. R. Chang, *Ind. Eng. Chem. Res.*, 2008, **47**, 9389–9395. Copyright 2008 American Chemical Society.

Other Techniques. Differential temperature analysis (DTA) is similar to heat flux DSC. The difference in temperature is reported, but not converted into heat flow. This gives a similar shaped curve, but only provides qualitative information rather than the quantitative information available from DSC. Its main advantage is when run simultaneously to TGA, it can provide insight into the cause of mass loss events; *e.g.* exothermic (*i.e.* burning) or endothermic (*i.e.* evaporation). Additionally, DTA instruments can operate over a wider temperature range than DSC.[78] Although this may be an advantage for thermal analysis of some materials (*e.g.* metals) that melt at high temperatures, the relatively low degradation temperature of agropolymers falls within the range of a typical DSC instrument.

In thermo-mechanical analysis (TMA) the change in dimensions under a minimal load is measured as a function of temperature.[83] This reveals the coefficient of thermal expansion (CTE) and can also be used to detect other transitions, such as the glass transition.

The heat deflection temperature (or heat distortion temperature) is an important material property mostly used to determine a material's useful temperature operating range. It refers to the temperature below which a moulded object can hold its own shape. It can be determined using a dynamic mechanical analyser set to apply a constant force. The HDT was determined for blends of plasticized soy flour (52% protein) and polyamide (nylon) as 45 °C when plasticized with 20 wt% sorbital, 35 °C when plasticized with 20 wt% glycerol, and 39 °C when plasticized with 10 wt% of each.[48] When such a blend is used to make composites with natural fibres, increasing content of natural fibres also increased the HDT.

Phase transition analysis uses an apparatus similar to a closed-chamber capillary rheometer. It measures displacement at a constant pressure. It yields glass transition results consistent with DMA, DSC and capillary rheometry.[80]

7.3.3.2 The Glass Transition

In both thermoplastic starch and thermoplastic proteins, the glass transition depends on numerous factors including moisture content, presence of plasticizers or other additives and processing history.

Reported glass transition temperatures for gelatinized starches are variable and depend on the methods and conditions used.[82] An extensive list of glass transition temperatures for thermoplastic starches and polymer blends containing thermoplastic starches of different compositions was compiled by Arvanitoyannis and Kassaveti.[90] These ranged from below –60 °C up to over 200 °C. The large range of contributing factors complicates a clear comparison between the T_g of materials produced in different studies, but do not preclude assessing the effect of specific conditions or additives.

The effect of sugar addition on the T_g of starch/glycerol/water systems was investigated using DMA. Adding sugar lowered the T_g and the elastic modulus suggesting that the presence of natural sugars in starch sources should be

factored into polymer design.[72] The T_g was also observed to decrease with an increase in amylose to amylopectin ratio.[14]

Glass transitions of dry, unplasticized proteins are typically in the range of 120–250 °C depending on protein structure.[91] For highly plasticized proteins, T_g can be well below ambient temperatures. For example, DSC of compression moulded soy protein sheets plasticized with 50–70 g ethylene glycol per 100 g soy protein revealed the T_g to be in the range of –90 to –70 °C.[92]

Miscibility of blends can be characterized by examining the glass transition with either DMA or DSC. Fully miscible blends show a single T_g, intermediate of those of the individual components, or phases. Two glass transitions corresponding to the individual components are seen in immiscible blends. Partial mixing is indicated by shifting of the distinct T_g values closer together.[79] The effect of different plasticizers or miscibility agents on the blend can be assessed in this way. Soy protein plastics plasticized with sorbitol were found to be more miscible with a polyester amide than those plasticized with glycerol.[48]

Bulk proteinaceous material used for agro-polymer production may contain more than one kind of protein subunit and, like blends, this may be reflected in multiple glass transitions related to the different subunits. Modulated DSC of plasticized, mechanically processed gluten revealed three glass transitions: one near –30 °C associated with molecular motion of free glycerol, along with one at 40 °C and one near 75 °C associated with the plasticized glutenin and gliadin gluten subunits respectively.[88] Likewise, DMA of thermoplastic soy protein isolates prepared with urea showed two glass transitions; a low T_g relating to 7s globulin, and a higher T_g relating to 11s globulin.[87] Depending on the instrument used, the resolution of the glass transition may or may not distinguish such phases. For a thermoplastic produced from soy protein isolate and 25 wt% glycerol, two glass transitions were observed in DMA, but only one was seen in DSC.[47]

7.3.3.3 Denaturing, Destructuring, Gelatinization and Physical Ageing

In starch, disruption of the ordered granular structure when heated in a solvent (usually water) is called destructuration or gelatinization. The temperature at which this occurs increases as the amount of solvent is decreased and is seen as an endothermic peak during the first scan in DSC.[93] Destructuration is an irreversible transition and, after cooling, an amorphous entanglement of amylose and amylopectin is formed.

An irreversible exothermic event has also been seen with some plasticizers. Mixtures of amylopectin and glycerol exhibited such a peak at 95–110 °C, mixtures of amylose and glycerol at 95–105 °C, mixtures of amylopectin and ethylene glycol at 70–85 °C and mixtures of amylose and ethylene glycol at 65–75 °C.[94] These peaks appear to be due to the formation of hydrogen bonding between the plasticizer and starch molecules and are not dependent on the crystallinity present in the polysaccharides.[94]

DSC is used by biochemists to quantitatively analyse the thermodynamics of protein folding and unfolding.[95] Any conformational change leading to disruption of protein functionality is called denaturation. Depending on conditions and the extent of conformational change, denaturing may be a reversible or irreversible process.[96] Historically, much work on protein denaturing has focussed on proteins in solution, rather than solid materials.[97] Like the glass transition, the denaturation temperature of a protein is dependent on water content, shifting to higher temperatures with decreasing water content.[98] In solution, protein denaturing typically occurs below 100 °C.[98] In thermoplastic proteins, denaturing occurs above the glass transition and for dry proteins this may be above 200 °C at temperatures close to degradation.[11]

Protein denaturing is seen as an endothermic peak in DSC. As with the glass transition, the phenomenon may be observed at multiple temperatures for blends containing multiple phases. Soy proteins exhibit two such peaks related to the denaturing of the 7s globulin and 11s globulin subunits.[87,98] Increased concentration of urea decreases the size of these peaks, confirming urea has partially or, at higher concentrations, fully denatured the subunits.[87]

Although, strictly speaking, denaturing refers to disruption of the native secondary, tertiary and quaternary structures, similar interactions are present in processed thermoplastic proteins. Depending on the protein used and the processing conditions with which it was plasticized, thermoplastic proteins may or may not exhibit a 'denaturing' peak in DSC. Cast films prepared from wheat gluten in the presence of sodium sulfite and ethanol exhibited an endothermic peak in modulated DSC, whereas thermo-mechanically prepared films prepared with glycerol in a torque rheometer did not.[88]

DSC was used to characterize soy protein plasticized with glycerol and modified with functional monomers that had been extruded and compression moulded. An endothermic peak corresponding to protein denaturing was seen at 152 °C in the absence of functional monomers. This temperature decreased after reactive extrusion with maleic anhydride or glycidyl methacrylate, but increased with styrene addition.[99] This provided information regarding the interaction of these monomers with the protein. For example, styrene is hydrophobic and does not interact with hydroxyl groups on the protein.

Ordered secondary structures like α-helixes and β-sheets occurring in thermoplastically processed proteins are effectively forms of crystallinity. In analysis of extruded feather keratin, which used sodium sulfite to break disulfide bridges, a shift from low crystallinity to higher crystallinity was seen between DSC scans of samples with 4% sodium sulfite and samples with 5% sodium sulfite.[100] Proteins may also contribute to the formation of ordered regions in polymers/protein blends. DSC analysis of crystal formation in soy protein/poly(butylene succinate) (PBS) blends showed soy protein both induced and accelerated PBS crystallization.[101]

An endothermic peak, just before the T_g, is seen for the first DSC scan in many proteins containing gluten subunits and has been suggested to be due to physical ageing.[80] Physical ageing is a characteristic of polymers in their glassy state and is a slow transformation of amorphous regions to a more ordered

structure.[79] It is accompanied by a reduction in internal energy and free volume and when heated through the glass transition causes an endothermic peak in DSC analysis.[47] Physical ageing is also readily apparent in thermoplastic starch as a form of retrogradation below the T_g.[102] This increase in crystallinity causes brittleness and limits the industrial applications of thermoplastic starches.[74] Retrogradation is studied with X-ray scattering techniques and is discussed further in Section 7.3.3.7.

Physical ageing has been observed for soybean protein plasticized with 25 wt% glycerol through enlargement of an endothermic peak at around 50–60 °C in the DSC scan of samples stored for increasing lengths of time at 50% RH.[47]

7.3.3.4 *Mass Loss and Degradation*

Thermal degradation of plasticized proteins, as determined by TGA, generally consists of four events that often overlap:[11]

(1) water elimination
(2) plasticizer elimination or decomposition
(3) weak bond cleavage contributing to peptide bond cleavage
(4) stronger bond cleavage leading to total degradation.

Soy proteins plasticized with ε-caprolactone/glycerol exhibit three mass loss regions under nitrogen atmosphere. Mass loss up to 120 °C was due to loss of moisture; between 120 °C and 260 °C due to volatilization of plasticizers and beyond 250 °C due to rupture of peptide bonds. Higher ε-caprolactone content imparted greater thermal stability, reducing the magnitude of the mass loss in the first two regions and shifted the volatilization of glycerol to a higher temperature.[86]

Soy proteins plasticized with acetimide exhibited similar regions, but had greater stability than those plasticized with glycerol.[54] Thermoplastic zein plasticized with polyethylene glycol (PEG) 400 only exhibited two significant mass loss regions, as the volatilization of the PEG occurred at similar temperatures to protein degradation.[103]

Acetylated gluten, zein, pea and soy proteins were found to be less stable than their unmodified counterparts. Nevertheless, the decomposition temperatures of the modified proteins are still above the softening temperatures required to process them.[104] Sorbitol plasticized soy protein/polyester blends exhibited greater thermal stability than glycerol plasticized soy protein/polyester blends.[48]

Thermal degradation of thermoplastic starch occurred after moisture loss and the degradation temperature was independent of the original moisture content in TGA.[105] Sealed high pressure DSC pans were used to study degradation of starch at high pressure and constant moisture content, simulating extrusion conditions. The onset of degradation and its broadness was dependent on moisture content which indicated that the decomposition mechanism was different from that occurring in unsealed TGA.[105]

7.3.3.5 The Importance of Moisture

The strong dependence of agro-polymer properties on moisture poses a particular challenge for thermal analysis of these materials. Some argue that the loss of plasticizer or moisture while testing at elevated temperatures implies that material properties are changing during testing and a different material is effectively tested.[106] These losses are an important consideration when designing applications for a material and are relevant. Nevertheless, techniques for containing water in the sample as it is heated are used. Coating samples with silicone oil was used to prevent moisture loss during DMA scans of gluten, corn zein and whey plasticized with water.[80]

Sealed pans can be used in DSC to restrict water loss.[73] However, data is more reliable when there is a larger contact area between the sample and the pan, giving preference to standard pans when moisture (or other volatile) loss is not significant.[79] This is rarely the case for agro-polymers and sealed pans are preferred.

Hermetically sealed aluminium pans are common and usually able to withstand internal pressures of up to 0.2 MPa.[79] In DSC analysis of starch, these pans ruptured at 110 °C, limiting the range of the experiment.[73] The use of high pressure stainless steel pans allowed scanning up to 300 °C; however, the extra mass of these pans reduced the accuracy to which changes in heat capacity of the sample could be detected.[73] It is recommended that moisture sensitive agro-polymers are tested in more than one kind of pan. When investigating the effect of water content on thermal properties of sunflower proteins both sealed aluminium pans and stainless steel pans with O-rings were used. The use of stainless steel pans allowed detection of a denaturing peak between 120 °C and 189 °C with moisture contents between 0% and 30 wt%.[107]

Alternatively, higher heating rates could reduce the affect of moisture loss on DSC results.[107] An advanced application of this is hyper DSC, which scans at very high heating rates and allows greater clarity in determination of the glass transition of thermoplastic starch than standard or modulated DSC.[105]

In agro-polymers, especially proteins, it is often necessary to distinguish between bound water (non-freezable) and free (freezable) water. Bound and freezable water content can be determined from water melting peaks detected in DSC.[108] The area of the endothermic peak represents the heat of fusion of the freezable fraction; division by the heat of fusion of pure water yields the mass of free water. Subtracting that value from the total water content of the sample gives the mass of bound water.[109]

The glass transition of sunflower proteins (by DSC) reduced from 180.8 °C with no water present to 5.3 °C with 26.12 wt% water. Up to 26.12 wt%, no endothermic peak was observed, indicating all moisture was bound. At 50 wt% water, a broad endothermic peak associated with the melting of freezable water obscured the glass transition.[107]

Similarly, in extruded soy proteins a strong endothermic peak for freezable water was observed in polymers containing 26 wt% water, but not at lower water contents.[58] It appeared that above a critical moisture content, the glass

transition does not continue to decrease but merges with the peak for water crystallizing.[58] The glass transition for these extruded soy protein sheets detected by DMA was lower than that detected in sealed DSC pans which may be due to water loss during the DMA scan.[58] On the other hand, some researchers have suggested moisture loss is more significant beyond the glass transition.[106]

DSC was used to determine the T_g of starch plasticized with either glycerol or xylital at different free water contents. Glycerol was shown to be the better plasticizer at lower water content, but xylital was found to be better at higher water content.[71] It has been postulated that in corn starch systems water exists in three phases: bound, loosely bound and free water.[110]

The hydrophilic nature of starch and proteins can be explained in terms of the chemical nature of their monomers. These contain many hydrophilic groups capable of hydrogen bonding. It is hydrogen bonding that dominates interactions with water, most plasticizers and most inter- and intra-molecular interactions in agro-polymers. Proteins also have a variety of side groups with different functionalities which may give rise to hydrophobic interactions and covalent cross-linking. These interactions give rise to ordered regions within polymers that may be characterized with techniques such as Fourier transform infrared spectroscopy (FT-IR) and X-ray scattering (XRS).

7.3.3.6 FT-IR

FT-IR is a technique used to investigate changes in the nature of chemical bonds. Different covalent interactions stretch, vibrate or bend at specific frequencies and allow the identification of specific interactions. With the exception of exact optical isomers, the same IR spectrum will not be observed for compounds with different structures.[111] Complete determination of the cause of every peak and elucidation of the exact chemical structure is not practical for mixtures of complex macromolecules. Rather, changes in the location or magnitude of characteristic peaks provide information about structural and chemical changes occurring during processing. Important changes after thermoplastic processing investigated by FT-IR include changes in secondary structures (α-helices and β-sheets or turns) in proteins and the interaction between chains and plasticizers in both starch and proteins.

Secondary Structure in Proteins. Characteristic peaks related to vibrations in peptides (forming the protein backbone) are shown in Table 7.4. Different molecular geometries and hydrogen bonding present in a protein's secondary structure contribute to different C=O stretching frequencies in the amide I region.[112] Deconvolution of this region allows estimation of protein secondary structure with good approximation.[112]

In solutions, the solvent dominates the FT-IR spectrum and must be subtracted, often causing distortions. In particular, the signal of water overlaps with the amide I region. For this reason, FT-IR of proteins is often performed

Table 7.4 Molecular motions responsible for characteristic FTIR absorbance peaks in peptide links.[112]

Molecular motion	*Characteristic frequency or frequency ranges (cm^{-1})*	*Designation*
N-H stretching	3300	Amide A
	3100	Amide B
C=O stretching	1600 – 1690	Amide I
C–N stretching and N–H bending	1480 – 1575	Amide II
	1229 – 1301	Amide III
O–C–N bending	625 –767	Amide IV
Out of plane N–H bending	640 – 800	Amide V
Out of plane C=O bending	537 – 606	Amide VI
Skeletal torsion	200	Amide VII

using dried protein powders in potassium bromide (KBr) pellets.[113] Plastic films may be mounted directly in FT-IR spectrophotometers.

Although the native secondary structure is denatured during thermoplastic processing, secondary structure elements may contribute to physical fixation as the processed material cools.[97] Changes to secondary structure induced by thermoplastic processing depend on the protein's primary structure, processing conditions and additives such as plasticizers or denaturing agents. In general, extrusion appears to favour an increase in ordered β-sheet regions at the expense of α-helices, but this is not always the case.[11] Time resolved FT-IR of soybean protein films held at 100 °C showed changes in the amide I region over time that may be attributed to an increase in β-turn or weak β-sheet structures.[114] The peaks in the amide I region overlap and some form of deconvolution is needed to distinguish the combined peak into separate peaks relating to different secondary type structures, as shown in Figure 7.17.

The amide I region for hot pressed films of egg albumin, lactalbumin, feather keratin and wheat gluten were analysed with deconvolution software. Increased order was observed in the form of β-sheets as glycerol content increased up to a critical value for each protein. Beyond this, critical value order decreased.[115] The result of the deconvolution for wheat gluten is summarized in Figure 7.18.

FT-IR analysis of film blown thermoplastic zein plasticized with polyethylene glycol highlighted the interdependence of structure and processing. Different batches of zein powder contained different ratios of β-sheets to α-helices and the best blown films were prepared from those with largest relative α-helical content. In turn, processing increased the α-helical content and decreased the presence of ordered β-sheet regions.[103] Cross-links induced by γ-radiation in whey, casein and soya films appeared to have reduced β-sheet regions.[116]

FT-IR analysis of thermoplastic sheets containing soy protein isolate and glycerol showed no change in the characteristic peaks of the individual components indicating that no covalent interactions formed between them.[117] In contrast, soy protein plastics plasticized with both ε-caprolactone and glycerol did not show peaks characteristic of caprolactone, indicating it had been consumed.[86]

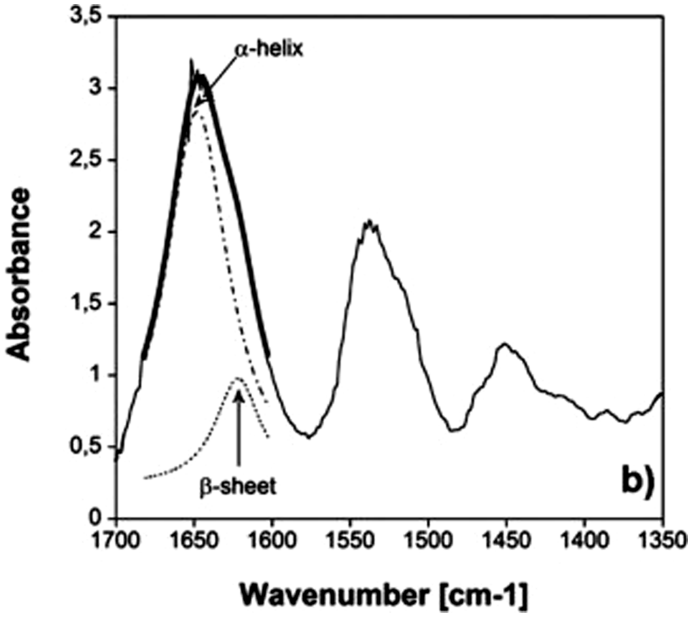

Figure 7.17 FTIR spectrogram of thermoplastic zein protein. The combined peak for the amide I region is separated as shown into component peaks relating to different secondary structures.[103] M. Oliviero, E. D. Maio and S. Iannace, Effect of molecular structure on film blowing ability of thermoplastic zein. *Journal of Applied Polymer Science*, 2010, **115**(1), 277–287. Copyright John Wiley and Sons. Reproduced with permission.

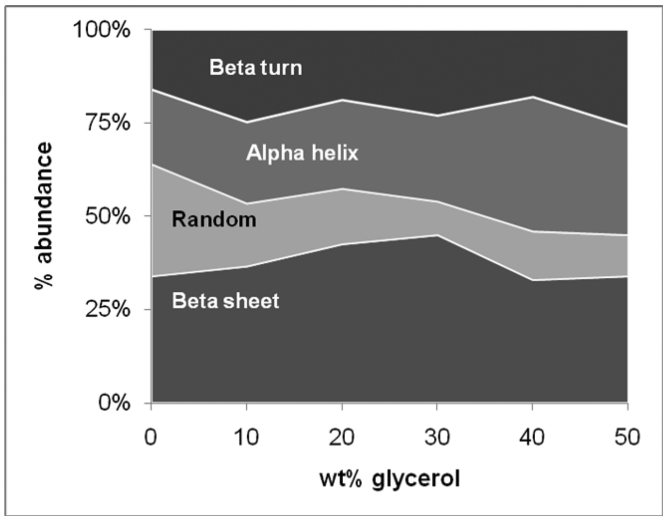

Figure 7.18 Secondary structure content of hot pressed wheat gluten films with glycerol as a plasticizer estimated by deconvolution of amide I region in FTIR spectrum.[115]

Starch/plasticizer Interactions. Peaks observed in thermoplastic starch between 992 and 1200 cm^{-1} have been associated with interaction between starch molecules and plasticizer and can be used to evaluate the efficiency of different plasticizers.[68]

Within this region, a peak at 1020 cm^{-1} can be attributed to C–O stretching in C–O–C bonds for native starch, while peaks at 1081 and 1156 cm^{-1} are indicative of C–O stretching in C–O–H bonds.[118] In thermoplastic starch, hydrogen bonding between starch and plasticizer causes absorbance to shift to lower wavenumbers.[118,119] Greater reduction in wavenumber is indicative of stronger plasticizer/starch interactions.[68] This shifting is apparent in the FT-IR spectra for native starch and TPS plasticized with ethanolamine, as shown in Figure 7.19. The effects of some plasticizers and ageing on these peaks are listed in Table 7.5.

As seen in Table 7.5, the peak for C–O–C stretching separates into two peaks as thermoplastic starch (10 wt% 30 pph glycerol) ages. This split peak is also seen in TPS with 30 pph glycerol and 1 pph citric acid prior to ageing and is unchanged after 70 days.[102]

In thermoplastic starch processed with 100 parts hydrous starch (20 % water content) and 30 pph glycerol and higher concentrations citric acid (10–40 pph),

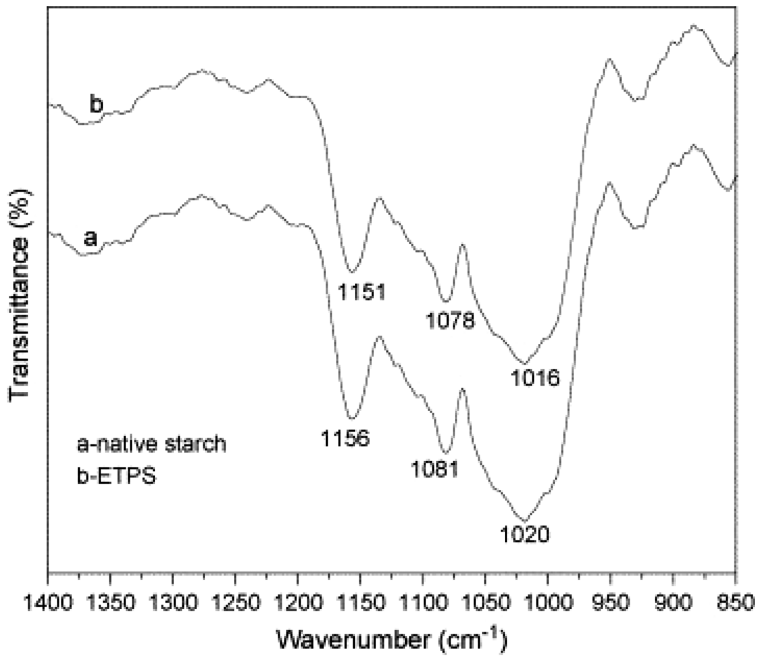

Figure 7.19 FTIR spectra of starch and ethanolamine plasticized thermoplastic starch (ETPS). Peaks which shift indicating H-bonding with plasticizer are labelled.[119] Reprinted from *Polymer Degradation and Stability*, **90**(3), M. F. Huang, H. G. Yu and X. F. Ma, Ethanolamine as a novel plasticiser for thermoplastic starch, 501–507, Copyright (2005), with permission from Elsevier.

Table 7.5 Shifts in some FITR peaks indicative of plasticiser H-bonding interactions in TPS.[70,102,118–120]

	Peak Postitions (cm^{-1})		
	C–O in C–O–C	*C–O in C–O–H*	
Native starch[102,118–120]	1020	1081	1156
TPS plasticised with Formamide[118]	1012	1077	1155
Ethanolamine[119]	1016	1078	1151
Ethylenebisformamide[120]	1016	1078	1150
Glycerol (30 pph) (after extrusion)[102]	1014	1078	1150
Glycerol (70 days aging)[102]	1016 and 996	1078	1150
Glycerol (30 pph) with citric acid (1 pph) (After extrusion)[102]	1012 and 990	1078	1150
Glycerol with citric acid (70 days aging)[102]	1012 and 990	1078	1150
Glycerol with high citric acid[70]	1024		1149

the peak for C–O stretching in C–O–C bonds was seen at 1024 cm^{-1}. Residual citric acid was removed by washing in deionized water after processing and before FT-IR. This peak decreased in size relative to the peak at 1149 cm^{-1} (C–O stretching in C–O–H bonds) as citric acid content increased, indicative of a reduction in molecular mass.[70]

Other peaks observed in thermoplastic starch provide further information about interactions between polysaccharide chains, water and plasticizer. A peak at 1644 cm^{-1} corresponds to water strictly bonded to starch.[68] A peak at 3389 cm^{-1} in native cornstarch is ascribed to free, intermolecular and intramolecular bound hydroxyl groups and decreased to 3325 cm^{-1} in TPS plasticized with ethanolamine.[119] Again, as with the peaks in Table 7.5, this indicates H-bonding interactions forming with the plasticizer at the expense of interactions between chains. Other researchers found a similar peak at 3413 cm^{-1} for native starch.[69] After processing with high glycerol contents, this peak shifted to lower wavenumbers and decreased in intensity. As thermoplastic starch aged (retrograded), this peak shifted back towards that seen in native starch. After 70 days, the peak had returned to 3413 cm^{-1} for TPS with 30% glycerol.[69] For higher glycerol contents this shifting slowed, suggesting the glycerol restricted retrogradation.[69]

A peak at 2931 cm^{-1} representing C–H stretching in CH_2 groups did not shift in TPS plasticized with ethanolamine, indicating the plasticizer did not interact with these groups.[119]

7.3.3.7 XRD/XRS

X-ray diffraction (XRD) and X-ray scattering (XRS) are techniques in which a sample is exposed to X-rays and the resultant scatter pattern is interpreted to provide information about the spatial arrangement of atoms. Strictly speaking, X-ray diffraction refers to the patterns of constructive and destructive interference due to the scattering of rays by crystal planes. Scattering is a more

general term also applicable to amorphous materials which show broad 'halo' peaks, rather than sharp peaks caused by diffraction. In practice, similar instrumentation is used for both techniques and the terms are often used interchangeably.[78] Wide angle X-ray diffraction (WAXD) and wide angle X-ray scattering (WAXS) (scattering angle $2\theta > 5^{\circ}$) are most commonly used for characterization of crystallinity in polymers.[78]

For thermoplastic starch and proteins, X-ray scattering techniques provide information about conformational changes induced by processing or ageing as well as information about the compatibility of plasticizers and cross-linking agents. Figure 7.20 shows examples of the plots of intensity versus scattering angle that are obtained as thermoplastic starches age and as plasticizer content changes for wheat gluten.

The original crystalline order of native starch is destroyed in the production of thermoplastic starch, but even below the T_g, chains exhibit enough mobility and re-order over time.[93] This re-forming of ordered crystalline regions is called retrogradation and can be observed using WAXS.[68,69,72,74,119] Different plasticizers and plasticizer content affect the rate of retrogradation and the type of crystallinity that forms. The types of crystallinity that can be identified using XRD are listed in Table 7.6.

Maize starch plasticized with 30 wt% glycerol displayed a shift from type-A crystallinity to type-V_H and type-V_A. Plasticization with 30 wt% of a mixture

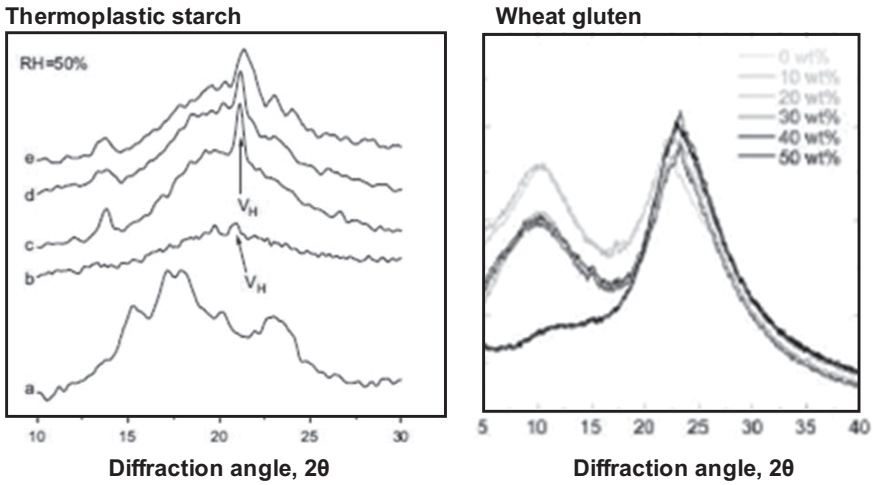

Figure 7.20 WAXS of (a) native starch and glycerol plasticized thermoplastic starch stored for 0, 30, 60 and 90 days respectively (b–e)[119] (Reprinted from *Polymer Degradation and Stability*, **90**(3), M. F. Huang, H. G. Yu and X. F. Ma, Ethanolamine as a novel plasticiser for thermoplastic starch, 501–507, Copyright (2005), with permission from Elsevier) and wheat gluten plasticized with different glycerol contents.[115] (Reprinted with permission from A. I. Athamneh, M. Griffin, M. Whaley and J. R. Barone, *Biomacromolecules*, 2008, **9**, 3181–3187. Copyright 2008 American Chemical Society.)

Table 7.6 Types of crystallinity in Starch.[68–69,93]

Crystallinity type	*Description*
A type (characteristic of maize)	Double helical structure characteristic of maize starch.[68] Denser and less hydrated than B type.[93]
B type (characteristic of potato)	Double helical structure.[69]
C type (characteristic of cassava)	Intermediate form between A and B.[93]
V type (complex with other molecules)	Amorphous or crystalline complex with other molecules (eg lipids in native starch, plasticiser or other polymer in TPS or TPS blends). Insoluble in water.[93] Single helical structure.[69] Can be either V_H (hydrated) or V_A (anhydrous) depending on moisture content.
E type (present in extruded starch)	Unstable form in TPS at low moisture. Rearranges to V type during conditioning.[93]

of urea and formamide produced an amorphous material, which was resistant to retrogradation.[68] Corn starch plasticized with ethanolamine has some type-V_H crystallinity induced during processing, but demonstrated no observable crystallinity after 30, 60 or 90 days at 50% relative humidity.[119] This is because ethanolamine forms stronger hydrogen bonds with starch than glycerol, restricting molecular rearrangements and the formation of new hydrogen bonding between starch molecules.[119] The same effect was seen using formamide as a plasticizer.[118] When glycerol is used as plasticizer, addition of a small amount of citric acid can strengthen the hydrogen bonding and restrict retrogradation.[102] This may be due to esterified citric acid groups bound to starch, inhibiting inter- and intra-molecular hydrogen bonding, while their free carboxyl groups increase solubility.[70]

XRD analysis during ageing of thermoplastic starch with high glycerol content (up to 60 wt%) showed that increased glycerol was helpful for forming single helix crystals (V-type complexes), but limited the formation of double helix B-type crystallinity.[69] V-type complexes may be useful when water resistance is a desired property as they are insoluble, even at high pressure and temperature.[93]

Storage conditions also affect the rate and type of retrogradation. Extruded corn meal (31 wt% moisture stored at 6 °C for 204 days) exhibited 31 % B and V_H-type crystallinity, whereas reducing the water content to 22 wt% lowered crystallinity to 3 %, mainly V_H-type. However, the T_g of the formulations was different; the former was stored above its T_g, while the latter was stored below its T_g.[106] As well as detecting crystallinity during ageing, WAXS is also used to investigate interactions between polymers and additives. Small molecules used as plasticizers may form crystals in the solid phase, giving rise to crystalline peaks of the pure plasticizer. If these peaks are absent in the thermoplastic it shows that the additive has dispersed throughout the polymer. For example, citric acid and glycerol were used in thermoplastic starch, where it was shown that the characteristic peaks of the plasticizers disappeared only if homogeneously distributed.[70]

Likewise, good compatibility was observed between soy protein isolate and acetamide used as plasticizer. The clear peaks observed for crystalline acetamide are not seen when mixed with soy protein isolate.[54] Starch blended with 30 wt% polystyrene and extruded to make loose fill packing foams formed new crystalline peaks not characteristic of either component.[121]

Alternatively, X ray scattering can demonstrate that cross-linking or reactive agents do not induce conformational changes. Comparison of WAXS plots of native starch and starch modified with sodium trimetaphosphate and sodium tripolyphosphate under alkaline conditions showed that no structural changes occurred other than cross-linking.[122]

X-ray scattering has also been used to investigate conformational changes in proteins. This is a different application than protein crystallography of highly purified protein crystals. Comparison between zein and thermoplastic zein suggested that alpha helical structures survived thermoplastic processing, but that inter-helical packing is disrupted.[103] Comparison between glycerol/SPI mixtures before and after compression moulding showed a smaller degree of crystallinity before processing, implying that heat and pressure induced rearrangement characteristic of strong intermolecular forces.[123] The same effect is seen compression moulded sheets of soy protein isolate and ethylene glycol.[92]

7.3.3.8 *Other Spectroscopic Techniques*

Other spectroscopic techniques are sometimes used to observe structural changes and polymer/plasticizer interactions. Vibrational circular dichroism spectroscopy has been used to investigate denaturing of protein films formed from bovine serum albumin.[124] Raman spectroscopy was used to investigate secondary structure changes in feather keratin extruded with sodium sulfite and revealed a transition from α-helices to β-sheets at sodium sulfite concentrations less than 4 wt%.[100] At higher sodium sulfite concentrations increased crystallinity was seen. Solid state NMR was used to investigate the interaction between dry starch and plasticizers, including glycerol and ethylene glycol, revealing a decrease in plasticizer mobility after heat treatment.[94] Although these are powerful techniques they are not as commonly used with thermoplastic starches and thermoplastic proteins and are beyond the scope of this chapter.

7.4 Conclusions

Thermoplastic agro-polymers are synthesized from starch and proteins. Both starch and protein experience a barrier to thermoplastic processing due to only a small difference between glass transition and degradation temperatures. For dry, unplasticized starch or protein, degradation occurs prior to the formation of a flowable melt. To overcome this, synthesis requires addition of plasticizers to reduce the T_g to temperatures which enable processing. For starch, the crystalline structure of starch granules also needs to be disrupted to allow processing and this is called gelatinization. Similarly, in proteins, formation of

thermoplastic melt disrupts higher order structures and this is called denaturing.

After processing, both starch and protein agro-polymers suffer the same drawback. Due to their hydophilicity, water is usually an effective plasticizer and is required for processing. Unfortunately, this hydrophilicity also causes the mechanical properties of products made from agro-polymers to depend on moisture content. Exposure to atmospheres of varying relative humidity leads to undesirable changes in properties. Furthermore, agro-polymers are often characterized by inferior mechanical properties compared to synthetic thermoplastics. These properties also depend on plasticizer content, although ductility is obtained at the expense of strength.

The most common techniques used for characterization of thermal properties and structure are TGA, DSC, DMA, FT-IR and XRD. Each of these techniques is used to elucidate specific aspects of agro-polymers.

TGA is used to assess thermal stability of agro-polymers. Starch and proteins degrade at temperatures around 200–250 °C which is not much higher than their glass transition temperatures. The T_g of agro-polymers in their native state and after thermoplastic processing is often determined by DSC and DMA. These techniques can also be used to determine the temperatures at which gelatinization, denaturing and crystallization occur. As with mechanical properties, thermal properties are dependent on moisture content and care needs to be taken to restrict or account for moisture loss by evaporation during thermal analysis.

FT-IR and XRD are used to assess the structural changes induced during thermoplastic processing and the interaction between plasticsers and polymer chains. For proteins the native secondary, tertiary and quaternary structures are destroyed by processing, but new secondary structure-like elements may be induced. Thermoplastic starch is semi-crystalline and tends to retrograde to higher crystalline content. XRD is extremely useful to determine the degree of crystallinity in starch.

The structure–property–processing relationship of agro-polymers is highly interdependent. A considerable research effort has been devoted to firstly obtain processible thermoplastics. Now, sustained efforts are required to overcome the water sensitivity and time-dependent properties of these materials.

References

1. A. Gandini, *Macromolecules*, 2008, **41**, 9491.
2. M. Flieger, M. Kantorova, A. Prell, T. Rezanka and J. Votruba, *Folia Microbiol.*, 2003, **48**, 27.
3. F. Chivrac, E. Pollet and L. Averous, *Mater. Sci. Eng., R*, 2009, **67**, 1.
4. L. Averous and P. J. Halley, *Biofuels Bioprod. Biorefin.*, 2009, **3**, 329.
5. L. Yu, K. Dean and L. Li, *Prog. Polym. Sci.*, 2006, **31**, 576.
6. X. L. Wang, K. K. Yang and Y. Z. Wang, *J. Macromol. Sci., Polym. Rev.*, 2003, **C43**, 385.
7. D. Le Corre, J. Bras and A. Dufresne, *Biomacromolecules*, **11**, 1139.
8. L. Averous, *J. Macromol. Sci., Polym. Rev.*, 2004, **C44**, 231.

9. A. Rouilly and L. Rigal, *J. Macromol. Sci., Polym. Rev.*, 2002, **C42**, 441.
10. C. J. R. Verbeek and L. E. van den Berg, *Recent Pat. Mater. Sci.*, 2009, **2**, 171.
11. C. J. R. Verbeek and L. E. van den Berg, *Macromol. Mater. Eng.*, 2010, **295**, 10.
12. R. F. T. Stepto, *Macromol. Symp.*, 2006, **245**, 571.
13. H. S. Liu, F. W. Xie, L. Yu, L. Chen and L. Li, *Prog. Polym. Sci.*, 2009, **34**, 1348.
14. R. A. de Graaf, A. P. Karman and L. Janssen, *Starch-Starke*, 2003, **55**, 80.
15. N. Follain, C. Joly, P. Dole and C. Bliard, *J. Appl. Polym. Sci.*, 2005, **97**, 1783.
16. I. Siro and D. Plackett, *Cellulose*, 2010, **17**, 459.
17. B. Cuq, N. Gontard and S. Guilbert, *Cereal Chem.*, 1998, **75**, 1.
18. R. H. Garrett and C. M. Grisham, *Biochemistry*, 2nd edn., Brooks/Cole-Thomson Learning, Pacific Grove, 1999.
19. *NZ Pat.*, NZ551531, 2009.
20. *US Pat.*, US5665152, 1997.
21. *WIPO Pat.*, WO2006017481A2, 2006.
22. *US Pat.*, US5710190, 1998.
23. *US Pat.*, US5523293, 1996.
24. *US Pat.*, US3615715, 1971.
25. *US Pat.*, US5882702, 1999.
26. K. A. Rosentrater and A. W. Otieno, *J. Polym. Environ.*, 2006, **14**, 335.
27. D. J. Gallant, B. Bouchet and P. M. Baldwin, *Carbohydr. Polym.*, 1997, **32**, 177.
28. L. Yu and G. Christie, *J. Mater. Sci.*, 2005, **40**, 111.
29. B. L. Deopura and I. Textile *Polyesters and Polyamides*, Woodhead Publishing in association with the Textile Institute; CRC Press, Cambridge, England and Boca Raton, FL, 2008.
30. J. Candlin, in *The Chemical Industry*, ed. A. Heaton, Chapman & Hall, London, 1994.
31. A. Heaton, *The Chemical Industry*, 2nd edn., Chapman & Hall, London, 1994.
32. W. D. Callister, *Materials Science and Engineering, An Introduction*, 6 edn., John Wiley & Sons, Inc., New York, 2003.
33. I. M. Ward and D. W. Hadley, *An Introduction to the Mechanical Properties of Solid Polymers*, 1st edn., Wiley, 1993.
34. B. Lagrain, B. Goderis, K. Brijs and J. A. Delcour, *Biomacromolecules*, 2010, **11**, 533.
35. H. C. Huang, T. C. Chang and J. Jane, *J. Am. Oil Chem. Soc.*, 1999, **76**, 1101.
36. O. Orliac, F. Silvestre, A. Rouilly and L. Rigal, *Ind. Eng. Chem. Res.*, 2003, **42**, 1674.
37. A. Rouilly, A. Mériaux, C. Geneau, F. Silvestre and L. Rigal, *Polym. Eng. Sci.*, 2006, **46**, 1635.

38. S. Lim and J. Jane, *J. Environ. Polym. Degrad.*, 1994, **2**, 111.
39. J. U. Otaigbe, H. Goel, T. Babcock and J. Jane, *J. Elastomers Plast.*, 1999, **31**, 56.
40. V. M. Hernandez-Izquierdo, D. S. Reid, T. H. McHugh, J. D. J. Berrios and J. M. Krochta, *J. Food Sci.*, 2008, **73**, E169.
41. D. J. Sessa, G. W. Selling, J. L. Willett and D. E. Palmquist, *Ind. Crops Prod.*, 2006, **23**, 15.
42. N. Leblanc, R. Saiah, E. Beucher, R. Gattin, M. Castandet and J.-M. Saiter, *Carbohydr. Polym.*, 2008, **73**, 548.
43. S. Sun, Y. Song and Q. Zheng, *Food Hydrocolloids*, 2007, **21**, 1005.
44. Q. Wu, H. Sakabe and S. Isobe, *Polymer*, 2003, **44**, 3901.
45. S. Sharma, J. N. Hodges and I. Luzinov, *J. Appl. Polym. Sci.*, 2008, **110**, 459.
46. M. Mastromatteo, S. Chillo, G. G. Buonocore, A. Massaro, A. Conte, A. Bevilacqua and M. A. D. Nobile, *J. Food Eng.*, 2009, **92**, 467.
47. X. Mo and X. Sun, *J. Polym. Environ.*, 2003, **11**, 15.
48. P. Tummala, W. J. Liu, L. T. Drzal, A. K. Mohanty and M. Misra, *Ind. Eng. Chem. Res.*, 2006, **45**, 7491.
49. Z. K. Zhong and S. X. Sun, *J. Appl. Polym. Sci.*, 2003, **88**, 407.
50. A. Taguet, M. A. Huneault and B. D. Favis, *Polymer*, 2009, **50**, 5733.
51. J. W. Zhang, L. Jiang and L. Y. Zhu, *Biomacromolecules*, 2006, **7**, 1551.
52. P. Mungara, T. Chang, J. Zhu and J. Jane, *J. Polym. Environ.*, 2002, **10**, 31.
53. P. Lodha and A. N. Netravali, *Ind. Crops Prod.*, 2005, **21**, 49.
54. D. Liu and L. Zhang, *Macromol. Mater. Eng.*, 2006, **291**, 820.
55. A. P. Mathew and A. Dufresne, *Biomacromolecules*, 2002, **3**, 1101.
56. V. M. Hernandez-Izquierdo and J. M. Krochta, *J. Food Sci.*, 2008, **73**, 30.
57. S. N. Swain, K. K. Rao and P. L. Nayak, *J. Appl. Polym. Sci.*, 2004, **93**, 2590.
58. J. Zhang, P. Mungara and J. Jane, *Polymer*, 2001, **42**, 2569.
59. M. Pommet, A. Redl, S. Guilbert and M.-H. Morel, *J. Cereal Sci.*, 2005, **42**, 81.
60. R. Mani and M. Bhattacharya, *Eur. Polym. J.*, 1998, **34**, 1467.
61. M. E. R. Ortiz, E. San Martin-Martinez and L. P. M. Padilla, *Starch-Starke*, 2008, **60**, 577.
62. D. Lourdin, L. Coignard, H. Bizot and P. Colonna, *Polymer*, 1997, **38**, 5401.
63. A. Hochstetter, R. A. Talja, H. J. Helén, L. Hyvönen and K. Jouppila, *LWT – Food Sci. Technol.*, 2006, **39**, 893.
64. Y. Zhang and J. Han, *J. Food Sci.*, 2008, **73**, E313.
65. L. Godbillot, P. Dole, C. Joly, B. Rogé and M. Mathlouthi, *Food Chem.*, 2006, **96**, 380.
66. A. Kumar and R. K. Gupta, *Fundamentals of Polymers*, 1st edn., McGraw-Hill International Editions, 1998.
67. *US Pat.*, US2238307, 1941.
68. R. Zullo and S. Iannace, *Carbohydr. Polym.*, 2009, **77**, 376.

69. R. Shi, Q. Y. Liu, T. Ding, Y. M. Han, L. Q. Zhang, D. F. Chen and W. Tian, *J. Appl. Polym. Sci.*, 2007, **103**, 574.
70. R. Shi, Z. Z. Zhang, Q. Y. Liu, Y. M. Han, L. Q. Zhang, D. F. Chen and W. Tian, *Carbohydr. Polym.*, 2007, **69**, 748.
71. D. S. Chaudhary, *J. Appl. Polym. Sci.*, 2010, **118**, 486.
72. E. M. Teixeira, A. L. Da Róz, A. J. F. Carvalho and A. A. S. Curvelo, *Carbohydr. Polym.*, 2007, **69**, 619.
73. L. Yu and G. Christie, *Carbohydr. Polym.*, 2001, **46**, 179.
74. A. L. Chaudhary, P. J. Torley, P. J. Halley, N. McCaffery and D. S. Chaudhary, *Carbohydr. Polym.*, 2009, **78**, 917.
75. C. M. Vaz, P. F. N. M. van Doeveren, G. Yilmaz, L. A. de Graaf, R. L. Reis and A. M. Cunha, *J. Appl. Polym. Sci.*, 2005, **97**, 604.
76. J. A. G. Areas, *Crit. Rev. Food Sci. Nutr.*, 1992, **32**, 365.
77. H. Madeka and J. L. Kokini, *J. Am. Oil Chem. Soc.*, 1996, **73**, 433.
78. Y. Leng, *Materials Characterization: Introduction to Microscopic and Spectroscopic Methods*, J. Wiley, Singapore and Hoboken, NJ, 2008.
79. J. D. Menczel and R. B. Prime, *Thermal Analysis of Polymers: Fundamentals and Applications*, John Wiley, Hoboken, NJ, 2009.
80. C. Bengoechea, A. Arrachid, A. Guerrero, S. E. Hill and J. R. Mitchell, *J. Cereal Sci.*, 2007, **45**, 275.
81. C. H. Tang, S. M. Choi and C. Y. Ma, *Int. J. Biol. Macromol.*, 2007, **40**, 96.
82. F. W. Xie, W. C. Liu, P. Liu, J. Wang, P. J. Halley and L. Yu, *Starch-Starke*, 2010, **62**, 350.
83. K. P. Menard, *Dynamic Mechanical Analysis: A Practical Introduction*, 2nd edn., CRC Press, Boca Raton, FL, 2008.
84. M. I. Beck, I. Tomka and E. Waysek, *Int. J. Pharm.*, 1996, **141**, 137.
85. W. Thakhiew, S. Devahastin and S. Soponronnarit, *J. Food Eng.*, 2010, **99**, 2164.
86. P. Chen, H. Tian, L. Zhang and P. R. Chang, *Ind. Eng. Chem. Res.*, 2008, **47**, 9389.
87. X. Q. Mo and X. Z. Sun, *J. Am. Oil Chem. Soc.*, 2001, **78**, 867.
88. A. Jerez, P. Partal, I. Martinez, C. Gallegos and A. Guerrero, *Biochem. Eng. J.*, 2005, **26**, 131.
89. G. K. Moates, T. R. Noel, R. Parker and S. G. Ring, *Carbohydr. Polym.*, 2001, **44**, 247.
90. I. S. Arvanitoyannis and I. Kassaveti, in *Biodegradable Polymer Blends and Composites from Renewable Resources*, ed. L. Yu, Wiley, Hoboken, NJ, 2009, pp. xi, 487.
91. S. Guilbert and B. Cuq, in *Handbook of Biodegradable Polymers*, eds. C. Bastioli and L. Rapra Technology, Rapra Technology, Shrewsbury, 2005, pp. xviii, 534.
92. Q. Wu and L. Zhang, *Ind. Eng. Chem. Res.*, 2001, **40**, 1879.
93. A. J. F. Carvalho, in *Monomers, Polymers and Composites from Renewable Resources*, eds. B. Mohamed Naceur, G. Alessandro, Elsevier, Amsterdam, 2008, pp. 321.

94. A. L. M. Smits, P. H. Kruiskamp, J. J. G. van Soest and J. F. G. Vliegenthart, *Carbohydr. Polym.*, 2003, **53**, 409.
95. C. K. Larive, S. M. Lunte, M. Zhong, M. D. Perkins, G. S. Wilson, G. Gokulrangan, T. Williams, F. Afroz, C. Schoneich, T. S. Derrick, C. R. Middaugh and S. Bogdanowich-Knipp, *Anal. Chem.*, 1999, **71**, 389R.
96. L. Zhang and M. Zeng, in *Monomers, Polymers and Composites from Renewable Resources*, eds. B. Mohamed Naceur and G. Alessandro, Elsevier, Amsterdam, 2008, pp. 479.
97. L. A. De Graaf, *J. Biotechnol.*, 2000, **79**, 299.
98. N. Kitabatake, M. Tahara and E. Doi, *Agric. Biol. Chem.*, 1989, **53**, 12012.
99. W. J. Liu, A. K. Mohanty, P. Askeland, L. T. Drzal and M. Misra, *J. Polym. Environ.*, 2008, **16**, 177.
100. J. R. Barone, W. F. Schmidt and N. T. Gregoire, *J. Appl. Polym. Sci.*, 2006, **100**, 1432.
101. Y. D. Li, J. B. Zeng, W. D. Li, K. K. Yang, X. L. Wang and Y. Z. Wang, *Ind. Eng. Chem. Res.*, 2009, **48**, 4817.
102. J. G. Yu, N. Wang and X. F. Ma, *Starch-Starke*, 2005, **57**, 494.
103. M. Oliviero, E. D. Maio and S. Iannace, *J. Appl. Polym. Sci.*, 2010, **115**, 277.
104. S. Brauer, F. Meister, R. P. Gottlober and A. Nechwatal, *Macromol. Mater. Eng.*, 2007, **292**, 176.
105. X. X. Liu, L. Yu, H. S. Liu, L. Chen and L. Li, *Polym. Degrad. Stabil.*, 2008, **93**, 260.
106. J. L. Brent, S. J. Mulvaney, C. Cohen and J. A. Bartsch, *J. Cereal Sci.*, 1997, **26**, 313.
107. A. Rouilly, O. Orliac, F. Silvestre and L. Rigal, *Polymer*, 2001, **42**, 10111.
108. Z. K. Zhong and X. S. Sun, *J. Appl. Polym. Sci.*, 2001, **81**, 166.
109. D. J. Muffett and H. E. Snyder, *J. Agric. Food Chem.*, 1980, **28**, 13035.
110. Z. Zhong and X. S. Sun, *J. Food Eng.*, 2005, **69**, 453.
111. J. L. Koenig, *Spectroscopy of Polymers*, 2nd edn. Elsevier, New York, 1999.
112. J. Kong and S. Yu, *Acta Biochim. Biophys. Sin.*, 2007, **39**, 549.
113. L. A. Forato, R. Bernardes and L. A. Colnago, *Anal. Biochem.*, 1998, **259**, 136.
114. K. Tian, D. Porter, J. Yao, Z. Shao and X. Chen, *Polymer*, 2010, **51**, 2410.
115. A. I. Athamneh, M. Griffin, M. Whaley and J. R. Barone, *Biomacromolecules*, 2008, **9**, 3181.
116. M. Lacroix, T. C. Le, B. Ouattara, H. Yu, M. Letendre, S. F. Sabato, M. A. Mateescu and G. Patterson, *Radiat. Phys. Chem*, 2002, **63**, 827.
117. P. Guerrero, A. Retegi, N. Gabilondo and K. de la Caba, *J. Food Eng.*, 2010, **100**, 145.
118. X. F. Ma and J. G. Yu, *J. Appl. Polym. Sci.*, 2004, **93**, 1769.

119. M. F. Huang, H. G. Yu and X. F. Ma, *Polym. Degrad. Stabil.*, 2005, **90**, 501.
120. J. H. Yang, J. G. Yu and X. F. Ma, *Carbohydr. Polym.*, 2006, **63**, 218.
121. H. A. Pushpadass, G. S. Babu, R. W. Weber and M. A. Hanna, *Packag. Technol. Sci.*, 2008, **21**, 171.
122. W.-J. Lee, Y.-N. Youn, Y.-H. Yun and S.-D. Yoon, *J. Polym. Environ.*, 2007, **15**, 35.
123. Q. Wu and L. Zhang, *J. Appl. Polym. Sci.*, 2001, **82**, 3373.
124. G. Shanmugam and P. L. Polavarapu, *Biophys. Chem.*, 2004, **111**, 73.

3

Thermal Transitions and Structural Relaxations in Protein-based Thermoplastics

An invited review paper

Published in

Macromolecular Materials and Engineering

by

JAMES M. BIER[1], C.J.R. VERBEEK AND M.C. LAY

[1]As first author, I prepared the initial draft manuscript, which was refined and edited in consultation with my supervisors, who have been credited as co-authors.

Macromolecular Journals

Macromolecular Materials and Engineering

Thermal Transitions and Structural Relaxations in Protein-Based Thermoplastics

James M. Bier,* Casparus J. R. Verbeek, Mark C. Lay

Protein-based thermoplastics resemble semi-crystalline polymers, suggesting the occurrence of a glass transition (T_g) and melting point. Denaturing a protein's native structure is often called melting, but this does not necessarily imply complete unfolding into a fully amorphous structure as true melting would. Protein secondary structures, such as α-helices and β-sheets, can remain after denaturing, stay intact above the T_g and do not necessarily melt at typical processing temperatures. This implies that consolidation of aggregated protein particles into a macroscopically monolithic material depends on inter-chain interactions in the amorphous phase and on newly formed secondary structures. Structural relaxations and transition temperatures of the amorphous phase are influenced and constrained by the presence of these secondary structures as well as heavily influenced by plasticizers.

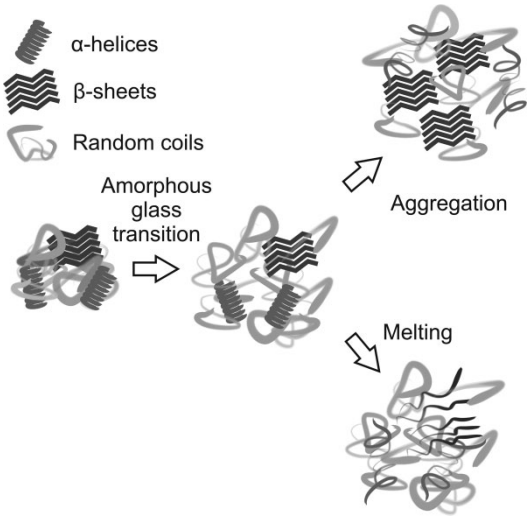

1. Introduction

Proteins have a long history of use as polymeric materials, from blood-based woodglue to caseinate buttons. Many of these early examples were thermosetting resins and involved irreversible crosslinking after processing into the desired shape. In recent years, attention has shifted to thermoplastic protein-based materials that can be extruded and injection moulded. Thermoplastic materials have been manufactured successfully from a variety of proteins from both plant and animal origin.[1] Examples include cast films,[2,3] injection moulded parts,[4–6] compression moulded sheets,[7,8] extruded sheets or films[9–11] and even blown films if adequate plasticizaton is provided.[2,12]

J. M. Bier, Dr. C. J. Verbeek, Dr. M. C. Lay
School of Engineering, University of Waikato, Knighton Road
Private Bag 3105, Hamilton, 3240, New Zealand
E-mail: jmb101@waikato.ac.nz

Although protein-based thermoplastics may be more efficient to produce than microbial-based polymers requiring energy intensive fermentation,[13,14] commercial uptake of protein-based thermoplastics has been slower than other bio-based polymers such as thermoplastic starch (TPS) and polylactic acid (PLA).[15] PLA is a chemically synthesized homopolymer with a very regular structure. Likewise, although starch has amylose and amylopectin sub-units with different degrees of crosslinking, the monomer is glucose in both. In contrast, proteins are heteropolymers of different amino acids, each with different side groups. Overall hydrophilicity, localized hydrophobic regions and covalent cross-linking contribute to making processing more difficult than with conventional plastics, and can lead to inferior properties.

Extrusion of protein-based thermoplastics requires protein chains to denature, disassociate, unravel, and align,[1] which requires the chains to be mobile. This enables flowing in the presence of heat and shear, filling the desired shape, and forming new molecular interactions

Macromol. Mater. Eng. **2013,** DOI: 10.1002/mame.201300248

on cooling. This mobility is achieved by heating and by adding plasticizers. Without plasticizers, the temperatures required for chain mobility in proteins are typically around their decomposition temperature.[1] Processing temperature also depends on protein secondary structure, which consists of α-helices, β-sheets, and amorphous regions (Figure 1) as well as the interactions between protein chains.

Although biopolymers such as proteins have been described as amorphous structures plasticized by water,[16] aspects of protein structure (ordered regions, such as α-helices and β-sheets) and thermal behavior (endothermic events) may resemble semi-crystalline materials. As a semi-crystalline thermoplastic is heated it undergoes a series of transitions. The first being the glass transition at which the amorphous regions become mobile, followed by the melting temperature, where crystalline regions melt. A third is the degradation temperature where polymer chains thermally decompose. Analysis these transitions and structures provides useful information on how to process proteins as thermoplastics.

DSC studies of plasticized proteins usually present an endothermic denaturing peak, similar in appearance to the melting of crystalline regions in semi-crystalline polymers. The temperatures at which these occur have been shown to be important in determining thermoplastic processing temperatures. For example, in whey plasticized with water and glycerol, an endothermic peak at about 146 °C was closely related to the melt temperatures of 143–150 °C necessary for extrusion into thin sheets.[11] X-ray scattering experiments of proteins showed regular spacings corresponding to β-sheet regions,[17] along with both intra-helical distances and inter-helix packing.[2,12] The size of crystalline regions in proteins may be very small (approximately 10 nm) compared to crystal aggregates in synthetic polymers (up to 100 nm for a single crystallite and diameters of up to a several mm for spherulites),[17,18] but have been shown to affect processing conditions. For example, zein protein with a higher proportion of α-helices to β-sheets produced better blown films than zein with lower α-helical content.[12]

The behavior of molecular transitions in proteins does differ for different proteins.[19] The purpose of this review is to discuss the similarities or differences between thermal behavior of dry native proteins, proteins in solution and protein-based thermoplastic materials. This is as important as successfully shaping useful products by extrusion and injection moulding requires processing above the softening temperature, or well above T_g, but also well below the degradation temperature. The structure–property relationship leading to observed properties is also discussed by evaluating expected thermal transitions and

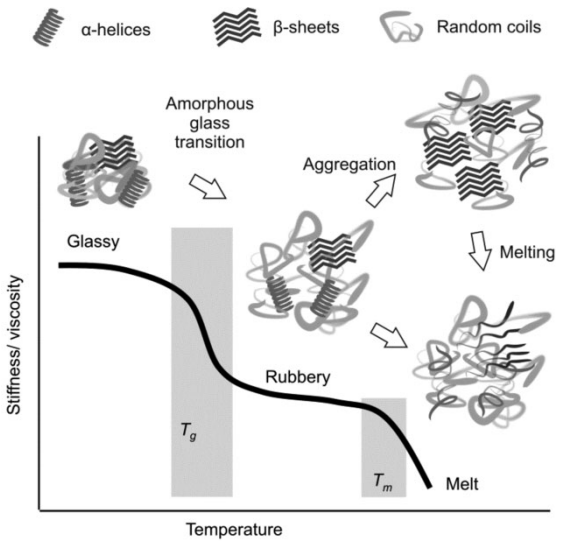

Figure 1. Regions of viscoelastic behavior of a typical semi-crystalline polymer and potential corresponding protein structure changes.

Dr. Verbeek is a Chemical Engineer, currently with the School of Engineering at the University of Waikato. He has more than 15 years experience in waste and by-product valorization with an emphasis on renewable materials and biological products. Since his tertiary studies, Johan's wealth of knowledge in the engineering field of sustainable products has skyrocketed, which has led to a number of innovative developments in the engineering industry. His research area covers a wide range of topics, such as polymer extrusion, rheology, material properties, protein analysis, chemical modification of proteins as well as protein composites and nano-composites.

James (Jim) Bier is a Research and Development Scientist at Aduro Biopolymers LP, a spin out from the University of Waikato. He holds a Bachelors (B.Sc.) degree in biochemistry from the University of Canterbury, and a Masters (M.Sc.) degree in Materials and Processing from the University of Waikato for which he investigated environmental impacts of producing Novatein™. Novatein is a protein based thermoplastic produced from bloodmeal, a by-product of the meat industry. His doctoral thesis examining structural changes and chain mobility during processing of this material is currently under examination.

Dr Mark Lay has a Ph.D. in Materials and Process Engineering and works in the School of Engineering and the Cooperative Education Unit at the University of Waikato. His research areas include bio-plastics, chromatography, protein recovery, pyrolysis and work integrated learning.

their approximate temperature ranges with a focus on proteins relevant to plastic production.

2. Structure and Mobility

2.1. Native Conformation of Proteins

From a biochemistry perspective, protein structure is defined at four levels. The primary structure is the sequence of amino acids making up the protein chain. The secondary structure is chain segments forming regular structures such as α-helices or β-pleated sheets. The tertiary structure is folding of the chain into a complex three-dimensional shape. The quaternary structure is multiple chains interacting to form larger structures. In solution, under biological conditions, proteins will typically self-assemble into a folded state with these levels of structure, stabilized by solvent and protein interactions.[19] Where specific protein–protein interactions are stronger than protein/solvent interaction, contraction can occur to increase protein–protein interactions, leading to a reduction in entropy.[19] This compares with the thermodynamic driving force of crystallization of polymers in general. Although the high degree of order in polymer crystals leads to a reduction in entropy compared with a randomly entangled melt, it is also associated with a large reduction in enthalpy.[20] Crystallization is thermodynamically favored if the latent heat, or enthalpy change, is larger than the reduction in entropy at T_m.[20] The folded native conformation of proteins is stabilized by a number of interactions, of varying bond strength, including hydrogen bonding (4–29 kJ mol^{-1}), electrostatic forces (4–25 kJ mol^{-1}), hydrophobic interactions (8–13 kJ mol^{-1}) and solvation effects.[21,22]

Protein native conformation, however, is not a fixed, rigid structure. As well as relaxation processes, where the system moves towards equilibrium from a non-equilibrium state, proteins experience equilibrium fluctuations – even in a stable state they change between multiple conformational substrates.[23] Although the "crystal" structures of thousands of proteins have been solved by macromolecular X-ray crystallography, such structures are really time averaged positions of atoms in molecules that undergo rapid fluctuations in solution.[22,24] Proteins move in very dynamic ways[23] and are flexible over a wide range of time scales and distances.[25] From a plastics perspective, this mobility more resembles a polymer well above its T_g. Denaturing of the native conformation is therefore not necessarily a transition from immobile to mobile, e.g., melting of a crystal, as proteins can also form insoluble stable aggregates upon denaturing.

2.2. Denaturing

Denaturing is the process of a protein transforming to a non-native (and for enzymes, inactive) conformation. This transformation may be induced by heating or chemical means, however there may still be residual structure in the unfolded state.[21] Depending on the conditions, denaturing can be reversible or irreversible.[26]

Although the words denaturing and unfolding were historically used interchangeably, it has been argued that it is useful to divide denatured states into two categories: "unfolded" referring only to a specific subset of denatured conformations in which there is little or no residual structure and which are open and exposed to solvent. This is in contrast to "compact" denatured conformations which may still be somewhat folded, but no longer in the native structure.[19]

When studied by DSC, the thermally induced denaturing temperature (T_d) is an endothermic peak.[27] In solution, this typically occurs below 100 °C.[27] The midpoint in the denaturing endothermic peak in solution is often called the protein's melting temperature (T_m), drawing an analogy with melting in solids.[24] Although also an endothermic event, care should be taken not to equate this with the melting temperature of crystals in synthetic polymers. As discussed above, the native structure is not typically a single rigid fixed conformation, but a time averaged approximation[22] and denatured states can still be somewhat folded. In contrast, melting in polymers is typically understood to involve a change from aligned chains to a mobile amorphous state. Although reversible denaturation to a fully unfolded state resembles this, non-reversible denaturation, if followed by aggregation, is a transformation from a flexible state to a more rigid state.

Irreversible thermal aggregation is often characterized as a two state model: first a reversible unfolding step, then the irreversible aggregation. It has been argued that the aggregation does not require fully unfolded proteins, merely unfolding of some regions to allow intermolecular interactions to form.[28] Thermally resolved FT-IR experiments of hemoglobin in solution suggested aggregation was a competing process to refolding, not a driving force of unfolding and hence aggregates may still contain a number of native structures.[28] Aggregation processes are important for protein-based thermoplastics, as new interactions between multiple chains are required to impart mechanical strength after consolidation. However, excessive aggregation too early in the melt can cause difficulties with processing.[1] There may also be ramifications for re-use, such as increased viscosity, if increased aggregation occurs after each heating cycle.

Endothermic events in dry or partially hydrated proteins have also been identified as protein denaturing.

In such cases, T_d depends on moisture content and increases as moisture content decreases.[27] Multiple T_ds may be observed if more than one protein is present. DSC of soy proteins exhibited two endothermic peaks, identified as denaturing of the 7s globulin and 11s globulin subunits.[27,29] The presence of two peaks does not always mean multiple proteins are present. Because proteins are complex heteropolymers with a wide variety of interactions, different parts of a single chain may respond differently and contribute to multiple thermal events. For example, DSC studies of thermal denaturation of BSA, both in solution and in powdered form with different moisture contents showed two endothermic events.[30,31] In solution, denaturation of BSA seemed to be irreversible irrespective of concentration of SDS, NaCl or pH, although both SDS and NaCl did have stabilizing effects.[30]

Additives such as urea are known to have de-stabilizing effects inducing denaturing. Increasing urea concentration decreased the size of the endothermic peaks observed for soy globulins, demonstrating that urea also denatured the subunits.[29] As with thermal denaturing, it was once assumed that the chemically denatured structure was an unfolded, random coil conformation, but some residual local structure persists even at high denaturant concentrations.[19]

The denaturing behaviors of both proteins in solution and of dry (or plasticized) proteins are relevant to processing protein-based thermoplastics. Formation of a consolidated plastic article requires new intermolecular interactions to be formed at the expense of existing intramolecular interactions or protein/solvent interactions. This would imply that a consolidated plastic will no longer contain proteins in their native state and that some denaturation is necessary.[32] Studies of denaturing in solution demonstrated that some order remained after denaturing. Rather than unfolding, it could be better thought of as partial re-folding or re-organization. The implication of this for protein-based thermoplastics is that secondary structure elements can remain above the T_d, and their presence may influence thermal behavior and rheological properties.

Protein-based thermoplastics should be thought of as semi-crystalline materials, and thermal transitions of proteins should be interpreted in this light. It is well known that for typical semi-crystalline polymers, amorphous regions undergo a T_g and that at some temperature above this, crystalline regions can be expected to melt. Although the term melting is sometimes applied to protein denaturing, this is not the same as melting of tightly packed crystal structures in other thermoplastics. In some cases, it is even the precursor to the formation of more tightly packed ordered structures.

3. The Amorphous Phase

Whereas both denaturing and melting involve latent heat, or sudden changes in enthalpy, transition from a glassy to rubbery state occurs without an increase in enthalpy. This transition is therefore usually described as a second order thermodynamic transition, although it shows a dependence on heating/cooling rate that should not be the case for a true second order thermodynamic transition.[20] Numerous properties change dramatically on heating or cooling through a narrow temperature range, or glass transition region, including heat capacity, coefficient of thermal expansion, mechanical damping, dielectric loss, stiffness, general appearance, and fracture mechanisms.[33] The glass transition is therefore regarded as the most significant phenomenon exhibited by a polymer.[33] The changes in properties and appearance are typically completely reversible and typically described as a function of molecular motions rather than change in polymer structure.[18]

As discussed above, proteins in solution at biological temperatures are highly mobile, but like any other polymer, this mobility slows as temperature is decreased, or with sufficient reduction in solvent or plasticizer. Proteins therefore also exhibit a T_g, below which some shorter range motions still occur, but larger scale cooperative motion is restricted. These motions are called relaxation processes as they can be studied for proteins, as with other polymers, through experimental techniques which involve applying a stress, force or field of some kind (mechanical, electric, magnetic), then measuring the response as the system relaxes to equilibrium due to molecules rearranging to dissipate the stress.[34] As molecular motion is a function of temperature, it follows that that these relaxations can be studied experimentally by either varying frequency at constant temperature, or varying temperature at constant frequency and in some cases, time and temperature can be mathematically superimposed.[35] One of the assumptions for this mathematical superposition is, however, that there is a single, simple relaxation. In proteins, the complex primary structure, with numerous side chains and interactions present a variety of different possible motions with overlapping time scales, and this assumption is not valid.

The terms transition and relaxation often seem to be used somewhat interchangeably, but more formally, transition temperatures are the temperatures at which macroscopic properties change on heating or cooling, and these are described in terms of specific molecular motions, or relaxations, occurring on the observational time scale. While often described in such kinetic terms, below T_g the motions of the α-relaxation process slow down sufficiently that when observed it appears motion is

Macromolecular Journals
Macromol. Mater. Eng. **2013,** DOI: 10.1002/mame.201300248

restricted, a purely kinetic model is insufficient to fully explain the glass transition, and attempts have been made to describe it as a thermodynamic transition.[36,37] Although widely described as a second order transition, there is still discussion as to the appropriateness of this as internal thermodynamic equilibriums do not exist on both sides of the T_g.[20] Early thermodynamic treatments successfully predicted many aspects of the behavior of plasticized polymers, co-polymers and the dependence of T_g on chain length,[18,36] but excluded any effect of intermolecular interactions between chains.[18]

Given that proteins contain large numbers of intermolecular interactions with a variety of strengths, any theoretical treatment of their T_g must take these interactions into account. Whereas many synthetic polymers are homopolymers with a single repeating unit, proteins are heteropolymers with a wide variety of side groups capable of interactions of different strengths, and almost every conceivable factor that affects T_g in some way is present in a protein-based thermoplastic (Table 1).

Some methods for predicting T_g of polymers have been developed that are also valid for proteins. Prediction of protein T_g from amino acid composition using an additive group contribution method showed good agreement with experimental data (DSC) extrapolated to zero plasticizer content for a number of food proteins.[39] The approach worked, even though the underlying assumptions did not consider higher structural levels of proteins (secondary, tertiary, and quaternary structures) or differences between native and denatured protein states. This suggests that the biochemical concept of a native conformation with defined tertiary and quaternary structure may have limited value in understanding transitions in protein-based thermoplastics, although side chain interactions are still important in their effect on T_g. The authors concluded that the T_g, denaturing and melting temperatures of globular proteins were in a narrow range at very low plasticization levels, but diverged as plasticizer content, such as water, increased.[39] This is consistent with experimental observations from DSC of sunflower proteins, in which T_d dropped from 189 °C with no moisture to 120 °C with 30 wt% water whereas T_g was 180.8 °C with no water and dropped to 5.3 °C with 26.12 wt% water.[40] Obviously, drastic conformational rearrangement requires large-scale molecular motions, implying that denaturing will only occur around or above the T_g. The implication for thermoplastic processing is that the separation of these temperatures means there are three different thermal events that may be relevant for processing (T_g, T_m, and T_d).

Bulk protein sources used for producing thermoplastics are typically dried powders before adding plasticizer. The glass transition of dried proteins is therefore discussed in the next section, before discussing the effect of moisture and other plasticizers.

3.1. Glass Transition Temperatures of Dry Proteins

Glass transitions and relaxation behavior of dried, or semi dried, proteins have been studied from both food and

Table 1. General factors influencing glass transition in polymers and their means of occurrence in proteins.[22,38]

Atttribute	Means of occurrence in protein
Factors increasing glass transition temperature	
Bulky side groups	Aromatic residues (phenylalanine, tyrosine, tryptophan) Other large residues (leucine, isoleucine, methionine, glutamine, lysine, arginine, histidine)
Stiffening groups	Proline residues, partial double bond character in C′–N bond in main polypeptide chain
Chain symmetry	Less common in proteins
Polar groups	Hydrogen bonding sites on main chain (C=O and N—H bonds), Polar residues (lysine, histidine, arginine, aspartic acid, threonine, serine, glutamic acid, tyrosine)
Cross-linking	Covalent disulfide crosslinkages (cysteine residues), Salt bridges between acidic residues (aspartic acid, glutamic acid) and basic residues (lysine, histidine, arginine)
Factors decreasing glass transition temperature	
Additives like plasticizers	Water or other plasticizers
Flexible main groups	Φ-bonds (N—C_α) and Ψ-bonds (C′—C_α), although there are steric limitations on which angles are allowed
Dissymetry	Many primary structure sequences
Non polar groups	Hydrophobic residues (proline, glycine phenylalanine, alanine, valine, leucine, isoleucine, methionine)

pharmaceutical perspectives. For example, in milk powders if the protein is above its T_g, there can be increased adhesion to equipment causing fouling.[41] From a pharmaceutical perspective, many proteins are often stored in a lyophilized (freeze dried) form for long-term stability, with a higher T_g than when hydrated.[42] Knowing the T_g of new pharmaceutical formulations is useful as storage below T_g ensures longer shelf life.[43,44] The T_g of dry, unplasticized proteins varies based on amino acid composition, but is typically in the range of 120–250 °C (Table 2).[45]

Until recently, powder materials were not able to be studied by mechanical relaxation techniques such as DMA, but the advent of material pockets now allows such analysis. Proteins including hen-egg white lysozyme, bovine pancreatic ribonuclease A, ovalbumin, and bovine serum albumin have been studied in such a pocket as lyophilized powders,[44] whilst frozen solutions of human serum albumin, porcine heparin, influenza antigen and neat human plasma have also been investigated to determine critical temperatures relevant during the freeze drying process itself.[46]

In calorimetric techniques, it can be difficult to distinguish T_g (reversible) and T_d (potentially irreversible) if they begin around the same temperature. At lower moisture contents, it is easier to identify T_g in proteins that have already lost some of their tertiary order.[31] Alternatively, modulated DSC techniques, using oscillating heating rates, can resolve overlapping thermal events in protein isolates.[51] Modulated DSC and simulations of human growth hormone unfolding suggested that dried proteins are thermodynamically unstable, even when formulated with excipients, such as disaccharides, and that kinetic limitations, such as low mobility, are what prevent their spontaneous unfolding.[52] This is again consistent with denaturing being constrained below T_g.

Table 2. Glass transition temperature of some dry protein sources.

Protein	T_g [°C]	Technique
Agricultural bulk protein sources		
Bloodmeal (90–95% denatured protein)[47]	220	DMA
Fish myofibrillar proteins[48]	220–250	DMA
Wheat gluten[49]	180	DSC
Sunflower protein isolate[40]	181	DSC
Soy protein isolate[50]	67 and 133	DSC
Purified proteins		
Lysozyme[44]	200	DSC
	212	DMA
Ovalbumin[44]	208	DSC
	214	DMA
Bovine serum albumin[44]	195	DSC
	216	DMA

3.2. Hydration Effects and Plasticization

Due to a protein's hydrophilic nature, its T_g is very moisture sensitive and typically drops around 10 °C for every 1% added water[45] (Figure 2). The implication is that with sufficient water, the T_g is lowered enough to create a processing window in which, on heating, the protein will soften before excessive degradation occurs, and be can be shaped using techniques such as extrusion and injection moulding.[1]

Some proteins can be plasticized solely with water, however, in practice many have additional interactions that must be overcome to allow thermoplastic processing. Reducing agents, such as sodium sulfite will break up cysteine/cysteine disulfide linkages; surfactants, such as sodium dodecyl sulfate will disrupt hydrophobic interactions, and protein denaturants, such as urea will assist in unfolding native structures.[1]

Although water is a very efficient plasticizer for proteins, plasticizers such as glycerol, sorbitol, and di, tri, or mono ethylene glycol are typically used in conjunction with or instead of water for thermoplastic applications.[1,5,56] Protein-based thermoplastics produced with water as the primary plasticizer become brittle as water desorbs over time. As the moisture content decreases, so does the plasticization level, leading to raised T_g. Hydrophobic interactions also influence protein processing and properties, and amphiphilic molecules such as octanoic or palmitic acid have also been used as plasticizers.[53,57] Appropriate plasticizers have low boiling points, low volatility and are

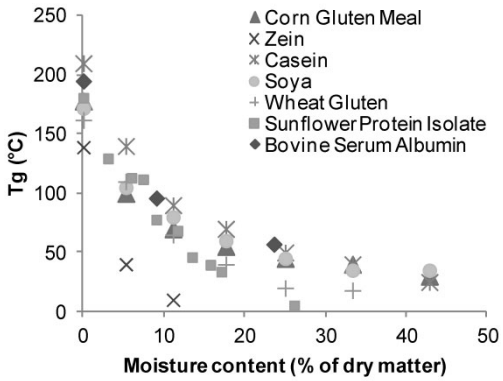

Figure 2. Change in glass transition with moisture content for a variety of proteins. Corn Gluten Meal (DSC),[53] Zein (DSC),[54] Casein, Soya, and Wheat Gluten (DMA, PTA, and DSC),[55] Sunflower protein isolate (DSC),[40] BSA (DSC).[31,44]

Macromolecular Journals
Macromol. Mater. Eng. **2013,** DOI: 10.1002/mame.201300248

compatible with the specific protein in question.[1,56] Success in plasticizing one protein type does not ensure a plasticizer is necessarily appropriate for all proteins due to the differences in primary structure (amino acid sequences) possible.[1]

Free volume theory is typically used to describe the mechanism in which plasticizers affect T_g and molecular mobility.[56,58] One way to increase free volume is to increase the concentration of chain ends in the polymer by decreasing its molecular mass. Chain ends are less constrained than the same chemical groups within the chain, so if there are more chain ends in the same amount of sample, there will be higher free volume at the same temperature.[33] Similarly, flexible side chains increase free volume at fixed points along the main chain. This is known as internal plasticization, but is not a common method of modifying T_g and processibility in proteins. Substitution of linear groups with hydrophobic ends by nucleophilic addition successfully reduced T_g of ovalbumin, but external plasticization was still found to be more practical in producing materials flexible at room temperature.[59] Similarly, processibility was improved after reacting certain proteins with aldehydes, but external plasticization was still required.[60] With external plasticizers, free volume increases in a manner proportional to the amount of plasticizer added, at any location along the polymer chain, increasing chain mobility and decreasing T_g. Plasticizers interfere with the three dimensional arrangement of a polymer, reducing opportunity for hydrogen bonding between protein chains and the energy required for molecular motions.[56]

The T_g of biopolymers as a function of plasticizer content can be calculated from the Couchman–Karasz relationship,[49]

$$\ln\left(\frac{T_g}{T_{g,pl}}\right) = \frac{w_p \ln\left(T_{g,up}/T_{g,pl}\right)}{w_{gly}\left(T_{g,up}/T_{g,pl}\right) + w_{up}} \quad (1)$$

where, T_g is the plasticized glass transition temperature, $T_{g,pl}$ is the glass transition temperature of the plasticizer (for example glycerol at 180 K), $T_{g,up}$ is the glass transition temperature of the unplasticized protein, and w_{pl} and w_{up} are respectively the mass fractions of plasticizer and protein.[49] This relationship predicted glycerol contents where T_g should be room temperature for glycerol plasticization of egg albumin, wheat gluten, and corn zein, which corresponded with critical glycerol contents where conformational changes were seen for these proteins.[49]

The Couchman–Karasz relationship holds for water plasticization of proteins as well, with the T_g for dry gluten, casein and soy proteins predicted using DSC results at different moisture contents showing good agreement with experimental data.[55]

3.3. Molecular Mobility in Protein-Based Thermoplastics

Thermal analysis is a useful technique for determining suitable operating temperatures for processing protein-based thermoplastics, along with effects from different environmental conditions, such as relative humidity (RH).[61] Not only are the material's final properties important, but thermal transitions in the material prior to processing are important as well, as these will have a direct influence on the processing window. As with dry proteins, the use of material pockets allowed DMA analysis of protein plastics prior to extrusion and consolidation,[47] or powders can be mounted directly in a DSC.

The vast array of factors affecting the T_g of a protein plastic, from the structural factors listed in Table 1, to different plasticizer choices, moisture contents, additional additives and processing histories limits the value of direct comparisons between T_g of materials produced in different studies. A common difficulty encountered when testing protein-based thermoplastics, especially where water is used as the primary plasticizer, is volatilization of plasticizer during testing. Some argue that such behavior means that at elevated temperatures the sample being tested is no longer the same material.[62] To combat this, some protein-based thermoplastics have been coated with silicone oil to prevent water loss during DMA scans.[55] Alternatively, sealed DSC pans are available which contain water when scanning water plasticized materials.[40,63,64] Kinetic studies have also shown that evaporation of water alone is not enough to explain the rate at which conformational changes occur when heating soy protein sheets.[65]

3.3.1. Blends and Multiple T_gs

Polymer blends that are fully miscible show a single T_g which is intermediate of the T_gs of individual components. Completely immiscible blends show T_gs corresponding to discrete phases of each component. Shifting of distinct T_gs closer together is indicative of partial miscibility.[63] One application of this is to investigate the effect of different plasticizers or miscibility agents on blends of protein-based thermoplastics with other polymers. For example, soy protein plastics were more miscible with a polyester amide when plasticized with sorbitol than with glycerol.[6] However, many bulk protein sources used for production of protein-based thermoplastics are themselves blends of different proteins, and as with T_d, showed multiple T_gs. Separate T_gs identified as belonging to the glutenin and gliadin subunits have been seen using modulated DSC of mechanically processed gluten, plasticized with glycerol.[66] Similarly, soy protein isolates contain both 7s and 11s globulins and dual T_gs have been identified in

plastics produced from soy protein isolate with both glycerol,[50,67] and urea.[49] Some researchers have argued the dual transition indicated plasticizer rich and protein rich phases, although the second transition was still present with no plasticizer.[50] This does not exclude the option that on adding plasticizer, one of the phases had higher affinity for the plasticizer than the other.

Some techniques are more sensitive than others at resolving multiple T_gs. DMA in particular is very sensitive, and revealed separate T_gs for sugar rich and protein rich phases in material pocket DMA of freeze dried powders that were not resolved in other techniques.[44] Similarly, for a glycerol plasticized soy protein isolate study, DMA showed two transitions where DSC only showed one.[67]

3.3.2. Secondary Transitions and Relaxations

Relaxation techniques such as DMA often reveal additional, or secondary, transitions below T_g. A peak in mechanical dampening (loss) is seen, with an associated rapid drop in elastic modulus, but not to the same extent as at the T_g. Protein is no exception to this. In dry bloodmeal (denatured protein), material pocket DMA detected a T_g at about 200 °C, along with smaller transitions at about 60 and −90 to 70 °C.[47] DMA of spider silk with a T_g of approximately 200 °C also showed a secondary transition around −70 °C.[68,69] Such a transition was also observed in silkworm silk.[70]

Certain secondary peaks are often seen at similar temperatures relative to the T_g when compared in an absolute temperature scale. For example, the β-transition (T_β), related to local chain movement is commonly seen around 0.75 of the T_g.[71,72] An additional transition at about 1.2 times the glass transition temperature (designated $T_{l,l}$) is also often seen.[72]

Four different types of motion that contribute to sub-T_g transitions have been described (Figure 3).[73] All of these are possible in plasticized proteins. As well as type A motion about the main polypeptide chain, different amino acid side chains may contribute to type B and type C motions. Type D motion is also possible for plasticized protein-based thermoplastics. For example, a separate transition relating to free glycerol was detected using modulated DSC in gluten films.[66]

There is often a correlation between β-transitions and polymer toughness. For this to occur, molecular motion must be large enough to absorb sufficient energy, such as localized main-chain motion, or very large side chain motions.[35] Secondary relaxations that involve all parts of a molecule are called Johari–Goldstein (JG) β-relaxations.[74] These were named after the researchers who discovered β-relaxations in glass forming materials consisting of only rigid molecules for which motion could only be explained by movement of the entire molecule.[74,75] It is the involvement of the entire molecule (or in the case of polymers, the entire repeat unit) that is the basis for classification as a JG-relaxation, rigidity is not a requirement.[74]

Early experiments using specific homopolymers, in which only certain motions were chemically possibly demonstrated that each type of motion illustrated in Figure 3 caused relaxations.[73] In proteins, the heterogeneous nature of the chains suggests it is not practical to specifically link an observed transition to a single specific type of motion or mode of relaxation. However, secondary transitions detectable by DMA do

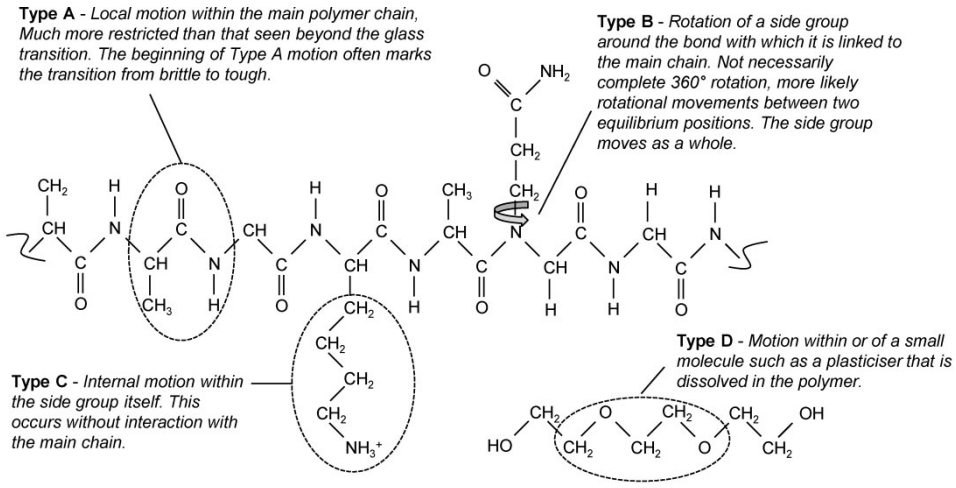

Figure 3. Motions causing secondary loss maxima in glassy amorphous polymers[73] and examples of their possible occurrence in proteins.

occur in protein-based thermoplastics and seem to be affected by plasticizer content. In thermoplastics produced from soy protein, a β-transition was detected that shifted with different moisture contents[10] (Figure 4). Similarly, in extruded sunflower protein films, T_β was shown to depend on plasticizer content (glycerol and water) and the die temperature used in processing. Sheets extruded at 85 °C with 50 parts glycerol and 20 parts water per 100 parts protein (equilibrated at 60%RH and 25 °C), had a T_β of −35.8 °C. This dropped to −49.4 °C for films produced at 160 °C.[9]

3.4. Models of Relaxation Temperature Dependence

At a given temperature, a characteristic relaxation time for molecular motion can described as:[34]

$$\tau = \frac{1}{2\pi f_m} \tag{2}$$

where f_m is the frequency at maximum loss during an oscillatory experiment such as dynamic mechanical analysis or di-electric analysis. The maximum dampening effect the material has on the oscillating system will be when the frequency of oscillation is on a similar timescale to molecular motions that can dissipate energy.

The simplest model used to relate observed transition temperature at a given experimental frequency or observed frequency at a given temperature is a modified form of the Arrhenius equation:

$$\ln f = \ln A - \left[\frac{E_A}{RT}\right] \tag{3}$$

where f is the oscillation frequency, related to relaxation time by Equation (2). A is a constant, E_A is the activation energy for the transition, R is the universal gas constant and T is the observed transition temperature. If ln f is plotted against $1/T$, Arrhenius behavior would predict a straight line with slope $-E_A/R$. Such a plot is often called a relaxation map.[76,77] In practice, while β-relaxations typically obey this Arrhenius relationship over broad frequency ranges,[73] the α-relaxation of proteins shows a super exponential temperature dependence, owing to collective behavior of many interactions giving rise to a curvature on the plot (Figure 5).[78] This curvature on is better represented by the Vogel Fulcher Tammann (VFT) equation[79]

$$\tau = \tau_0 \, e^{(DT_0/T-T_0)} \tag{4}$$

where A, D, and T_0 are constants and τ is the relaxation time at a temperature, T. The D parameter gives an indication of how well the system follows Arrhenius behavior (the case when D is infinite).[80] $1/T_0$ is an asymptotic restriction on the α-relaxation (Figure 5) and different D values will change the position of T_0 relative to T_g.[80] As frequency of maximum loss is related to the relaxation time by Equation (2), Equation (4) can also be written in terms of frequency

$$f_m = A \, e^{(DT_0/T-T_0)} \tag{5}$$

where $A = 2\pi\tau_0$.

Curvature in the relaxation map is not unique to proteins. Rather, it is a generic property of the α-relaxation in glass forming materials. The curvature has its origins in the co-operative nature of the motions responsible for T_g, so can be used as a test to determine if a relaxation is co-operative. As

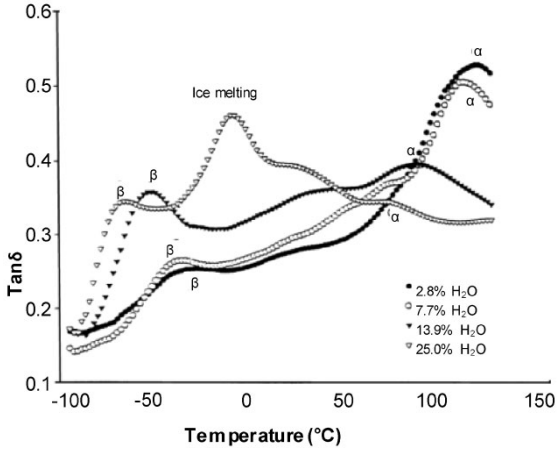

Figure 4. Peaks in tanδ from DMA for extruded soy protein sheets with different moisture contents.[10] Reproduced with permission.[10]. Copyright 2001, with permission from Elsevier.

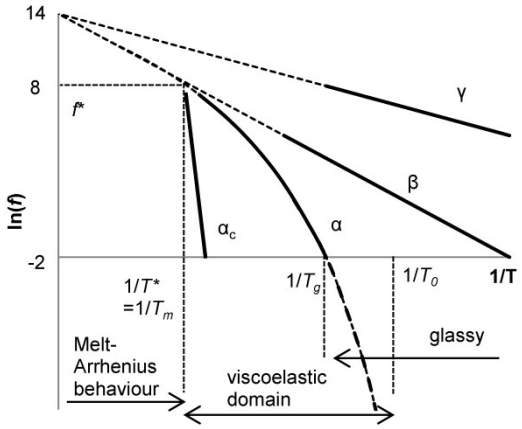

Figure 5. Typical relaxation frequency-temperature dependence in glass forming semi-crystalline polymers[76] Reproduced with permission.[76] Copyright 2000, with permission from Elsevier.

discussed earlier, numerous secondary motions also occur in proteins (Figure 3). Analysis of their frequency dependence may assist in identifying which types of motion are being observed. Whilst secondary relaxations follow an Arrhenius dependence, a distinction can be made between the response of JG-relaxations, involving whole repeat units and strongly related to the larger range motions responsible for T_g,[74] and other types of secondary relaxation. When plotted on a relaxation map, the time/temperature dependence of JG-relaxations merges with the α-relaxation at a critical temperature, denoted T^*, and frequency, denoted f^* [76,81] (Figure 5). Above this temperature, large-scale motion is effectively unconstrained and the α-relaxation also follows Arrhenius temperature/frequency dependence. This temperature may have further relevance, if protein-based thermoplastics are viewed as semi-crystalline, as it typically also corresponds to the melting temperature of crystalline regions in semi-crystalline polymers and the α_c relaxation (motion in the crystalline phase) also merges at T^*.[76]

Other types of secondary relaxation, which could occur in proteins due to side groups or plasticizers, would not be expected to merge with the α-relaxation and are called statistically independent β-fluctuations. Below a crossing temperature T_{cr} these motions are expected to be faster than the cooperative α-process, and above it they are slower.[81]

The deviation of a liquid's behavior from Arrhenius is described as its fragility.[79] The D parameter in Equations (5) and (6) can be seen as a measure of the strength of a liquid. Higher D values are closer to Arrhenius behavior and classified as strong. Lower values are typical of most polymers and classified as fragile. Proteins have been described a "both strong and fragile," depending on which relaxation processes are being examined.[79]

3.5. Glass Transitions in Highly Plasticized/Solvated Proteins

As well as sub-ambient secondary transitions at low to medium plasticization, the T_g itself may be well below ambient temperature for highly plasticized proteins. For example, DSC showed a T_g of –90 to –70 °C for compression moulded soy protein sheets plasticized with 33–40 wt% ethylene glycol.[7] Similarly, blood protein-based thermoplastics with approximately 35 wt% water had a T_g at about –80 °C prior to extrusion.[47]

As discussed earlier, water itself is a very effective plasticizer for proteins, and the importance of protein/water interactions cannot be overstated. Protein function typically depends on the protein being hydrated.[81] When T_g has been studied for a given protein over a wide range of water contents, several observations have been apparent. At lower moisture contents, bulk water was not observed, and T_g decreased as water content increases. Above a critical water content (about 26% for both sunflower and extruded soy proteins) the T_g was obscured by, or merged with the endothermic event associated with water melting in DSC.[10,40] In lysozyme, T_g decreased markedly with increasing water content up to 25% then stabilized at about –90 °C.[82] In BSA, it stabilized at about –80 °C at 30% water content, above which unbound water appeared to have crystallized on cooling.[83] In both lysozyme and BSA, three relaxation regions were identified:[83]

- Local relaxation of polar groups on the protein surface, thought to also have a contribution from bound, uncrystallized water.
- Relaxation of the crystallized bulk water phase.
- The α-relaxation responsible for the glass transition of the hydrated protein.

The low T_g observed when there was enough water to form a separate freezable phase resembled that of proteins fully dissolved in solution, in which a transition is seen at approximately –70 to –90 °C (or around 200 K).[25] The relationship between relaxation of fully hydrated proteins, and relaxation of the solvent has been described as symbiotic[84] and that the T_g of the protein is "slaved" to the JG-relaxation of the solvent.[85] In solution, proteins have a hydration shell of solvent molecules bonded to the protein. For example, myglobin in solution has a hydration shell approximately 5 Å thick, with approximately 200 water molecules interacting in a manner distinguished from the background by high resolution X-ray crystallography.[81] The transition involves co-operative motion of both the protein and the solvent in the hydration shell.[85] This transition has been seen independent of the specific protein, but its temperature is broad and depends on the solvent.[25]

The implication of a T_g at –70 °C for dissolved or highly plasticized proteins is that at ambient conditions, they are well above their glass transition temperature, and theoretically, in a very mobile state. However, at biological temperatures, proteins are typically described as having a native structure, stabilized by numerous interactions. In contrast, dry proteins are well below their T_g at ambient conditions and must be heated to provide molecular mobility necessary for thermoplastic processing. The T_g of dry proteins is often around or above their decomposition temperature and plasticizers are therefore used to lower T_g, enabling processing without excessive degradation.[1] This results in a thermal behavior intermediate of dissolved and dry proteins, where denaturing is restricted by the T_g, which is influenced by plasticizer interactions.

3.6. Physical Aging and Sub-T_g Endotherms

Another endothermic event is often observed for proteins during the first heating scan in DSC, and has been thought to

be due to physical aging.[55] Below T_g, amorphous regions of polymers are in a meta-stable state and volume, enthalpy and entropy in the glassy phase can be higher than they would be at equilibrium. The polymer therefore undergoes slow chain relaxation processes towards an equilibrium conformation with reduction in internal energy and free volume.[63] Annealing is essentially the same process at elevated temperatures, although typically still below T_g.[63] For a typical amorphous polymer, either of these causes an endothermic peak in the vicinity of the T_g, detectable during a heating scan in DSC.[67] It should be noted that heat treatment of semicrystalline polymers and the resulting change in crystal structure is also called annealing, but would lead to increased crystallinity.

In dry or partially hydrated proteins, an endothermic peak which has been ascribed to aging seems to occur at around 60–80 °C,[55] which may be above or below the T_g depending on how the T_g is shifted by moisture content. Such a peak has been seen in many proteins that contain gluten sub-units.[55] This behavior has also been observed in soy proteins plasticized with glycerol that had been stored at 50%RH[67] as well as in BSA, both in the native state and after thermal denaturation at water contents below 20%.[31] Because of this, it should not simply be assumed that any endothermic peak observed around T_g is due to denaturing-especially if the protein has already been denatured, as is the case in processed protein plastics.

Figure 6 shows example DSC plots for BSA, revealing both an upper endothermic peak, which would correspond to denaturing temperature, and lower temperature peak, which has been linked with aging.[31] It is interesting to note that while the upper denaturing peak and the T_g shift greatly with moisture content, the lower temperature peak does not, and ends up below T_g at lower moisture content. The molecular rearrangements responsible for a pre-T_g endothermic event in proteins at low moisture content and implications for storage are subject to ongoing discussion.[86] Although not present on an immediate second scan, in BSA the peak returns if samples are left for 3 or more hours before a second scan.[31] It has also recently been shown that this event has a co-operative nature, similar to the α-relaxation responsible for T_g, and suggested that it may be due to internal motion within protein molecules.[86]

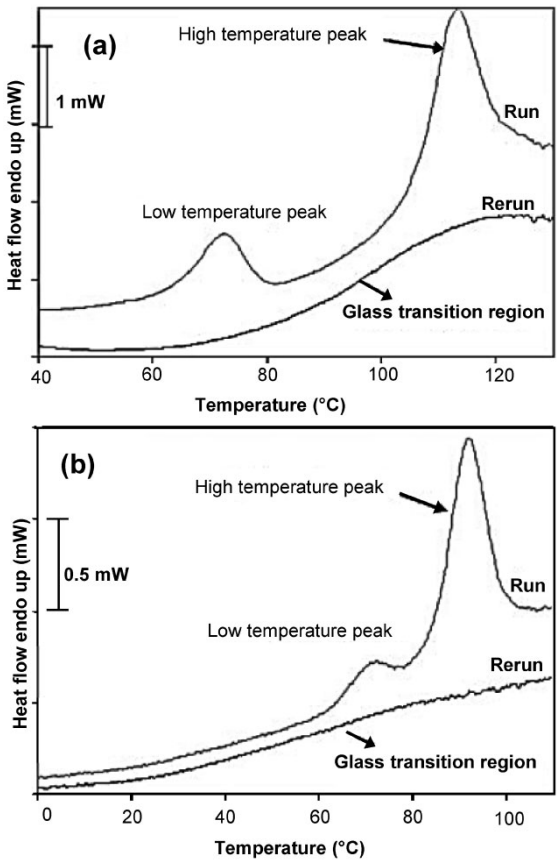

Figure 6. DSC thermogram traces for BSA conditioned at (a) 40 °C and 53% RH (moisture content 8.3% wet basis) and (b) 40 °C and 82%RH (moisture content 19.1% wet basis).[31] Reproduced with permission.[31]

4. The Crystalline Phase

4.1. Protein Crystallinity from a Plastics Perspective

It is hard to mention crystallinity and proteins without conjuring up images of X-ray crystallography to solve native structures. However, a protein "crystal" still typically contains 40–60% solvent, with large solvent channels between adjacent native protein molecules.[22] Protein-based thermoplastics, are not widespread crystals of entire proteins. To impart reasonable mechanical properties, interactions between molecules are required.[32] Nevertheless, the presence of α-helix and β-sheet secondary structures resemble crystalline zones as seen in other polymers.[45] Inter-chain distances corresponding to these structures have been detected in proteins by wide angle X-ray scatting (WAXS), both before and after thermoplastic processing. Two peaks are typically observed in proteins. The first corresponds to a d-spacing of approximately 10 Å, and has been attributed to both inter-helix packing in proteins with predominantly helical structures and to inter-sheet separation in proteins with a large proportion of β-sheets.[87] The second is a d-spacing of 4–5 Å attributed to repeating distances within each structure, due to hydrogen bonding

either along the backbone of α-helical proteins or between strands in β-sheets.[87]

These structures are stabilized by extensive hydrogen bonding between sites that would otherwise interact with water. Folding from random coils to ordered secondary structure conformations involves the loss of approximately one-third of the water of solvation to the bulk solvent.[22] In α-helices, hydrogen bonding is intramolecular and along the protein backbone. In β-sheets it can either be inter or intramolecular as bonding between aligned chain segments. In the same way that the low temperature T_g of proteins in solution has been described slaved to the bound solvent, some researchers have associated denaturing with a transformation of solvent molecules changing from a bound oscillator to a freely mobile molecule.[68] This removes constraints to the Φ and Ψ bond torsional angles (bond rotation angles about the N–C_α and C′–C_α bonds of the polypeptide backbone, respectively), and allows chains to rotate more freely and then potentially misfold.[68]

Hydrogen bonding in secondary structures means that the melting point of these structures is typically high. Keratin is the protein that is the major constituent of hair and wool. Helical crystallites in human hair (conditioned to 11.6 wt% water, at 20 °C and 65%RH) had a melting point of 175 °C.[88] Isothermal studies of β-sheet crystallization in films of silk fibroin have been performed at crystallization temperatures of around 200 °C, implying that the crystals were stable below this temperature.[17] These studies were performed by time resolved FT-IR and WAXS at elevated temperature and revealed a phase separation of crystallizable and uncrystallizable blocks.[17]

4.2. Effects of Crystallinity on Glass Transitions

The presence of crystalline phases in proteins does not just introduce a potential thermodynamic melting event, but also constrains amorphous chain motions in a non-uniform manner. This gives rise to a broader α-relaxation, or T_g in amorphous regions of semi-crystalline polymers than in purely amorphous polymers.[76,89] Typically, T_g of chains constrained between crystallites increases by 6–10 °C for a 10% increase in degree of crystallinity.[76] Furthermore, an additional broad relaxation, often designated the α_c-relaxation, emerges between T_g and T_m due to motions in the crystalline phase.[76] For secondary structures found in proteins, several motions are possible. α-helices can stretch (accordion like motion), rotate, rotate and extend simultaneously (torsional extension), or slip past adjacent helices.[90] Similarly, β-sheet structures are also capable of stretching in accordion like motion, while β-barrels (effectively a rolled up β sheet) have been described as "breathing".[91] Such motions typically involve stretching to the hydrogen bonds that stabilize the secondary structure.

4.3. Structure and Processing

The presence of secondary structures in protein-based thermoplastics has important implications for processing. Such secondary structure elements may contribute to fixing an article's physical shape on cooling.[32] This is important for commercial production of injection-moulded parts because shape fixation needs to be rapid and sufficient enough for effective mould release.

Another important implication is that these structures may or may not still be present in the "melt." Thermoplastic processing tends to favor an increase in ordered β-sheet regions,[1] often at the expense of α-helices, but this is not always the case. Increased crystallinity was seen after compression moulding sheets of soy protein isolate plasticized with either glycerol or with ethylene glycol.[7,92] This would imply increased formation of ordered secondary structures, at the expense of random coils. For hot pressed films from egg albumin, feather keratin and wheat gluten, increasing glycerol content increased ordered β-sheet content up to a critical plasticization level, beyond which it decreased a little.[49] To optimize processing it is important to understand whether these structures were forming on cooling from the melt, or forming at elevated temperatures within it.

If processing is conducted above T_g, but below T_m for the secondary structures present, they will not melt and may even crystallize further. This situation would be analogous to denaturing followed by aggregation in solution, with random coiled/amorphous regions of the protein polymer undergoing conformational change leading to stronger intermolecular interactions. When time resolved FT-IR was performed on soybean protein films held at 100 °C, spectral changes attributed to an increase in β-turns or β-sheet structures were observed.[65] Comparison of WAXS patterns of zein and thermoplastic zein suggested that some helical structures survived processing, although the tight packing of these structures was disrupted.[12] In the same study, the best blown films were prepared from zein with higher α-helical content relative to β-sheets. In this case, processing increased the α-helical content and decreased the presence of ordered β-sheet regions,[12] indicating some break up of β-sheets. Where the above soybean study used compression moulding, this work on zein used extrusion (to feed film blowing) and the level of shear would have been drastically different. Shear therefore may assist in breaking up and dispersing β-sheets in protein melts.

Severe aggregation can cause increased viscosity and restrict processing. The time between denaturing and excessive aggregation, known as the processing window,

also depends on the type of protein and its amino acid sequence.[93] Processing of proteins that do not aggregate extensively (such as zein, gliadins, and gelatin) is more easily controlled than processing of those that aggregate readily (such as egg white, whey, and sodium caseinate).[93–95] Plasticizers typically widen the processing window and aggregation can further be controlled by choosing appropriate processing conditions or other chemical additives.[93]

Secondary structure and crystallinity are not the only factors influencing processability of protein-based thermoplastics. Crosslinking and degradation also change protein structure and in turn influence processability.

4.3.1. Crosslinking

Cysteine bonding in proteins resists conformational change that would otherwise be bought about by plasticization and contributes to a higher rubbery modulus at temperatures above T_g.[49] In extruded feather keratin, where sodium sulfite was used to break disulfide bonds, a shift from low crystallinity to higher crystallinity was seen as sodium sulfite was increased.[96] This suggests that based on backbone interactions alone, thermoplastic processing favors a shift to a more crystalline material, but side chain interactions may prevent this. Similarly, whey, casein and soy films appeared to have reduced β-sheet regions when crosslinking was induced by γ-radiation.[97]

The formation of a cross-linked network made proteins with higher cysteine content less sensitive to plasticization.[49] Proteins with fewer cysteine groups and large numbers of polar side groups, especially if these contained carbonyl groups (glutamine, asparagine, glutamic acid, and aspartic acid) had increased sensitivity to plasticization by polar molecules such as glycerol. Increased order in the glassy states was seen with increased plasticizer content.[49] Again, this seemed to be a case of a preference of more order along the backbone or increased hydrogen bonding between main chains if side chain interactions were reduced.

4.3.2. Degradation

The other thermal event of huge significance for processing protein-based thermoplastics is degradation. Whereas denaturation takes place without rupture to peptide bonds that link amino acids in proteins, these bonds will rupture if exposed to high temperatures. Thermogravimetric analysis (TGA) of protein-based thermoplastics reveals four typical events, which may overlap:[1]

(i) volatilization of water,
(ii) volatilization or decomposition of other plasticizers,
(iii) cleavage of weaker bonds contributing to peptide bond cleavage, and
(iv) cleavage of stronger bonds leading to total degradation.

The reason degradation is important is that it imposes upper temperature limits on thermoplastic processing. Although large mass losses (other than loss of solvent or

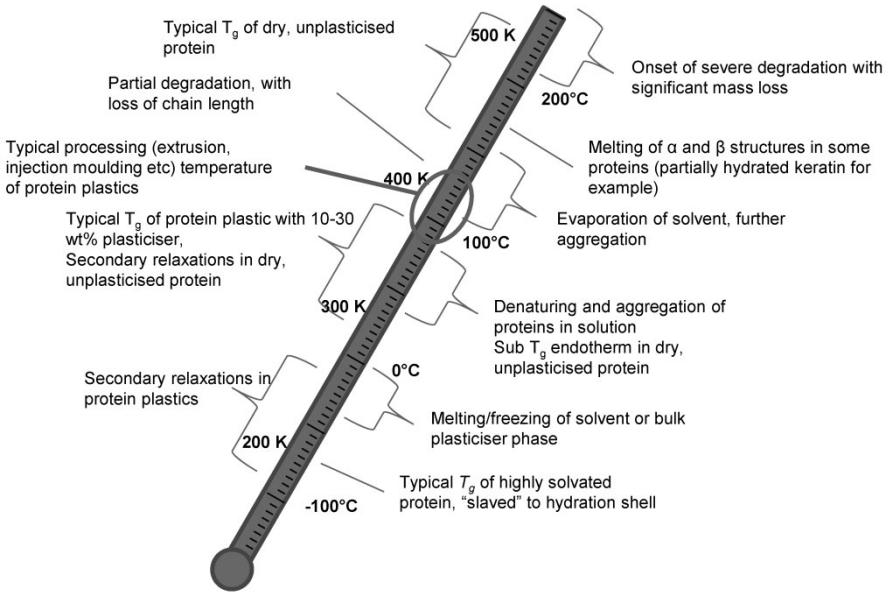

Figure 7. Typical temperatures at which thermal events occur in proteins (dry,plasticized,and in solution).

volatile plasticizers) are not typically seen in TGA until around 200 °C, some degradation occurs below this temperature. Changes in mechanical properties and increase in solubility indicated that some degradation had occurred when processing soy protein/starch blends by injection moulding at 140 °C.[98] Similarly, whey protein sheets plasticized with glycerol, compression moulded at 140 °C or above, showed signs of degradation within a 2 min residence time.[99] The main products of protein degradation in the range 120–260 °C are H_2O, CO_2, and NH_3.[100] It is the authors' own experience that when injection moulding protein plastics above 140 °C ammonia was smelt, indicating some degradation had occurred, even though moulded articles could still be produced.

Although optimal processing temperature depends on both the amino acid sequence of a particular protein and the level of plasticization used,[1] it needs to be above the softening temperature but below temperatures that cause excessive degradation. For proteins, the softening, or melt temperature is typically 40 °C above the T_g [1,55]. Typical processing temperatures in the window below degradation are in the range of 70–130 °C.

5. Conclusion

Several important transition regions in proteins have been identified along with the important changes in molecular motion responsible for those. The temperature range over which these typically occur for dry, plasticized and fully solvated proteins are summarized in Figure 7.

In dry proteins, T_g, T_d, and T_m of secondary structures fall in a narrow range, close to or around the degradation temperature. With increased plasticization, these events separate, with T_g as the lowest temperature major transition, as low as –70 to 90 °C at high levels of plasticization or in solution. T_d is the next major thermal transition. Although denaturation of proteins in solution is referred to as melting by analogy with solids, it is not the same as melting of crystalline regions in synthetic polymers. Denaturation is defined in terms of loss of biological function or long-range molecular order. Secondary structures may remain after denaturing, and further aggregation may even occur. Upon further heating, melting of secondary structures occurs, resembling T_m in other thermoplastics.

As well as denaturation, true melting of ordered regions and the broadening effect of crystallinity on the T_g should be taken into consideration when optimizing thermal processing conditions for protein-based thermoplastics. Extrusion of a consolidated protein-based material requires denaturing and new interactions to form, but may not necessarily involve the destruction of secondary structures. Some secondary structures may therefore be present in the melt, which could affect viscosity. Additionally, newly folded secondary structures may form in the melt and on cooling, which along with inter-chain interactions in the amorphous phase contribute to consolidation.

Received: June 20, 2013; Accepted: August 6, 2013;Published online: DOI: 10.1002/mame.201300248

Keywords: denaturing; glass transition; plasticiser; protein; secondary structure

[1] C. J. R. Verbeek, L. E. van den Berg, *Macromol. Mater. Eng.* **2010**, *295*, 10.
[2] Y. Wang, F. Lopes, P. Geil, G. W. Padua, *Macromol. Biosci.* **2005**, *5*, 1200.
[3] L. F. Drummy, D. M. Phillips, M. O. Stone, B. L. Farmer, R. R. Naik, *Biomacromolecules* **2005**, *6*, 3328.
[4] C. A. Vaz, J. F. Mano, M. Fossen, R. F. van Tuil, L. A. de Graaf, R. L. Reis, A. A. Cunha, *J. Macromol. Sci. Phys.* **2002**, *B41*, 33.
[5] O. Orliac, F. Silvestre, A. Rouilly, L. Rigal, *Ind. Eng. Chem. Res.* **2003**, *42*, 1674.
[6] P. Tummala, W. J. Liu, L. T. Drzal, A. K. Mohanty, M. Misra, *Ind. Eng. Chem. Res.* **2006**, *45*, 7491.
[7] Q. Wu, L. Zhang, *Ind. Eng. Chem. Res.* **2001**, *40*, 1879.
[8] D. Liu, L. Zhang, *Macromol. Mater. Eng.* **2006**, *291*, 820.
[9] A. Rouilly, A. Mériaux, C. Geneau, F. Silvestre, L. Rigal, *Polym. Eng. Sci.* **2006**, *46*, 1635.
[10] J. Zhang, P. Mungara, J. Jane, *Polymer* **2001**, *42*, 2569.
[11] V. M. Hernandez-Izquierdo, D. S. Reid, T. H. McHugh, J. D. J. Berrios, J. M. Krochta, *J. Food Sci.* **2008**, *73*, E169.
[12] M. Oliviero, E. D. Maio, S. Iannace, *J. Appl. Polym. Sci.* **2010**, *115*, 277.
[13] J. M. Bier, C. J. R. Verbeek, M. C. Lay, *Int. J. Environ. Cult. Econ. Soc. Sustain.* **2011**, *7*, 145.
[14] J. Bier, C. Verbeek, M. Lay, *Int. J. Life Cycle Assess.* **2012**, *17*, 314.
[15] E. Rudnik, *Compostable Polymer Materials*, Elsevier, Amsterdam, London **2008**, p. xii.
[16] A. Rouilly, O. Orliac, F. Silvestre, L. Rigal, *Thermochim. Acta* **2003**, *398*, 195.
[17] X. Hu, Q. Lu, D. L. Kaplan, P. Cebe, *Macromolecules* **2009**, *42*, 2079.
[18] J. M. G. Cowie, V. Arrighi, *Polymers: Chemistry and Physics of Modern Materials*, 3rd ed. CRC Press, Boca Raton **2008**, p. 499.
[19] K. A. Dill, D. Shortle, *Annu. Rev. Biochem.* **1991**, *60*, 795.
[20] R. J. Young, P. A. Lovell, *Introduction to Polymers*. 3rd ed., Taylor and Francis Group LLC, Boca Raton **2011**.
[21] R. Sowdhamini, P. Balaram, in *Thermostability of Enzymes* (Ed: M. N. Gupta), Narosa Publishing House/Springer, New Delhi/Berlin, New York **1993**, p. vi.
[22] T. M. Devlin, *Textbook of Biochemistry: With Clinical Correlations*. 7th ed. John Wiley & Sons, Hoboken, NJ **2011**, p. xxxii.
[23] H. Frauenfelder, S. G. Sligar, P. G. Wolynes, *Science* **1991**, *254*, 1598.
[24] D. Voet, J. G. Voet, *Biochemistry*. 3rd ed. *John Wiley & Sons*, Hoboken, NJ **2004**, p. xv.
[25] D. Ringe, G. A. Petsko, *Biophys. Chem.* **2003**, *105*, 667.

[26] L. Zhang, M. Zeng, in *Monomers, Polymers and Composites from Renewable Resources*, (Eds: B. Mohamed Naceur and G. Alessandro), Elsevier, Amsterdam **2008**, p. 479.
[27] N. Kitabatake, M. Tahara, E. Doi, *Agric. Biol. Chem.* **1989**, *53*, 1201.
[28] Y. B. Yan, Q. Wang, H. W. He, H. M. Zhou, *Biophys. J.* **2004**, *86*, 1682.
[29] X. Q. Mo, X. Z. Sun, *J. Am. Oil Chem. Soc.* **2001**, *78*, 867.
[30] C. Giancola, C. De Sena, D. Fessas, G. Graziano, G. Barone, *Int. J. Biol. Macromol.* **1997**, *20*, 193.
[31] A. Farahnaky, F. Badii, I. A. Farhat, J. R. Mitchell, S. E. Hill, *Biopolymers* **2005**, *78*, 69.
[32] L. A. De Graaf, *J. Biotechnol.* **2000**, *79*, 299.
[33] K. Chynoweth, in *Polymer Update: Science and Engineering* (Eds: W.D. Cook G. B. Guise), Polymer Division Royal Australian Chemical Institute, Parkville, Vic. **1989**, p. xx.
[34] G. Allen, in *Molecular Basis of Transitions and Relaxations: Papers*. (Eds: R. F. Boyer, D. J. Meier, Midland Macromolecular Institute, and Dow Chemical Company), Gordon and Breach Science Publishers, London, New York **1978**, p. xii.
[35] K. P. Menard, *Dynamic Mechanical Analysis: A Practical Introduction*, 2nd ed.n CRC Press, Boca Raton, FL **2008**, p. xix.
[36] J. H. Gibbs, E. A. DiMarzio, *J. Chem. Phys.* **1958**, *28*, 373.
[37] W. Kauzmann, *Chem. Rev.* **1948**, *43*, 219.
[38] C. E. Carraher, R. B. Seymour, *Seymour/Carraher's Polymer Chemistry*, 7th ed. CRC Press, Boca Raton **2008**, p. 738.
[39] Y. I. Matveev, V. Y. Grinberg, I. V. Sochava, V. B. Tolstoguzov, *Food Hydrocolloids* **1997**, *11*, 125.
[40] A. Rouilly, O. Orliac, F. Silvestre, L. Rigal, *Polymer* **2001**, *42*, 10111.
[41] N. Silalai, Y. H. Roos, *J. Food Sci.* **2010**, *75*, E285.
[42] S. Kadoya, K. Fujii, K.-I. Izutsu, E. Yonemochi, K. Terada, C. Yomota, T. Kawanishi, *Int. J. Pharm.* **2010**, *389*, 107.
[43] J. K. Towns, *J. Chromatogr. A* **1995**, *705*, 115.
[44] J. Carpenter, D. Katayama, L. Liu, W. Chonkaew, K. Menard, *J. Therm. Anal. Calorim.* **2009**, *95*, 881.
[45] S. Guilbert, B. Cuq, in *Handbook of Biodegradable Polymers* (Es: C. Bastioli), , Rapra Technology, Shrewsbury **2005**, p. xviii.
[46] J. Gearing, K. P. Malik, P. Matejtschuk, *Cryobiology* **2010**, *61*, 27.
[47] J. M. Bier, C. J. R. Verbeek, M. C. Lay, *J. Therm. Anal. Calorim.* **2012**, 1.
[48] B. Cuq, N. Gontard, S. Guilbert, *Polymer* **1997**, *38*, 4071.
[49] A. I. Athamneh, M. Griffin, M. Whaley, J. R. Barone, *Biomacromolecules* **2008**, *9*, 3181.
[50] P. Chen, L. Zhang, *Macromol. Biosci.* **2005**, *5*, 237.
[51] C. H. Tang, S. M. Choi, C. Y. Ma, *Int. J. Biol. Macromol.* **2007**, *40*, 96.
[52] M. J. Pikal, D. Rigsbee, M. J. Akers, *J. Pharm. Sci.* **2009**, *98*, 1387.
[53] L. di Gioia, S. Guilbert, *J. Agric. Food Chem.* **1999**, *47*, 1254.
[54] H. Madeka, J. L. Kokini, *J. Am. Oil Chem. Soc.* **1996**, *73*, 433.
[55] C. Bengoechea, A. Arrachid, A. Guerrero, S. E. Hill, J. R. Mitchell, *J. Cereal Sci.* **2007**, *45*, 275.
[56] M. G. A. Vieira, M. A. da Silva, L. O. dos Santos, M. M. Beppu, *Eur. Polym. J.* **2011**, *47*, 254.
[57] M. Pommet, A. Redl, S. Guilbert, M.-H. Morel, *J. Cereal Sci.* **2005**, *42*, 81.
[58] A. Kumar, R. K. Gupta, *Fundamentals of Polymers*, 1st ed. McGraw-Hill International Editions, New York, **1998**.
[59] N. K. Budhavaram, J. A. Miller, Y. Shen, J. R. Barone, *J. Agric. Food Chem.* **2010**, *58*, 9549.
[60] US. US2238307 (1941), Secretary, agriculture of invs.: G. H. Brother, L. L. Mckinney.
[61] C. Verbeek, N. Koppel, *J. Mater. Sci.* **2011**, *47*, 1187.
[62] J. L. Brent, S. J. Mulvaney, C. Cohen, J. A. Bartsch, *J. Cereal Sci.* **1997**, *26*, 313.
[63] J. D. Menczel, R. B. Prime, *Thermal Analysis of Polymers: Fundamentals and Applications*, John Wiley, Hoboken, NJ **2009**, p. x.
[64] L. Yu, G. Christie, *Carbohydr. Polym.* **2001**, *46*, 179.
[65] K. Tian, D. Porter, J. Yao, Z. Shao, X. Chen, *Polymer* **2010**, *51*, 2410.
[66] A. Jerez, P. Partal, I. Martinez, C. Gallegos, A. Guerrero, *Biochem. Eng. J.* **2005**, *26*, 131.
[67] X. Mo, X. Sun, *J. Polym. Environ.* **2003**, *11*, 15.
[68] D. Porter, F. Vollrath, *BBA-Proteins Proteomics* **2012**, *1824*, 785.
[69] F. Vollrath, D. Porter, *Soft Matter* **2006**, *2*, 377.
[70] J. Guan, D. Porter, F. Vollrath, *Biomacromolecules* **2013**, *14*, 930.
[71] D. W. van Krevelen, K. t. Nijenhuis, *Properties of Polymers: Their Correlation with Chemical Structure: Their Numerical Estimation and Prediction from Additive Group Contributions*, 4th, completely rev./ed, Elsevier, Amsterdam, Boston **2009**, p. xxvi.
[72] R. F. Boyer, in *Molecular Basis of Transitions and Relaxations: Papers*. (Eds.: R. F. Boyer, D. J. Meier, Midland Macromolecular Institute, and Dow Chemical Company), Gordon and Breach Science Publishers, London, New York **1978**, p. xii.
[73] J. Heijboer, in *Molecular Basis of Transitions and Relaxations: Papers*. (Eds.: R. F. Boyer, D. J. Meier, Midland Macromolecular Institute, and Dow Chemical Company), Gordon and Breach Science Publishers, London, New York **1978**, p. xii.
[74] K. L. Ngai, M. Paluch, *J. Chem. Phys.* **2004**, *120*, 857.
[75] G. P. Johari, M. Goldstei, *J. Chem. Phys.* **1970**, *53*, 2372.
[76] J. Rault, *J. Non-Cryst. Solids* **2000**, *271*, 177.
[77] S. E. Pagnotta, S. Cerveny, A. Alegria, J. Colmenero, *Phys. Chem. Chem. Phys.* **2010**, *12*, 10512.
[78] W. Doster, *BBA-Proteins Proteomics* **2010**, *1804*, 3.
[79] J. L. Green, J. Fan, C. A. Angell, *J. Phys. Chem.* **1994**, *98*, 13780.
[80] C. A. Angell, *Science* **1995**, *267*, 1924.
[81] H. Frauenfelder, G. Chen, J. Berendzen, P. W. Fenimore, H. Jansson, B. H. McMahon, I. R. Stroe, J. Swenson, R. D. Young, *Proc. Natl. Acad. Sci. USA* **2009**, *106*, 5129.
[82] A. Panagopoulou, A. Kyritsis, A. M. Aravantinou, D. Nanopoulos, R. S. I. Serra, J. L. G. Ribelles, N. Shinyashiki, P. Pissis, *Food Biophys.* **2011**, *6*, 199.
[83] A. Panagopoulou, A. Kyritsis, R. S. I. Serra, J. L. G. Ribelles, N. Shinyashiki, P. Pissis, *BBA-Proteins Proteomics* **2011**, *1814*, 1984.
[84] K. L. Ngai, S. Capaccioli, N. Shinyashiki, *J. Phys. Chem. B* **2008**, *112*, 3826.
[85] N. Shinyashiki, W. Yamamoto, A. Yokoyama, T. Yoshinari, S. Yagihara, R. Kita, K. L. Ngai, S. Capaccioli, *J. Phys. Chem. B* **2009**, *113*, 14448.
[86] M. Mizuno, M. J. Pikal, *Eur. J. Pharm. Biopharm.* **2013**, in press.
[87] W. M. Elshemey, A. A. Elfiky, W. A. Gawad, *Protein J.* **2010**, *29*, 545.
[88] J. Cao, *Thermochim. Acta* **1999**, *335*, 5.
[89] R. H. Boyd, *Polymer* **1985**, *26*, 323.
[90] M. Takayanagi, in *Molecular Basis of Transitions and Relaxations: Papers*. (Eds.: R. F. Boyer, D. J. Meier, Midland Macromolecular Institute, and Dow Chemical Company), Gordon and Breach Science Publishers, London, New York **1978**, p. xii.
[91] K. C. Chou, *Biophys. J.* **1985**, *48*, 289.

[92] Q. Wu, L. Zhang, *J. Appl. Polym. Sci.* **2001**, *82*, 3373.
[93] C. J. R. Verbeek, L. E. van den Berg, *Recent Pat. Mater. Sci.* **2009**, *2*, 171.
[94] A. Jerez, P. Partal, I. Martinez, C. Gallegos, A. Guerrero, *Rheol. Acta* **2007**, *46*, 711.
[95] A. Jerez, P. Partal, I. Martínez, C. Gallegos, A. Guerrero, *J. Food Eng.* **2007**, *82*, 608.
[96] J. R. Barone, W. F. Schmidt, N. T. Gregoire, *J. Appl. Polym. Sci.* **2006**, *100*, 1432.
[97] M. Lacroix, T. C. Le, B. Ouattara, H. Yu, M. Letendre, S. F. Sabato, M. A. Mateescu, G. Patterson, *Radiat. Phys. Chem.* **2002**, *63*, 827.
[98] H. C. Huang, T. C. Chang, J. Jane, *J. Am. Oil Chem. Soc.* **1999**, *76*, 1101.
[99] V. M. Hernandez-Izquierdo, J. M. Krochta, *J. Food Sci.* **2008**, *73*, 30.
[100] P. Chen, H. Tian, L. Zhang, P. R. Chang, *Ind. Eng. Chem. Res.* **2008**, *47*, 9389.

4

Thermal and Mechanical Properties of Bloodmeal-Based Thermoplastics Plasticised with Tri-ethylene glycol

A paper

Published in

Macromolecular Materials and Engineering

by

JAMES M. BIER[1], C.J.R. VERBEEK AND M.C. LAY

[1]As first author for this paper, I prepared the initial draft manuscript, which was refined and edited in consultation with my supervisors, who have been credited as co-authors. For the effect of different TEG contents, I determined which formulations to trial based on reviewing those used in previous research, I prepared all samples and I ran the analysis (mechanical testing DMA, DSC and WAXS). The FT-IR results reported were collected in collaboration with my supervisors during beamtime at the Australian Synchrotron in November 2011. The main experiment from that beamtime is reported in Chapter 7, but the scans reported here were not used in that analysis. For the factorial experiment I assisted in injection moulding the specimens, ran all the DMA analysis, and performed the statistical analysis on mechanical properties and DMA results.

Thermal and Mechanical Properties of Bloodmeal-Based Thermoplastics Plasticized with Tri(ethylene glycol)

James M. Bier,* Casparus J. R. Verbeek, Mark C. Lay

Thermoplastic protein produced from bloodmeal (BM) becomes brittle as moisture desorbs from the material. Tensile tests, DMA, DSC and WAXS are used to determine the effect of replacing water with TEG. Specimens containing 0–30 pph_{BM} TEG and combined water and TEG content prior to extrusion of 60 pph_{BM} are extruded, injection-moulded and conditioned. TEG increases the strain at break while reducing strength. 20 pph_{BM} is chosen as an appropriate compromise between strength and ductility with a tensile strength of 6 MPa, a Young's modulus of 250 MPa, a toughness of 2.8 MPa and a strain at break of 0.53. When TEG is held at 20 pph_{BM} and the amounts of other additives varied urea has the largest effect on conditioned properties, showing that H-bonding still dominates protein/protein interactions.

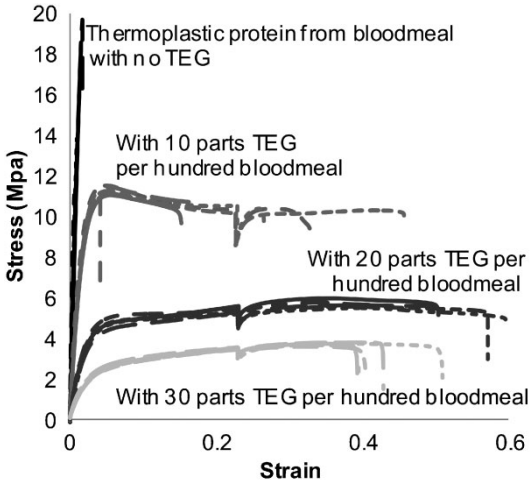

1. Introduction

Renewable alternatives to petro-chemical polymers can be produced by converting biomass sources into new polymers [e.g., poly(lactic acid) (PLA) or poly(hydroxy-alkanoates) (PHA)] or by modifying biopolymers to enable thermoplastic processing. Thermoplastic starch is available commercially, while thermoplastics have been produced from proteins such as wheat, soy and sunflower, gelatine, keratein, casein, whey and bloodmeal.[1]

Bloodmeal is a denatured protein by-product of the meat processing industry produced by steam coagulation and drying of blood. Treating bloodmeal with a combination of water, a protein denaturant (urea), a reducing agent (sodium sulfite, SS) and surfactant (sodium dodecylsulfate, SDS) produced a thermoplastic which can be extruded and injection-moulded.[2,3] These additives are required to reduce hydrogen bonding, covalent crosslinking and hydrophobic interactions between proteins present in bloodmeal. In the absence of additives, the temperature required to overcome these interactions is higher than the protein's thermal degradation point. Water is an efficient plasticizer for proteins[1,4] and in conjunction with the other additives reduces the softening temperature to below the onset of excessive degradation.[3]

After processing, water desorbs from the moulded plastic over time. The material becomes brittle and although strength increases due to increased protein/protein interactions, the material loses toughness. With sufficient urea, a material can be produced from bloodmeal

J. M. Bier, C. J. R. Verbeek, M. C. Lay
School of Engineering, University of Waikato, Knighton Road, Private Bag 3105 Hamilton 3240, New Zealand
E-mail: jmb101@waikato.ac.nz

that remains somewhat ductile after conditioning.[5] Urea is capable of strong hydrogen bonding and is used to disrupt protein/protein interactions during processing. However, protein/protein interactions are stronger than protein/urea interactions and urea leaches out from protein-based plastics over time, leaving a white residue on the surface.[6,7] Protein plastics produced with alternative plasticizers are typically more flexible and show a greater extension at break than those produced with urea.[1]

Although hydrogen bonding is an important interaction stabilising proteins, hydrophobic interactions also play a role.[8,9] For this reason, amphiphilic plasticizers, containing both polar and nonpolar regions, have been shown to be more efficient plasticizers than polar molecules when compared on a molar or H-bonding capability basis.[4] One such plasticizer is tri(ethylene glycol) (TEG). Table 1 compares basic properties and the number of H-bonding sites by mass for water, urea and TEG.

The purpose of this research was to investigate plasticisation of bloodmeal-based thermoplastics by assessing changes in mechanical and thermal properties after replacing different amounts of water with TEG. The amounts of other additives were chosen to provide a formulation that embrittled without TEG, so that the effect of TEG could clearly be observed. After exploring the effect of TEG at a constant level of these additives, the roles of these additives at a constant level of TEG was assessed. This was achieved using a factorial experiment with urea, SDS, SS and water content as variables.

2. Experimental Section

2.1. Materials and Sample Preparation

Bloodmeal-based thermoplastic has been developed earlier and patented by Novatein Ltd. and is marketed under the trade name Novatein Thermoplastic Protein (NTP), New Zealand.[2] In this study, different formulations were produced to assess the effect of varying TEG contents (Table 2) and effects of different levels of other additives at constant TEG content (Table 3). Urea, SS

Table 1. Comparison of hydrogen bonding sites by mole and by mass for water, urea and TEG.

Property	Water	Urea	TEG
molar mass [g·mol^{-1}]	18	60.6	150.17
melting point [°C]	0	133	−7
boiling point [°C]	100	decomposition	285
H-bonding hydrogen [mol·mol^{-1}]	2	4	2
lone electron pairs [mol·mol^{-1}]	2	4	8
H-bonding hydrogen [mol·g^{-1}]	0.11	0.07	0.01
lone electron pairs [mol·g^{-1}]	0.11	0.07	0.05
hydrophilic groups [%]	100	100	44

Table 2. Design of experiment to assess effect of variation in TEG content.

			Composition [pph$_{BM}$ [a)]]			
Reagent	Source	Grade	V0	V1	V2	V3
bloodmeal	Wallace Co.	agricultural	100	100	100	100
urea	Ballance Agrinutrients	agricultural	10	10	10	10
water	produced on site from town supply	distilled	60	50	40	30
sodium dodecyl sulfate	Merck	technical	3	3	3	3
sodium sulfite	Merck	technical	3	3	3	3
tri(ethylene glycol)	Merck	for synthesis	0	10	20	30

[a)] g per 100 g bloodmeal.

Macromolecular Journals
Macromol. Mater. Eng. **2013,** DOI: 10.1002/mame.201200460

Table 3. Factorial design of formulations used to assess effects of other additives in the presence of 20 pph_{BM} TEG.

Formulation	Urea [pph_{BM}]	Water [pph_{BM}]	SS [pph_{BM}]	SDS [pph_{BM}]
F1	15	40	3	3
F2	15	40	3	6
F3	15	40	6	3
F4	15	40	6	6
F5	15	30	3	3
F6	15	30	3	6
F7	15	30	6	3
F8	15	30	6	6
F9	5	40	3	3
F10	5	40	3	6
F11	5	40	6	3
F12	5	40	6	6
F13	5	30	3	3
F14	5	30	3	6
F15	5	30	6	3
F16	5	30	6	6

and SDS (sources and grades as per Table 2) were dissolved in distilled water at 50 °C and mixed with bloodmeal in a high speed mixer for 10 min. TEG was added after the first 6 min. The resulting mixture, pre-extruded NTP (PNTP), was left overnight in sealed plastic bags at <4 °C then extruded using a ThermoPrism TSE-16-TC twin-screw extruder with a temperature profile and screw configuration as shown in Figure 1, using a screw speed of 150 rpm. Actual melt temperatures were within 2–5 °C of the set temperatures. The screw diameter was 16 mm, with an *L/D* ratio of 25 and the extruder was fitted with a single 10 mm diameter circular die. A relative torque of 60–75% of the maximum allowed in the extruder was maintained (12 N · m per screw maximum) by adjusting the mass flowrate of the feed. The extruded material (ENTP) was granulated using a tri-blade granulator from Castin Machinery Manufacturer Ltd. (New Zealand).

The granulated extrudate was injection-moulded into Type 1 tensile test specimens[10] through a cold runner into a water heated mould with a 30 kN locking force. Samples with varying TEG content were moulded using a BOY-35A injection moulder with 24 mm screw, temperature profile of 100, 115, 120, 120, 120 °C from feed zone to die, a screw speed of 200 rpm and a maximum injection pressure of 1100 bar. Samples with different additive levels at constant TEG content were moulded using a BOY 15S injection moulder with 22 mm screw, temperature profile of 100, 105, 115, 120 °C from feed zone to die, a screw speed of 150 RPM and a maximum injection pressure of 1200 bar.

Test pieces were conditioned at 50% RH and 23 °C for 7 days, producing conditioned NTP (CNTP) and tested in a climate controlled room.

2.2. Analysis

Mechanical properties of CNTP at different TEG contents were measured in tension at 5 mm · min^{-1} in an Instron model 33R4204 fitted with a 50 mm gauge length extensometer. A secant modulus was calculated between 0.0005 and 0.0025 strain and toughness was determined from the area under the stress/strain graph. Mechanical properties of CNTP at different additive levels, but at constant TEG content, were measured in tension at 5 mm · min^{-1} in a Lloyd Instruments LR 100K tensile tester. Due to the absence of an extensometer, only ultimate tensile strength and elongation at break (crosshead displacement in mm) have been reported for this portion of the experiments.

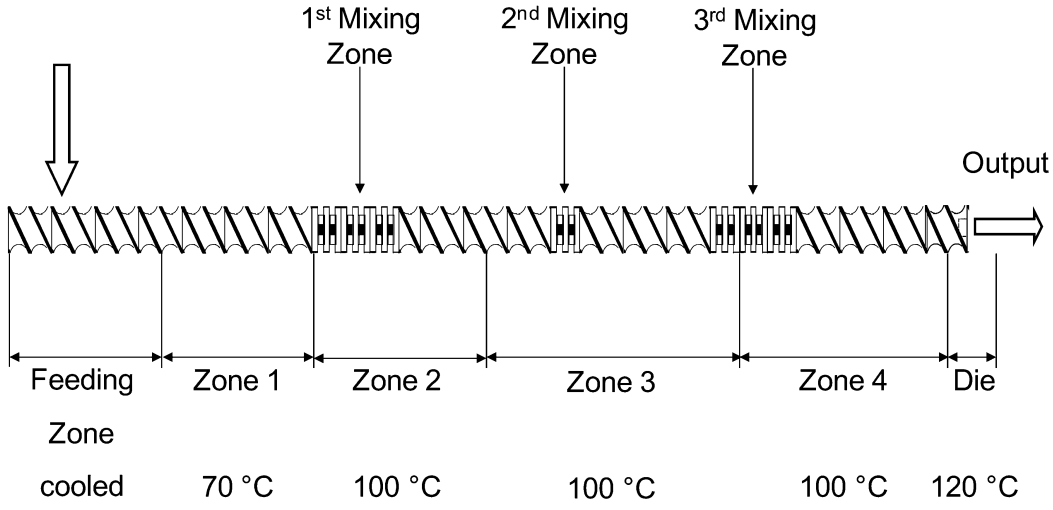

Figure 1. Extruder screw configuration and temperature profile.

Dynamic mechanical analysis (DMA) was performed using a Perkin-Elmer DMA8000 fitted with a high temperature furnace and cooled with liquid nitrogen. CNTP samples of approximately $3.5 \times 6.5 \times 30\ mm^3$ were cut from larger moulded pieces and tested between −100 and 120 °C at a programmed heating rate of $2\ °C\ min^{-1}$ in single cantilever bending mode (1 Hz, 12.5 mm free length, 0.03 mm dynamic displacement). PNTP samples were examined by mounting approximately 50 mg of powder in $\approx 1.0 \times 7.4 \times 28\ mm^3$ (folded dimensions) material pockets (Perkin-Elmer)[11] and tested with a dynamic displacement of 0.05 mm and other parameters as per self-supporting samples.

Differential scanning calorimetry (DSC) on PNTP was performed in a Perkin-Elmer DSC8500 cooled with liquid nitrogen. Crimped auto-sampler pans (Perkin-Elmer) with approximately 10 mg of sample were cooled to −100 °C at $50\ °C \cdot min^{-1}$ and held for 5 min, before heating at $50\ °C \cdot min^{-1}$ to +100 °C. Samples were weighed to ensure no mass had been lost, and then scanned a second time with the same profile. Additional samples were also scanned from −100 to +150 °C at $300\ °C \cdot min^{-1}$.

Powder wide angle X-ray scattering (WAXS) was performed on PNTP using a Phillips X'Pert system with a wavelength of 1.54 Å (PW3373/00 Cu LFF DK233995 X-ray tube at 40 kV and 40 mA). Samples were scanned from $2\theta = 2$ to 60° at 0.020° steps.

Synchrotron-based FT-IR (S-FT-IR) experiments on conditioned plastics were undertaken on the infrared microspectroscopy beamline at the Australian Synchrotron, Victoria, Australia. Samples with 0 and 20 pph_{BM} were dried over two nights in a Freezone 2.5 Litre benchtop freeze dryer (Labconco Corporation, Kansas City) set to auto mode (collector temperature −50 °C, vacuum <11 Pa.). Sections 2 μm thick were cut using stainless steel blades (TBS Inc.) on a TBS Cut 4060 RE microtome (TBS Inc.) lit by a microlight 150 (Fibreobtic Lightguides, Australia) and flattened between two diamond cells removing the top of the cell for analysis. Spectra were collected using a Bruker Hyperion 3000 with an MCT collector and XY stage using Opus 6.5 software (Bruker Optik GmbH 2009). Representative points were chosen on a video image of the microtomed section. For each point, 32 spectra were collected with a resolution of $4\ cm^{-1}$ between 3900 and $700\ cm^{-1}$ and averaged. The resulting data were baseline corrected (10 iteration concave rubber band with 64 baseline points) and min max normalized between 800 and $1800\ cm^{-1}$ using Opus 6.5.

3. Results and Discussion

3.1. Plasticizer Content

3.1.1. Mechanical Properties

A total plasticizer (water + TEG) content of 60 pph_{BM} was used for processing to determine the effect of TEG. However, moisture evaporates during conditioning, reducing the amount of total plasticizer present in CNTP. TEG is less volatile, so samples with a higher ratio of TEG to water retain a higher level of plasticisation after conditioning (Table 4), partly due to TEG also being hydrophilic, thereby having higher equilibrium moisture contents.

The mechanical properties of CNTP with different TEG content are shown in Figure 2. Specimens prepared without TEG were the stiffest and strongest, but these were also very brittle (low strain at break) and had very low toughness. Higher plasticizer content increased chain mobility, which reduced strength, but also allowed for some chain rearrangements in response to the applied force. This resulted in a tougher material with a higher strain at break. 20 pph_{BM} was chosen as good compromise between strength and toughness with the best strain at

Table 4. Transition temperatures identified at different TEG contents (temperatures from a single cryo scan of each and moisture contents for those very samples).

		T_g [°C]			T_β [°C]				TEG		H bonding sites [mol per g bloodmeal]			
Sample	Exp.	E'	E''	tanδ	E'	E''	tanδ	Moisture [%]	[pph_{BM}]	[%]	From water	From TEG	From urea	Total
CNTP	V0	51	–	81	−28	−21	–	6	0	0	0.016	0.000	0.013	0.03
	V1	40	–	71	−44	−25	–	6.50	10	7	0.019	0.007	0.013	0.04
	V2	17	–	66	−45	29	–	8	20	14	0.026	0.013	0.013	0.05
	V3	7	–	56	–	−38	–	8.50	30	19	0.030	0.020	0.013	0.06
PNTP	V0	−25	21	−17	−76	−91	90	38	0	0	0.150	0.000	0.013	0.16
	V1	−48	−32	−28	−84	−84	−82	33	10	6	0.128	0.007	0.013	0.15
	V2	−64	−36	−32	−64	84	−82	27	20	11	0.106	0.013	0.013	0.13
	V3	−79	−71	−64	–[a)]	–	–	21	30	17	0.084	0.015	0.013	0.12

[a)] Merges with above.

Macromolecular Journals
Macromol. Mater. Eng. **2013,** DOI: 10.1002/mame.201200460

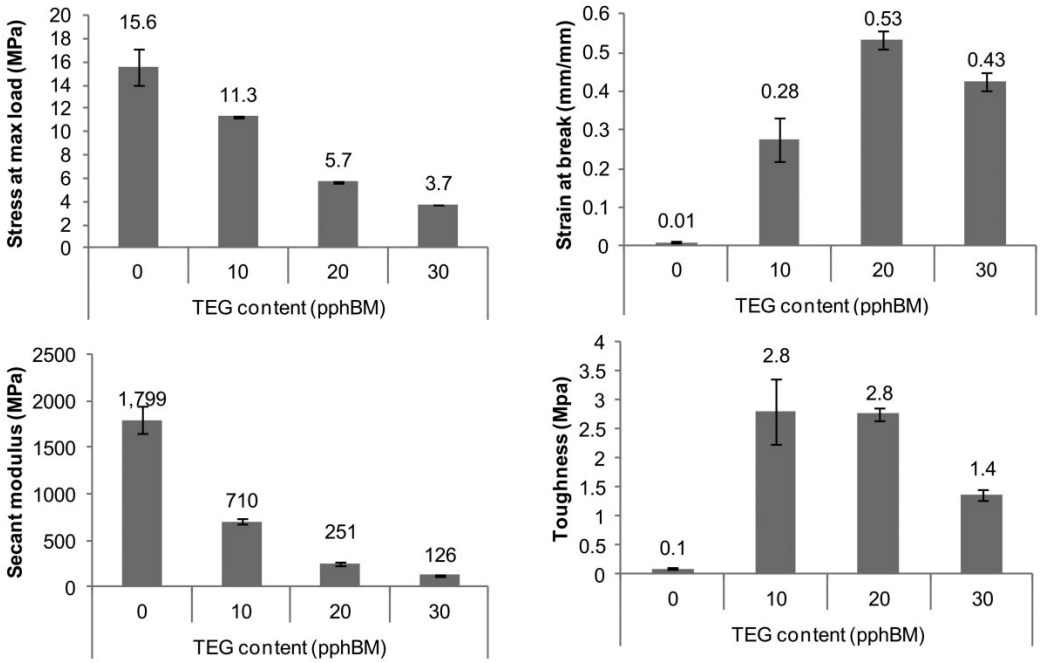

Figure 2. Mechanical properties of conditioned test pieces with varying TEG content. Error bars denote standard error of the mean.

break of the four formulations. Using 30 pph_{BM} TEG reduced toughness again, implying too much reduction of chain entanglements.

3.1.2. Thermal Properties

Dynamic mechanical analysis (DMA) of CNTP showed two transitions in the temperature range of −100–120 °C (Figure 3). The upper transition was characterized by a peak in tan δ and a drop of two orders of magnitude in E', both features consistent with a glass transition (T_g). Increased TEG broadened this transition and shifted it to lower temperatures, despite only a small difference in moisture content (Table 3), demonstrating the plasticising effect of TEG. The second, lower transition was thought to be a β-transition, associated with short-range relaxations and therefore less affected by TEG. It is interesting to note that as TEG is increased, the relative size of these transitions in the loss modulus curve changed and the upper transition merged into the lower. β-relaxations in polymers typically involve motion of an entire repeat unit.[12] It seems that with sufficient TEG, the protein/protein interactions that prevent larger scale motions were reduced in CNTP, so that there was a smaller difference between the onset of motion of one or two repeat units and longer range co-operative motions, characteristic of a T_g.

Two transitions were also seen as distinct peaks in tan δ for PNTP samples with lower TEG contents, merging at higher TEG contents. It has previously been discussed that the peak just below zero degrees likely represents freezable water, or a freezable water plus TEG phase when TEG is present.[13] The lower transition was not seen with only bloodmeal and water without the other processing aids[13] and was believed to be the heavily plasticized T_g of PNTP. The shifting together of these two peaks at 30 pph_{BM} TEG implies that at higher TEG contents the bulk frozen plasticizer and protein phases are less distinct.

DSC of PNTP revealed similar observations to DMA that there was a separate freezable phase. A peak corresponding to the melting of free/unbound water was observed at about zero degrees in PNTP with no TEG, appearing at lower temperatures as water was replaced with TEG (Figure 4, Table 5). This peak slightly reduced in size during a second heating cycle, but was observed at the same temperature. This reduction was not due to removal of water, as samples were weighed before and after scanning to ensure no moisture was lost from the sample. At 300 °C · min^{-1}, the endothermic peaks were again visible at 0 and 10 pph_{BM} TEG, but were not apparent at 20 or 30 pph_{BM} TEG. At this higher heating rate, the peaks were shifted to higher temperatures, which is a normal response for DSC results.

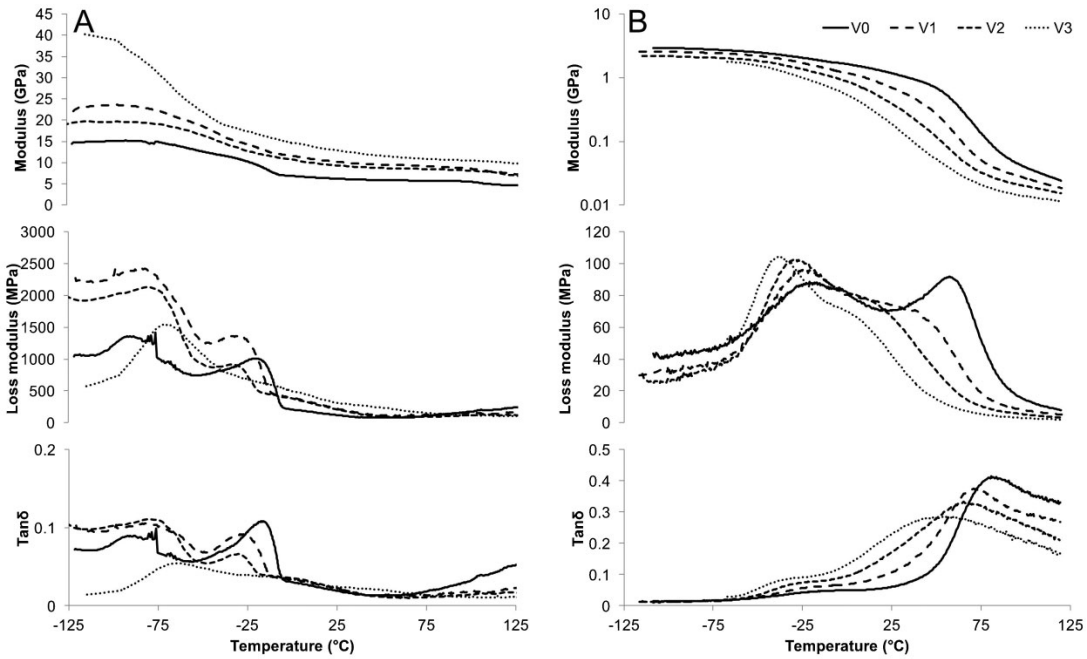

Figure 3. 1 Hz dynamic mechanical properties of (A) PNTP in powder pockets and (B) CNTP bars.

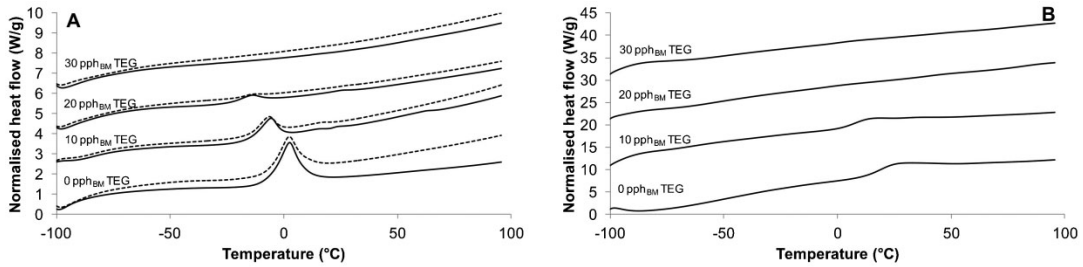

Figure 4. DSC curves (endothermic up, stacked for clarity) for PNTP at different TEG contents. (A) Two heating cycles at 50 °C · min^{-1} (solid line: first heating, dashed line: the second heating), (B) one heating cycle at 300 °C · min^{-1}.

Table 5. Location and size of endothermic peaks detected in DSC.

		First heating at 50 °C·min^{-1}		Second heating at 50 °C·min^{-1}		Single heating at 300 °C·min^{-1}	
Sample	Exp.	Position [°C]	Size [J·g^{-1}]	Position [°C]	Size [J·g^{-1}]	Position (°C)	Size [J·g^{-1}]
PNTP	V0	2.5	27.3	2.4	24.0	27.7	17.9
PNTP	V1	−5.8	10.1	−6.6	7.8	15.7	14.2
PNTP	V2	−14.0	3.6	−14.0	0.9	–	–
PNTP	V3	–	–	–	–	–	–

Macromolecular Journals
Macromol. Mater. Eng. **2013,** DOI: 10.1002/mame.201200460

The existence of freezable water at higher moisture content is consistent with other protein systems used to make plastics. For example, in DSC of sunflower proteins and extruded soy proteins, such a peak appears at about 26% moisture and the T_g merges with or is obscured by this peak.[14,15] It is interesting that as a greater mass of water is replaced by TEG this separate freezable phase decreases. The existence of a freezable plasticizer phase implies hydrogen bonding of plasticizer molecules with each other, rather than between protein chains. For the same mass, TEG has fewer H-bonding sites than water (Table 1). This may mean that saturation of available hydrogen bonding sites on the protein is not occurring at 30 pph_{BM} water/30 pph_{BM} TEG whereas it does at 60 pph_{BM} water. Alternatively, the reduction in peak size could be due to the amphiphilic nature of TEG having a compatibilising effect between the water and protein.

An implication of this separate freezable phase is that there may be more water in the formulation than is required for successful extrusion. If all available H-bonding sites on the protein are bound to plasticizer, further plasticisation may be unnecessary. The formulation containing 30 pph_{BM} TEG could still be extruded and injection moulded successfully, even though there are fewer plasticizer H-bonding sites (Table 4) available and no separate phase. It should, however, be noted that some protein/protein H-bonding is desirable to impart strength. Furthermore, saturation of available H-bonding sites on a folded protein does not mean a complete lack of protein/protein H-bonding interactions. Even in solution, with vast excess water, native proteins are stabilized into a folded confirmation by a variety of interactions, including H-bonding along or between chains. These interactions stabilize ordered secondary structures, such as α-helices and β-sheets. This was investigated further using X-ray scattering.

3.1.3. WAXS

X-ray scattering enables estimation of inter-chain distances (d) in glassy polymers. This is done by identifying peak positions in the inter-chain correlations region (1–2.5 $Å^{-1}$) of the WAXS scattering vector s, where $s = 4\pi \sin\theta/\lambda$.[16] For the wavelength used in this study, this corresponds to a 2θ range of approximately $5 - 35^\circ$. Using Braggs law ($n\lambda = 2d \sin\theta$), the scattering angle of these peaks can be related to inter-chain distances. Two such peaks are typical in proteins, found at $2\theta \approx 8 - 9^\circ$ ($d \approx 10$ Å) and 19° ($d \approx 4$–5 Å) for the wavelength used in this study. The first is attributed to inter-helix packing in helix rich proteins and inter-sheet separation in beta sheet rich proteins. The second peak is similarly attributed to either hydrogen bonding along the backbone in helices, or to bonding between strands in β-sheets.[17] Both were seen in thermoplastics derived from bloodmeal (Figure 5). The former peak reduced in size when TEG was included, suggesting some disruption to the packing of ordered secondary structures when TEG was included. The peak at $2\theta = 19^\circ$ demonstrated that even in the presence of enough plasticizer to form a freezable phase, protein/protein H-bonding interactions were maintained, at least at room temperature.

To further clarify, a Gaussian peak representing scattering by amorphous regions was fitted under the curve and used to estimate the degree of crystallinity (Table 6). Bloodmeal and PNTP without TEG showed similar degrees of crystallinity. Crystallinity increased with a small amount

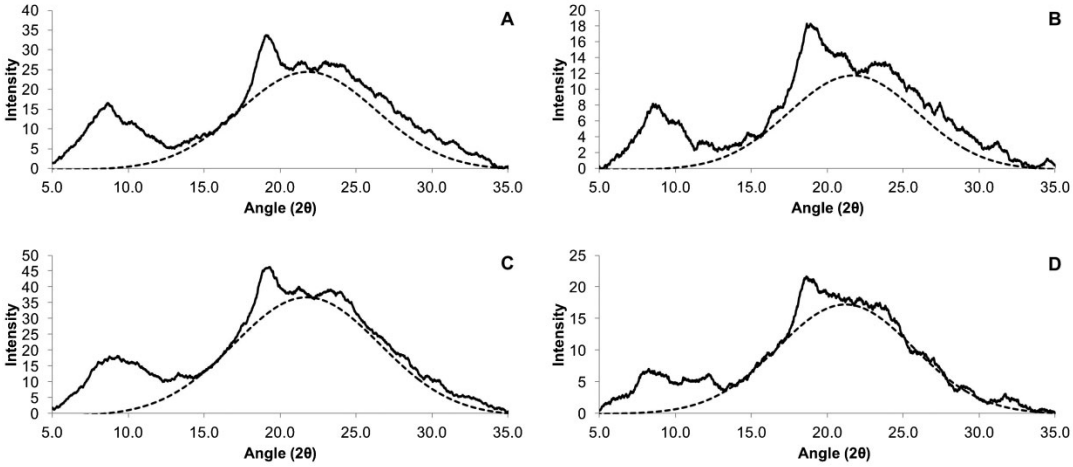

Figure 5. WAXS scattering for PNTP with (A) 0 pph_{BM} TEG, (B) 10 pph_{BM} TEG, (C) 20 pph_{BM} TEG, 30 pph_{BM} TEG.

Table 6. Estimated crystallinity from WAXS of PNTP.

Sample	Exp.	Crystallinity [%]	Halo centre (2θ) [°]
SBM	–	35	22.0
PNTP	V0	34	21.8
PNTP	V1	39	21.7
PNTP	V2	26	21.7
PNTP	V3	22	21.2

of TEG and then decreased as more was added. This suggests that including TEG disrupted some protein/protein interactions prior to extrusion that were not disrupted by water and the other additives alone. This may be due to the increased compatibility between TEG and protein because it is amphiphilic.

3.1.4. FT-IR

FT-IR spectra for fully processed plastic showed a peak between 1040 and 1090 cm^{-1} in samples with TEG which was not present in samples without TEG (Figure 6A). This peak was thought to be due to the C–OH functional groups in TEG. The amide I region, corresponding to C═O stretching, also changed shape when TEG was included, with the emergence of a secondary peak at lower wavenumber (Figure 6B). This is indicative of stronger hydrogen bonding interactions reducing electron density in the C═O bond.[18] The amide III region, which occurs due to in phase N–H bending and C–N stretching, also changed shape (Figure 6C). The most prominent feature in this region was a peak thought to be a convolution of overlapping absorbance of beta sheets (1220–1250 cm^{-1}) and random coils (1250–1270 cm^{-1}).[19] Consistent with the decrease in crystallinity seen in WAXS, this convoluted peak changed shape further towards wavenumbers corresponding to random coils. Together, this suggests that strong H-bonding interactions with the plasticizer replaced protein/protein H-bonding interactions, leading to a more random structure.

3.2. Compositional Effects

Based on the previous discussion, it is clear that TEG had a plasticising effect on bloodmeal-based thermoplastics, and was retained in the material after conditioning. Different amounts of TEG may be used to tailor properties as desired. However, the results have also suggested that including TEG disrupts protein/protein H-bonding prior to extrusion. This may mean less urea or water is required in the final product formulation.

A TEG content of 20 pph_{BM} was chosen as a reference to assess the affect of varying levels of the other additives in CNTP. It was found that at this level of TEG, the effect of urea was quite significant. The 16 formulations assessed as part of this factorial experiment could clearly be divided into two broad groups with respect to tensile properties (Figure 7). Samples with 15 pph_{BM} urea had a higher elongation at break and reduced strength compared to samples containing 5 pph_{BM} (Table 7). The same grouping was apparent from DMA results where samples with the higher level of urea showed a lower and broader thermal transition (peak in tan δ) than samples containing 5 pph_{BM}

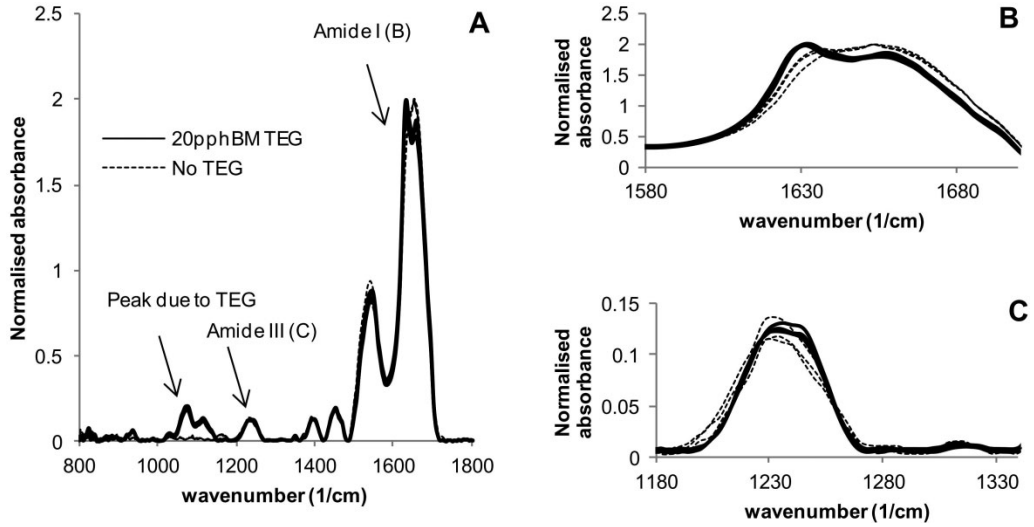

Figure 6. S-FT-IR spectra for processed bloodmeal-based thermoplastics, with and without TEG.

Macromolecular Journals
Macromol. Mater. Eng. **2013,** DOI: 10.1002/mame.201200460

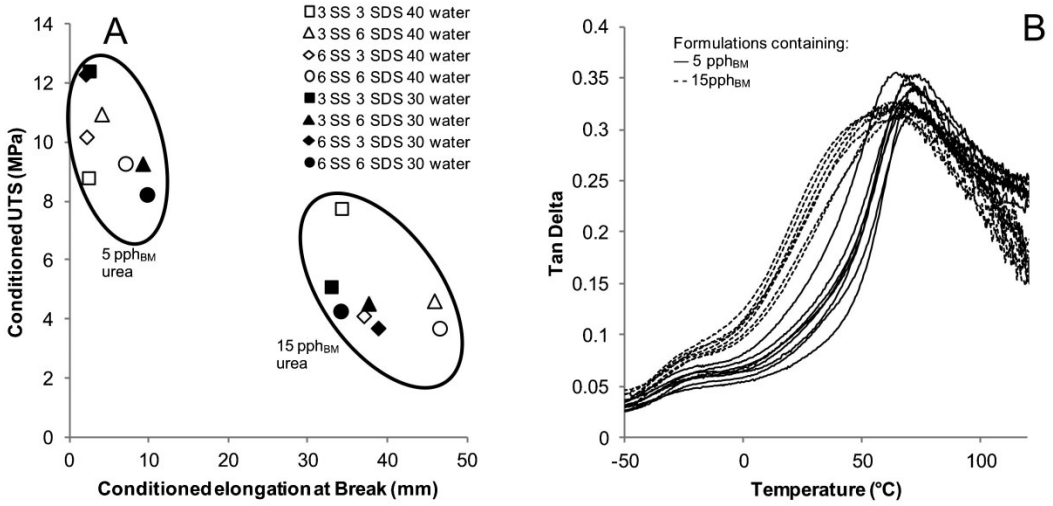

Figure 7. Grouping of factorial experiment results showing clusters based on urea content; (A) mechanical properties, (B) tan δ.

(Table 7). This would suggest that urea, TEG and water can be considered as plasticizers in this context.

Although the importance of urea was clear from Figure 7, the influence of other additives was less obvious but can be explored using analysis of variance (ANOVA). As expected, urea contributed significantly ($p < 0.05$) to changes in T_g and had the largest percentage contribution at the additive levels tested. SDS level was also significant, but had much smaller percentage contribution than urea (Table 8).

Table 7. Mechanical properties (average of 5 and standard deviations) and glass transition temperature of conditioned plastics, varying additive levels.

					UTS [MPa]		Elongation at break [mm]		1 Hz T_g [°C]	Moisture [%]
Formulation	Urea [pph_{BM}]	Water [pph_{BM}]	SS [pph_{BM}]	SDS [pph_{BM}]	Mean	Std. dev.	Mean	Std. dev.	(peak in tanδ)	
F1	15	40	3	3	7.7	0.2	34.3	4.1	61.6	7.6
F2	15	40	3	6	4.6	0.2	45.9	2.1	64	7.4
F3	15	40	6	3	4.1	0.5	37.1	2.3	69.3	8.1
F4	15	40	6	6	3.7	0.1	46.6	2.3	63.5	8.3
F5	15	30	3	3	5.1	0.4	33.0	4.7	67.2	7.5
F6	15	30	3	6	4.5	0.2	37.7	5.7	65.7	7.4
F7	15	30	6	3	3.7	0.1	38.9	2.4	60.8	8.7
F8	15	30	6	6	4.3	0.3	34.1	3.9	59.8	8.0
F9	5	40	3	3	8.8	1.3	2.4	0.6	72.4	6.9
F10	5	40	3	6	11.0	0.5	4.1	1.0	72.2	6.9
F11	5	40	6	3	10.2	0.7	2.2	0.2	72.9	6.8
F12	5	40	6	6	9.3	0.9	7.1	3.0	70.6	6.9
F13	5	30	3	3	12.4	0.9	2.5	0.3	70.7	6.9
F14	5	30	3	6	9.3	0.5	9.2	5.0	68.7	7.1
F15	5	30	6	3	12.3	0.7	2.1	0.1	72.7	6.9
F16	5	30	6	6	8.2	0.5	9.8	2.9	65	7.5

Table 8. ANOVA *p* values and ^{2} values for effect size on conditioned properties. Values found to be significant at the 95% confidence interval are in bold.

	***p* Value**					**Contribution [%]**				
Property	**Urea**	**Water**	**SS**	**SDS**	**Error**	**Urea**	**Water**	**SS**	**SDS**	**Error**
T_g (1 Hz tan δ)	0.00	0.18	0.49	0.13	0.00	59	5	1	7	28
UTS	0.00	0.85	0.00	0.00	0.00	78	0	2	4	16
Elongation at break	0.00	0.10	0.25	0.00	0.00	92	0	0	2	6

Urea, SDS and SS contributed significantly to changes in mechanical properties, although urea had the largest percentage contribution. This demonstrated that H-bonding was still the most important interaction determining mechanical properties and that there were sufficient available H-bonding sites after TEG was added for urea to have a significant contribution.

Between the two levels of water considered, the amount added to the sample prior to extrusion did not contribute significantly to changes in T_g and mechanical properties. This can be expected as water is removed during conditioning. However, in previous work the amount of processing water was significant when TEG was excluded, suggesting a minimum level of plasticisation is necessary for processing.[5] Current work would suggest that TEG can partially replace water required for processing.

Figure 8 shows changes in group-means caused by factors found to be significant using ANOVA. SDS and SS should be used at 3 pph_{BM} to maximize mechanical properties and reduce T_g. Using 5 pph_{BM} urea resulted in a low elongation at break, whereas 15 pph_{BM} had reduced strength. An intermediate quantity of 10 pph_{BM} urea is recommended as a tradeoff between strength and ductility. Even though water content was insignificant, its effect on processing has not been considered. The amount of water present during processing may affect properties such as melt viscosity, which could influence the types of products that can be produced. It

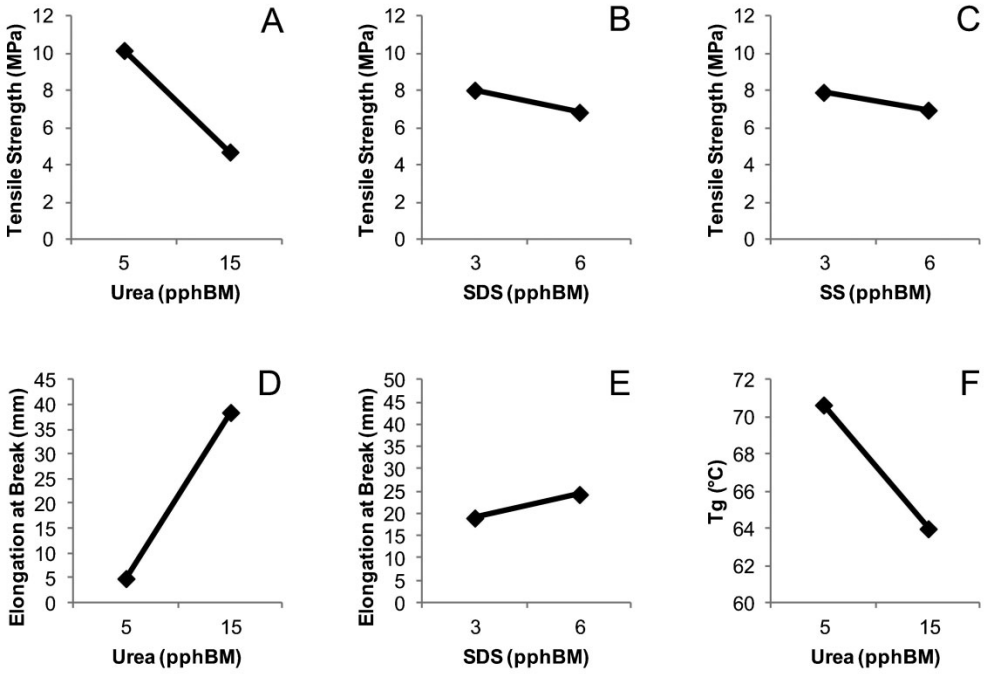

Figure 8. Significant effects on group means from ANOVA. (A) Influence of urea on tensile strength, (B) influence of SDS on tensile strength, (C) influence of SS on tensile strength, (D) influence of urea on elongation at break, (E) influence of SDS on elongation at break, (F) influence of urea on T_g.

Macromolecular Journals
Macromol. Mater. Eng. **2013,** DOI: 10.1002/mame.201200460

is recommended that such effects be investigated further in future work.

4. Conclusion

DMA and DSC of pre-extruded material revealed that unbound water can form a distinct phase in NTP. As water is replaced with TEG this phase separation is reduced such that at equal proportions of TEG and water there was no longer a separate phase present. This implies that the interactions between TEG and proteins are stronger than between water and protein. This was also supported by X-ray scattering results for pre-extruded material, which showed decreasing crystallinity as the proportion of TEG increased. The decrease in crystallinity suggests TEG was more disruptive to ordered secondary structures, which are stabilized by H-bonding interactions, than by water and the other additives alone. FT-IR confirmed that stronger H-bonding was seen when TEG was included, evidence of protein-plasticizer H-bonding interactions replacing a portion of protein/protein interactions.

TEG has a plasticising effect, reducing tensile strength and glass transition temperature, but increasing ductility. Materials with 10, 20 or 30 pph_{BM} TEG were ductile after conditioning with increased strain at break and toughness. ANOVA revealed that urea was the most significant factor influencing the conditioned material's properties at a constant TEG content. This suggested that even at that level of TEG plasticisation, hydrogen bonding between chains is still the most important factor influencing NTP mechanical properties.

The implication of the above findings is that a range of materials with varying ductility and strength after conditioning can be produced by changing the additive levels. With 40 pph_{BM} water, 20 pph_{BM} TEG, 10 pph_{BM} urea, 3 pph_{BM} SDS and 3 pph_{BM} SS, a material is produced with strength intermediate of the formulations used in this study, but with much higher toughness than conditioned samples without TEG.

Acknowledgements: The FT-IR portion of this research was undertaken on the infrared microspectroscopy beamline at the Australian Synchrotron, Victoria, Australia. Proposal number AS113/IRMFI/4267. The authors would especially like to acknowledge the technical assistance of Dr. Mark Tobin. Travel funding support was received from the New Zealand Synchrotron Group Ltd. The authors wish to thank Velram Balaji Mohan for assistance in sample preparation and mechanical testing in the factorial experiment.

Received: December 21, 2012; Revised: March 13, 2013; Published online: DOI: 10.1002/mame.201200460

Keywords: glass transitions; mechanical properties; plasticization; proteins; thermoplastics

[1] C. J. R. Verbeek, L. E. van den Berg, *Macromol. Mater. Eng.* **2010**, *295*, 10.
[2] C. J. R. Verbeek, C. Viljoen, K. L. Pickering, L. E. van den Berg, (Waikatolink Ltd.), NZ 551531, **2009**.
[3] C. J. R. Verbeek, L. E. van den Berg, *J. Polym. Environ.* **2010**, 1.
[4] L. di Gioia, S. Guilbert, *J. Agric. Food Chem.* **1999**, *47*, 1254.
[5] C. J. R. Verbeek, L. E. van den Berg, *Macromol. Mater. Eng.* **2011**, *296*, 524.
[6] M. Pommet, A. Redl, S. Guilbert, M.-H. Morel, *J. Cereal Sci.* **2005**, *42*, 81.
[7] X. Mo, X. Sun, *J. Polym. Environ.* **2003**, *11*, 15.
[8] A. Jerez, P. Partal, I. Martinez, C. Gallegos, A. Guerrero, *Rheol. Acta* **2007**, *46*, 711.
[9] M. Pommet, A. Redl, M. H. Morel, S. Guilbert, *Polymer* **2003**, *44*, 115.
[10] ASTM International. *D638-03 Standard Test Method for Tensile Properties of Plastics*, ASTM International, West Conshohocken, PA, USA **2004**.
[11] P. G. Royall, C. Y. Huang, S. W. J. Tang, J. Duncan, G. Van-de-Velde, M. B. Brown, *Int. J. Pharm.* **2005**, *301*, 181.
[12] K. L. Ngai, M. Paluch, *J. Chem. Phys.* **2004**, *120*, 857.
[13] J. M. Bier, C. J. R. Verbeek, M. C. Lay, *J. Therm. Anal. Calorim.* **2012**, 1.
[14] A. Rouilly, O. Orliac, F. Silvestre, L. Rigal, *Polymer* **2001**, *42*, 10111.
[15] J. Zhang, P. Mungara, J. Jane, *Polymer* **2001**, *42*, 2569.
[16] A. Elicegui, J. J. Del Val, J. L. Millan, C. Mijangos, *J. Non-Cryst. Solids* **1998**, *235*, 623.
[17] W. M. Elshemey, A. A. Elfiky, W. A. Gawad, *Protein J.* **2010**, *29*, 545.
[18] M. Jackson, H. H. Mantsch, *Crit. Rev. Biochem. Mol. Biol.* **1995**, *30*, 95.
[19] S. W. Cai, B. R. Singh, *Biophys. Chem.* **1999**, *80*, 7.

5

Identifying Transition Temperatures in Bloodmeal-Based Thermoplastics Using Material Pocket DMTA

A paper

Published in

Journal of Thermal Analysis and Calorimetry

by

JAMES M. BIER[1], C.J.R. VERBEEK AND M.C. LAY

[1]As first author for this paper, I prepared the initial draft manuscript, which was refined and edited in consultation with my supervisors, who have been credited as co-authors. I prepared all of the samples tested, ran all the DMA scans and processed the data to the form in which it is presented.

J Therm Anal Calorim (2013) 112:1303–1315
DOI 10.1007/s10973-012-2680-0

Identifying transition temperatures in bloodmeal-based thermoplastics using material pocket DMTA

J. M. Bier · C. J. R. Verbeek · M. C. Lay

Received: 8 June 2012 / Accepted: 31 August 2012 / Published online: 29 September 2012

Abstract Bloodmeal can be used to manufacture thermoplastics, but requires water, urea, sodium sulphite, and sodium dodecyl sulphate to modify chain mobility. Transition temperatures of bloodmeal, modified bloodmeal, and processed bloodmeal-based thermoplastics were compared using material pocket dynamic mechanical thermal analysis. The glass transition temperature (T_g) of bloodmeal dropped from 493 to 263 K using only water as a plasticizer but was restored when freeze dried. Modifying bloodmeal lowered T_g to 193 K. This was raised by drying, but not to that of unmodified bloodmeal indicating a permanent change. Three additional transitions were identified above T_g, for modified bloodmeal between 300 and 480 K. These were thought to be transitions of dehydrated bulk amorphous regions, amorphous regions between crystallites and chains segments in crystallites and were also seen at lower temperatures when replacing some water with triethylene glycol (TEG). Material pockets increased resolution in processed samples. One broad T_g was observed in consolidated bars, at 335 or 350 K with or without TEG. In material pockets, these resolved into three transitions, similar to those observed before processing. Changes in relative magnitudes suggested some chain rearrangement leading to more bulk amorphous regions. Differences were detected between onset of drop in storage modulus and peaks in loss modulus and tan δ in pockets or bars, but generally led to the same conclusions. For bar samples, it was helpful to compare natural and log modulus scales. Good practice would use all these techniques in parallel to correctly identify relaxation temperatures.

J. M. Bier (✉) · C. J. R. Verbeek · M. C. Lay
School of Engineering, University of Waikato, Private Bag 3105, Hamilton 3240, New Zealand
e-mail: Jmb101@waikato.ac.nz

Keywords Relaxation · Dynamic mechanical thermal analysis (DMTA) · Thermoplastic protein · Bioplastics · Glass transition

Introduction

Environmental concerns regarding conventional plastics have led to the development of bio-based alternatives using proteins or polysaccharides. Thermoplastics have been produced from plant and animal proteins, including wheat gluten, soy, sunflower, corn, gelatine, keratin, casein, whey and bloodmeal [1]. Bloodmeal is highly denatured protein that is readily available as a by-product of the meat processing industry. Protein crosslinking induced by heat treatment prevents the formation of an extrudable melt from bloodmeal and water alone [2]. Sodium sulfite (SS), sodium dodecyl sulfate (SDS) and urea are also added. SS disrupts chemical crosslinking (by reducing disulfide bonds) and SDS disrupts hydrophobic interactions. Urea, a protein denaturant, disrupts secondary structures such as beta sheets [3]. The combination of these modifies bloodmeal into a thermoplastic which can be extruded and injection moulded [2, 4, 5]. Extrusion relies on the material having a low enough glass transition temperature (T_g) for large scale chain rearrangements without protein degradation at the processing temperature [1]. The T_g can be modified further by adding additional plasticisers such as polyols.

Dynamic mechanical thermal analysis (DMTA) is a well-known technique for detecting thermal transitions in polymers by measuring the response of a sample to an oscillating force while varying frequency or temperature. For viscoelastic materials, the response is described by the complex modulus (E^*) which is made up of two components, the storage modulus (E') and the loss modulus (E'').

The ratio of E''/E' is called tan δ and used as a measure of mechanical damping. Typically, for an amorphous polymer, E' drops rapidly by two orders of magnitude, while E'' and tan δ show maxima at the onset of large scale co-operative chain movements seen as the T_g. At lower temperatures, smaller drops in E' and accompanying peaks or shoulders in E''/tan δ relate to the onset of shorter range chain movements. A key advantage of DMTA is sensitivity to relaxations near or below the glass transition [6] and the ability to identify these additional transitions that are not apparent in DSC or thermo-mechanical analysis (TMA) [7].

A newer application of DMTA is the use of material pockets which allow powders and other non-self-supporting samples to be analysed [8]. The technique relies on the metal pocket behaving elastically within the temperature and frequency range studied and that any tan δ peak observed is due to relaxation in the pocket's contents [9]. This is a reasonable assumption as the pocket has a modulus several orders of magnitude higher than the contents. Such pockets are now commercially available from Tritech and Perkin Elmer, and have been used to successfully identify glass transitions and study relaxation behaviour of freeze-dried proteins [10], carbohydrates [8, 11], milk powders [12], solutions containing bio-materials [13] and thermosetting resins [14]. The technique has been mostly applied to pharmaceutical or food-based materials, with only a few studies concerned with plastics [9, 14], none of which considering protein-based thermoplastics.

The objective of this paper was to investigate the use of material pocket DMTA to determine transition temperatures in thermoplastic proteins derived from bloodmeal. In particular, the relaxation behaviour of bloodmeal, modified bloodmeal (pre-processed thermoplastic) and the resultant thermoplastic were compared using powdered samples. Analysing bloodmeal and modified bloodmeal required the material pocket as these materials are only available in powder form. As a comparison, solid bars (i.e. injection moulded thermoplastics) of the resultant product were also analysed.

A further objective was assessing the validity of various methods of identifying relaxation temperatures, specifically relating to the material pocket. Different techniques used were the peak in tan δ, onset of drop in storage modulus (E') or peak in loss modulus (E''). These can typically vary by 10–25 °C [7]. One of the challenges of interpreting DMTA results is the inconsistent use of these identification techniques. In Table 1, a summary is given of the techniques used to identify transition temperatures in studies where the material pocket was used [8–20].

Several earlier studies have demonstrated that T_g values obtained by material pocket DMTA show agreement with other mechanical and calorimetric techniques (Table 1) and validation using other thermal techniques has not been repeated in this work.

Methods

Materials and sample preparation

Thermoplastic protein was produced from bloodmeal using a patented process [4], with and without tri-ethylene glycol (TEG) as plasticizer. 20 g urea (Ballance Agri-nutrients), 6 g sodium dodecyl sulphate (SDS) (Merck) and 6 g sodium sulphite (SS) (Ajax Finechem) were dissolved in 120 g distilled water at 50 °C. The solution was mixed with 200 g sieved bloodmeal (Wallace Corporation) in a high speed mixer for 10 min. To prepare the material with TEG, the amount of water was reduced to 80 g, and 40 g of TEG (Merck) was added after the first 6 min of blending. The resultant mixtures were stored below 4 °C overnight in sealed plastic bags. Sample descriptions, compositions in parts per hundred bloodmeal (pph_{BM}) and abbreviations are shown in Table 2. WBM was prepared in the same manner as PPM and PPM–TEG, but with 60 pph_{BM} distilled water as the only additive.

The mixtures were extruded in a Thermoprism TSE-16-TC twin screw extruder at 150 RPM. The temperature settings were 70, 100, 100, 100, and 120 °C from feed zone to die. Granulated extrudate was injection moulded into Type 1 tensile test specimens [21] using a BOY-35A injection moulder with a temperature profile of 100, 115, 120, 120, 120 °C from feed zone to die and a screw speed of 200 RPM. The injection pressure was set to 110 bar in profile sections 0–4 and 30 bar in sections 5–7. The mould was heated to 70 °C using water. Injection moulded specimens were conditioned in a humidity chamber set to 23 °C and 50 % relative humidity for a minimum of 7 days prior to testing.

All samples were tested at their respective moisture contents after conditioning or as freeze-dried powders (Table 2). Samples were dried over two nights in a Freezone® 2.5 Litre Benchtop freeze dryer (Labconco Corporation, Kansas City) set to auto mode (Collector temperature −50 °C, vacuum <11 Pa).

Dynamic mechanical thermal analysis

Samples were tested in single cantilever mode using a DMA 8000 (Perkin Elmer) fitted with a high temperature furnace and controlled with DMA software version 14306. The instrument was cooled to below 173 K by evaporation of liquid nitrogen after mounting each sample. Evaporated nitrogen was then fed back into the chamber as a purge gas. Experiments were performed at a programmed heating rate

Table 1 Published studies making significant use of the material pocket DMTA technique

Year/citation	Materials analysed	Method of determining T_g from material pocket DMTA	Other techniques used to validate T_g values[a]
2005 [8]	Lactose	Peak in tan δ	MDSC
2005 [15]	Celocoxib	Peak in tan δ	DSC
2007 [14]	Benzoxazine monomers	Peak in tan δ	DEA
2008[11]	Xanthan powder	Peak in tan δ	PTA DSC/T_g not seen
2009 [10]	Hen egg white lysozyme, bovine pancreatic ribonuclease A, ovalbumin, bovine serum albumin, sucrose, trehalose and hydroxyethyl starch	Peak in tan δ and onset of E' drop both shown. Onset of drop used for fitting	DSC/HDSC, TMA
2008 [16]	Poly(D,L-lactic acid), neat and blended with cyclodextrin	Peak in tan δ	DSC
2009 [9]	Poly(D,L-lactic acid), neat and blended with cyclodextrin	Peak in tan δ	None
2010 [17]	Ball-milled cellulose	Peak in tan δ	DSC
2010 [18]	Pharmaceuticals and polymer blends	Not stated	DSC
2010 [13]	Human serum albumin, porcine heparin, trehalose, lactose, dextran, influzena antigen, and neat human plasma analysed in solution	Peak in tan δ	MDSC
2010 [6]	Milk powders with varying lactose and protein contents	Onset of E' drop	DEA
2011 [12]	Milk powders withvarying lactose and protein contents	Peak in E''	DEA
2011[19]	Skim milk/maltodextrin systems	Peak in E''	DSC
2011 [20]	Phosphate based 2-hydroxyethyl methacrylate hydrogels	Peak in tan δ	DSC

[a] Technique abbreviations: *DSC* differential scanning calorimetry, *MDSC* modulated DSC, *HDSC* hyper DSC, *DEA* dielectric analysis, *TMA* thermomechanical analysis, *PTA* phase transition analysis

Table 2 Sample formulations used and their abbreviations

Sample description	Sample formulation/pph_{BM}						Abbreviation	Moisture content[a]	Moisture content/freeze dried[b]
	Bloodmeal	Water	Urea	SS	SDS	TEG			
Sieved bloodmeal	100						SBM	7.2 %/TG	N/A
Wet bloodmeal	100	60					WBM	40 %/TG	3 %/TG
Pre-processed thermoplastic protein without TEG	100	60	10	3	3	0	PPM	35 %/TG	5.5 %/TG
Pre-processed thermoplastic protein with TEG	100	40	10	3	3	20	PPM–TEG	28 %/TG	5.2 %/TG
Moulded thermoplastic protein	PPM extruded, injection moulded and conditioned at 23 °C and 50 % relative humidity.						MTP	7.9 %/oven drying	6.5 %/TG
Moulded thermoplastic protein with TEG	PPM–TEG extruded, injection moulded and conditioned at 23 °C and 50 % relative humidity						MTP–TEG	8.4 %/oven drying	3.1 %/TG

[a] Method used to determine moisture content shown in brackets

[b] Moulded bar samples were ground prior to freeze drying

of 2 K min^{-1} up to 523.15 K for powders. For self-supporting bars, the stiffness drops before this and samples were stopped at 393.15 K. Self-supporting samples were cut from larger injection moulded pieces with approximate geometry of 3.5 × 6.5 × 30 mm. Powder samples were analysed by mounting ~50 mg powder in ~1.0 × 7.4 × 28 mm (folded dimensions) material pockets (Perkin Elmer) [8] which were then crimped with pliers. Material pockets and self-

supporting samples were tested using a free length of 12.5 mm and a dynamic displacement of 0.05 mm at 0.1, 0.3, 1, 3 10, and 30 Hz.

Multi strain scans of sieved blood meal (SBM) were also performed at 1 Hz with displacements from 0.01 to 0.1 mm confirming that at the displacement of 0.05 mm was within the linear elastic region across the temperatures tested. All samples were weighed before and after testing to determine any mass loss.

Transition temperatures determined at different frequencies were examined for their correlation to the modified Arrhenius equation [6, 8]:

$$\ln f = \ln A - \left[\frac{E_A}{RT}\right], \quad (1)$$

where f is the test frequency, A is the pre-exponential factor, E_A is the Arrhenius activation energy, R is the universal gas constant and T transition temperature determined from peak in tan δ, onset of drop in E' or peak in E'' at test frequency (K).

Moisture content

Moisture content of powdered samples was assessed using thermogravimetic analysis (TG) in a Texas Instruments SDT 2960 analyser. Approximately, 10 mg powdered sample was placed in the sample crucible and heated at 10 K/min from room temperature to 873 K under constant air flow. Moisture content was determined from the cumulative mass loss up to 393 K.

The moisture content of injection moulded samples was determined gravimetrically by oven drying for 24 h at 376 K and recording the mass loss before and after drying.

Results and discussion

Thermoplastic processing techniques such as extrusion and injection moulding require a polymer to be in a molten state, or several Kelvin above its softening point. This would imply a temperature above the material's T_g if it is amorphous or the melting point for crystalline or semi-crystalline materials. To evaluate the additives efficiency at reducing the processing temperature, thermal transitions in bloodmeal were compared to those in modified bloodmeal (pre-extruded thermoplastic protein) as well as to bloodmeal with additional water added.

Bloodmeal and modified bloodmeal

From Fig. 1a, three peaks in tan δ were apparent for bloodmeal (labelled $T_i - T_{iii}$ from left to right). Although E' and E'' represent composite moduli of the pocket and the polymer, peaks in E'' and the onset of the drop in E' were consistent with the tan δ peaks. T_i, at 182.4 K, was thought to be a gamma relaxation, involving side chains or very small portions of main chains.

The temperature of T_{ii} at 336 K is similar to the denaturation temperature of haemoglobin or bovine serum albumin in solution [22, 23]. However, bloodmeal is already denatured and is a dehydrated protein with only 7 % moisture. It was thought that this was a β-relaxation, relating to onset of similar, but shorter range motions to the T_g. β-relaxations typically obey an Arrhenius relationship over a broad frequency range [24]; however, T_{ii} in bloodmeal did not (Table 3). It was thought that the loss of residual water during testing up to this temperature obscured the frequency dependence of this transition.

Bloodmeal's T_{iii}, at 493 K, was thought to be the T_g, associated with the α-relaxation, indicating the onset of large range chain motions. Good correlation with the Arrhenius equation ($r^2 > 0.99$) indicated a frequency dependence characteristic of long-range chain relaxation (Table 3). However, TG revealed the onset of significant mass loss immediately beyond this temperature (Fig. 2). Degradation would prevent processing at temperatures near this T_g, requiring plasticisers to lower the T_g to a temperature well below 393 K.

Using 60 pph_{BM} water as plasticiser, a peak in tan δ was found at $T_i = 263$ K (Fig. 1b). Although the temperature of this transition decreased at lower frequencies, it did not fit an Arrhenius frequency relationship (Table 3). This peak was thought to be a hybrid of the T_g of water plasticised protein, and the melting of any bulk or free water in the sample. Melting of bulk water has previously been shown to exhibit a peak just below 273 K at 1 Hz in material pocket DMTA [11]. In DSC studies of sunflower proteins and extruded soy proteins, no peak for freezable water was seen below about 26 % moisture [25, 26]. Above this moisture content, it appears the T_g is obscured [25], or merges with the peak for water melting [26]. Wet bloodmeal contained about 40 wt% water so this is likely also the case here. The significant drop in storage modulus in the same temperature region further supported the conclusion that this peak was indeed the plasticised T_g.

At higher temperature, T_{iv} for WBM was thought to be the dry T_g of bloodmeal after evaporation of water during testing. A small minima in tan δ was also seen around 350–360 K with an associated peak in E' at $T_{iii} = 366$ K. This dip gave rise to what appeared to be two peaks in tan δ (T_{ii} and T_{iii}). In gluten-based plastics, a drop in tan δ and increase in modulus were seen as evidence of denaturation by means of crosslinking [27]. Although bloodmeal is already denatured and crosslinked, this behaviour is reminiscent of cured thermosetting resins, which exhibit additional crosslinking on heating [7]. If this is the case, it

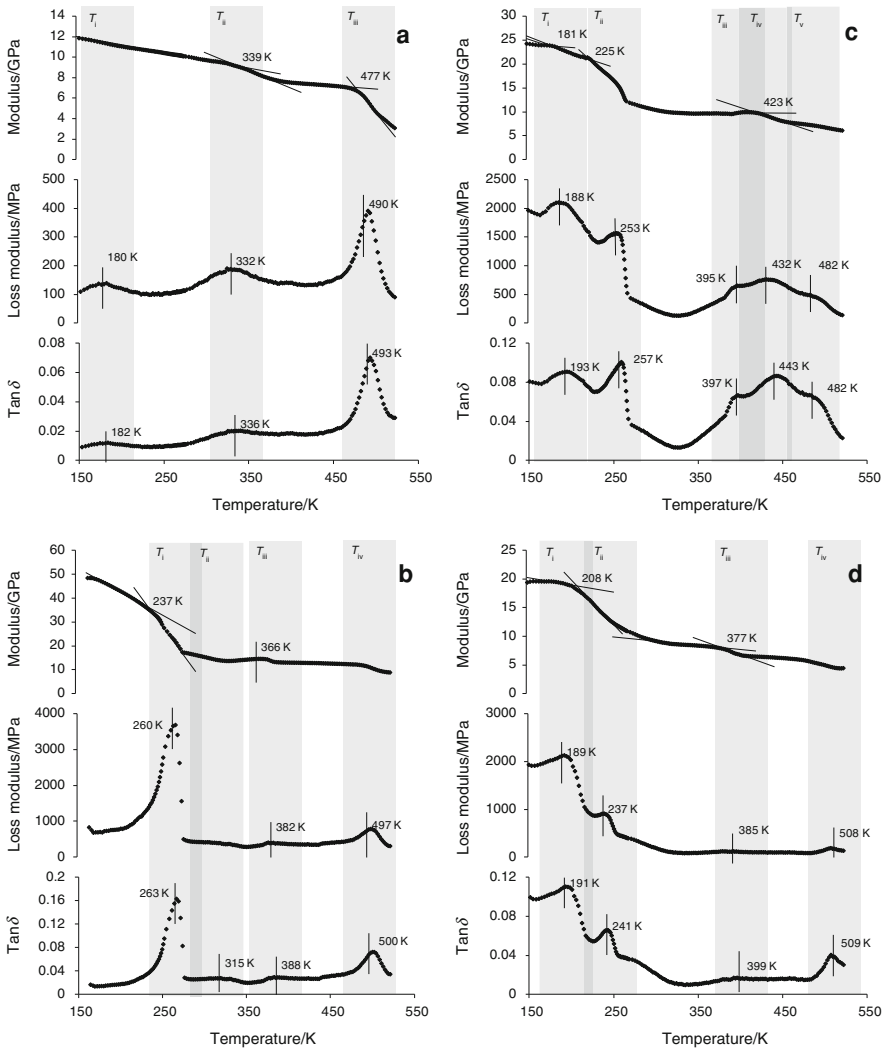

Fig. 1 Representative 1 Hz DMTA data for: **a** sieved bloodmeal, **b** sieved bloodmeal plus 60 pph_{BM} water, **c** pre-processed material without TEG and **d** pre-processed material with TEG

would be expected that the storage modulus show little drop at the end of the rubbery plateau, similar to synthetic crosslinked polymers. However, such effects are obscured as the pocket supporting the sample also restricts the drop in modulus.

It has previously been demonstrated that the plasticising effect of water alone was not enough to allow bloodmeal to be processed via extrusion [2]. Although a transition region is seen below 273 K in wet bloodmeal, excessive cross-linking will prevent thermoplastic flow. This required the use of additional additives for processing.

Figure 1c shows the DMTA trace for modified bloodmeal (PPM). As with wet bloodmeal, there is a peak in tan δ, a little below the freezing point of water ($T_{ii} = 257$ K). There was also an additional peak (T_i) at 193 K detected also as a peak in E'' and a drop in E'. It was thought that T_{ii} represents melting of unbound water, depressed due to colligative interactions with protein chains, with T_i the glass transition of PPM, lowered by the addition of urea, SDS and sodium sulphite. These additives reduce chain interactions and would increase the free volume by increased chain mobility. The behaviour was similar to native BSA, which is one of the components of bloodmeal. The T_g of BSA determined by DSC as been shown to be 193 K at a water content allowing free water to crystallise [28].

At high temperatures, behaviour is more complex. Three peaks were seen above 390 K, by which stage water was expected to have evaporated, compared to only one peak in SBM and WBM. The central peak (T_{iv} in Fig. 1c) showed very good agreement with the Arrhenius equation over a temperature range of >30 K with the frequencies tested (Table 3). It was thought that this was the main dry

Table 3 Transition temperatures identified from peaks in tan δ in bloodmeal and pre-processed material

Sample	Figure label	Temperature/K for each frequency/Hz						Fits to Arrhenius model		
		0.1	0.3	1	3	10	30		E_A/kJ/mol	r^2
SBM	T_i	n/a	176	**182**	189	195	197	Yes	59	0.964
	T_{ii}	338	337	**336**	336	340	342	No	n/a	n/a
	T_{iii}	488	490	**493**	496	499	504	Yes	754	0.983
WBM	T_i	257	261	**263**	264	265	265	No	n/a	n/a
	T_{ii}	304	310	**315**	315	317	318	No	n/a	n/a
	T_{iii}	388	388	**388**	388	n/a	386	No	n/a	n/a
	T_{iv}	494	497	**500**	502	506	508	Yes	842	1.000
PPM	T_i	203	195	**193**	192	189	190	No	n/a	n/a
	T_{ii}	252	255	**257**	259	259	260	Yes	352	0.905
	T_{iii}	397	397	**397**	392	398	395	No	n/a	n/a
	T_{iv}	425	434	**443**	449	453	457	Yes	279	0.962
	T_v	479	479	**482**	486	490	497	Yes	587	0.914
PPM–TEG	T_i	191	190	**191**	191	189	187	No	n/a	n/a
	T_{ii}	240	241	**241**	241	239	237	No	n/a	n/a
	T_{iii}	400	400	**399**	399	414	424	No	n/a	n/a
	T_{iv}	497	510	**510**	509	508	501	No	n/a	n/a
FD WBM	T_i	195	199	**205**	210	228	227	Yes	56	0.940
	T_{ii}	346	350	**355**	361	355	353	No	n/a	n/a
	T_{iii}	490	493	**496**	500	504	508	Yes	688	0.996

1 Hz data is in bold. Transitions were deemed to fit to the Arrhenius model over the frequency range tested if $r^2 > 0.90$

Table 4 Transition temperatures identified from peaks in tan δ in freeze-dried bloodmeal and pre-processed material

Sample	Figure label	Temperature/K for each frequency/Hz						Fits to Arrhenius model		
		0.1	0.3	1	3	10	30		E_A/kJ/mol	r^2
FD WBM	T_i	195	199	**205**	210	228	227	Yes	56	0.940
	T_{ii}	346	350	**355**	361	355	353	No	n/a	n/a
	T_{iii}	490	493	**496**	500	504	508	Yes	688	0.996
FD PPM	T_i	n/a	207	**215**	217	227	240	Yes	58	0.956
	T_{ii}	361	366	**360**	363	365	364	No	n/a	n/a
	T_{iii}	419	422	**427**	431	437	443	yes	372	0.994
	T_{iv}	472	472	**477**	477	473	471	no	n/a	n/a
FD PPM–TEG	T_i	199	204	**206**	211	225	229	yes	66	0.948
	T_{ii}	266	266	**269**	275	282	282	yes	176	0.916
	T_{iii}	326	330	**337**	342	347	354	yes	194	0.996
	T_{iv}	506	503	**504**	504	504	504	no	n/a	n/a

1 Hz data is in bold

amorphous glass transition, after the plasticization effect of urea, SDS and SS. The broadness of this peak and the appearance of the two smaller peaks were attributed to the blend proteins in bloodmeal (mainly bovine serum albumin and haemoglobin), each of which is a complex heteropolymer. In both gluten- and soy protein-based plastics with more than one protein subunit, multiple T_gs have been detected [27, 29, 30]. Furthermore, as well as random coils, proteins fold into ordered regions (α-helices and β-sheets) suggesting a semi-crystalline nature, detectable by wide-angle X-ray scattering (WAXS) [31]. Crystallinity both broadens the glass transition [32] and sometimes causes multiple glass transitions, arising from a purely amorphous phase, amorphous material restrained by crystallites, crystal slippage and hindered rotation of chains inside folded crystals [33]. Determination of which transitions correspond to

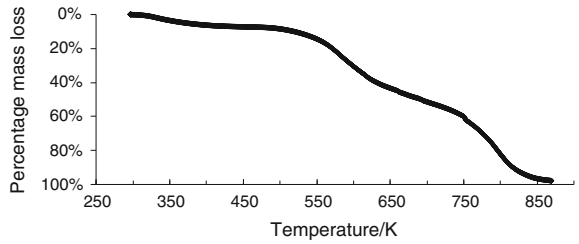

Fig. 2 Mass loss versus temperature for SBM determined by T_gA

each of these possible relaxations is beyond the scope of this paper, but it is important to note that behaviour is not characteristic of one simple amorphous phase.

When TEG was included (Fig. 1d), two peaks in tan δ were again observed below 273 K. T_i, at 191 K, was comparable that seen without TEG and again thought to be the T_g of plasticised proteins in the material. Similarly, it was again thought that T_{ii} could correspond to a bulk freezable plasticiser phase, as the same mass of total plasticiser (water plus TEG) was present. In PPM–TEG, however, T_{ii} dropped further to 241 K, 32 K below the freezing point of water alone. TEG is a known freezing point depressor in aqueous solutions [34], so a plasticiser phase consisting of both water and TEG should have a lower transition temperature than a phase of water alone.

While replacing some water with TEG made only small difference to the low temperature relaxation behaviour, it made a profound difference to above ambient properties. The broad transition, previously centred at 428 K without TEG, was not apparent with TEG. It was thought that TEG increased mobility such that the material was in a rubbery state at this temperature, even after some moisture evaporated. Since TEG is present at a relatively low proportion, a dehydrated T_g was still observed at $T_{iv} = 505$ K.

Using material pockets has enabled chain relaxation behaviour of both bloodmeal and pre-processed modified bloodmeal to be investigated. Large differences in T_g were seen between SBM (493 K) and WBM (263 K) due to the plasticising effect of water. Both PPM and PPM–TEG showed transitions at $\sim$191 K, believed to be the plasticised T_g after the effect of processing additives. Altering the plasticiser composition to replace some water with TEG does not affect the wet T_g, but reduces the dry T_g such that it is not seen after water evaporation during scanning. While water alone is not enough to ensure processibility of bloodmeal, the alpha relaxation of pre-processed thermoplastic protein is heavily influenced by interactions with water. Because of large differences in moisture content (Table 2), samples were freeze dried in subsequent experiments to minimise the effect of water on relaxation behaviour. Further investigation into compositional effects by varying TEG or moisture content are beyond the scope of this paper, but these effects have previously been explored for processed bar samples conditioned at different relative humidity [35].

Freeze-dried pre-processed material

DMTA plots of freeze-dried WBM (Fig. 3a, b) were very similar to SBM (Fig. 1a) suggesting addition of water did not cause any irreversible change in its relaxation behaviour. The shift of T_i and T_{ii} to the right, when compared with SBM is to be expected as moisture content has been reduced from 7 to 3 %, effectively a decrease in plasticisation. This shift confirms that T_{ii} is affected by water, supporting the earlier hypothesis that evaporation could obscure the frequency dependence in this region.

FD PPM (Fig. 3c) showed similar three peak behaviour to its non-freeze-dried counterpart at elevated temperatures, confirming the hypothesis that in PPM these were dry relaxations seen after water evaporation. Again, the middle of these three showed good correlation with the Arrhenius equation over a wide temperature range (Table 4). Below ambient, the freeze-dried sample differed from the wet sample. One low temperature tan δ peak was seen at 215 K. Given the amount of water that has been removed, this will be only a local motion, rather than the long range motions responsible for the peak at 193 K without freeze drying. Minimal drop in modulus in the freeze-dried sample confirmed this. It was, therefore, concluded that T_i and T_{ii} seen earlier in the wet samples (Fig. 2) were glass transitions in water-plasticized protein.

Including TEG further plasticised the freeze-dried material (Fig. 3D), even in the absence of water. The tan δ peak at 337 K (labelled T_{iii}) was considered to be the glass transition, corroborated by a large drop in modulus and good frequency dependence (Table 4). The peak at 269 K (T_{ii}) would then be a β-transition and also showed frequency dependence. The peak labelled T_i at 206 K was thought to represent the same short-range motions responsible for T_i in FD PPM without TEG and FD WBM. This is justified as all these peaks showed similar Arrhenius activation energy (Table 4). The high temperature peak at $T_{iv} = 504$ K in FD PPM–TEG was thought to be an unplasticised dry-T_g similar to T_{iv} for FD PPM (Fig. 3C).

The results for freeze-dried material showed that urea, SDS and sodium sulphite had a plasticising effect in dry protein and that TEG caused additional plasticisation even after drying.

Processed material

Consolidated bars

Figure 4 shows the results for processed material as self-supporting bar samples, (a) without and (b) with TEG. In both the cases, a large peak in tan δ is apparent (labelled

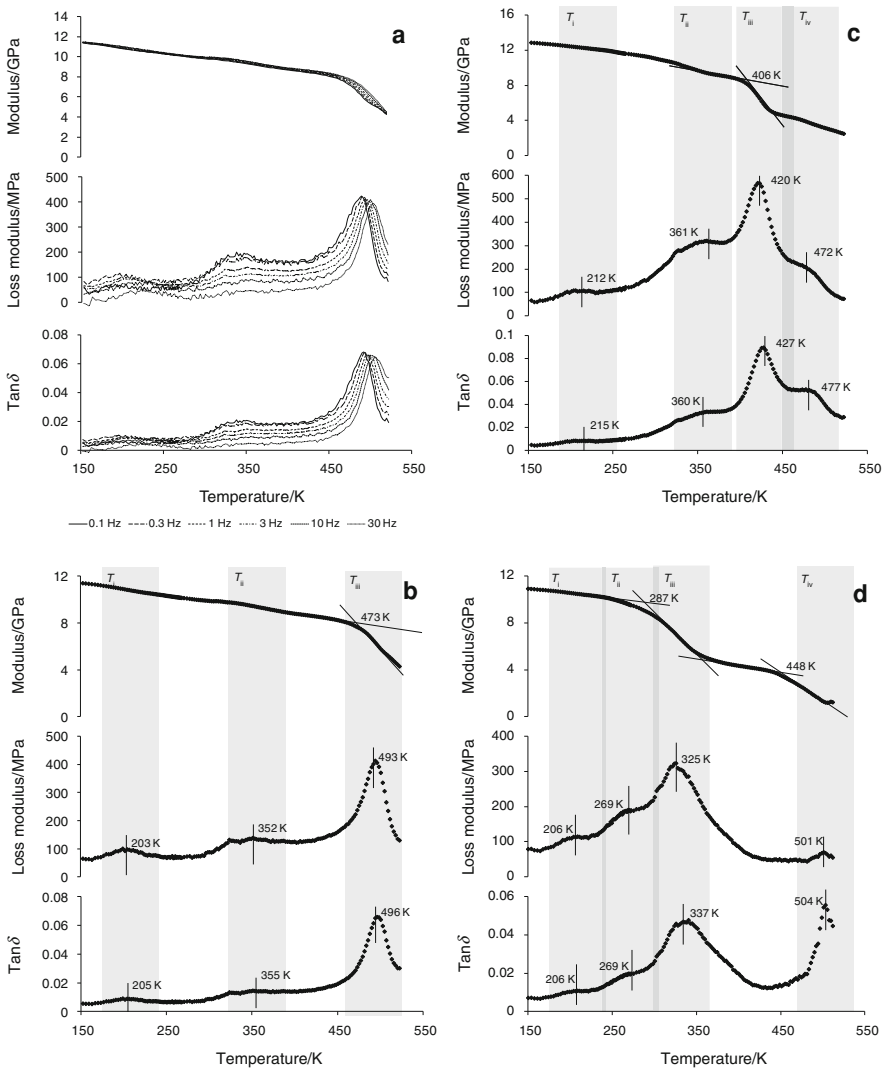

Fig. 3 **a** Multifrequency DMTA data for freeze-dried bloodmeal plus 60 pph_{BM} water and **b** representative 1 Hz DMTA data. **c** Modified bloodmeal without TEG after freeze drying and **d** modified bloodmeal with TEG after freeze drying

T_{ii}), with a second peak at $T_i = 0.74T_{ii}$, T_{ii} and T_i were thought to be the glass transition and a beta relaxation, respectively, as it has long been recognised that due to similar, but more localised motions, $T_\beta \cong 0.75T_g$ in amorphous and semi-crystalline polymers [33, 36].

If the onset of drop in E' had been used to determine T_g, it could mistakenly have been identified 100 K lower than the temperature from the large tan δ peak, as the drops in modulus for both transitions appeared convoluted. Variation of up to 20 K (indicated by the grey shading in Fig. 4) is normal and to be expected [7], but differences of 100 K indicate different transitions are being identified by the two techniques. To clarify this further, the modulus curves were also plotted on a logarithmic scale (Fig. 5). Natural and logarithmic E' scales give different onset values, but are both accepted for assigning T_g values [37]. Natural scales have been used for the bulk of this work as the pocket prevents sample stiffness dropping more than an order of magnitude. In the case of the bar samples; however, the logarithmic scale clarifies that the drop of two orders of magnitude, typical of T_g, is associated with the *upper* tan δ peak (T_{ii}). The onset of this drop is still $\sim$50 K lower than the peak in tan δ, (308 K compared with 350 K in PPM and 287 K compared with 335 K in PPM–TEG) and the peaks themselves, especially with TEG, are rather broad. This is typical of low crystallinity polymers, in which crystals restrict the general long range segmental motions responsible for the amorphous T_g, leading to a broad transition [38].

Comparison between bars and ground processed material

A direct comparison between pre-processed material and processed bar samples is restricted because of the absence

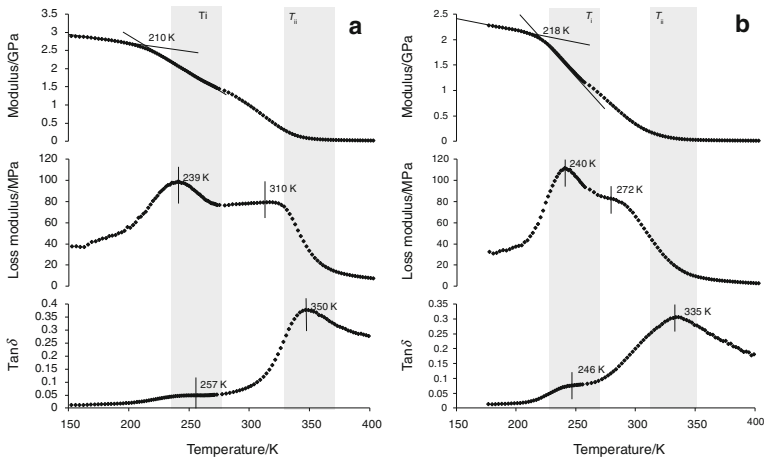

Fig. 4 Representative 1 Hz DMTA plots of **a** processed bar sample with no TEG, **b** processed bar sample with 20 pph_{BM} TEG. The *grey shading* represents ±20 K from the peaks identified in tan δ

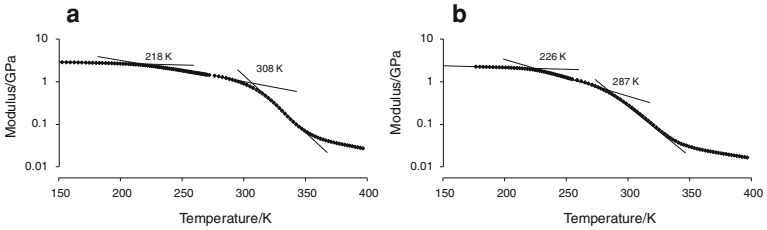

Fig. 5 Representative log scale 1 Hz DMTA E' plots of **a** processed bar sample with no TEG and **b** processed bar sample with 20 pph_{BM} TEG

of the stiff pocket and extensive moisture loss during processing. To overcome these, bar samples were ground and analysed in material pockets before and after freeze drying (Fig. 6). DMTA results of bar and ground-processed samples indicated that material pockets can successfully be used to detect transitions present in the bulk material. In addition, as the pocket maintains stiffness, it enables analysis at higher temperatures at which stiffness drops in self-supporting samples.

In ground MTP, peaks in tan δ were seen at $T_i = 257$ and $T_{ii} = 344$ K (Fig. 6a), corresponding to peaks at T_i and T_{ii} seen in the bar (Fig. 4a). The higher temperature transition seen in Fig. 4a (T_{ii}), resolved into two peaks, $T_{ii} = 344$ K and $T_{iii} = 380$ K (Fig. 6a) using the material pocket. This would suggest the material pocket is more sensitive to determine multiple transitions, typically appearing convoluted in a bar sample.

In ground MTP–TEG, a transition was seen at $T_i = 236$ K, thought to correspond to T_i in the bar sample. The bar sample had a broad transition centred at $T_{ii} = 335$ K, while the ground sample showed peaks at $T_{ii} = 308$ K at $T_{iii} = 375$ K (Fig. 6b). Previous studies of protein/sugar mixtures found that material pocket DMTA was more sensitive to phase transitions than other techniques [8, 10]. The difference in MTP–TEG could be due to resolution of multiple T_gs being enhanced in the material pocket. Two glass transitions are sometimes distinguished in semi-crystalline polymers, T_g(L), arising from the purely amorphous phase and T_g(U), arising from amorphous material restrained by crystallites. A general rule when this is the case is that $T_g(U) \cong (1.2 \pm 0.1)T_g(L)$ [33]. In MTP–TEG, $T_{iii}/T_{ii} = 1.2$, suggesting that the stiffness of the pocket has resolved the broad T_g seen in the MTP–TEG bar into these two components.

While the material pocket technique offered better resolution of phases as detected by peaks in tan δ, it does not mean that the transitions detected in bar samples were wrong. The peak in tan δ seen in bars at 354 K (without TEG) or 339 K (with TEG) is the behaviour of the bulk material when not constrained by a non-dampening metal. Where self-supporting samples can be prepared, the material pocket may be useful for resolving multiple transitions, but should not replace self-supporting samples to determine average behaviour of bulk material.

With samples that cannot be self supporting, it should be remembered that results are for the hybrid system. From the results presented here, the shape of the E'' curves were quite different to the shape of the tan δ curves for bar samples (Fig. 5), while they were similar in material pockets (Fig. 6). In DMTA, E'' is not directly measured, but calculated from the phase lag and sample stiffness, which is a combined property of the material pocket and the sample. The material pocket stiffness is much higher than the polymer which may distort E'' resulting in a response that appears different, but still gives similar transition temperatures.

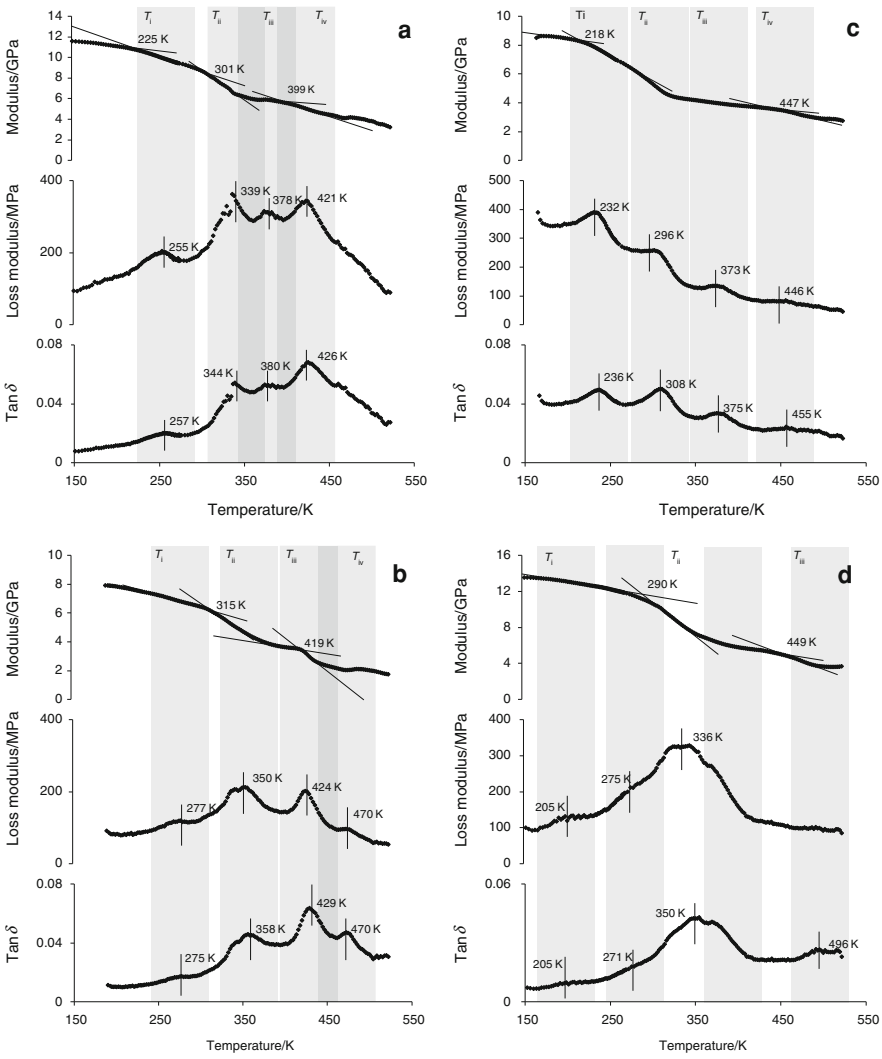

Fig. 6 Representative scans of **a** MTP in material pocket, **b** freeze-dried MTP in a material pocket, **c** MTP–TEG in a material pocket and **d** freeze-dried MTP–TEG in a material pocket

Because of this composite effect between the material pocket and the material, differences between transition temperature assignment were compared when using E', E'' and tan δ (Table 5). Low temperature transitions (T_i) were very similar between all methods used for assigning the transition temperature, regardless of using bar or material pocket samples. However, the second transition seen in bar samples (T_{ii}) resolved into two peaks when using the material pocket technique (T_{ii} and T_{iii}). T_{ii} detected in bar samples varied with about 40 K between the methods used to determine the transition. When this peak was resolved into two peaks in the material pocket, the variation between the temperature assignments using the different techniques was also about 40 K for T_{ii}, but much less for T_{iii}.

One could, therefore, conclude that between the methods used to define transition temperatures, the variation is reasonable for material pockets, but more severe in bar samples. It would be good practise to use E', log E', E″ and tan δ to assign transitions and material pockets may also offer greater resolution

Comparison of freeze-dried material before and after processing

For a comparison at similar moisture content, pre-processed and processed powders were compared after freeze drying. The results are shown in Figs. 3c and 6b for materials without TEG and Figs. 3d and 6d for materials with TEG. The general shape of the tan δ curves was very similar before and after processing. However, the relative magnitude of the triple peaks between 300 and 500 K was different before and after processing for both cases. It was thought that assessing the materials as semi-crystalline (α-helix and β-sheets), T_{ii} would correspond to a glass

Table 5 Transitions identified in processed material for bar and material pocket samples

		Transition temperatures/K[a]				
	Bar:	T_i	T_{ii}			
	Pocket:		T_{ii}		T_{iii}	T_{iv}
MTP						
tan δ	Bar	257	–	350	–	–
				64/0.945		
	Pocket	257	344	–	380	426
			986/0.978		−453/0.980	410/0.987
E''	Bar	239	–	310	–	–
		195/0.916				
	Pocket	255	339		378	421
			673/0.972		−336/0.943	395/0.98
E'	Bar	210	–	Not detected	–	–
		186/0.960				
	Pocket	225	301	–	399	408
			384/0.992			
LogE'	Bar	218	–	308	–	–
	Pocket	222	304	–	Not detected	402
						308/0.936
MTP–TEG						
tan δ	Bar	246		335		
		154/0.922				
	Pocket	236	308	–	375	455
			287/0.993			
E''	Bar	240	–	272	–	–
		202/0.987		126/0.986		
	Pocket	232	296	–	373	446
			141/0.934			
E'	Bar	218	–	Not detected	–	–
		245/0.959				
	Pocket	228	Not detected	–	Not detected	448
		86/0.979				
LogE'	Bar	223	–	285	–	–
		231/0.950		395/0.959		
	Pocket	226	285	–	Not detected	450

[a] If the transition has fit the Arrhenius equation, activation energy (E_A/kJ/mol) and goodness of fit (r^2) are shown after the temperature. Data for other frequencies not shown (0.1, 0.3, 3, 10 and 30 Hz)

transition of bulk amorphous material, T_{iii} to chains trapped between crystallites and T_{iv} to a relaxation temperature of chains within crystallites. On this premise, it would appear that extrusion and injection moulding resulted in chain rearrangement leading to more bulk amorphous chains evident from a greater drop in E' at lower temperatures. This was less evident in samples containing TEG as these would be significantly more plasticised leading to much lower transition temperatures.

Conclusions

Bloodmeal had a T_g at 493 K which is too high for thermoplastic processing. Adding water lowered the T_g to 263 K, although a low T_g alone is not enough to ensure processing.

Modified bloodmeal had a much lower T_g of 193 K due to urea, SS and SDS reducing chain interactions. Modified bloodmeal also showed complex transitions at temperatures above the T_g. These transitions were thought to be

associated with dehydrated bulk amorphous chains, amorphous sections between crystallites and short chain segments within crystalline regions. Including TEG as plasticiser lowered these transitions considerably.

It was concluded that bloodmeal's T_g was largely affected by water even after modification in pre-processed material. Analysis before and after freeze drying revealed that without protein modification the material resorted to the relaxation behaviour of standard bloodmeal, while modification resulted in a permanently lowered T_g.

The material pocket technique gave similar results compared to injection-moulded bar samples at low temperatures, but had increased resolution at higher temperatures. For processed materials, higher temperature transitions seen in bar samples, resolved into three peaks using the material pocket due to the semi-crystalline nature of the material. The relative proportion of these transitions appeared different in processed material compared to pre-processed materials suggestion that some chain rearrangement occurred resulting in more bulk amorphous regions.

Using the material pocket did not lead to additional difficulties in identifying transitions. However, it was found that the technique used for identifying a transition lead to slightly different transition temperatures. Using the onset in E', peak in E'' or tan δ should be used in combination, preferably checking for transitions on a natural and logarithmic scale. This phenomenon was even more pronounced in consolidated bar samples.

References

1. Verbeek CJR, van den Berg LE. Extrusion processing and properties of protein-based thermoplastics. Macromol Mater Eng. 2010;295(1):10–21. doi:10.1002/mame.200900167.
2. Verbeek CJR, van den Berg LE. Development of proteinous bioplastics using bloodmeal. J Polym Environ. 2010;1:1–10. doi:10.1007/s10924-010-0232-x.
3. Bennion BJ, Daggett V. The molecular basis for the chemical denaturation of proteins by urea. Proc Natl Acad Sci USA. 2003;100(9):5142–7. doi:10.1073/pnas.0930122100.
4. Verbeek CJR, Viljoen C, Pickering KL, van den Berg LE. Plastics material. NZ Patent NZ551531. Waikatolink Limited, Hamilton (2009).
5. Verbeek CJR, van den Berg LE. Structural changes as a result of processing in thermoplastic bloodmeal. J Appl Polym Sci. 2012. doi:10.1002/app.36964.
6. Silalai N, Roos YH. Dielectric and mechanical properties around glass transition of milk powders. Dry Technol. 2010;28(9):1044–54. doi:10.1080/07373937.2010.505520.
7. Menard KP. Dynamic mechanical analysis: a practical introduction. 2nd ed. Boca Raton, FL: CRC Press; 2008.
8. Royall PG, Huang CY, Tang SWJ, Duncan J, Van-de-Velde G, Brown MB. The development of DMA for the detection of amorphous content in pharmaceutical powdered materials. Int J Pharm. 2005;301(1–2):181–91. doi:10.1016/j.ijpharm.2005.05.015.
9. Pinheiro A, Mano JF. Study of the glass transition on viscous-forming and powder materials using dynamic mechanical analysis. Polym Test. 2009;28(1):89–95. doi:10.1016/j.polymertesting.2008.11.008.
10. Carpenter J, Katayama D, Liu L, Chonkaew W, Menard K. Measurement of t-g in lyophilized protein and protein excipient mixtures by dynamic mechanical analysis. J Therm Anal Calorim. 2009;95(3):881–4. doi:10.1007/s10973-007-8986-7.
11. Raschip IE, Yakimets I, Martin CP, Paes SS, Vasile C, Mitchell JR. Effect of water content on thermal and dynamic mechanical properties of xanthan powder: a comparison between standard and novel techniques. Powder Technol. 2008;182(3):436–43.
12. Silalai N, Roos YH. Coupling of dielectric and mechanical relaxations with glass transition and stickiness of milk solids. J Food Eng. 2011;104(3):445–54.
13. Gearing J, Malik KP, Matejtschuk P. Use of dynamic mechanical analysis (DMA) to determine critical transition temperatures in frozen biomaterials intended for lyophilization. Cryobiology. 2010;61(1):27–32.
14. Gârea S-A, Iovu H, Nicolescu A, Deleanu C. Thermal polymerization of benzoxazine monomers followed by GPC, FTIR and DETA. Polym Test. 2007;26(2):162–71.
15. Gupta P, Bansal AK. Devitrification of amorphous celecoxib. AAPS PharmSciTech. 2005;6(2):E223–30. doi:10.1208/pt060232.
16. Mano JF. Thermal behaviour and glass transition dynamics of inclusion complexes of alpha-cyclodextrin with poly(D,L-lactic acid). Macromol Rapid Commun. 2008;29(15):1341–5. doi:10.1002/marc.200800180.
17. Paes SS, Sun SM, MacNaughtan W, Ibbett R, Ganster J, Foster TJ, et al. The glass transition and crystallization of ball milled cellulose. Cellulose. 2010;17(4):693–709. doi:10.1007/s10570-010-9425-7.
18. Williams MA, Jones DS, Andrews GP. A study of drug-polymer miscibility using dynamic mechanical thermal analysis. J Pharm Pharmacol. 2010;62(10):1400.
19. Silalai N, Roos YH. Mechanical relaxation times as indicators of stickiness in skim milk-maltodextrin solids systems. J Food Eng. 2011;106(4):306–17.
20. Kemal E, Adesanya KO, Deb S. Phosphate based 2-hydroxyethyl methacrylate hydrogels for biomedical applications. J Mater Chem. 2011;21(7):2237–45. doi:10.1039/c0jm02984j.
21. ASTM International. D638-03 standard test method for tensile properties of plastics. PA 19428-2959. ASTM International, West Conshohocken, PA; 2004.
22. Guo JX, Harn N, Robbins A, Dougherty R, Middaugh CR. Stability of helix-rich proteins at high concentrations. Biochemistry. 2006;45(28):8686–96. doi:10.1021/bi060525p.
23. Michnik A. Thermal stability of bovine serum albumin DSC study. J Therm Anal Calorim. 2003;71(2):509–19. doi:10.1023/a:1022851809481.
24. Heijboer J, Secondary loss peaks in glassy amorphous polymers. In: Boyer RF, Meier DJ. Midland macromolecular institute. In Dow Chemical Company, editors. Molecular basis of transitions and relaxations: papers. Midland macromolecular monographs. London: Gordon and Breach Science Publishers; 1978. p. xii, 429.
25. Rouilly A, Orliac O, Silvestre F, Rigal L. DSC study on the thermal properties of sunflower proteins according to their water content. Polymer. 2001;42(26):10111–7.
26. Zhang J, Mungara P, Jane J. Mechanical and thermal properties of extruded soy protein sheets. Polymer. 2001;42(6):2569–78.
27. Jerez A, Partal P, Martinez I, Gallegos C, Guerrero A. Rheology and processing of gluten based bioplastics. Biochem Eng J. 2005;26(2–3):131–8. doi:10.1016/j.bej.2005.04.010.

6

Short term Visco-elastic Properties of Bloodmeal-Based Thermoplastics

A paper

submitted for review and publication in

Advances in Polymer Technology

by

JAMES M. BIER[1], C.J.R. VERBEEK, M.C. LAY AND D. VAN DER MERWE

[1]As first author for this paper, I prepared the initial draft manuscript, which was refined and edited in consultation with my supervisors, who have been credited as co-authors. I had the assistance of University of Waikato Summer Research Scholarship student with sample preparation and data collection to my specifications. I processed all of the data into the form it is presented in within, and did all of the modelling and statistical analysis reported.

Short Term Visco-elastic Properties of Bloodmeal-Based Thermoplastics

Abstract

The effects of sodium sulphite content and injection moulding temperature on the visco-elasticity of bloodmeal based thermoplastics were assessed using creep, recovery and stress relaxation. Both sodium sulphite content and processing temperature affected standard mechanical properties and time dependent behaviour. Increased sodium sulphite led to greater creep, greater strain at break and reduced modulus and strength. Higher injection moulding temperature also reduced modulus and strength, while increasing the fraction of creep recovered in twenty minutes. These results, along with standard pull to break tensile tests, confirmed that increased sodium sulphite increased chain mobility and that injection moulding at 140°C instead of 120°C did not cause excessive thermal crosslinking.

Introduction

Thermoplastic protein is an alternative to petroleum-based polymer and can be produced from agricultural by-products, such as bloodmeal [1]. Proteins are much more complex than synthetic homo-polymers and have a wide range of inter-molecular interactions that reduce molecular mobility and increase the glass transition (T_g) to around their degradation temperature [2]. Plasticisers such as water or other low molecular weight compounds are necessary to lower T_g for processing to precent excessive degradation [2].

Bloodmeal is produced by drying slaughterhouse blood from the meat industry. The resulting powder contains more than 90 wt% protein and is highly denatured and cross-linked. In addition to plasticisation, thermoplastic processing of bloodmeal requires additives to break covalent cross-links (sodium sulphite, SS), disrupt hydrophobic interactions (sodium dodecyl sulphate, SDS) and disrupt hydrogen bonding that stabilises secondary structures (urea, a protein denaturant) [1]. With these additives, bloodmeal can be converted into a thermoplastic material that can be extruded and injection moulded [3].

While the combined effect of these additives reduces crosslinking (either physical or chemical), increasing chain mobility [4], high processing temperatures and specific mechanical energy input can cause excessive degradation and crosslinking in proteins [2]. For example, degradation at injection moulding temperatures above 130°C negatively impacts on the mechanical properties of soy protein/starch blends [5]. On the other hand, crosslinking reduces chain mobility, which will slow the rate at which chains can rearrange to dissipate forces at constant strain (relaxation) or slide past each other in response to constant stress (creep).

Viscoelastic models typically consist of an arrangement of Hookean springs (with stress proportional to strain) and Newtonian dashpots (with stress proportional to strain rate). A spring and dashpot in series (Maxwell model) predicts stress relaxation at constant strain but not creep. A spring and dashpot in parallel (Voigt or Kelvin model (VK)) predicts creep at constant load, but not stress relaxation. Introducing additional elements to these ideal models more closely simulates experimental behaviour of real polymers [6].

The four element Burgers model (a Maxwell element in series with a VK element (Figure 1) is typically used to describe both creep and recovery. For relaxation, simpler generalised Maxwell models are typically used. However, if a four element model is used for stress relaxation, it allows the constants determined to be compared with those from creep experiments [7]. The governing equations for stress relaxation at constant load for the four elements have previously been solved by Laplace transforms and, using constants obtained from creep experiments, shown to predict relaxation of polyisobutylene [7].

In the Burgers model, the Maxwell spring (E_1), Maxwell dashpot (η_1) and the combined VK element all experience the same stress and the overall strain is the sum of the individual strains for these elements. For the VK element, the spring (E_2) and dashpot (η_2) experience the same strain and the total stress is the sum of the stress on these two elements. If these parameters are known, the model predicts total creep compliance at time t, under a constant load σ_0 and predicts recovery after the load is removed at a time, t_1 [6].

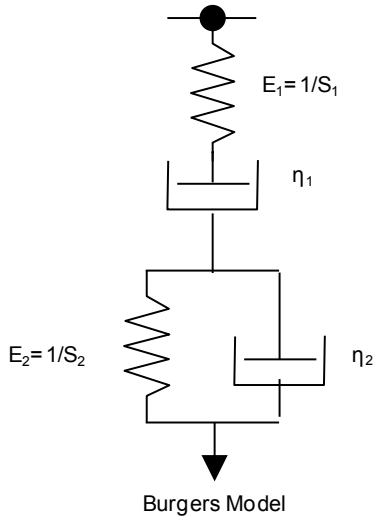

Figure 1: Four element model of viscoelastic behaviour, consisting of a Maxwell element (E_1 and η_1) in series with a Voigt/Kelvin element (E_2 and η_2) [6].

In practice, real polymer behaviour has a distribution of retardation times, and a better fit can be obtained with a generalisation of many VK elements in parallel. The governing equation for compliance can be approximated to four parameters, like the Burgers model, while maintaining characteristics of the generalised VK model, as the modified four element (MFE) model [8-9]:

$$S_t = S_1 + t/\eta_1 + t/(\eta_2 + E_2 t) \quad 1$$

$$\tau_{ret} = \eta_2 / E_2 \quad 2$$

Parameters fitted to Equations 1-2 have been demonstrated to fit experimentally observed creep behaviour of food biopolymers including extrudates of glutinous rice [8, 10] and denatured protein gels [11]. In equation 1-2, symbols have the following meaning:

E = Elastic or relaxation modulus (MPa),
S = Compliance, 1/E (MPa^{-1})
t = time (s)
η = viscosity, σ/(dε/dt) (MPa.s or GPa.s)
τ_{ret} = retardation time (s)
The use of subscripts denotes which element in Figure 1a given parameter corresponds to.

In this paper visco-elasticity of bloodmeal-based thermoplastics was used to assess the effect of sodium sulphite content and injection moulding temperature on the strength of chain interactions. Using a modified four element model,

experimental results from creep, recovery and stress relaxation were modelled to compare fitted parameters of the MFE which should reflect chain mobility and the strength of chain interactions in polymers.

Experimental

Materials

Agricultural grade bloodmeal (Wallace Corporation, Hamilton, New Zealand), agricultural grade urea (Ballance Agrinutrients, Kapuni, New Zealand), distilled water, tri-ethylene glycol (TEG) for synthesis (Merck), technical grade sodium dodecyl sulphate (SDS) (Merck) and technical grade sodium sulphite (SS) (Merck) were used for the manufacturing of polymer samples.

Preparation of test specimens

Thermoplastic protein was prepared from bloodmeal (formulations shown in Table 1) by blending in a high speed mixer as described previously [1, 12]. The blended mixture was extruded in a Thermoprism TSE-16-TC twin screw extruder (screw diameter was 16 mm, L/D ratio of 25) fitted with a single 10 mm diameter circular die using previously described parameters [1, 12].

Table 1: Formulations produced and tested in this work

Injection moulding temperature	**Sample formulation (g per 100 g bloodmeal)**						**Sample name**
(From feed zone to die) and sample names	Blood meal	Water	Urea	SS	SDS	TEG	
100, 115, 120, 120, 120 °C	100	40	10	2	3	20	2-120
	100	40	10	3	3	20	3-120
	100	40	10	4	3	20	4-120
100, 120, 135, 140, 140 °C	100	40	10	2	3	20	2-140
	100	40	10	3	3	20	3-140
	100	40	10	4	3	20	4-140

Granulated extrudate was injection moulded into Type 1 tensile test specimens [13] through a cold runner into a water heated mould using a BOY-35A injection moulder with 24 mm screw. Two injection moulding temperature profiles were used (Table 1). In both profiles, a screw speed of 200 RPM, a maximum injection pressure of 1100 Bar and 30 kN locking force were used.

Test pieces were conditioned at 50% RH and 23°C for 7 days and tested in a climate controlled room. Equilibrium moisture content was between 7-8% for all sample types, tested by oven drying for a minimum of 48 hours at 103°C.

Mechanical testing

Three kinds of tests were performed using an Instron model 33R4204 fitted with a 50 mm gauge length extensometer:

- Pull to break: samples were subjected to constant strain rate of 5 mm/min until fracture to determine ultimate tensile strength (UTS) and strain to break. A secant modulus was calculated between 0.0005 and 0.0025 strain. Toughness was calculated as the area under the stress/strain curve. Five specimens were tested for each sample type [13].
- Creep and recovery: samples were pulled to a strain of 1% at 50 mm/min then held at the corresponding load for 20 minutes while strain was measured. The load was then removed and strain measured for an additional 20 minutes. Three specimens of each sample type were tested.
- Stress relaxation: samples were pulled to a strain of 1% at 50 mm/min then held at constant strain for 20 minutes while load was measured. Three specimens of each sample type were tested.

The glass transition temperature (T_g) was determined using a DMA8000 (Perkin Elmer) fitted with a high temperature furnace, controlled with DMA software version 14306 and cooled with liquid nitrogen. Samples were cut from larger injection moulded pieces with approximate geometry of 3.5 x 6.5 x 30 mm and tested in single cantilever bending mode with a free length of 12.5 mm, dynamic displacement of 0.03 mm and frequency of 1 Hz. Experiments were performed between -100 and 120°C at a programmed heating rate of 2°C/min. T_g was determined from the peak in tanδ.

Modelling and statistical analysis

Creep, recovery and stress relaxation were modelled separately using the modified four element (MFE) model (Equation 1). For creep and relaxation the following relations were used:

$$S_1 = S_{(t=0)} = \varepsilon_0 / \sigma_0 \quad 3$$

Where ε_0 is the initial strain of 0.01 and σ_0 is initial stress required to achieve this strain.

$$\eta_1 = 1/(dS/dt) \quad 4$$

Where *dS/dt* is the slope of *S(t)* in the linear region (t > 1000s).

Excel Solver was then used to determine η_2 and E_2 by minimising the sum of square errors between model and experimental data.

While the pre-loading conditions were identical for creep and stress relaxation, the initial condition for recovery was the conclusion of a creep test. For recovery, S_1 was calculated using σ_0 from the creep experiment preceding it and ε_0 was determined from the first data point to show greater than 0.01 recovered strain after the load was removed. Again, η_2 and E_2 were determined using Excel Solver to minimise the sum of square errors between model and experimental data. The following relation was then used to determine η_1:

$$\eta_1 = \sigma_0 t_1 / \varepsilon_p \quad 5$$

Where ε_p is the unrecovered (permanent) creep predicted after fitting η_2 and E_2, σ_0 is the stress from the creep portion of the experiment and t_1 is the time the load was removed.

Analysis of variance (ANOVA) was conducted using STATISTICA version 11 [14]. The experimental design included sodium sulphite at three levels, and injection moulding temperature profiles (maximum temperatures of 120°C and 140°C respectively) at two levels, (Table 1). Pull to break results were analysed using SS, temperature and their interaction as predicting factors. For the time dependent experiments, fitted MFE parameters were analysed using experiment type (creep, recovery or relaxation), SS and temperature as predicting factors. In addition, final values which did not depend on model parameters were included in the statistical analysis. For creep, this was the final compliance ($S_{t=1200s} = \epsilon_{t=1200s}/\sigma_0$), for recovery, the fraction of creep recovered ($1-\epsilon_{t=2400s})/\epsilon_{t=1200s}$) and for stress relaxation, the fraction of stress relaxed ($1-\sigma_{t=1200s})/\sigma_0$). A 95% confidence interval was used, such that factors with p values <0.05 were deemed to be

significant. Percentage contribution (η^2) was calculated from the sum of square errors for significant factors.

Results and discussion

Pull to break

Pull to break tests revealed typical thermoplastic stress/strain behaviour. Parameters determined from these tests are shown in Table 2. A reduction in strength was seen in samples 4-120 and 4-140, indicating that higher SS content reduced intermolecular interactions. Similarly, samples 2-120 and 2-140 showed smaller strain at break, revealing lower ductility than at higher SS contents. An interactive effect manifested for samples with 3 pph_{BM} SS, which showed reduced strength and modulus at the higher moulding temperature.

Table 2: Pull to break tensile results. Mean ± standard deviation for five samples of each formulation. (Only 2 samples of each for Tg)

Moulding temp (°C)	SS content (pph_{BM})	UTS (MPa)	Toughness (MPa)	Strain at break	Secant modulus (MPa)	T_g (°C)
120	2	7.9 ±0.1	2.7 ±0.2	0.40 ±0.03	375 ±42	62.2 ±1.3
	3	7.6 ±0.2	3.4 ±0.1	0.50 ±0.02	380 ±35	64.6 ±0.6
	4	5.6 ±0.1	2.6 ±0.3	0.54 ±0.05	238 ±33	59.7 ±0.9
140	2	7.6 ±0.2	3.1 ±0.4	0.46 ±0.04	388 ±9	63.5 ±3.5
	3	6.3 ±0.3	3.1 ±0.6	0.56 ±0.10	282 ±34	63.3 ±1.6
	4	5.7 ±0.2	2.7 ±0.4	0.54 ±0.08	241 ±34	57.6 ±0.1

This suggests that at the intermediate SS level, higher thermal energy reduced cross-linking. At higher SS concentration, there was enough reducing agent present that this effect was not seen. ANOVA revealed the effect of sodium sulphite contents was significant at a 95% confidence interval for strength, toughness, elongation at break and modulus, whereas the two moulding temperatures did not have a significant effect on toughness or elongation at break (Table 3, Figure 2).

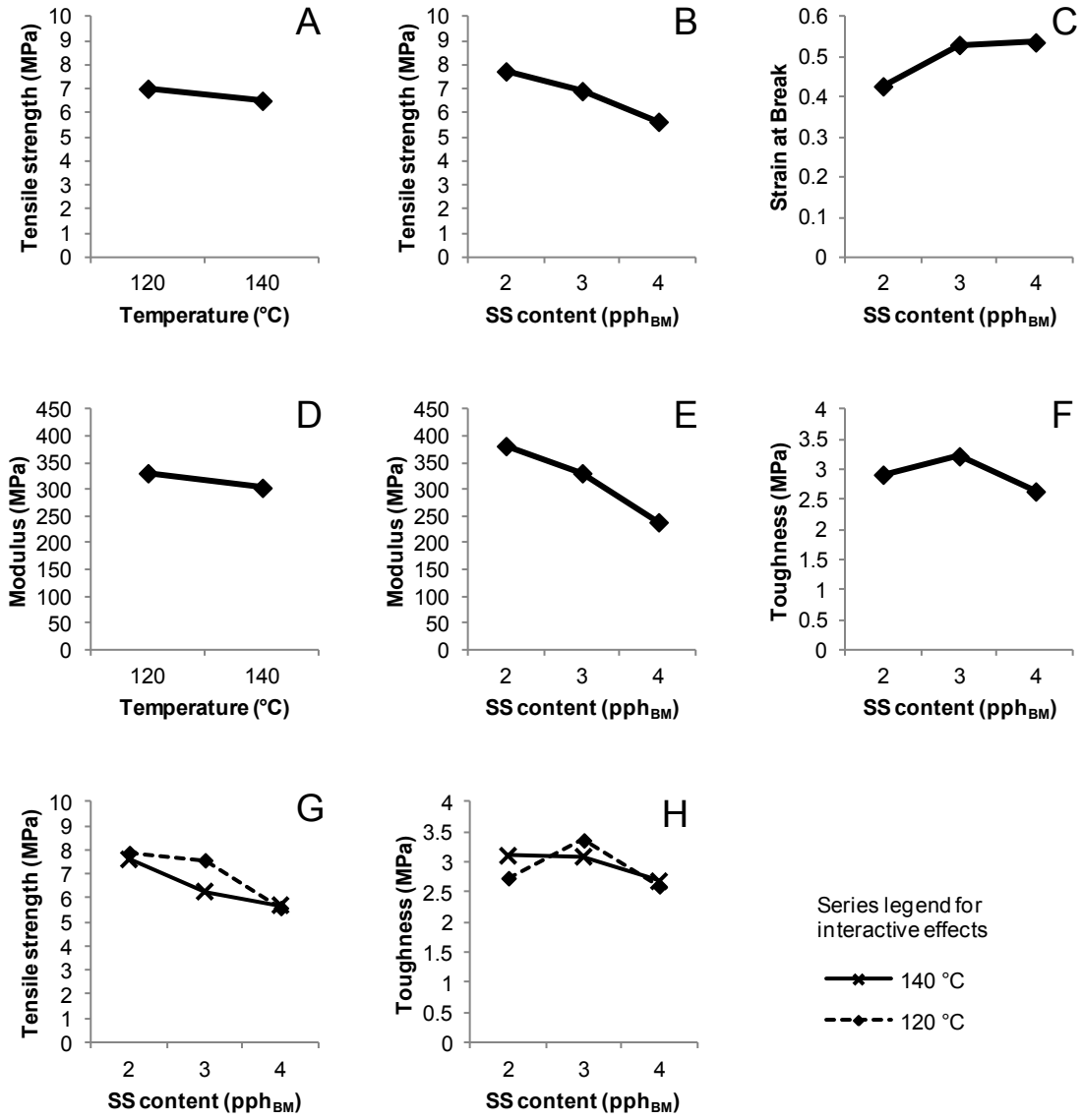

Figure 2: ANOVA group means for significant factors. A) effect of temperature on strength, B) effect of SS on strength, C) effect of SS on strain at break, D) effect of temperature on modulus, E) effect of SS on modulus and F) effect of SS on toughness, G) Effect of interaction of SS and temperature on strength, H) Effect of interaction of SS and temperature on toughness.

For strength and modulus, in which the moulding temperature was significant, the interaction between SS content and temperature was also significant (Table 3). Group-means for significant factors (Figure 2) revealed that even when temperature was significant (modulus and strength), its percentage contribution was very small (Table 3), with only a small difference in group-mean between the two melt temperautres (Figure 2). SS was always the dominant factor, significant for all parameters tested. At higher SS content, it consistently lowered properties (Figure 2), which demonstrates that it was successfully breaking bonds. Toughness first increased, and then decreased with increasing SS. This can be

explained as a small amount of chain movement is good for energy absorption, but too much movement compromises strength, thereby reducing toughness.

Table 3: p values and percentage contribution from factorial ANOVA on conditioned pull to break tensile results Values found to be significant at the 95% confidence interval are in bold. Percentage contributions have been pooled with error for factors not found to be significant

	Tensile strength	Toughness	Strain at break	Secant modulus	T_g
p-value					
Temperature	**<0.01**	0.69	0.09	**0.03**	0.52
SS content	**<0.01**	**0.01**	**<0.01**	**<0.01**	**0.01**
Temperature*SS content	**<0.01**	0.17	0.46	**<0.01**	0.41
Error	**<0.01**	**<0.01**	**<0.01**	**<0.01**	**<0.01**
Percentage contribution					
Temperature	**7%**	pooled	pooled	**4%**	pooled
SS content	**80%**	**31%**	**43%**	**68%**	**71%**
Temperature*SS content	**10%**	pooled	pooled	**12%**	pooled
Error	**3%**	**69%**	**57%**	**16%**	**29%**
	100%	100%	100%	100%	100%

Stress relaxation

NTP held at constant strain showed considerable drop in stress with as much as 68-74% of the initial stress dissipating in 1200 seconds (Table 4). Plots of stress decay versus time are shown in Figure 3. Although neither SS level nor moulding temperature significantly affected the fraction of the initial stress that was dissipated in 1200 seconds (Table 5), this structural relaxation provides evidence that chain rearrangements occured on a time scale comparable to the experimental time at room temperature.

Amorphous polymers below their T_g are meta-stable and chain rearrangements still occur, albeit more slowly than in a polymer melt. The ratio of relaxation time to experimental observation time is called the Deborah number [15]. At low Deborah number (relaxation time >> observation time), elastic behaviour is observed, while at high Deborah numbers (observation time >> relaxation time), viscous behaviour is observed. If the observation time and relaxation time are similar, (Deborah number ≈ 1) viscoelastic phenomena are apparent, as seen in these experiments. An experimental time of 1200 seconds (20 minutes) was therefore adequate for exploring chain rearrangements, whereas the frequencies

needed to detect such motions at room temperature in dynamic mechanical analysis would need to be very low (<0.01 Hz). The conditioning period of seven days is significantly longer than the timescale of observed structural relaxation, so it is possible that polymer aging (chain rearrangement to reduce internal energy and entropy) may have occurred during conditioning. Also, the material will creep over a similar time scale in applications where the material is exposed to similar stresses to those applied in this experiment.

Table 4: Extent of relaxation, creep and recovery after twenty minutes of each. Average and standard deviation from three samples (only two for 4-140 recovery)

Moulding temp (°C)	SS content (pph_{BM})	Fraction relaxed		Creep compliance (1/Mpa)		fraction recovered	
120	2	0.68	±0.01	0.023	±0.002	0.82	±0.02
	3	0.72	±0.02	0.028	±0.001	0.79	±0.00
	4	0.69	±0.01	0.029	±0.002	0.79	±0.00
140	2	0.69	±0.02	0.025	±0.002	0.81	±0.01
	3	0.69	±0.01	0.025	±0.002	0.81	±0.00
	4	0.74	±0.00	0.035	±0.001	0.95	±0.01

Table 5: p-values and percentage contributions of main effects ANOVA on extent of relaxation, creep and recovery in twenty minutes. Bold p-values indicate significance at the 95% confidence interval.

	Fraction relaxed	Creep Compliance (1/MPa)	Fraction recovered
p-value			
Temperature	0.40	0.36	**0.03**
SS content	0.21	**0.00**	0.11
Percentage contribution			
Temperature	pooled	pooled	25%
SS content	pooled	54%	pooled
Error	100%	46%	75%
	100%	100%	100%

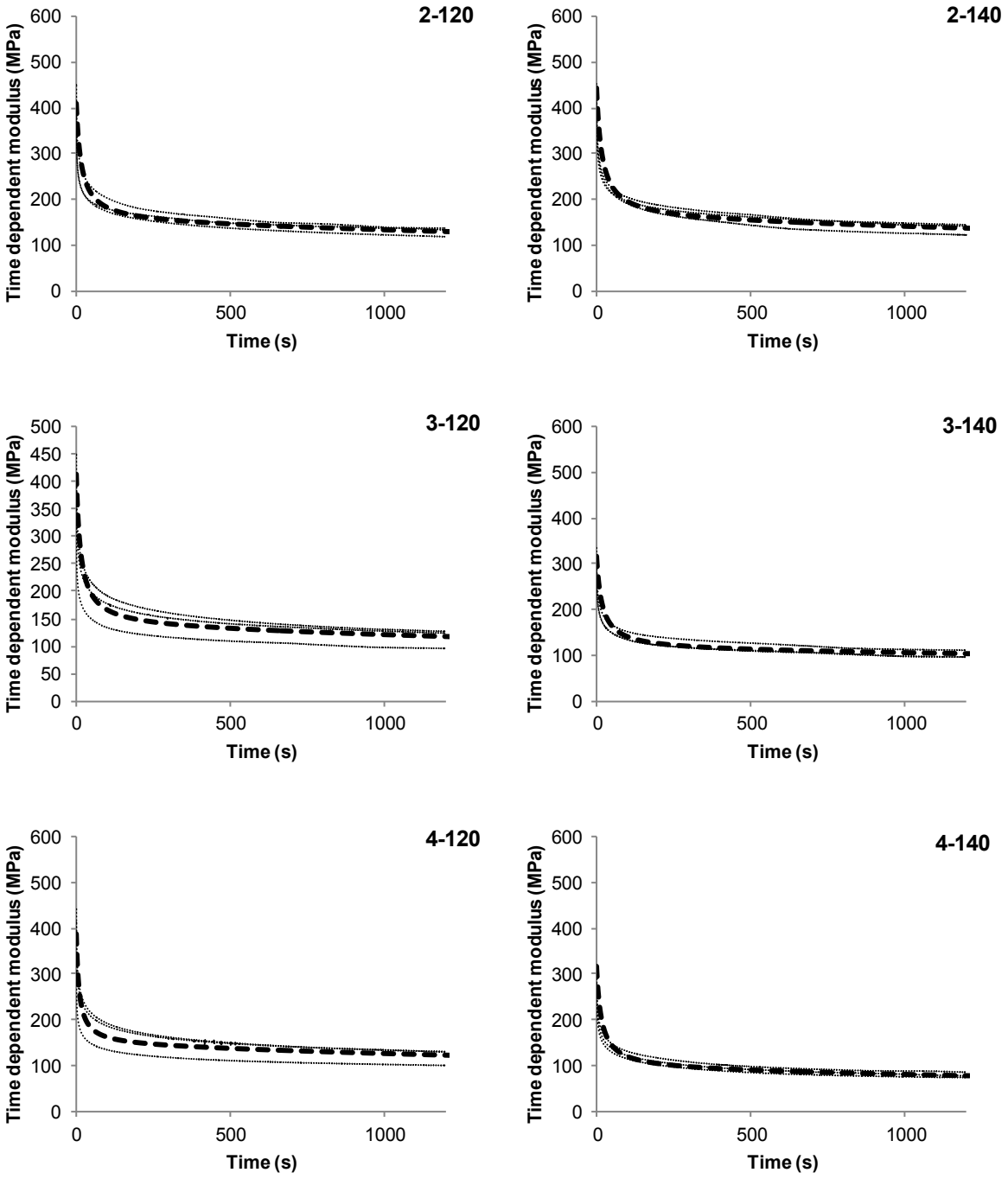

Figure 3: Comparison of experimental data and fitted parameter predictions for relaxation experiments.

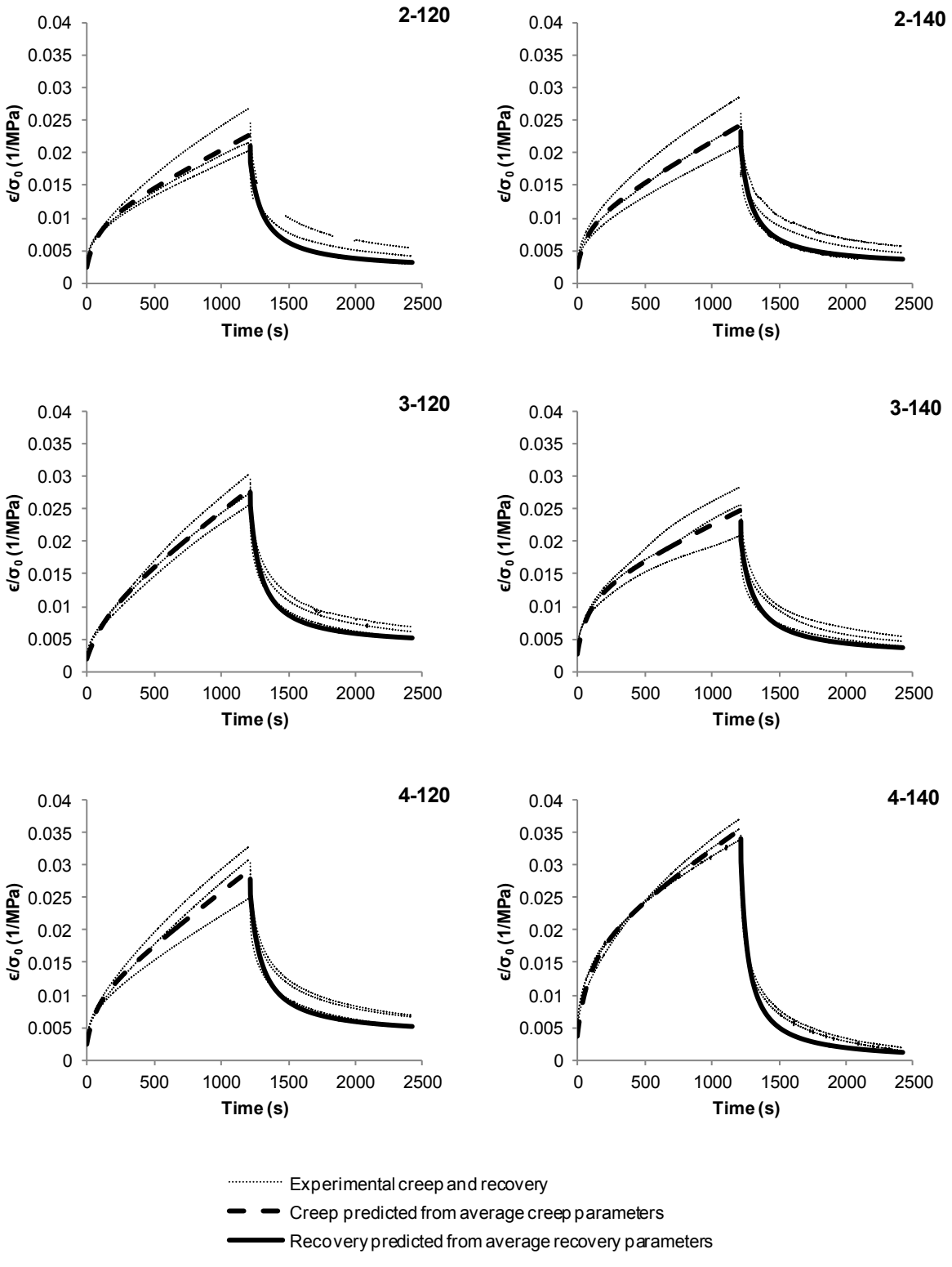

Figure 4: Comparison of experimental data and fitted parameter predictions for creep and recovery experiments. Y-axis is ϵ/σ_0, which is equivalent to creep compliance during the creep portion of the experiment.

Creep and recovery

Appreciable creep was observed within the experimental time of 1200 seconds and each sample reached a state where compliance rose linearly (Figure 4). When the load was removed, significant but incomplete recovery was seen within 1200 seconds (Figure 4). Creep and recovery were not symmetric, with the first few minutes of recovery showing greater recovered strain than creep to the equivalent time, before levelling off (Figure 4).

For each formulation, creep was started at the load corresponding to 0.01 strain to match the starting conditions for relaxation. However, since the instantaneous modulus varied between each experiment, the load at 0.01 strain was different as well. To overcome this, formulations were compared based on the creep compliance at 1200 seconds ($S_{t=1200s} = \epsilon_{t=1200s}/\sigma_0$) and the fraction strain recovered in 1200 seconds after creep ($1-\epsilon_{final}/\epsilon_{initial}$). These parameters were evaluated using ANOVA to determine the effect of temperature and SS (Table 4, Table 5 and Figure 5).

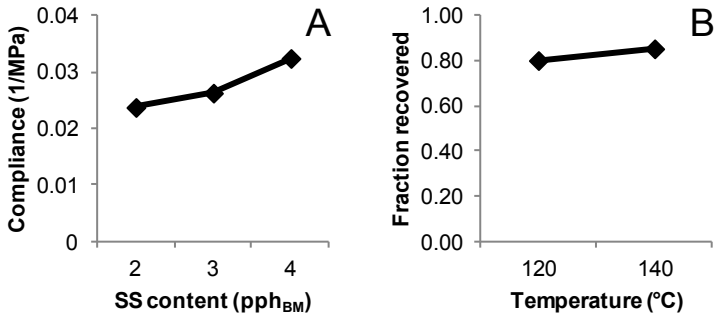

Figure 5: Group means for significant factors in main effects ANOVA on final values after twenty minutes.

After 1200 seconds of stress relaxation, the fractional stress relaxed was independent of melt temperature as well as SS content. This implied that chains must have enough manoeuvrability to dissipate the applied load. In other words, even at the lowest SS level there is still enough chain movement and melt temperature does not further restrict this. However, increasing SS content did lead to a statistically significant rise in creep compliance. This would imply that breaking further cross-links (by adding SS) does increase chain mobility, but this is over and above that required for stress relaxation. Although melt temperature

appeared to have been significant, it is more likely that the value at 140°C with 4 pph_{BM} SS skewed the results.

Modelling

To provide for further comparison between chain mobility in the different formulations and melt temperature, the modified four element model was fitted to the data, giving the parameters E_1, E_2, η_2 and η_1, which could then be compared. Non-linear regression can be used, along with equations 3-5, to determine the constants in the model.

Prior to the linear region, the shape of the compliance curve is determined by the VK element. The spring constant, E_1, would determine instantaneous reversible deformation in the MFE model. E_2 would effectively dictate the extent of recoverable creep, while η_2 controls the rate. This implies that the VK element represents reversible time dependent properties, while the dashpot from the Maxwell element (η_1) would account for non-reversible deformation.

Figure 4 shows the experimental creep compliance and recovery, along with behaviour predicted from parameters fitted to each portion of the experiment. Similarly, Figure 3 shows the experimental time dependent modulus during relaxation along with predictions from the MFE model. The MFE model was fitted to each of the three time dependent experiments with good agreement; however different model parameters were required for each (Table 6). The goodness of fit (R^2) was at least 0.92 for each sample group and experiment type, however the best fits were obtained for creep (R^2>0.99).

One of the most striking differences is the magnitude of Maxwell element viscosity (η_1) between the three experiment types (Table 6). Linear steady state creep was observed for all samples which could not be predicted by a three element model, such as the standard linear solid. However, predicted permanent deformation based on the linear region was much greater than experimental values (*x* in Figure 6). This meant creep and recovery could not be modelled using the same parameters for both processes (Figure 6), although linear visco-elasticity and the Boltzman superposition principle would suggest that these two processes should be additive. If the material is left to recover after 20 minutes of creep, model parameters based on creep data would suggest a much greater non-

recoverable strain. Recovery was seen to happen faster and to a greater extent than what would be predicted from the creep data (Figure 6). Similarly parameters fitted to recovery predict faster initial creep than experimentally observed.

Table 6: Modifed four element model parameters for each formulation fitted relaxation, creep and recovery

Moulding temp (°C)	SS content (pph_{BM})	E_1 (MPa)		E_2 (MPa)		η_2 (GPa.s)		η_1 (GPa.s)		τ_{ret}(s)		Goodness of model fit (R^2)	
Relaxation													
120	2	412	±24	237	±17	10.6	3.3	1,383	±565	47	±17	0.973	±0.011
	3	416	±24	201	±26	8.6	1.8	958	±80	43	±6	0.974	±0.012
	4	396	±41	227	±15	5.8	2.3	906	±42	25	±10	0.926	±0.047
140	2	443	±8	241	±15	12.0	0.5	1,183	±225	50	±6	0.966	±0.008
	3	316	±10	171	±8	8.6	0.6	1,284	±132	50	±1	0.951	±0.007
	4	316	±6	131	±14	7.0	0.7	564	±117	56	±11	0.979	±0.007
Creep													
120	2	412	±13	125	±12	10.8	1.5	95	±10	91	±21	0.998	±0.001
	3	530	±6	114	±6	20.7	1.1	66	±4	183	±10	0.999	±0.000
	4	422	±6	119	±13	9.4	1.2	64	±6	81	±11	0.998	±0.001
140	2	438	±18	118	±20	10.6	1.1	86	±5	96	±19	0.998	±0.001
	3	366	±11	92	±13	8.1	1.2	103	±10	97	±29	0.996	±0.001
	4	268	±14	61	±3	6.1	1.2	73	±5	102	±24	0.998	±0.000
Recovery													
120	2	404	±14	60	±5	6.0	±.8	433	±120	100	±6	0.972	±0.007
	3	491	±15	46	±3	3.9	±.3	241	±19	84	±1	0.976	±0.003
	4	434	±20	46	±4	4.2	±.4	238	±25	91	±1	0.976	±0.001
140	2	406	±15	55	±4	4.7	±.4	349	±65	87	±6	0.974	±0.002
	3	338	±6	56	±6	5.8	±.7	341	±31	104	±7	0.982	±0.002
	4	311	±69	32	±2	1.9	±.4	1,249	±534	58	±8	0.947	±0.018

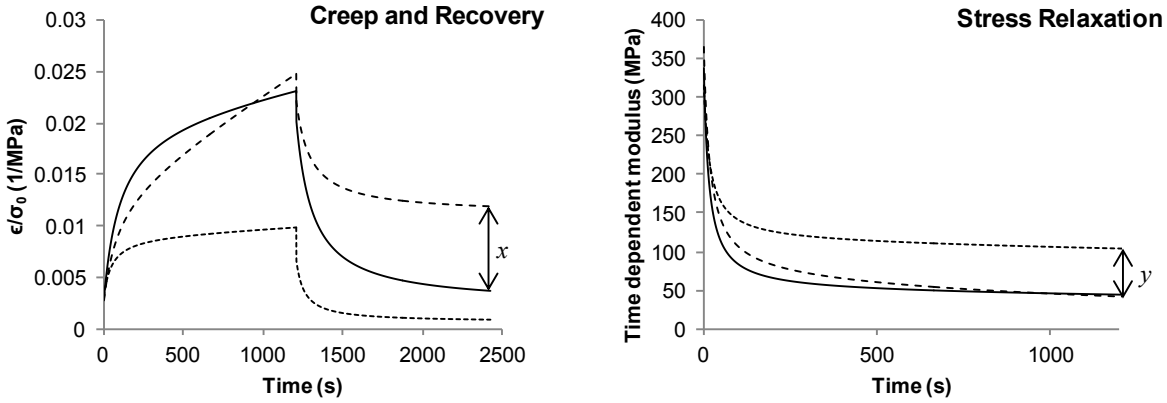

Figure 6: Comparison of predicted behaviour from MFE constants fitted to each experiment type. Example is one sample of 4-140.

The reason for this behaviour is likely the way in which protein chains react to an applied stress. Under creep, significant intermolecular forces need to be overcome to enable chain rearrangement, while chains could simply rearrange into a different conformation during recovery, leading to a faster rate. Proteins are complex heteropolymers with multiple side groups, of different sizes and hydrophobicity. Steric hindrance from some of these groups may slow creep down, as bulky side groups must push past each other to allow chain rearrangement. After some time creeping, these groups may have been pushed into a conformation in which they are no longer in each others' way, resulting in steady state creep, and allowing for rapid recovery.

ANOVA confirmed that that there was no statistically significant difference between E_1 calculated by the three time dependent tests (creep, recovery and relaxation). Moulding temperature and SS level, were both significant and a similar trend was seen with the secant modulus from the pull to break tests (Table 2 and Table 6). The modulus at higher melt temperature and higher SS decreased (Figure 7). However, strictly speaking, these two moduli are not equivalent. The secant modulus was determined between 0.0005 and 0.0025 strain during extension at 5 mm/minute, whereas E_1 was determined from the instantaneous stress after a 50 mm/minute extension to 0.01 strain. Typically, a higher rate will lead to a higher modulus.

For the VK element parameters, only experiment type was significant for τ_{ret}, (η_2/E_2) (Table 7), despite both temperature and SS content being significant for E_2 itself and SS being significant for η_2. The retardation time seen in creep was

greater than that seen for recovery, consistent with the above observation that the first few minutes of recovery were faster than initial creep.

Because experiment type was the dominant factor for many of the fitted parameters (Table 7), there was the possibility it obscured the significance of more subtle differences in response due to SS or melt temperature within each experiment type. P values and percentage contribution of SS and melt temperature were also calculated within each experiment type (Table 8). Consistent with the overall ANOVA, neither temperature nor SS were significant for modelled η_1 or τ_{ret} in any of the experiment types. SS and temperature were both significant for E_1 determined from individual start conditions in creep or relaxation. In the overall ANOVA, both SS and temperature were significant for E_2. Consistent with this, temperature had a significant influence on E_2 fitted to creep and relaxation, while SS had a significant influence on E_2 fitted to recovery and relaxation. The overall ANOVA also showed a significant influence of SS on modelled η_2. Again, consistent with this, in creep and relaxation individually, SS also showed a significant effect on η_2. In recovery, a p-value of 0.06 was observed, only just outside the confidence interval taken as significant. If a 90% confidence interval had been used instead, this would have been taken as significant and the calculated percentage contribution would have been 35%. Similarly, the overall ANOVA had a p-value of 0.06 for the effect of temperature on η_2 (Table 7). In this case, a significant influence was seen for η_2 fitted to creep, but not to recovery or relaxation. Nevertheless, it seems that results of ANOVAs within each experiment type support the conclusions from the overall ANOVA on which parameters were significantly affected by temperature and SS.

In relaxation, the total strain is held constant, but the strain on the various elements changes, dissipating the initial stress. Fitting the same model to stress relaxation, τ_{ret} does not represent the relaxation time. Rather, it is the retardation time of the VK element within the four element model. The overall relaxation time of the model involves decay of stress from the Maxwell spring into both the VK element and Maxwell dashpot as well as decay of stress from the VK element to Maxwell dashpot. The compliance and viscosities determined from stress relaxation greatly under-predict creep and similarly those determined from creep and recovery predict greater relaxation than that seen in twenty minutes (y in Figure 6). This suggests that this model does not fully describe real thermoplastic

protein behaviour. Nevertheless, the constants determined for each mode of testing can be used to compare the effect of melt temperature and SS on chain mobility.

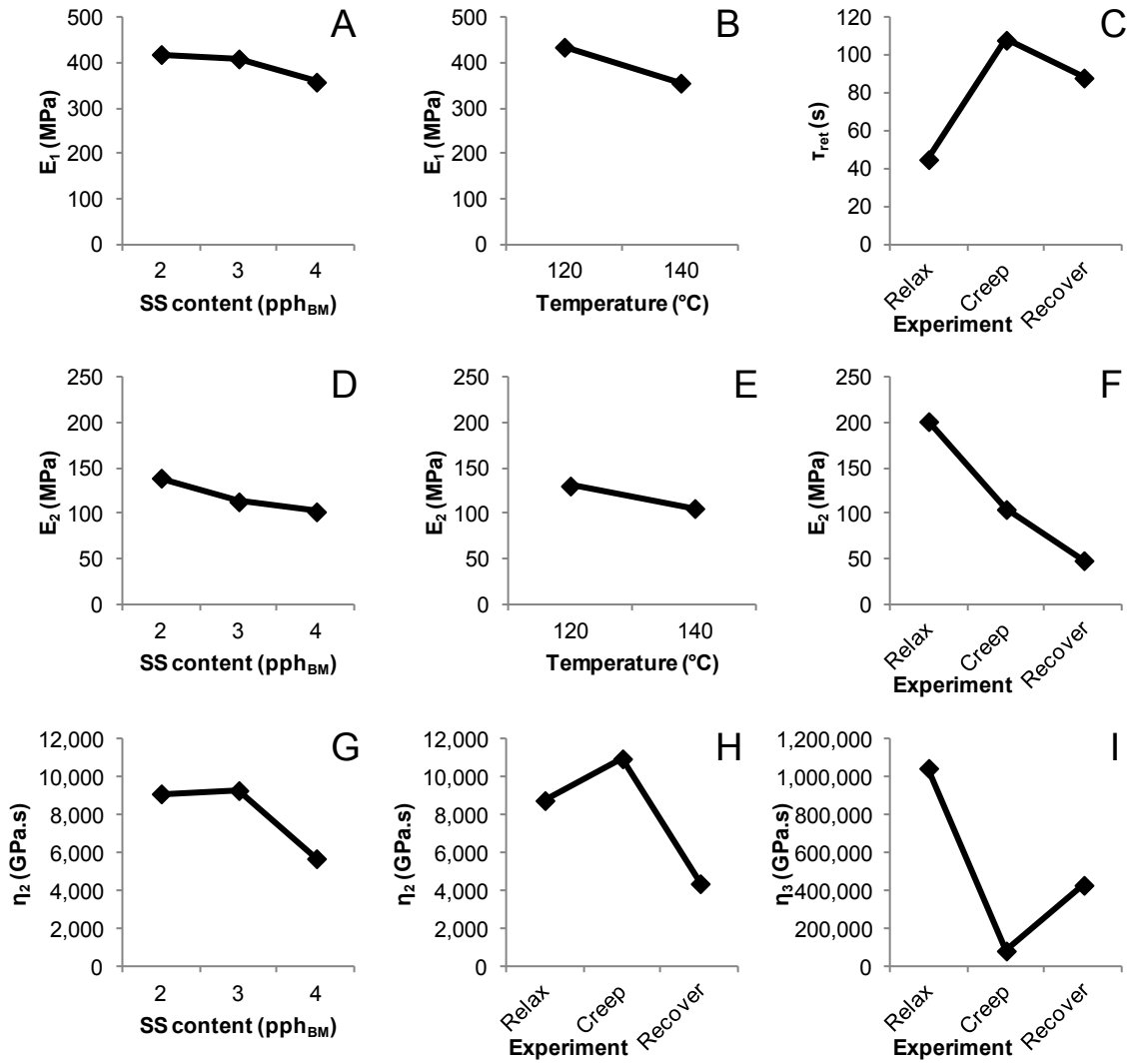

Figure 7: Group means for significant factors in main effects ANOVA of fitted modified four element model parameters: A) effect of SS on E_1, B) Effect of temperature on E_1, C) Effect of experiment type on τ_{ret}, D) Effect of SS content on E_2, E) Effect of temperature on E_2, F) Effect of experiment type on E_2, G) Effect of SS content on η_2, H) Effect of experiment type on η_2, I) Effect of experiment type on η_1.

Although more complicated constitutive models do exist, these have many more material constants which must be fitted to experimental data [16]. With a multitude of adjustable parameters, such a model was deemed unsuitable for a direct comparison of the effects of sodium sulfite and temperature. The modified four element model has the advantages of a good fit to experimental data and fewer unknowns to solve for.

Table 7: p-values and percentage contributions of main effects ANOVA on fitted modified four element model parameters. Bold p-values indicate significance at the 95% confidence interval

	E_1 (MPa)	E_2 (MPa)	η_2 (GPa.s)	η_1 (GPa.s)	τ_{ret} (s)
p-value					
Experiment type	0.43	**0.00**	**0.00**	**0.00**	**0.00**
Temperature	**0.00**	**0.00**	0.06	0.52	0.59
SS content	**0.00**	**0.00**	**0.00**	0.59	0.06
Percentage contribution					
Experiment type	pooled	79%	37%	59%	45%
Temperature	32%	3%	pooled	pooled	pooled
SS content	14%	5%	13%	pooled	pooled
Error	54%	13%	50%	41%	55%
	100%	100%	100%	100%	100%

Table 8: p-values and percentage contributions of main effects ANOVA on fitted modified four element model parameters within each experiment type. Bold p-values indicate significance at the 95% confidence interval

	E_1 (MPa)	E_2 (MPa)	η_2 (GPa.s)	η_1 (GPa.s)	τ_{ret} (s)
p-value					
Creep					
Temperature	**0.00**	**0.02**	**0.01**	0.12	0.33
SS content	**0.01**	0.10	**0.02**	0.08	0.11
Recovery					
Temperature	**0.00**	0.63	0.51	0.11	0.33
SS content	0.48	**0.03**	0.06	0.22	0.15
Relaxation					
Temperature	**0.05**	**0.03**	0.55	0.74	0.11
SS content	**0.05**	**0.02**	**0.04**	0.13	0.68
Percentage contribution					
Creep	36%	26%	30%	pooled	pooled
Temperature	30%	pooled	31%	pooled	pooled
SS content	34%	74%	40%	100%	100%
Error	100%	100%	100%	100%	100%
Recovery					
Temperature	45%	pooled	pooled	pooled	pooled
SS content	pooled	42%	pooled	pooled	pooled
Error	55%	58%	100%	100%	100%
	100%	100%	100%	100%	100%
Relaxation					
Temperature	18%	20%	pooled	pooled	pooled
SS content	29%	34%	36%	pooled	pooled
Error	53%	46%	64%	100%	100%
	100%	100%	100%	100%	100%

Overall, by increasing temperature or sodium sulphite, E_2 was significantly reduced, corresponding to higher spring compliance in the VK element, or increased recoverable creep within twenty minutes. This suggests partial reduction in cross-linkages, which restrict the extent of creep, but not to such an extent that

a large number of bonds were broken. Enough cross-links remained to prevent extensive permanent deformation or significant chain slippage. SS also had a significant effect on η_2, reducing it approximately by half at 4 pph_{BM} SS (Figure 7G). Sample 4-140 showed greater recovery than the other five sample types, suggesting there could be some interaction between temperature and SS, as seen for tensile strength and secant modulus in the pull to break analysis.

Dynamic mechanical analysis

Dynamic mechanical analysis revealed a glass transition in the range of 58-65°C for all samples (Table 2), therefore all samples were at least 30°C below T_g when tested for viscoelasticity. Although differences between the formulations were minor the samples containing 4 pph_{BM} had the lowest T_g, at both melt temperatures. T_g is normally assumed to be an indication of chain mobility. In this work large differences in the T_g were not observed, but clear differences were observed when evaluating the time-dependant properties. Short term viscoelastic testing was therefore useful to evaluate subtle differences between chain mobility. There was little difference between 2 and 3 pph_{BM} SS, but 4 pph_{BM} did make a significant difference (Table 3). However, the overall goal is not to increase chain mobility too much, as strength drops accordingly. This too was evident from pull to break results.

Conclusions

Thermoplastic protein produced from bloodmeal shows appreciable creep, recovery and stress relaxation on an experimental time scale of 20 minutes. This has implications for use in some product types, for example anything weight bearing where a product is under load or tension where creep may not be desirable. Nevertheless, high recovery of creep is seen, suggesting that, although the material shows time dependent deformation, most of this is not permanent at the stresses and strains investigated.

A modified four element model was able to be fitted individually stress relaxation, creep and recovery; however model parameters were different for each experiment type. Recovery was seen to occur faster than creep, and to a greater extent than that predicted from parameters fitted to the creep portion of the

experiment. Although a model could be fitted to stress relaxation data, the parameters obtained greatly under-predicted creep.

Both sodium sulphite content and processing temperature were shown to affect standard mechanical properties and time dependent behaviour. Increased sodium sulphite led to greater extent of creep in twenty minutes (total and recoverable), greater strain at break and reduced modulus and strength. The higher injection moulding temperature also reduced modulus and strength, while increasing the fraction of creep recovered in twenty minutes

Together, these results confirmed that increased sodium sulphite increased chain mobility. Additionally, it was found that injection moulding at 140°C instead of 120°C did not cause excessive thermal crosslinking, but rather increased chain mobility at some sodium sulphite contents. While increased chain mobility in the conditioned plastic comes at the expense of strength, and is not always desirable, this widens the range of acceptable injection moulding parameters which may be useful in adjusting injection settings for appropriate filling of different moulds.

References

[1] C.J.R. Verbeek, L.E. van den Berg, Development of Proteinous Bioplastics Using Bloodmeal, J. Polym. Environ., (2010) 1-10.

[2] C.J.R. Verbeek, L.E. van den Berg, Extrusion Processing and Properties of Protein-Based Thermoplastics, Macromol. Mater. Eng., 295 (2010) 10-21.

[3] C.J.R. Verbeek, C. Viljoen, K.L. Pickering, L.E. van den Berg, NZ551531: Plastics material, in: IPONZ (Ed.), Waikatolink Limited, New Zealand, 2007.

[4] C.J.R. Verbeek, L.E. van den Berg, Structural changes as a result of processing in thermoplastic bloodmeal, J. Appl. Polym. Sci., 125 (2012) E347-E355.

[5] H.C. Huang, T.C. Chang, J. Jane, Mechanical and physical properties of protein-starch based plastics produced by extrusion and injection molding, J. Am. Oil Chem. Soc., 76 (1999) 1101-1108.

[6] D.W. van Krevelen, K.t. Nijenhuis, Properties of polymers :their correlation with chemical structure : their numerical estimation and prediction from additive group contributions, 4th, completely rev. / ed., Elsevier, Amsterdam ;Boston, 2009.

[7] D.D. Joye, Stress-relaxation in 3-element and 4-element mechanical models of viscoelastic materials, Journal of Applied Polymer Science, 47 (1993) 345-350.

[8] G.C.-C. Chuang, A.-I. Yeh, Creep Deformation Modeling of Glutinous Rice Cakes (Mochi), Cereal Chem., 83 (2006) 179-187.

[9] S. Purkayastha, M. Peleg, M.D. Normand, Presentation of the creep curves of solid biological-materials by a simplified mathematical version of the generalized Kelvin-Voigt model, Rheol. Acta, 23 (1984) 556-563.
[10] G.C.-C. Chuang, A.-I. Yeh, Rheological characteristics and texture attributes of glutinous rice cakes (mochi), Journal of Food Engineering, 74 (2006) 314-323.
[11] J.T. de Faria, V.P.R. Minim, L.A. Minim, Evaluating the effect of protein composition on gelation and viscoelastic characteristics of acid-induced whey protein gels, Food Hydrocolloids, 32 (2013) 64-71.
[12] J.M. Bier, C.J.R. Verbeek, M.C. Lay, Identifying transition temperatures in bloodmeal-based thermoplastics using material pocket DMTA, J. Therm. Anal. Calorim., (2012) 1-13.
[13] ASTM International, D638 -03 Standard Test Method for Tensile Properties of Plastics, in, ASTM International,, West Conshohocken, PA 19428-2959, United States., 2004.
[14] StatSoft Inc, STATISTICA (data analysis software system) version 11., in, 2012.
[15] K.P. Menard, Dynamic mechanical analysis :a practical introduction, 2nd ed., CRC Press, Boca Raton, FL, 2008.
[16] A.D. Drozdov, J.D. Christiansen, Viscoelasticity and viscoplasticity of semicrystalline polymers: Structure-property relations for high-density polyethylene, Comput. Mater. Sci., 39 (2007) 729-751.

7

Using Synchrotron FT-IR Spectroscopy to Determine Secondary Structure Changes and Distribution in Thermoplastic Protein

A paper

published in

Journal of Applied Polymer Science

by

JAMES M. BIER[1], C.J.R. VERBEEK AND M.C. LAY

[1]As first author for this paper, I prepared the initial draft manuscript, which was refined and edited in consultation with my supervisors, who have been credited as co-authors. This work reported results from beamtime at the Australian synchrotron in November 2011. In discussion with my supervisors, I designed the experiment and drafted the beamtime proposal. The synchrotron proposal system does not permit students to register as "lead researchers," however I was registered as co –proposer. I prepared the samples and liaised with the synchrotron regarding obtaining appropriate import permits to take them into Australia. Together with my supervisors, I travelled to the Australian Synchrotron to conduct the experiments. I then performed the data analysis in OPUS software and Microsoft Excel, and ran the statistical analysis in Statistica.

JOURNAL OF Applied Polymer SCIENCE

Using Synchrotron FTIR Spectroscopy to Determine Secondary Structure Changes and Distribution in Thermoplastic Protein

James Michael Bier, Casparus Johannes Reinhard Verbeek, Mark Christopher Lay
School of Engineering, Faculty of Science and Engineering, University of Waikato, Hamilton 3240, New Zealand
Correspondence to: J. M. Bier (E-mail: jmb101@waikato.ac.nz)

ABSTRACT: Blood meal is a high protein, low value by-product of the meat processing industry that can be converted into a thermoplastic material by extrusion with a combination of a surfactant, urea, a reducing agent, water, and plasticiser. Changes in protein structure after each processing step (mixing with additives, extrusion, injection molding, and conditioning) were explored using synchrotron FTIR microspectroscopy. Blood meal particles were found to have higher β-sheet content around the perimeter with a randomly structured core. α-Helices were either located near the core or were evenly distributed throughout the particle. Structural rearrangement consistent with consolidation into a thermoplastic was seen after extrusion with processing additives, resulting in reduced α-helices and increased β-sheets. Including triethylene glycol as a plasticiser reduced α-helices and β-sheets in all processing steps. At all processing stages, regions with increased β-sheets could be identified suggesting blood meal-based thermoplastics should be considered as a semicrystalline polymer where clusters of crystalline regions are distributed throughout the disordered material.

KEYWORDS: proteins; thermoplastics; spectroscopy; extrusion; microscopy

Received 9 December 2012; accepted 6 February 2013; published online
DOI: 10.1002/app.39134

INTRODUCTION

Renewable alternatives to petrochemical polymers can be produced by converting biomass sources into new polymers (e.g., PLA or PHA) or by modifying biopolymers to enable thermoplastic processing. Thermoplastic starch is available commercially and thermoplastics have been produced from many proteins, including wheat, soy, and sunflower from plants as well as gelatine, keratein, casein, whey, and blood meal from animals.[1] Blood meal is a denatured protein by-product of the meat processing industry produced by steam coagulation and drying of blood. Treating blood meal with a combination of water, a protein denaturant, a reducing agent and a surfactant produces a thermoplastic, which can be extruded and injection molded.[2,3]

Proteins in their native and denatured states typically contain regions of secondary structures such as α-helices, β-sheets, and random coils. Extrusion and injection molding of proteins require chain rearrangement, implying changes to protein secondary structure. This structural rearrangement is a major challenge in developing protein-based thermoplastics.[4] For processing, existing chain interactions in and between proteins must be overcome using denaturants, reducing agents, surfactants, and heating, forming a homogenous melt, followed by new interactions forming during cooling to consolidate the molded or extruded article.[1,5] Although not exclusively the case, thermoplastic processing tends to increase β-sheet content at the expense of α-helices.[1] β-Sheets have stronger hydrogen bonding interactions than α-helices, potentially creating stronger interchain interactions and hence stronger materials. For example, strong natural fibrous proteins such as spider silk are known to have high β-sheet content. However, for some applications, such as film blowing, higher helical contents have been shown to be favorable.[6]

Not only is it of interest to determine what secondary structures are present, but their spatial distribution is also relevant. Dynamic mechanical analysis of blood meal based thermoplastics suggests a semicrystalline character with some phase separation after processing.[7] Microcrystalline regions in synthetic polymers can increase mechanical properties such as toughness, therefore spatial secondary structure variation in proteins may mimic this. Spatial resolution of protein secondary structures may determine if there is separation into α-helix rich and β-sheet rich regions, or plasticiser rich and protein rich phases. This will provide insight into chain rearrangements induced by processing, and may suggest future manipulations to improve properties.

FTIR is an established protein structure characterisation technique, particularly useful for exploring changes in secondary

Table I. Band Assignments in Determination of Protein Secondary Structures

Region	Secondary structure	Band assignment (cm^{-1})
Amide III[18]	α Helix	1295-1330
	β-Turns	1270-1295
	Random coils	1250-1270
	β-Sheets	1220-1250
Amide I[8]	Antiparallel β-sheet/ aggregated strands	1675-1695
	3_{10}-Helix	1660-1670
	α-Helix	1648-1660
	Unordered	1640-1648
	β-Sheet	1625-1640
	Aggregated strands	1610-1628

structure.[8] Determining absolute secondary structures (rather than just relative change) with FTIR relies on several assumptions, which may not necessarily always be valid for proteins, for example, that all structures absorb equally at the same concentration.[9] Nevertheless, quantitative estimation of secondary structures using the technique shows good agreement with X-ray data.[10,11]

Synchrotron IR sources are typically 100–1000 times brighter than conventional globar/thermal IR sources due to their highly collimated nature and small effective source size.[12,13] Very little light from a globar source will pass through a 10 μm aperture, whilst >80% of the light from a synchrotron source will, leading to much higher signal to noise ratios at high spatial resolutions.[12]

Synchrotron based FTIR microscopy (S-FTIR) has been used for spatial resolution of secondary structures in a variety of agricultural protein sources including animal feeds and feather proteins.[9,13–15] Relative estimates of the ratio of α-helices and β-sheets were able to be mapped, showing distributions across plant tissues as well as differences between feed sources known to have different digestibility. S-FTIR has also been used to examine phase separation of biopolymer blends such as gelatin with maltodextrin and quantification of peak intensities may enable analysis of compositional fractions *in situ*.[16]

Protein FTIR spectra contain several regions relating to vibrations along the polypeptide backbone. The amide I region (1600–1700 cm^{-1}), occurring mostly due to C=O bond vibration, is the most commonly used for secondary structure determination.[8] Stronger hydrogen bonds reduce electron density in the C=O bond, shifting its absorbance to lower wavenumbers. Different secondary structures have different hydrogen bonding strength leading to different characteristic absorbencies.[8] In practice, the amide I region is a convoluted peak, and techniques such as Fourier self deconvolution or second derivative analysis (2DA) are necessary to identify individual peak components.[10]

Although the amide I peak is typically the strongest absorbing peak of proteins, it also overlaps with an absorbance band of H_2O. For this reason, dry proteins or proteins dissolved in deuterated water are typically used for analysis. A further complication is that urea absorbs strongly in this region, at wavenumbers typically associated with β-sheets. As urea is used to prepare thermoplastic protein from blood meal, it may contribute to a perceived increase in β-sheets.[17] The amide III absorbance region (1200–1350 cm^{-1}) is due to in phase N—H bending and C—N stretching. Although, typically 5–10 times weaker than the amide I region, the amide III region is also sensitive to structural changes, and not subject to interference from H_2O[18] nor urea. Typical band assignments for protein secondary structures are given in Table I.

The objective of this research was to determine if there was spatial variation of protein secondary structures in blood meal and blood meal-based thermoplastics. This was explored using FTIR microspectroscopy at the Australian Synchrotron. Specifically, changes induced by processing were evaluated, which should demonstrate consolidation. The multiphase behavior implied by dynamic mechanical thermal properties could then be correlated with structural changes. Increased understanding of the interdependent relationship between structures, properties, and processing in thermoplastic protein may then suggest future directions to enhance processing methods and improve resultant material properties.

EXPERIMENTAL

Materials

Novatein thermoplastic protein (NTP) was prepared from the reagents shown in Table II. Two variants were produced,

Table II. Materials Used and NTP Compositions

Reagent	Source	Grade	Composition g/100 g blood meal (pph_{BM}) V0	V2
Blood meal	Wallace Corporation	Agricultural	100	100
Urea	Ballance Agrinutrients	Agricultural	10	10
Water	Produced on site from town supply	Distilled	60	40
Sodium dodecyl sulfate	Merck	Technical	3	3
Sodium sulphite	Merck	Technical	3	3
Triethylene glycol	Merck	For synthesis	0	20

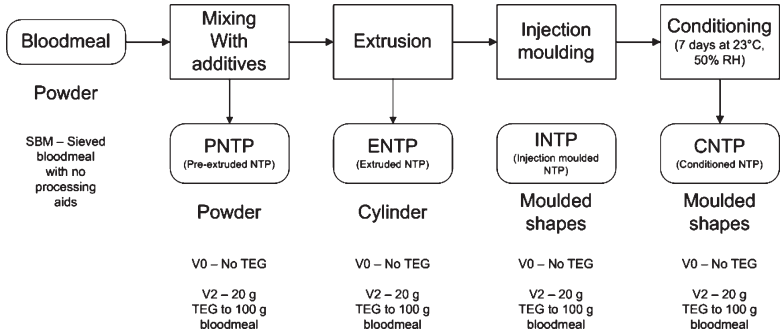

Figure 1. Samples prepared for synchrotron analysis.

differing in whether or not the plasticiser triethylene glycol (TEG) was included in the formulation.

Experimental Design

Samples were prepared at different stages of processing starting with blood meal up to a conditioned thermoplastic material, as shown in Figure 1. Two formulations were used, with and without TEG as an additional plasticiser (Table II). This resulted in eight NTP sample types, in addition to blood meal. For each sample type, a minimum of three rectangles were mapped.

Statistical Analysis. Analysis of variance (ANOVA) on secondary structure scores of the protein plastics were conducted in Statistica version 10 (StatSoft).[19] Data was filtered for a minimum area under the amide I region to exclude points mapped outside particle surfaces. A factorial experimental design was followed (Table III) and ANOVA was used to assess the effects of processing stage and the inclusion or exclusion of plasticiser on secondary structure.

Methods

Mixing with Additives. Urea, sodium sulfite, and sodium dodecyl sulphite were dissolved in distilled water at 50°C in the ratios shown in Table II, and mixed with blood meal in a high speed mixer for 10 min. If TEG was included, it was added after the first 6 min blending.

Extrusion. Extrusion was performed using a ThermoPrism TSE-16-TC twin-screw extruder with a temperature profile and screw configuration as shown in Figure 2 using a screw speed of 150 rpm. Actual melt temperatures were within 2–5°C of the set temperatures. The screw diameter was 16 mm, with an L/D ratio of 25 and it was fitted with a single 10 mm diameter circular die. A relative torque of 60–75% of the maximum allowed in the extruder was maintained (12 Nm per screw maximum) by adjusting the mass flow rate of the feed. Extruded material was granulated using a tri-blade granulator from Castin Machinery Manufacturer, New Zealand.

Table III. Array Design for ANOVA of Effects of Processing and Plasticizer Content

	Without TEG	With TEG
Pre-extrusion	PNTP-V0	PNTP-V2
Extruded	ENTP-V0	ENTP-V2
Injection molded	INTP-V0	INTP-V2
Conditioned	CNTP-V0	CNTP-V2

Injection Molding. Granulated extrudate was injection molded into Type 1 tensile test specimens[20] using a BOY-35A injection molder with 24 mm screw (L/D ratio of 24). A temperature profile of 100, 115,120, 120, and 120°C from feed zone to die, a screw speed of 200 RPM and a mold locking force of 30 kN were used. The mold was heated to 70°C using water and the injection pressure was set to 1100 bar in profile sections zero to four and 300 bar in sections 5–7.

Conditioning and Freeze Drying. Injection molded samples were placed in a chamber kept at 23°C and 50% relative humidity for 7 days. Apart from blood meal, which was already a dry powder, all samples were dried over two nights in a Freezone^{TM} 2.5 L benchtop freeze dryer (Labconco Corporation, Kansas City) set to auto mode (collector temperature −50°C, vacuum < 11 Pa).

Synchrotron based FTIR

Data Collection. Spatially resolved FTIR experiments were undertaken on the infrared microspectroscopy beamline at the Australian Synchrotron, Victoria, Australia. Spectra were collected using a Bruker Hyperion 3000 with an MCT collector and XY stage using Opus 6.5 software (Bruker Optik GmbH 2009).Video images were captured of each sample and a minimum of three representative grids (5 μm spot size) were mapped on each. For each grid point, 32 spectra were collected with a resolution of 4 cm^{-1} between 3900 and 700 cm^{-1} and averaged. Data acquisition took $\sim$ 11 s per grid point with the subtracted background also rescanned every five points, plus additional time for sample preparation and mounting.

For solid samples, microtomed ribbons were flattened between two diamond cells removing the top of the cell for analysis. Sections 2 μm thick were cut using stainless steel blades (TBS^{TM}) on a TBS Cut 4060 RE microtome (TBS^{TM}) lit by a microlight 150 (Fibreobtic Lightguides, Australia).

For powders, fine particles were chosen and flattened between diamond cells. Initially, the top was also removed for analysis, however this proved problematic as samples decompressed during analysis. It was found that more reliable and cleaner spectra were obtained from powders with the top cell left in place.

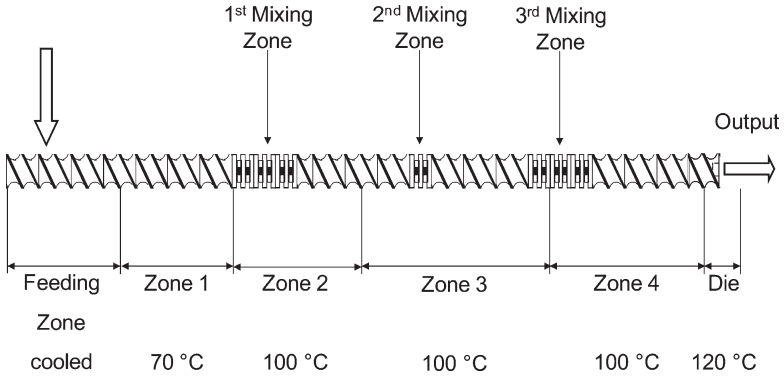

Figure 2. Extruder screw configuration and temperature profile.

Data Processing. Second derivative peaks in the amide III region have previously been used for quantitative analysis of protein secondary changes during mixing of gluten,[21] demonstrating their usefulness for analysis of changes in solid phase mixtures containing non-native protein. Derivation offers two main advantages: first, sloping baselines are removed without the need for subjective corrections.[22] This is advantageous for grid maps where the baseline shape may not be constant across the entire map. Second, spectral resolution of overlapping bands is increased.[22] This is advantageous for both the amide I and amide III regions of proteins, which contain overlapping bands corresponding to different secondary structure conformations.

There are two challenges in using 2DA for quantitative structure determination: noise increases through the introduction of peak side-lobes; and second derivative peak heights are sensitive to the half width at half height (HWHH) of original peaks, with narrower peaks giving higher second derivative peaks.[23] This has led to criticism of the reliability of determining protein secondary structure composition using 2DA.[24] However, if the same calculation procedure is used for all samples and the same peaks are of interest, relative differences can still be explored.[23] Demonstrations using poly L-lysine and hemoglobin as model proteins have shown that neither the side lobes nor HWHH issues affected quantitative results using 2DA.[24]

The second derivative of the original spectra (with no baseline correction) was determined using the Savitzky-Golay algorithm in Opus 6.5 using nine point smoothing. The second derivative was inverted by dividing by negative one and peak heights above the zero line were compared. Spatial maps were drawn using OPUS 6.5 based on the ratios A''_α/A''_β, A''_t/A''_β, and A''_r/A''_β, where A''_x is the maximum height of the inverted second derivative peak within the wavenumber range associated with α-helices, β-sheets, turns, and random coils (Table I) indicated, respectively, by the subscripts α, β, t, and r. The molar fraction for each secondary structure type was calculated using eqs. (1)–(5) and spatial maps were drawn based on these compositions using Microsoft Excel.

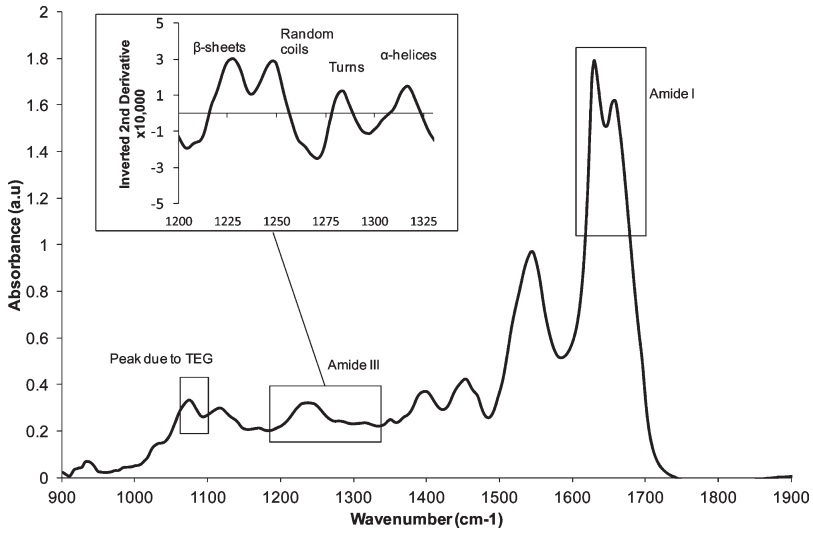

Figure 3. Example spectra of ENTP V2 from a single 5 μm spot on a mapped grid.

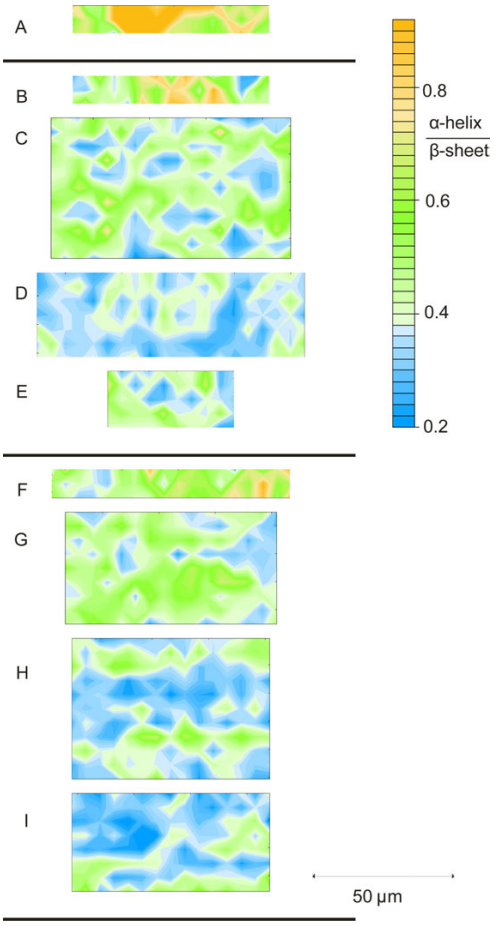

Figure 4. Representative maps showing second derivative peak height ratios (α-helices/β-sheets) for (A) Blood meal, (B) PNTP V0, (C) ENTP V0, (D) INTP V0, (E) CNTP V0, (F) PNTP V2, (G) ENTP V2, (H) INTP V2, and (I) CNTP V2. All maps have been drawn at the same scale and intensity scale. [Color figure can be viewed in the online issue, which is available at wileyonlinelibrary.com.]

$$\alpha + \beta + t + r = 1 \quad (1)$$

$$\beta = \frac{1}{A''_\alpha/A''_\beta + A''_t/A''_\beta + A''_r/A''_\beta + 1} \quad (2)$$

$$\alpha = \beta \frac{A''_\alpha}{A''_\beta} \quad (3)$$

$$t = \beta \frac{A''_t}{A''_\beta} \quad (4)$$

$$r = \beta \frac{A''_r}{A''_\beta} \quad (5)$$

The composition approximates a mole fraction of peptide linkages in each structural conformation, each of which absorbs differently in the amide III region. Spatial maps of TEG distribution were constructed by comparing the area ratio of the peak at 1040–1090 cm^{-1} to the total area of the amide III region.

WAXS

Powder wide angle X-ray scattering (WAXS) was conducted using a Phillips system running X'Pert Data Collector vs. 2.0b and XPERT-MPD vs. 2.7 control software. A PW3373/00 Cu LFF DK233995 X-ray tube was used at a voltage of 40 kV and current of 40 mA, which provided X-rays with a wavelength of 1.54 Å. Samples were scanned from $2\theta = 2°–60°$ at 0.020° steps. As well as analysing the sample types taken to the Synchrotron in powder form, conditioned plastics were ground and then freeze dried for WAXS.

RESULTS AND DISCUSSION

Classification of Peaks and Ratio of α-Helices to β-Sheets

A typical FTIR spectra from the protein plastic is shown in Figure 3 along with an inverted second derivative in the amide III region demonstrating the resolution of this region into four peaks. Based on assignments in literature these were taken to represent α-helices, turns, random coils, and β-sheets in order of decreasing wave number.[18,21] It should be emphasised that Figure 3 only represents one 5 μm spot on one sample of the plastic. Changes in the relative heights of these peaks could be used as a comparison reflecting relative differences in protein secondary structure spatially across a sample (Figure 4).

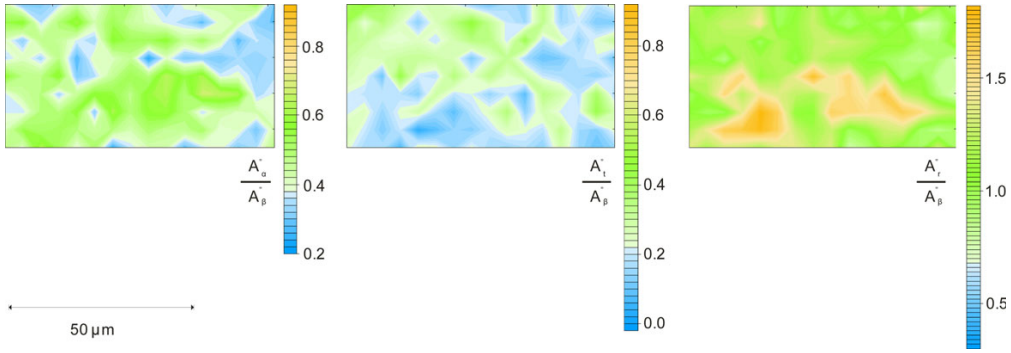

Figure 5. Maps of second derivative peak height ratios in ENTP V2. From left to right: α-helix/β-sheet, turn/ β-sheet, and random coil/β-sheet. [Color figure can be viewed in the online issue, which is available at wileyonlinelibrary.com.]

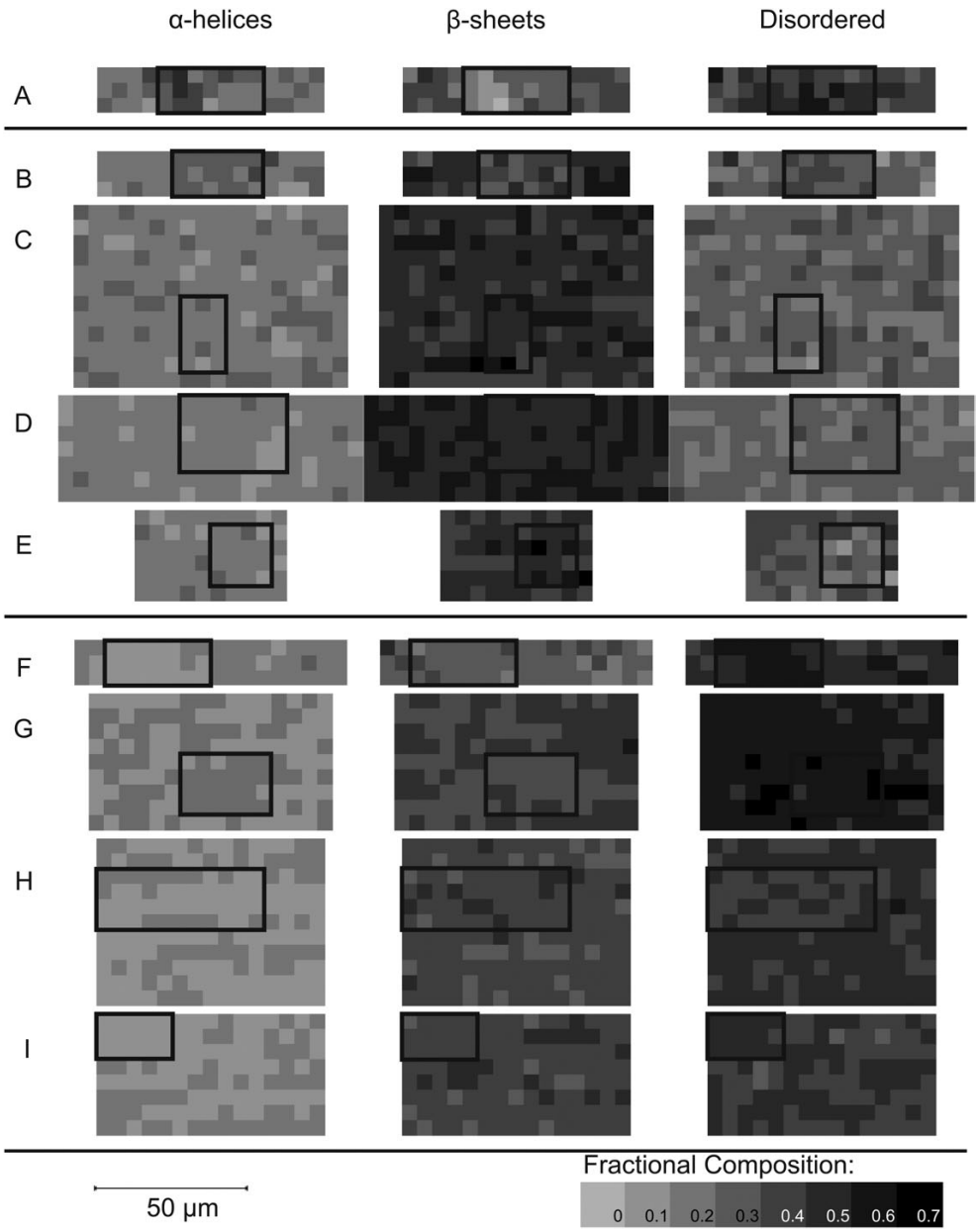

Figure 6. Representative maps showing fractional secondary structure for (A) Blood meal, (B) PNTP V0, (C) ENTP V0, (D) INTP V0, (E) CNTP V0, (F) PNTP V2, (G) ENTP V2, (H) INTP V2, and (I) CNTP V2. All maps have been drawn at the same distance and intensity scale. Each pixel represents a 5 μm spot and the shading represents the relative composition calculated from the inverted second derivative spectra.

Comparison of peak height ratios across a map, rather than actual peak height, has the advantage of correcting for any differences in thickness.[13] Such a method has been used in conjunction with S-FTIR to compare ratios of α-helices and β-sheets in a variety of agricultural protein sources including animal feeds and coproducts of biofuel production.[13–15]

The ratio of α-helix to β-sheet peak height was typically well below one, suggesting that there are more β-sheets than helices. Although the main proteins in bovine blood (haemoglobin and bovine serum albumin) are known to have helical structures, a higher proportion of β-sheets is consistent with thermal aggregation during blood meal production. In blood meal and pre-processed material, the regions with the highest helical content, relative to β-sheets, are in the centre of particles (Figure 4). It is worth noting that extrusion caused drastic changes in the appearance of the spatial maps, but the material looks similar

Table IV. ANOVA Results for Effect of Formulation and Processing on Fractional Secondary Structure

		Helix		Turn		Random coil		Sheet	
Factor	DOF	*F*	Contrib.	*F*	Contrib.	*F*	Contrib.	*F*	Contrib.
Formulation	1	730	15 %	207	6 %	4454	53 %	4175	43 %
Processing	3	244	15 %	41	3 %	184	7 %	781	24 %
Formulation × Processing	3	17	1 %	59	5 %	48	2 %	11	0.3 %
Error	3236		69 %		86 %		38 %		32.7 %
Total	3423		100 %		100 %		100 %		100 %

		Helix/sheet ratio		Turn/sheet ratio		Random coil/sheet ratio	
Factor	DOF	*F*	Contrib.	*F*	Contrib.	*F*	Contrib.
Formulation	1	56	1 %	401	10 %	2557	37 %
Processing	3	383	25 %	82	6 %	364	16 %
Formulation × Processing	3	55	4 %	71	5 %	27	1 %
Error	3236		70 %		79 %		46 %
Total	3423		100 %		100 %		100 %

after injection molding and conditioning. After processing, there is reduced overall helical content relative to β-sheets, but there was still spatial variation with regions showing a higher ratio of α -helices than other portions of the same map. Although this suggests some structural changes are caused by extrusion, thermoplastic protein is better thought of as a four component system comprised of helices, sheets, random coils, and turns. Limiting analysis to the ratio of α-helices to β-sheets does not make the distinction between whether the effect of processing is to decrease helices, increase sheets, or both. The ratio of random coils to β-sheets and of turns to β-sheets were also found to vary spatially across each map (Figure 5) showing that variations in these also need to be taken into account.

Changes in Fractional Composition

Figure 6 shows maps of fractional composition calculated from the second derivative peak height ratios for representative grids for each sample. While Figure 6 only shows a single mapped rectangle for each sample type, a minimum of three maps were scanned for each, visually inspected, and included in the statistical analysis. Both α-helices and β-sheets are ordered structures whereas random coils and turns are have been grouped together to represent the disordered amorphous fraction. When viewed in this way, it is apparent that the variation in α-helix/β-sheet ratio seen in Figure 4 was partly caused by clusters of helix rich regions, higher amounts of β-sheets near blood meal particle edges, and a more disordered particle core. Processing additives induced some chain rearrangement in blood meal prior to extrusion. This is important as protein cross-linking (physical and chemical) fixes chains in place, preventing thermoplastic flow during heating. The additives disrupted cross-linking and the chain rearrangements observed here demonstrates that disruption occurred prior to extrusion.

Results from a factorial ANOVA, considering the effect of both formulation and processing stages, are shown in Table IV and Figure 7. Formulation, processing and their interaction were significant at >99% confidence level for all four structures. Formulation had the greatest percentage contribution to the

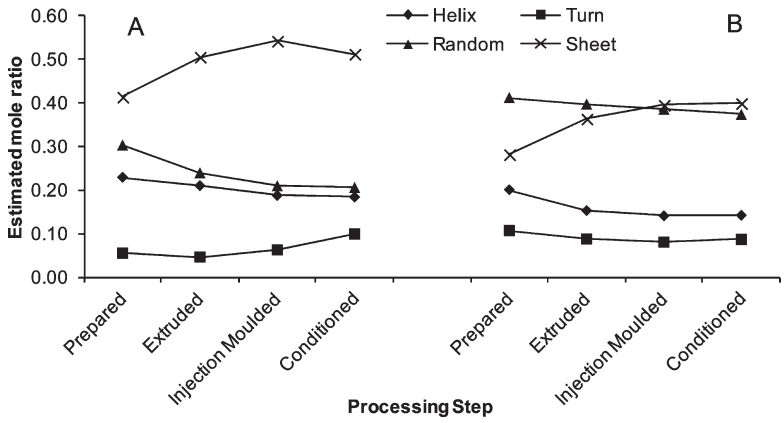

Figure 7. ANOVA means results demonstrating effect of formulation and processing on mean compositions. (A) Formulation V0 (no TEG) and (B) formulation V2 (with 20 pph_{BM} TEG).

Table V. Summary Statistics

	Fractional Composition of Each Structure					T-Test Results		
	Mean	Std. dev	Lower quartile	Median	Upper quartile	Rectangle mean	Subset mean	*P*-value
α-Helices								
SBM	0.24	0.06	0.19	0.23	0.28	0.26	0.30	0.15
PNTP V2	0.20	0.07	0.15	0.19	0.24	0.17	0.14	0.00
ENTP V2	0.15	0.03	0.14	0.15	0.17	0.15	0.17	0.00
INTP V2	0.14	0.03	0.12	0.14	0.16	0.14	0.14	0.74
CNTP V2	0.14	0.03	0.12	0.14	0.16	0.14	0.11	0.00
PNTP V0	0.23	0.04	0.20	0.23	0.26	0.24	0.28	0.03
ENTP V0	0.21	0.04	0.18	0.21	0.24	0.21	0.21	0.99
INTP V0	0.19	0.03	0.16	0.19	0.21	0.19	0.19	0.57
CNTP V0	0.18	0.04	0.15	0.18	0.21	0.19	0.20	0.34
β-Sheets								
SBM	0.35	0.09	0.29	0.36	0.41	0.30	0.23	0.01
PNTP V2	0.28	0.07	0.23	0.29	0.33	0.31	0.31	0.63
ENTP V2	0.36	0.04	0.33	0.36	0.39	0.35	0.32	0.00
INTP V2	0.39	0.05	0.36	0.39	0.43	0.39	0.42	0.00
CNTP V2	0.40	0.05	0.37	0.40	0.43	0.41	0.39	0.30
PNTP V0	0.41	0.06	0.37	0.41	0.45	0.46	0.39	0.00
ENTP V0	0.50	0.05	0.47	0.51	0.54	0.48	0.51	0.02
INTP V0	0.54	0.04	0.51	0.54	0.57	0.54	0.52	0.01
CNTP V0	0.51	0.07	0.46	0.51	0.56	0.48	0.52	0.04
Disordered structures								
SBM	0.41	0.09	0.35	0.40	0.47	0.43	0.47	0.09
PNTP V2	0.52	0.08	0.47	0.52	0.57	0.52	0.56	0.01
ENTP V2	0.48	0.04	0.46	0.48	0.51	0.49	0.51	0.19
INTP V2	0.46	0.04	0.44	0.46	0.49	0.46	0.44	0.00
CNTP V2	0.46	0.04	0.43	0.46	0.49	0.45	0.49	0.00
PNTP V0	0.36	0.07	0.32	0.36	0.40	0.30	0.34	0.11
ENTP V0	0.29	0.06	0.25	0.29	0.32	0.30	0.28	0.04
INTP V0	0.27	0.05	0.24	0.27	0.30	0.27	0.30	0.01
CNTP V0	0.30	0.07	0.25	0.31	0.36	0.33	0.28	0.02

amount of random coils and β-sheets, but processing also had a reasonable contribution to β-sheets. By comparing the means shown in Figure 7, going from prepared to an extruded material had a greater effect than subsequent injection molding and conditioning. Without TEG, addition of processing additives led to an increase in β-sheets, whereas including TEG with the additives increased disordered structures. After thermal processing, the samples with TEG continue to have more disordered structures and less β-sheets than samples without TEG. This effect was not apparent when simply looking at the α-helix/β-sheet ratio in Figure 4. Similarly, the ANOVA showed only a 1% contribution to the α-helix/β-sheet ratio, but larger contributions to both the individual helix and sheet content were observed.

The error terms for each structure showed that there was some variability not accounted for by the tested factors. In other words, although the means were significantly different between groups, there was still considerable variability within groups. This variability within groups was quantified in terms of standard deviation and quartiles within each sample type (Table V). In some cases, the difference between the upper and lower quartile within a sample was greater than the difference between the means between sample types. When considering this in conjunction with what is observed in Figure 6, it can be concluded that there was variation in secondary structure at different points within plastic sample as extreme as the difference in average composition before and after extrusion. A T-test between the highlighted subsections of each rectangle shown in Figure 6 and the rectangles themselves showed that regions of adjacent points could be identified with a significantly different composition to the map's average. The *P*-values obtained are shown in Table V. For each sample type, a region could be identified with a significantly different ($P < 0.05$) fractional content of at least two structure types (alpha helices, β- sheets, or disordered structures).

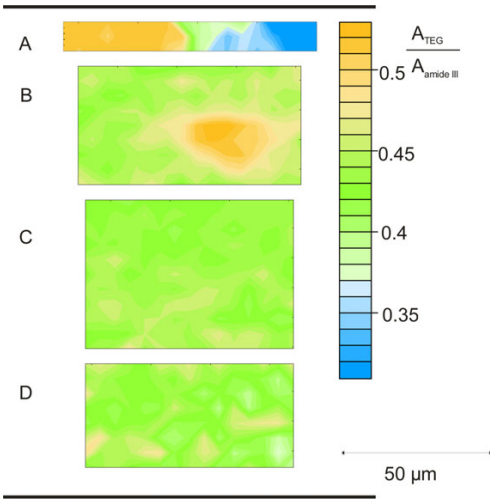

Figure 8. Spatial distribution of TEG in NTP. Representative maps of (A) PNTP, (B) ENTP, (C) INTP, and (D) CNTP. All four maps are on the same distance and intensity scale. [Color figure can be viewed in the online issue, which is available at wileyonlinelibrary.com.]

TEG Distribution

Spectra for samples with TEG showed a peak between 1040 and 1090 cm^{-1}, which was not present in samples without TEG. This peak was thought to be due to the C-OH functional groups in TEG. The ratio of this peak area to the amide III peak (baselines drawn across the bottom of each peak) was taken as representative of variations in TEG concentration across the sample. Variation in this ratio was seen in the samples, suggesting the presence of TEG rich regions and TEG poor regions (Figure 8). In PNTP, the centre of a large particle was relatively TEG poor compared with the perimeter suggesting TEG was unable to diffuse into the centre. After extrusion, regions of high TEG concentration suggested some heterogeneity. Injection molding appeared to have led to a finer dispersion, with heterogeneity returning after conditioning.

WAXS

WAXS for blood meal showed a sharp peak at $s = 1.3$ $Å^{-1}$, corresponding to a d-spacing of 4.8 Å, and another peak at about $s = 0.6$ $Å^{-1}$, corresponding to a d-spacing of 10.5 Å (Figure 9). Peaks corresponding to these distances are commonly seen in WAXS patterns of proteins and have alternately been described as corresponding to β-sheet structures or α-helix structures.[25] Both of these were reduced dramatically in pre-processed material with TEG, but less so when TEG was absent. Protein secondary structures are stabilized by hydrogen bonding interactions along the main chain (α-helices) or between adjacent chains (β-sheets). TEG contains function groups capable of hydrogen bonding, so it is reasonable to expect some disruption to secondary structure as protein-plasticiser interactions replace protein-protein interactions. A d-spacing of 4–5 Å corresponds to regular distances within structures, while a d-spacing of about 10.5 Å corresponds to interstructure packing (either stacked β-sheets or adjacent helices). That both peaks decrease in size with TEG supports observations from FTIR that TEG reduced overall α-helix and β-sheet content, and disrupted tight packing. Comparison of preprocessed material with ground conditioned material showed little difference within each formulation, and the difference between the two formulations was pronounced at both processing steps.

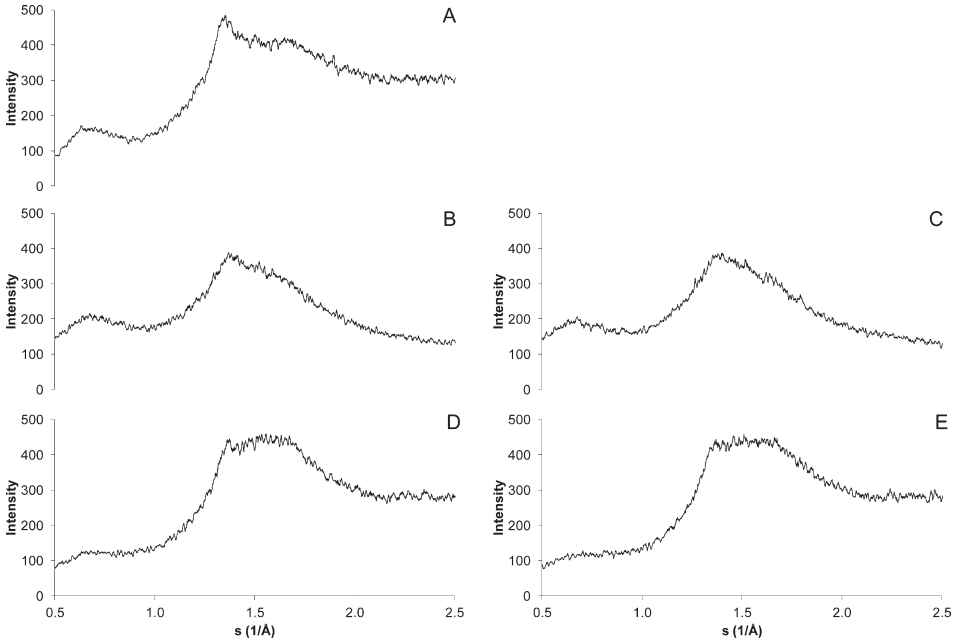

Figure 9. WAXS plots for (A) blood meal, (B) PNTP V0, (C) CNTP V0, (D) PNTP V2, and (E) CNTP V2.

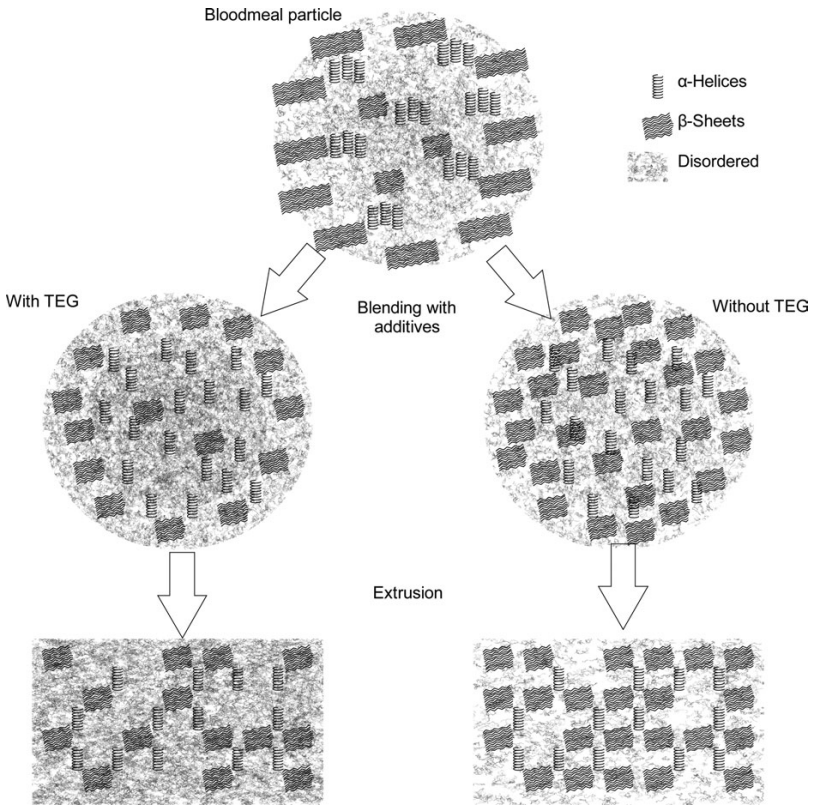

Figure 10. Schematic of proposed model for changes in structural dispersion as blood meal is processed into a thermoplastic.

Proposed Model for Structural Changes

Blood meal predominantly contains a uniform dispersion of helical structures and turns. Some blood meal particles suggested there were more α-helices in the centre, but this was not consistent throughout all particles tested. A higher concentration of β-sheets was consistently observed toward the edge of particles and a higher proportion of random coils in the middle of particles. Two aspects of blood meal production may contribute to this. Blood meal production involves coagulation followed by steam drying. The coagulation step may force hydrophobic side chains to aggregate, with hydrophilic regions still facing outward. These hydrophobic side group interactions then result in a random coil structure, rather than forming α-helices and β-sheets by hydrogen bonding. Additionally, cysteine–cysteine crosslinking is known to occur at elevated temperatures and may further stabilize the coagulated conformation. As additional heat is supplied and water is evaporated, β-sheet aggregation may then occur as water is removed from the hydrophilic regions at the edges of the coagulated particle. A second, alternative explanation is that β-sheets, being more crystalline, may be more brittle than random coils, and breakages may occur at these brittle regions when blood meal passes through a hammer mill at the end of blood meal production.

Transformation of blood meal into a thermoplastic involves the addition of urea to disrupt hydrogen bonding, sodium dodecyl sulfate to disrupt hydrophobic interactions and sodium sulfite to disrupt cysteine–cysteine crosslinkages. This destabilizes the side chain interactions in the disordered core, allowing formation of additional β-sheets prior to extrusion in the formulation without TEG. With TEG, an increase in disorder and a decrease in α-helices were observed. This observation can be explained by the presence of TEG contributing additional free volume and preventing new tightly packed interactions from occurring necessary for forming additional β-sheets. This is further supported by WAXS, which revealed that the tight packing of secondary structures observed in blood meal was preserved without TEG, but was reduced with it. A schematic of the changes thought to be occurring is shown in Figure 10.

The next transformation involves applying heat and shear in an extruder. This causes radical chain rearrangements necessary for consolidation of individual particles into a continuous extrudate. On an average structure level, this leads to an increase in β-sheets and reductions in both random coils and α-helices. More β-sheets were seen without TEG than with it, although both formulations showed evidence of spatial variations in their distribution. A decrease in turns suggested intermolecular β-sheets were formed rather than β-sheets consisting of chains folding back on themselves. Together, this suggests chain unravelling during heating and reformation of β-sheets

upon cooling, with some nucleation effects potentially leading to variations in β-sheet concentration across maps.

Injection molding involves heating to rearrange chains and allow them to flow under pressure. However the transformation from extruded to injection molded material was not nearly as drastic as what occurs when first extruded. Average composition did change slightly in favor of β-sheets, but the spatial map of β-sheet concentration looked comparable between extruded and injection molded samples. The slight effect of this second heating and cooling cycle confirmed the thermoplastic nature of NTP.

Conditioning was the final processing step in producing NTP test pieces and was included because NTP is hydrophilic and moisture sensitive. Changes in macroscopic properties such as tensile strength and glass transition temperature have previously been observed after conditioning.[7,26] Average secondary structure and the spatial distribution thereof appeared to change little between unconditioned and conditioned injection molded samples suggesting the changes in macroscopic properties were mostly due to changes in moisture content, rather than reformation of α-helices and β-sheets.

CONCLUSIONS

Blood meal-based thermoplastics should be considered as a semicrystalline polymer consisting of clusters of crystalline regions of α-helices and β-sheets distributed throughout a randomly coiled protein structure. The additives used to process blood meal into a thermoplastic caused structural rearrangement implying cysteine–cysteine crosslinking between protein chains was disrupted and chain mobility has increased. Extrusion caused drastic structural rearrangement, resulting in a more uniform structure implying consolidation had occurred. In blood meal particles, β-sheets were concentrated around the perimeter of particles, while in extruded and injection molded materials, β-sheet rich regions were distributed evenly throughout a more disordered matrix. Including TEG as a plasticizer reduced α-helices and β-sheets and increased the amount of disordered protein chains at each processing stage. These findings are consistent with earlier work, which indicated that NTP exhibited multiphase behavior beyond simple plasticizer separation. The results also suggest that if these structures and the distribution thereof can be manipulated, material properties could potentially be tailored for different applications.

ACKNOWLEDGMENTS

This research was undertaken on the infrared microspectroscopy beamline at the Australian Synchrotron, Victoria, Australia. Proposal number AS113/IRMFI/4267. The authors would especially like to acknowledge the technical assistance of Dr. Mark Tobin. Travel funding support was received from the New Zealand Synchrotron Group Ltd.

REFERENCES

1. Verbeek, C. J. R.; van den Berg, L. E. *Macromol. Mater. Eng.* **2010**, *295*, 10.
2. Verbeek, C. J. R.; Viljoen, C.; Pickering, K. L.; van den Berg, L. E. Plastic Matetial. NZ Patent NZ551531, **2007**.
3. Verbeek, C. J. R.; van den Berg, L. E. *J. Polym. Environ.* **2010**, *19*, 1.
4. Pickering, K.; Verbeek, C.; Viljoen, C. *J. Polym. Environ.* **2012**, *20*, 335.
5. Verbeek, C. J. R.; van den Berg, L. E. *Recent Pat. Mater. Sci.* **2009**, *2*, 171.
6. Oliviero, M.; Maio, E. D.; Iannace, S. *J. Appl. Polym. Sci.* **2010**, *115*, 277.
7. Bier, J. M.; Verbeek, C. J. R.; Lay, M. C. *J. Therm. Anal. Calorim.* **2012**, 1. Available at: http://dx.doi.org/10.1007/s10973-012-2680-0.
8. Jackson, M.; Mantsch, H. H. *Crit. Rev. Biochem. Mol. Biol.* **1995**, *30*, 95.
9. Yu, P. Q. *Spectr.-Int. J.* **2006**, *20*, 229.
10. Mantsch, H. H.; Casal, H. L.; Jones, R. N. In Spectroscopy of Biological Systems; Clark, R. J. H., Hester, R. E., Eds.; Wiley: Chichester, **1986**; pp 547.
11. Kong, J.; Yu, S. *Acta Biochim. Biophys. Sin.* **2007**, *39*, 549.
12. Miller, L. M. In Infrared and Raman Spectroscopic Imaging; Salzer, R., Siesler, H. W., Eds.; Wiley-VCH: Weinheim, **2009**, pp 510.
13. Yu, P. Q.; McKinnon, J. J.; Christensen, C. R.; Christensen, D. A. *J. Agric. Food Chem.* **2004**, *52*, 7353.
14. Yu, P.; Christensen, D. A.; Christensen, C. R.; Drew, M. D.; Rossnagel, B. G.; McKinnon, J. J. *Can. J. Anim. Sci.* **2004**, *84*, 523.
15. Yu, P. Q.; Niu, Z. Y.; Damiran, D. *J. Agric. Food Chem.* **2010**, *58*, 3460.
16. De Giacomo, O.; Cesaro, A.; Quaroni, L. *Food Biophys.* **2008**, *3*, 77.
17. Verbeek, C. J. R.; van den Berg, L. E. *J. Appl. Polym. Sci.* **2012**, *125*, E347.
18. Cai, S. W.; Singh, B. R. *Biophys. Chem.* **1999**, *80*, 7.
19. Statistica version 10, Statsoft Inc. Statsoft.com. **2011**.
20. ASTM International. ASTM International: West Conshohocken, PA, **2004**.
21. Seabourn, B. W.; Chung, O. K.; Seib, P. A.; Mathewson, P. R. *J. Agric. Food Chem.* **2008**, *56*, 4236.
22. Diem, M.; Matthäus, C.; Chernenko, T.; Romeo, M. J.; Milijkovic, M.; Bird, B.; Schubert, J.; Papamarkakis, K.; Laver, N. In Infrared and Raman spectroscopic imaging; Salzer, R., Siesler, H. W., Eds.; Wiley-VCH: Weinheim, **2009**; pp 510.
23. Saarakkala, S.; Rieppo, L.; Rieppo, J.; Jurvelin, J. S. In Microscopy: Science, Technology, Applications and Education; Méndez-Vilas, A., Díaz, J., Eds.; Formatex Research Center: Badajoz, Spain, **2010**; pp 403.
24. Zhang, J.; Yan, Y.-B. *Anal. Biochem.* **2005**, *340*, 89.
25. Elshemey, W. M.; Elfiky, A. A.; Gawad, W. A. *Protein J.* **2010**, *29*, 545.
26. Verbeek, C. J. R.; van den Berg, L. E. *Macromol. Mater. Eng.* **2011**, *296*, 524.

8

Thermally Resolved Synchrotron FT-IR Microscopy of Structural Changes in Bloodmeal-Based Thermoplastics

A paper

Published in

Journal of Thermal Analysis and Calorimetry

by

JAMES M. BIER[1], C.J.R. VERBEEK AND M.C. LAY

[1]As first author for this paper, I prepared the initial draft manuscript, which was refined and edited in consultation with my supervisors, who have been credited as co-authors. This work reported results from beamtime at the Australian synchrotron in June 2012. As with the experiment reported in chapter 7, I designed the experiment and drafted the beamtime proposal in discussion with my supervisors. I was again registered as co –proposer. I prepared the samples with appropriate documentation to take them into Australia. Together with my supervisors, I travelled to the Australian Synchrotron to conduct the experiments. I then performed the data analysis using OPUS software and Microsoft Excel, and ran the statistical analysis in Statistica.

J Therm Anal Calorim
DOI 10.1007/s10973-013-3340-8

Thermally resolved synchrotron FT-IR microscopy of structural changes in bloodmeal-based thermoplastics

James Michael Bier · Casparus Johannes Reinhard Verbeek · Mark Christopher Lay

Received: 25 May 2013 / Accepted: 17 July 2013

Abstract Synchrotron FT-IR micro-spectroscopy was used to determine thermally induced structural changes in thermoplastic protein produced from bloodmeal after mixing with sodium sulphite, sodium dodecyl sulphate, urea, tri-ethylene glycol and water. Changes in protein secondary structure at elevated temperature were assessed using second derivative peak height ratios in the amide III region (1,200–1,330 cm^{-1}) and compared with DSC and DMA results over the same temperature range. The results show an increase in ordered β-sheet structures with temperature at the expense of random coils, and that these β-sheets do not melt in the temperature range up to extrusion temperature of 120 °C. The implication of this is that during melt processing, β-sheet clusters may remain intact, similar to dispersed particulate fillers.

Keywords Secondary structure estimation · Infrared-spectroscopy · Thermoplastic protein · Synchrotron radiation · Differential scanning calorimetry · Dynamic mechanical analysis

Introduction

Competition of land use for food, bio-fuels and biopolymer production has motivated research into producing biopolymers from low value by-products of existing agricultural and horticultural processes. One such by-product is bloodmeal, a powder produced by steam coagulating and drying slaughterhouse blood from the meat industry [1]. After drying, this powder is approximately 90 % protein [1–3], and can be modified to exhibit thermoplastic behaviour using urea, sodium dodecyl sulphate and sodium sulphite to reduce interactions between protein chains. The resulting material can be extruded and injection moulded on conventional polymer processing equipment [4, 5].

Thermoplastic processing involves three steps: heating to overcome inter-chain interactions; shaping the melt using pressure; and cooling to reintroduce chain interactions to stabilise the newly formed shape (fixation). In proteins, secondary structure elements may contribute to this fixation [6]. Understanding how protein secondary structures such as α-helices and β-sheets are transformed and distributed by processing will better enable the manipulation of these structures to improve material properties. For example, impact behaviour in semi-crystalline polymers can be improved by optimising crystalline morphology [7].

The protein primary structure is a long chain of amino acids; the secondary structure is local folding of the chain into random coils or ordered structures such as α-helices and β-sheets; the tertiary structure is the global conformation of an entire chain, and the quaternary structure involves more than one chain coming together to make a functional protein. This three dimensional structure is stabilised by covalent cross linkages, hydrophobic interactions, salt bridges and hydrogen bonding, both within the protein and between the protein and solvent or other protein chains [8, 9]. Where protein–protein interactions are stronger than protein–solvent interactions, contraction to increase protein–protein interactions can be energetically favourable enough to overcome entropic barriers to protein folding [10].

Secondary structure changes induced by thermoplastic processing depend on the protein's primary structure, along

J. M. Bier (✉) · C. J. R. Verbeek · M. C. Lay
School of Engineering, University of Waikato, Private Bag 3105, Hamilton 3240, New Zealand
e-mail: jmb101@waikato.ac.nz

Published online: 08 August 2013

with processing conditions and any additives such as plasticisers or denaturing agents. In general, thermoplastic processing favours an increase of ordered β-sheet regions at the expense of α-helices, although this is not always the case [11]. As an example, in hot-pressed films of egg albumin, lactalbumin, feather keratin and wheat gluten, β-sheet content increased as glycerol content increased up to a critical value for each protein after which order decreased [12]. An increase of α-helices was seen after zein was film-blown. Furthermore, samples with higher α-helix content produce better blown films than those with high β-sheet content [13], indicating that the presence and distribution of secondary structures has an effect on processing and the resultant product.

The chain mobility necessary for shaping a polymer by extrusion or injection moulding implies that processing should occur above the material's softening point, which for proteins is typically about 40 °C above the glass transition temperature (T_g) [11, 14]. However, the presence of protein secondary structures suggests that the material is better treated as semi-crystalline, rather than purely amorphous, and therefore other thermal events, such as melting, may also be important. Conventional semi-crystalline polymers would typically be processed above both the T_g of amorphous regions and the melting temperature (T_m) of crystalline regions.

Melting of polymers is typically assessed by differential scanning calorimetry (DSC), however there are complications when using DSC alone to study melting in protein-based thermoplastics. As well as two types of ordered secondary structure (α-helices and β-sheets) that may melt at different temperatures, ageing effects and denaturing also can produce endothermic peaks [15]. Denaturing refers to disruption of the native conformation of a protein leading to loss of function, but can occur without complete unfolding of secondary structures [10].

Specific structural changes associated with melting or crystallisation in polymers can be observed using thermally resolved FT-IR or time-resolved FT-IR at elevated temperature. For example, changes to the relative heights of carbonyl peaks associated with amorphous and crystalline fractions in polycaprolactone correlated well with melting temperature and onset of recrystallisation determined by DSC [16]. The implication is that using FT-IR over the same temperature range as DSC may reveal which structures are or are not unfolding and refolding at particular temperatures. In proteins, time-resolved FT-IR at an isothermal temperature of 100 °C revealed an increase in β-turns or weak β-sheet structures in soybean protein films [17]. Another example is the growth of β-sheet crystals in silk fibroin above the dry T_g of 178 °C [18]. These examples demonstrate that thermal energy alone may not disrupt the strong hydrogen bonds that stabilise β-sheets in protein plastics at typical extrusion temperatures of around 120 °C. However, bloodmeal-based thermoplastics also contain additives to reduce protein–protein interactions and the effect may be different in the presence of these.

Protein secondary structure can be estimated from the absorbance in key fingerprint areas such as the amide I (1,500–1,600 cm^{-1}) and amide III (1,180–1,350 cm^{-1}) regions. The amide I vibration has a large contribution from the carbonyl C=O bond and hydrogen bonding environments characteristic of different secondary structures affect the electron density within this bond, shifting its vibration. Deconvolution of this region allows estimation of protein secondary structure with good approximation [19]. Bloodmeal-based thermoplastics contain urea as a denaturant and plasticiser, which also absorbs in the amide I region, obscuring results. However, the amide III region (in phase N–H bending and C–N stretching) is also sensitive to structural changes, but is not influenced by urea.

The amide III region is typically 5–10 times weaker than the amide I region [20] requiring a good signal-to-noise ratio for quantitative analysis. Synchrotron IR sources are highly collimated with low dispersion, and are typically 100–1,000 times brighter than conventional globar/thermal IR sources [21, 22]. This gives much higher signal-to-noise ratios at high-spatial resolutions [21]. Using an FT-IR microscope connected to a synchrotron source, spectra can be collected for quantitative analysis in the amide III region on micrometre-sized samples and sample areas [23], rapidly enough for spatial and thermally resolved experiments.

Previous spatially resolved experiments found bloodmeal-based thermoplastics are characterised by clusters of ordered α-helical and β-sheet regions distributed within randomly coiled protein chains [24]. Bloodmeal has higher β-sheet content towards the edge of particles and heat and shear during extrusion causes rearrangement of these regions. After extrusion, a more homogenous distribution was observed, with increased β-sheet content [24], however, the dynamic behaviour of this transformation may be important for process design. Currently, it is unknown whether β-sheets melt during processing at elevated temperatures then refold on cooling, or whether β-sheets persist in the melt, or even aggregate further.

The aim of this research was to characterise the changes in bloodmeal-based thermoplastic protein secondary structure, during heating through its glass transition temperature, and up to a typical extrusion temperature for the material. Results concerning structural changes were compared with dynamic mechanical analysis (DMA) and DSC results over the same temperature range.

Experimental

Materials

Agricultural grade bloodmeal (Wallace Corporation, Hamilton, New Zealand), agricultural grade urea (Ballance Agrinutrients, Kapuni, New Zealand), distilled water (produced on site from town supply), tri-ethylene glycol (TEG) for synthesis (Merck), technical grade sodium dodecyl sulphate (Merck) and technical grade sodium sulphite (Merck) were used to prepare polymer specimens.

Methods

Sample preparation

20 g urea, 6 g sodium dodecyl sulphate, and 6 g sodium sulphite were dissolved in 80 g distilled water at 50 °C. The solution was mixed with 200 g of sieved bloodmeal in a high-speed mixer. The mixture was blended for 6 min, after which 40 g TEG was added, followed by an additional 4 min blending. The resultant mixture [pre-extruded Novatein thermoplastic protein bioplastic (PNTP)] was equilibrated overnight in sealed plastic bags below 4 °C.

Equilibrated samples were dried over two nights in a Freezone® 2.5 l Benchtop freeze dryer (Labconco Corporation, Kansas City) set to auto mode (collector temperature −50 °C, vacuum < 11 Pa). Moisture content of freeze-dried specimens (FD-PNTP) was determined as 1.2 ± 0.3 % from mass loss to 120 °C in TG (mean and standard deviation from three samples).

Synchrotron microscopy

Spatially resolved FT-IR experiments were undertaken on the infrared microspectroscopy beamline at the Australian Synchrotron, Clayton, VIC, Australia. Particles were compressed in a diamond cell then transferred onto a barium fluoride slide. This was placed in Linkam heated stage connected to a Bruker Hyperion 3000 with an MCT collector and XY stage. For each point, 32 spectra were collected with a resolution of 4 cm^{-1} between 3,900 and 700 cm^{-1} and averaged using Opus 6.5 software (Bruker Optik GmbH 2009).

A minimum of three representative grids (10 μm × 10 μm spot size) on video images of particles of FD-PNTP and bloodmeal were mapped in *xy*-coordinates. After spectra collection for each point in the grid, at room temperature, the mounted samples were heated in the Linkam stage to 120 °C, held isothermally for 2 min then cooled back to room temperature. Grids with the same *xy* co-ordinates as originally scanned were then mapped a second time.

As a second experiment, smaller representative grids (10 μm spot size) were mapped at room temperature on freshly mounted particles of FD-PNTP. This sample was then heated to 50 °C, held isothermally for 10 min, then the grids with the same *xy* co-ordinates were mapped again. This process was repeated at 70, 90, 110, and 130 °C.

As a third experiment, a freshly mounted sample of FD-PNTP was cooled to −120 °C. To average out spatial variations, a single 50 μm spot was chosen on this sample, and then spectra were collected at 30 s intervals during a constant heating ramp to 120 °C at 2 °C min^{-1}.

Thermal analysis

DSC was conducted in a Perkin Elmer DSC 8500 hyper DSC fitted with an autosampler accessory and cooled with liquid nitrogen. Approximately 10 g of sample was weighed into autosampler pans (Perkin Elmer) which were then crimped, providing a seal and placed into the auto sampler. FD-PNTP samples were scanned between −100 and 200 °C at 50, 100, 250 and 500 °C min^{-1}. Additional samples of FD-PNTP were given heat treatments of 5 min isothermally at 50, 70, 90, 110 and 130 °C in the DSC, then cooled down and scanned between −100 and 200 °C at 50 and 250 °C min^{-1} to determine changes induced by prior thermal treatment. Glass transition temperature (half C_p extrapolated) was determined using Pyris 7 software (Perkin Elmer).

DMA was performed using a Perkin Elmer DMA 8000 fitted with a high-temperature furnace and cooled with liquid nitrogen. FD-PNTP samples were examined by mounting approximately 50 mg of powder in ~1.0 × 7.4 × 28 mm (folded dimensions) material pockets (Perkin Elmer) [25] and tested at 1 Hz with a dynamic displacement of 0.05 mm and free length of 12.5 mm.

Thermogravimetric analysis (TG) was performed in a Texas Instruments SDT 2960 analyser. Approximately 10 mg powdered sample was placed in the sample crucible and heated at 10 °C min^{-1} from room temperature to 700 °C under constant air flow. Moisture content was determined from the cumulative mass loss up to 120 °C.

Data analysis

The output from the synchrotron experiments was a collection of spectra with *xy* coordinates and corresponding to different temperatures. Relative peak height in the amide III region of inverted second derivative spectra was used to estimate how relative fractional composition of corresponding secondary structures varied spatially and with temperature across maps. Data were filtered for a minimum area under the amide III region to exclude points mapped outside particles from the analysis.

Second derivative analysis has two main advantages. Spectral resolution of overlapping bands is increased and sloping baselines are removed without subjective corrections [26]. Although side lobes may increase noise and the height of second derivative peaks is dependent on the half width at half height of the original peaks, it has been demonstrated that neither of these issues affected quantitative results obtained from the second derivative for poly-L-lysine and haemoglobin as model proteins [27]. Relative differences can be explored if the same peaks are of interest and the same calculation procedure used for all samples [28]. Quantitative analysis of peaks in the amide III region has previously been used to assess secondary structure changes during mixing of gluten [29], and for bloodmeal based-thermoplastics after different processing steps [24].

The second derivative of the original spectra (with no baseline correction) was determined using the Savitzky-Golay algorithm in Opus 6.5 using nine point smoothing. The second derivative was inverted by dividing by -1 and peak heights above the zero line were compared. The ratios A''_{α}/A''_{β}, A''_{t}/A''_{β} and A''_{r}/A''_{β} were calculated using Opus 6.5, where A''_{x} is the maximum height of the inverted second derivative peak within the wavenumber range associated with α-helices, β-sheets, turns and random coils (Table 1) indicated respectively by the subscripts α, β, t and r. The molar fraction for each secondary structure type was calculated using Eqs. 1–5 and spatial maps were drawn based on these compositions using Microsoft Excel.

$$\alpha + \beta + t + r = 1. \tag{1}$$

$$\beta = \frac{1}{A''_{\alpha}/A''_{\beta} + A''_{t}/A''_{\beta} + A''_{r}/A''_{\beta} + 1} \tag{2}$$

$$\alpha = \beta \frac{A''_{\alpha}}{A''_{\beta}} \tag{3}$$

$$t = \beta \frac{A''_{t}}{A''_{\beta}} \tag{4}$$

$$r = \beta \frac{A''_{r}}{A''_{\beta}} \tag{5}$$

The composition approximates a mole fraction of peptide linkages in each structural conformation, each of which absorbs differently in the amide III region.

Table 1 Peak assignment in the amide III region [20]

Region	Secondary structure	Wavenumber/cm^{-1}
Amide III	α Helix	1295–1,330
	β-turns	1,270–1,295
	random coils	1,250–1,270
	β-sheets	1,220–1,250

Results and discussion

Isothermal heat treatment

A 2-min isothermal heat treatment at 120 °C followed by cooling to room temperature was chosen to simulate the temperature and residence time encountered during extrusion. Secondary structure maps before and after this heating cycle are shown for one sample in Fig. 1. For clarity, random coils and turns have been grouped as disordered structures. Clusters of higher concentrations of α-helices and β-sheets were observed. Clusters were still observed after thermal treatment, but the map appeared more heterogeneous after heat treatment. A similar trend was seen for other rectangles, whereas previous results had suggested a more even distribution of structures after extrusion [24]. It should be noted that the present case is purely a heat treatment cycle and excludes shear and mixing encountered during extrusion.

The segregated nature of the maps made it hard to visually get an impression of the overall structural change, so the average and standard deviation were also calculated for all points mapped in this portion of the experiment (Fig. 2). For the mapped area as whole, a significant increase in α-helices and β-sheets at the expense of random coils was observed. Consistent with increased heterogeneous nature seen in the maps, the standard deviation of the mean also increased for α-helices and β-sheets.

In contrast, when the same experiment was performed on bloodmeal (without any of the additives necessary for thermoplastic processing) no significant changes in fractional composition were seen (Fig. 2). These results show structural arrangement is not occurring during with the 2-min thermal treatment of unmodified bloodmeal. Localised chemical changes, for example formation of additional S–S crosslinks may be occurring but was not confirmed in this study. After the addition of processing chemicals, structural changes occurred within 2 min at 120 °C, even for the freeze-dried samples analysed here. These findings are consistent with DMA which showed the glass transition temperature (T_g) of dry bloodmeal to be approximately 220 °C and FD-PNTP to be approximately 80 °C [30]. This shows that FD-PNTP would have enough chain mobility for structural changes to occur, as observed by FT-IR (Fig. 2).

Spatial and thermal resolution

Figure 3 shows changes to secondary structure for a smaller grid at 20 °C temperature intervals after 10 min thermal treatment at each temperature. At the initial temperature of 23 °C, disordered regions dominated, with a moderate amount of β-sheets and relatively fewer

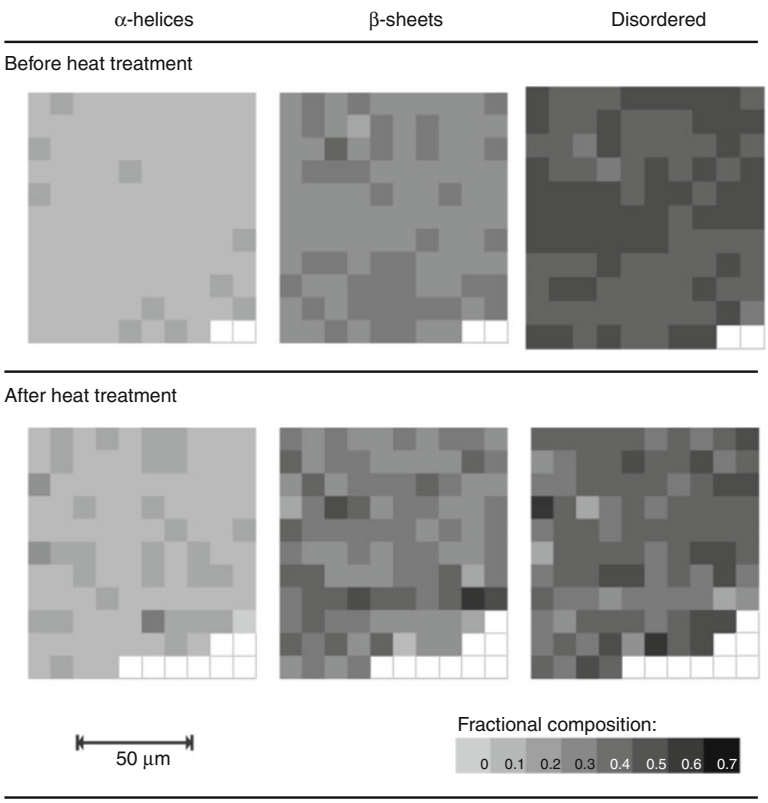

Fig. 1 Representative maps showing fractional secondary structures for PNTP before and after thermal treatment at 120 °C. Each *pixel* represents a 10 μm spot and the *shading* represents the relative composition of the labelled structure calculated from the inverted second derivative spectra

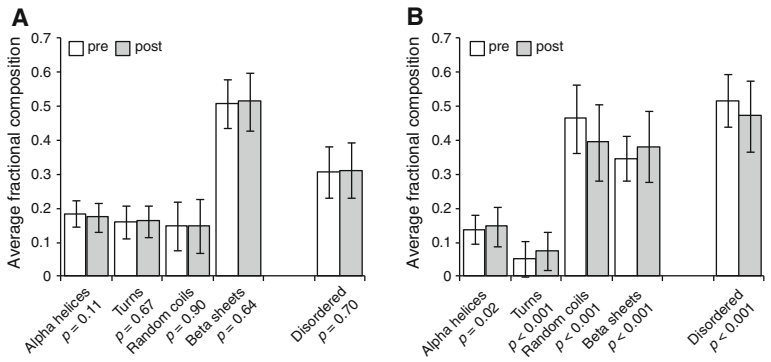

Fig. 2 Average secondary structure fractional composition of **a** bloodmeal and **b** FD-PNTP before and after thermal treatment at 120 °C, followed by cooling to room temperature. *Error bars* denote standard deviation and *p* values for a two tailed *t* test are shown. A *p* value of less than 0.05 indicates significance at a 95 % confidence interval

α-helices. As indicated by the change in shading intensity in Fig. 3, an increase in ordered β-sheet structures was seen at the expense of disordered regions as the sample was heated. Again, although only one representative grid is shown, average and standard deviations were calculated for all points mapped across three grids on separate particles at each temperature step (Table 2). Consistent with the first experiment, a large increase in β-sheets was seen at the expense of random coils. The standard deviation also increased, suggesting a more heterogeneous distribution of β-sheet concentrations after treatment. Analysis of variance revealed that the effect of temperature was significant (>99 % confidence) for all structural types, however the contribution was small for α-helices and β-turns. Partial η^2 values indicated that variation in the amount of these structures with temperature was small compared to the variation across a map. In contrast, for random coils, β-sheets and total disordered structures, the contribution was large (partial η^2 values were $\sim$0.6). This shows that although there is some change in α-helices and turns, the predominant structural changes are from disordered to β-sheets.

Table 2 Temperature resolved change in average fractional composition of maps and results of one way analysis of variance with temperature as the independent variable. p values <0.05 indicate significance at the 95 % confidence level and partial η^2 gives the effect size relative to structural variation across maps not due to temperature

Temperature/°C	α-Helices	Turns	Random coils	β-sheets	Total disordered
23	0.14 ± 0.02	0.05 ± 0.02	0.49 ± 0.05	0.33 ± 0.04	0.53 ± 0.04
50	0.15 ± 0.03	0.05 ± 0.03	0.42 ± 0.07	0.38 ± 0.05	0.47 ± 0.06
70	0.15 ± 0.03	0.05 ± 0.03	0.38 ± 0.07	0.43 ± 0.05	0.42 ± 0.06
90	0.16 ± 0.03	0.05 ± 0.03	0.33 ± 0.07	0.46 ± 0.06	0.38 ± 0.06
110	0.16 ± 0.02	0.05 ± 0.03	0.29 ± 0.06	0.50 ± 0.05	0.34 ± 0.06
130	0.16 ± 0.03	0.06 ± 0.04	0.25 ± 0.09	0.53 ± 0.08	0.31 ± 0.09
Key results of one way ANOVA versus temperature for each structure					
p	<0.001	0.006	<0.001	<0.001	<0.001
Partial η^2	0.08	0.03	0.58	0.60	0.59

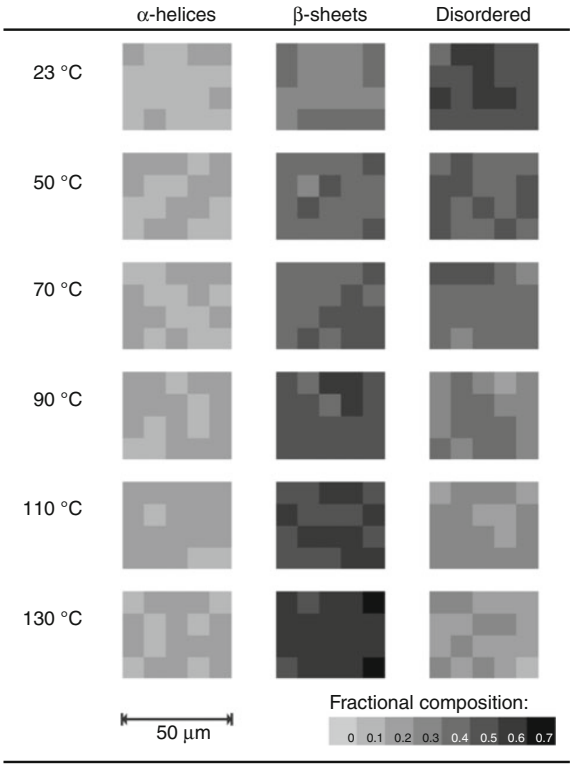

Fig. 3 Representative maps showing fractional secondary structure for PNTP after 10 min isothermal treatments at 20 °C temperature increments. Each *pixel* represents a 10 µm spot and the *shading* represents the relative composition of the labelled structure calculated from the inverted second derivative spectra

Thermal treatments at the same temperatures were performed using DSC. With no prior heating cycle (23 °C), FD-PNTP showed a small endothermic peak and a glass transition in the range of 30–90 °C (Fig. 4). This peak became smaller and shifted to higher temperature after progressively higher thermal treatment temperatures, and is no longer apparent after the 90 °C treatment. The results would suggest that structural changes responsible for this peak were incomplete below 90 °C evident from the endothermic peak observed below 90 °C. At higher temperatures, complete and irreversible transformation occurred during thermal treatment leading to the absence of this event during DSC scans after heat treatments above 90 °C. Scanning at 250 °C min^{-1} suggested that the T_g remained after thermal treatment (Fig. 4b), albeit a very broad transition.

Table 3 Thermal events associated with the glass transition in FD-PNTP

Method	T_g/°C	Peak of endothermic event/°C
DSC at 50 °C min^{-1}	46	55
DSC at 100 °C min^{-1}	57	67
DSC at 250 °C min^{-1}	73	82
DSC at 500 °C min^{-1}	98	109
DMA at 1 Hz/onset of drop in modulus	24	N/a
DMA at 1 Hz/peak in tan delta	77	

Temperature-dependent structural changes

As a further experiment, temperature-induced structural changes over time were investigated using a 50 µm spot size at a constant heating rate of 2 °C min^{-1}. Figure 5 shows the change in shape of the amide III region at 30, 60 and 90 °C. The convoluted peak centred around 1,235 cm^{-1} broadened and shifted slightly towards lower wavenumbers. Considering the second derivative (Fig. 5 inset), it was clear that significant change occurred at two peak locations; 1,245 cm^{-1} (random coils) and 1,220 cm^{-1} (β-sheets).

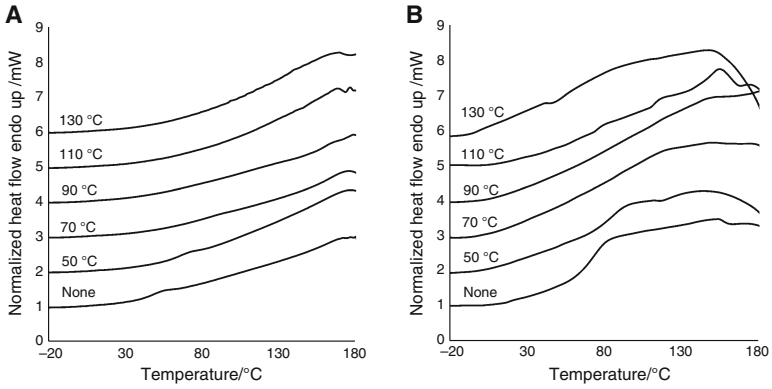

Fig. 4 DSC traces at **a** 50 °C min^{-1} and **b** 250 °C min^{-1} for FD-PNTP after 5 min held isothermally at the marked temperatures. Traces have been stacked for legibility

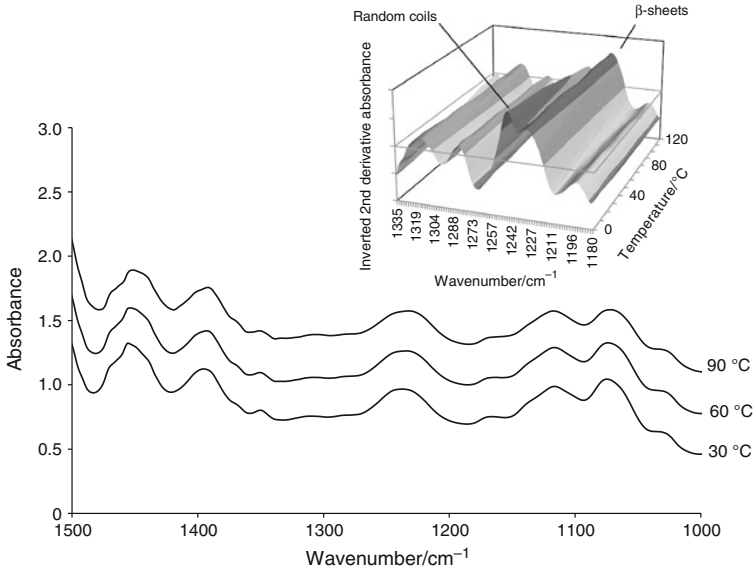

Fig. 5 Temperature-resolved change in the Amide III spectral region. Original spectra are shown at 30, 60 and 90 °C. Inset shows inverted second derivative

The fractional composition was calculated for each time step using the same method as before and plotted against temperature, in conjunction with changes in thermal and dynamic mechanical properties over the same range (Fig. 6). Above room temperature a gradual increase in α-helices and β-sheets was seen, with a corresponding drop in random coils. This corresponds with the region above the onset of drop in modulus (24 °C, Table 3), determined from DMA at the same scanning rate. Material pocket DMA represents a hybrid modulus of the material pocket and the sample, but stainless steel shows no major transitions in this region and the rapid drop in modulus and increase in mechanical damping are that of the sample. Although the corresponding peak in tanδ is 77 °C, it is a wide transition, and it has previously been thought that it could be a hybrid transition of purely amorphous regions and regions constrained by ordered structures [30]. It is therefore not inconsistent for some structural rearrangement to occur below this peak temperature.

As discussed with respect to the effects of thermal treatment, DSC revealed a hybrid endothermic peak and T_g between 30 and 90 °C, suggesting some structural rearrangement that required thermal energy to occur. The midpoint of the endothermic peak was consistently about 10 °C higher than the T_g, with both shifting to higher temperatures at higher heating rates (Table 3). Scanning at a higher rate emphasised the T_g, confirming the presence of chain relaxation in disordered regions. The observed thermal behaviour should be seen as a hybrid between chain relaxations (as determined from DMA) and structural rearrangement (DSC and FT-IR). No major decrease in ordered secondary structures was observed, suggesting the small endothermic peak must have a different origin than melting of secondary structure. It may be the disruption of

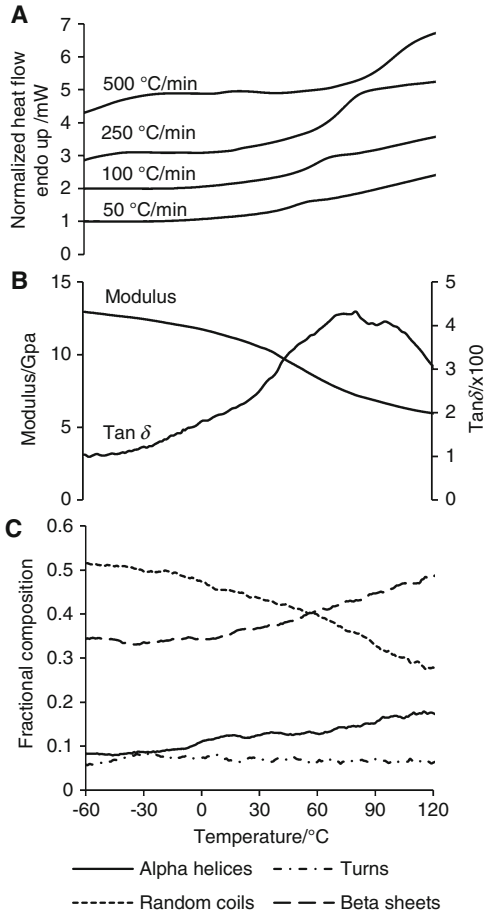

Fig. 6 Changes in **a** thermal properties, **b** thermo-mechanical properties and **c** structure during heating of FD-PNTP. Change in fractional secondary structure during heating at 2 °C min^{-1} is from a 50 μm × 50 μm spot and has been smoothed using a ten-point moving average

small amounts of residual tertiary structure in random coil regions as these become more mobile or may represent the thermal energy required to bring about the chain rearrangement observed.

While denaturing is typically observed as an endothermic peak, it should be noted that bloodmeal has already been thermally denatured before conversion to a bioplastic. Nevertheless, some residual regions of tertiary structure or tightly packed amorphous regions may remain. An endothermic peak around the T_g of proteins has previously been described as due to physical ageing [31]. This relates to the onset of mobility of tightly packed amorphous regions with reduced internal energy and free volume prior to the T_g [32]. Physical ageing is common in proteins containing gluten subunits [14] and has been seen in soy protein plasticised in glycerol [31]. Of particular relevance for bloodmeal-based plastics, physical ageing has been demonstrated in both native and denatured bovine serum albumin [33].

It is not unreasonable to find that ordered structures in dry bloodmeal-based thermoplastics do not melt below 120 °C. In other dry proteins, such as dry silk fibroin (T_g of 178 °C), formation of β sheets was shown to occur above the T_g [18]. Similarly, α-helix type crystallinity in human hair with a conditioned moisture content of 11.6 % did not melt until 175 °C [34]. However, the implications for processing are important. Rather than melting and the realigning, results suggest that consolidation happens due to interactions between amorphous regions, with small aggregated β-sheets dispersed amongst this amorphous material in a similar fashion to particulate fillers.

This study simulated the temperatures used in extruding bloodmeal-based thermoplastics, however extrusion also involves input of mechanical energy and shear forces. Although the present apparatus does not enable the effect of these to be simulated, spatial resolution of secondary structure distribution for bloodmeal-based thermoplastics after extrusion and injection moulding has been previously reported [24]. In light of those findings and this present work, it would seem that while heating induces formation of additional β-sheets, shear during extrusion dispersed these β-sheet particles more evenly than what occurs during heating alone.

Conclusions

Bloodmeal-based thermoplastic, even when freeze dried, still has considerable chain mobility at a typical extrusion processing temperature of 120 °C. After heating to this temperature for 2 min, significant increases in ordered structures (α-helices and β-sheets) were observed indicating refolding of protein chains. In contrast, bloodmeal alone, with none of the additives required for processing, showed negligible change to average secondary structure after heating to 120 °C.

No melting of secondary structures was observed during heating at 2 °C min^{-1} between −120 and 120 °C. However, above room temperature, a gradual increase in ordered structures occured at temperatures corresponding to the glass transition region, consistent with amorphous chains realigning into more ordered structures. An irreversible endothermic event was also observed in the glass transition region which may be due to ageing effects or disruption to residual tertiary structure.

Although these results were obtained in the absence of shear and water, the results suggested that thermoplastic protein derived from bloodmeal does not form a complete melt on heating, rather aggregates of ordered structures

flow within an amorphous matrix, similar to dispersed particulate fillers. This has importance for future attempts to modify the viscosity of the material.

Acknowledgements This research was undertaken on the infrared microspectroscopy beamline at the Australian Synchrotron, Clayton, VIC, Australia. Proposal number AS122/IRMFI/4951. The authors would especially like to acknowledge the technical assistance of Dr. Mark Tobin and Dr. Danielle Martin. Travel funding support was received from the New Zealand Synchrotron Group Ltd.

References

1. Filstrup P. Processes and equipment for protein by-products in the meat industry. In: Grant RA, editor. Applied protein chemistry. London: Applied Science Publishers Ltd; 1980. p. 181–222.
2. Swan JE. Animal By-Product Processing. In: Francis FJ, editor. Wiley encyclopedia of food science and technology. 2nd ed. New York: Wiley; 2000. p. 4 v, (xxi, 2768).
3. Fernando T. Blood Collection and Processing. Richmond: School of Food Sciences, Hawkesbury Agricultural College; 13th–17th May 1984.
4. Verbeek CJR, Viljoen C, Pickering KL, van den Berg LE, Inventors. Waikatolink Limited, assignee. NZ551531: Plastics material. New Zealand Patent 551531. Granted 2009 21 Nov 2007.
5. Verbeek CJR, van den Berg LE. Development of proteinous bioplastics using bloodmeal. J Polym Environ. 2010;19:1–10. doi:10.1007/s10924-010-0232-x.
6. De Graaf LA. Denaturation of proteins from a non-food perspective. J Biotechnol. 2000;79(3):299–306.
7. Perkins WG. Polymer toughness and impact resistance. Polym Eng Sci. 1999;39(12):2445–60. doi:10.1002/pen.11632.
8. Devlin TM. Textbook of biochemistry: with clinical correlations. 7th ed. Hoboken: Wiley; 2011.
9. Sowdhamini R, Balaram P. Protein Structrure and Stability. In: Gupta MN, editor. Thermostability of enzymes. New York: Springer; 1993. p. vi, 213.
10. Dill KA, Shortle D. Denatured states of proteins. Annu Rev Biochem. 1991;60:795–825. doi:10.1146/annurev.bi.60.070191.004051.
11. Verbeek CJR, van den Berg LE. Extrusion processing and properties of protein-based thermoplastics. Macromol Mater Eng. 2010;295(1):10–21. doi:10.1002/mame.200900167.
12. Athamneh AI, Griffin M, Whaley M, Barone JR. Conformational changes and molecular mobility in plasticized proteins. Biomacromolecules. 2008;9(11):3181–7. doi:10.1021/bm800759g.
13. Oliviero M, Maio ED, Iannace S. Effect of molecular structure on film blowing ability of thermoplastic zein. J Appl Polym Sci. 2010;115(1):277–87.
14. Bengoechea C, Arrachid A, Guerrero A, Hill SE, Mitchell JR. Relationship between the glass transition temperature and the melt flow behavior for gluten, casein and soya. J Cereal Sci. 2007;45(3):275–84.
15. Verbeek CJR, Bier JM. Synthesis and characterisation of thermoplastic agro-polymers. In: Sharma SK, Mudhoo A, editors. A handbook of biopolymers: synthesis, degradation and applications. Cambridge: RSC Publishing; 2011. p. 197–242.
16. Murphy SH, Leeke GA, Jenkins MJ. A Comparison of the use of FTIR spectroscopy with DSC in the characterisation of melting and crystallisation in polycaprolactone. J Therm Anal Calorim. 2012;107(2):669–74. doi:10.1007/s10973-011-1771-7.
17. Tian K, Porter D, Yao J, Shao Z, Chen X. Kinetics of thermally-induced conformational transitions in soybean protein films. Polymer. 2010;51(11):2410–6.
18. Hu X, Lu Q, Kaplan DL, Cebe P. Microphase separation controlled beta-sheet crystallization kinetics in fibrous proteins. Macromolecules. 2009;42(6):2079–87. doi:10.1021/ma802481p.
19. Kong J, Yu S. Fourier transform infrared spectroscopic analysis of protein secondary structures. Acta Biochim Biophys Sin. 2007;39(8):549–59. doi:10.1111/j.1745-7270.2007.00320.x.
20. Cai SW, Singh BR. Identification of beta-turn and random coil amide III infrared bands for secondary structure estimation of proteins. Biophys Chem. 1999;80(1):7–20. doi:10.1016/s0301-4622(99)00060-5.
21. Miller LM. Biomedical applications of infrared microspectroscopy using synchrotron radiation. In: Salzer R, Siesler HW, editors. Infrared and Raman spectroscopic imaging. Weinheim: Wiley-VCH; 2009. p. xx, 510.
22. Yu PQ, McKinnon JJ, Christensen CR, Christensen DA. Using synchrotron-based FTIR microspectroscopy to reveal chemical features of feather protein secondary structure: comparison with other feed protein sources. J Agric Food Chem. 2004;52(24):7353–61. doi:10.1021/jf0490955.
23. Ling SJ, Qi ZM, Knight DP, Shao ZZ, Chen X. Synchrotron FTIR microspectroscopy of single natural silk fibers. Biomacromolecules. 2011;12(9):3344–9. doi:10.1021/bm2006032.
24. Bier JM, Verbeek CJR, Lay MC. Using synchrotron FTIR spectroscopy to determine secondary structure changes and distribution in thermoplastic protein. J Appl Polym Sci. 2013;130(1):359–69. doi:10.1002/app.39134.
25. Royall PG, Huang CY, Tang SWJ, Duncan J, Van-de-Velde G, Brown MB. The development of DMA for the detection of amorphous content in pharmaceutical powdered materials. Int J Pharm. 2005;301(1–2):181–91. doi:10.1016/j.ijpharm.2005.05.015.
26. Diem M, Matthäus C, Chernenko T, Romeo MJ, Milijković M, Bird B et al. Infrared and Raman spectroscopy and spectral imaging of individual cells. In: Salzer R, Siesler HW, editors. Infrared and Raman spectroscopic imaging. Weinheim: Wiley-VCH; 2009. p. xx, 510.
27. Zhang J, Yan Y-B. Probing conformational changes of proteins by quantitative second-derivative infrared spectroscopy. Anal Biochem. 2005;340(1):89–98.
28. Saarakkala S, Rieppo L, Rieppo J, Jurvelin JS. Fourier transform infrared (FTIR) microspectroscopy of immature, mature and degenerated articular cartilage. In: Méndez-Vilas A, Díaz J, editors. Microscopy: science, technology, applications and education vol. 1. FORMATEX Microscopy Series No. 4, 2010. p. 403–14.
29. Seabourn BW, Chung OK, Seib PA, Mathewson PR. Determination of secondary structural changes in gluten proteins during mixing using Fourier transform horizontal attenuated total reflectance spectroscopy. J Agric Food Chem. 2008;56(11):4236–43. doi:10.1021/jf703569b.
30. Bier JM, Verbeek CJR, Lay MC. Identifying transition temperatures in bloodmeal-based thermoplastics using material pocket DMTA. J Therm Anal Calorim. 2013;112(1303):1315. doi:10.1007/s10973-012-2680-0.
31. Mo X, Sun X. Effects of storage time on properties of soybean protein-based plastics. J Polym Environ. 2003;11(1):15–22.
32. Menczel JD, Prime RB. Thermal analysis of polymers: fundamentals and applications. Hoboken: Wiley; 2009.
33. Farahnaky A, Badii F, Farhat IA, Mitchell JR, Hill SE. Enthalpy relaxation of bovine serum albumin and implications for its storage in the glassy state. Biopolymers. 2005;78(2):69–77. doi:10.1002/bip.20265.
34. Cao J. Melting study of the [alpha]-form crystallites in human hair keratin by DSC. Thermochim Acta. 1999;335(1–2):5–9.

9

Plasticiser Migration in Bloodmeal-Based Thermoplastics

A paper

Published in

Journal of Applied Polymer Science

by

JAMES M. BIER[1], C.J.R. VERBEEK AND M.C. LAY

[1]As first author for this paper, I prepared the initial draft manuscript which was refined and edited in consultation with my supervisors, who have been credited as co-authors. The data was collected during the same two visits to the Australian Synchrotron reported on in Chapter 7 and Chapter 8. I then performed the data analysis using OPUS software and Microsoft Excel.

Journal of Applied Polymer Science

Plasticizer Migration in Bloodmeal-Based Thermoplastics

James Michael Bier, Casparus Johannes Reinhard Verbeek, Mark Christopher Lay
School of Engineering, University of Waikato, Private Bag 3105, Hamilton 3240, New Zealand
Correspondence to: J. M. Bier (E-mail: jmb101@waikato.ac.nz)

ABSTRACT: Tri-ethylene glycol (TEG) is an effective plasticizer for many protein-based thermoplastics because of its low volatility, however, partial miscibility with the protein matrix may still lead to some phase separation. Spatial variation of TEG concentration in bloodmeal-based thermoplastics as a result of processing was investigated using synchrotron-based FT-IR micro-spectroscopy. Although TEG forms strong hydrogen bonding with proteins, for the protein to fold into β-sheets bound plasticizer must be released. TEG can then migrate, pooling into localized areas, rich in plasticizer. Further heating causes further migration towards the edge of plasticized bloodmeal particles where the TEG may evaporate. Thermo-gravimetric analysis confirmed that loss of TEG by evaporation may occur at 120°C, given enough time for diffusion. Efficient mixing combined with a short residence time at elevated temperature mean significant plasticizer loss is unlikely during processing. However, it does limit long-term use at elevated temperatures. © 2013 Wiley Periodicals, Inc. J. Appl. Polym. Sci. **2013**, *000*, 39969.

KEYWORDS: biopolymers and renewable polymers; plasticizer; proteins; spectroscopy; thermogravimetric analysis

Received 31 May 2013; accepted 12 September 2013
DOI: 10.1002/app.39969

INTRODUCTION

Bloodmeal is a by-product of the meat processing industry, which can be extruded into a bio-based thermoplastic by mixing with a reducing agent, protein denaturant, surfactant, and plasticizer.[1,2] The resulting material is known as Novatein™ thermoplastic protein (NTP). Extrusion of proteins involves applying heat and shear to produce a homogenous melt. This involves denaturing, disassociation, unravelling, and re-alignment of protein chains.[3] After compounding, NTP can be extruded or injection moulded using conventional polymer processing equipment.

Water is a common plasticizer for protein-based thermoplastics, but evaporation after processing can result in a brittle material.[4] For this reason, less volatile plasticizers are often used instead of or in conjunction with water. Tri-ethylene glycol (TEG) has been shown to be an effective plasticizer in bloodmeal-based thermoplastics; remaining in injection-moulded test pieces during conditioning, resulting in a tougher and more ductile plastic material.[5]

Urea is included in NTP to assist in disrupting protein–protein interactions during processing. Urea also has a plasticising function, and in the absence of TEG a ductile material can be produced if enough urea is included in the formulation.[4] However, urea can leach out of protein plastics forming a white residue on the plastic's surface.[3,6,7] Urea, water, and TEG all contain polar groups and hydrogen bond to protein chains. TEG also contains hydrophobic groups and therefore should show slower leaching rates compared to urea and water. A study of corn protein-based thermoplastics with a wide variety of plasticizers suggested polar plasticizers interact with easily accessible polar amino acids, but amphiphilic plasticizers could interact with more difficulty to access nonpolar zones, buried with the protein.[8]

Plasticizer migration in conventional plastics faces public scrutiny because of concerns about biological impacts, for example concerns about potential carcinogenicity and endocrine disruption effects of phthalates.[9,10] Traditional plasticizers used with synthetic polymers are not necessarily suitable for some bio-based plastics and along with water, polyols are more common.[11,12] Nevertheless, plasticizer migration is still of interest for protein-based materials, as it has potential implications for both processing and resultant material properties. If the plasticizer concentration is too high, it can exceed the compatibility limit leading to phase separation and plasticizer exclusion.[11] Phase separation into plasticizer-rich and plasticizer-poor phases has been implicated in the presence of multiple thermal transitions in soy protein-based plastics.[13] In wheat gluten composites reinforced with natural fibers, migration of plasticizer from the matrix to the fiber results in a more brittle matrix with higher glass transition temperature. This effect reduces processability at high fiber contents.[14]

The migration rate of plasticizers in proteins depends on the physicochemical properties of the plasticizer,[8] but is also influenced by other factors such as protein conformation and environmental conditions. A study of plasticized wheat gluten films suggested plasticizer migration may be reduced by a more

aggregated protein structure.[15] Certain plasticizers may have different compatibilities with different proteins. For example, polyethylene glycol was found to be compatible with wheat grain protein, but less compatible with β-lactoglobulin or soy protein isolate, as evidenced by the formation of an oily surface residue.[16] Environmental factors such as humidity may also promote migration of plasticizer from proteins.[17] For films made of sunflower protein, reasonable barrier properties for water vapor were obtained, but resistance to water was limited, in part because of migration of hydrophilic plasticizers into the water.[12] Another environmental consideration is temperature. Even with conventional plastics, materials used in high temperature environments often need frequent replacement because of becoming brittle and cracking as plasticizers evaporate or degrade over time.[9] It is therefore of interest to determine how protein/plasticizer interactions are affected during heating.

FT-IR is commonly used with protein-based plastics to estimate relative amounts of secondary structures using the amide I (1600–1700 cm^{-1}) or amide III (1180–1330 cm^{-1}) regions of the spectra. Analysis of peaks corresponding to plasticizer functional groups can yield more information about the interactions of the protein with the plasticizer. For example, FT-IR analysis revealed no covalent interactions had formed between glycerol and protein sheets prepared from soy protein isolate, as no changes were observed in the peaks characteristic of each component.[18] However, FT-IR of soy protein plastics plasticized with both glycerol and caprolactone indicated that caprolactone had been consumed in their preparation as its characteristic peaks were not observed.[19]

TEG contains both ether and alcohol functional groups and absorbance peaks corresponding to these are present in bloodmeal-based plastics containing TEG.[5] Analysis of how these peaks change relative to characteristic protein peaks across a sample should reveal how plasticizer content changes spatially as the result thermoplastic processing.

Spatially resolved secondary structure changes occurring in bloodmeal-based plastics because of processing have previously been reported.[20] β-sheets were concentrated around the perimeter of bloodmeal particles, whereas after extrusion and injection moulding, β-sheet-rich regions were distributed more evenly throughout a disordered matrix. At each processing stage, the inclusion of TEG as a plasticizer resulted in more random coils and less α-helices and β-sheets throughout the material. Because urea also has a carbonyl absorbance peak in the amide I region, analysis relied on the amide III region. Although weaker than the amide I, it is also sensitive to structural changes.

The work presented here discusses the spatial distribution of TEG and include peaks corresponding to both the alcohol and ether groups from TEG. The primary objective was to determine how these change relative to the amide III region on heating pre-extruded powder as well as after different processing steps. Results are used to explain how protein/plasticizer interactions vary spatially on a microscale and how these are influenced by heating and thermoplastic processing.

Table I. Composition, in Parts Per Hundred Bloodmeal (pph_{BM}) of the Pre-extruded Formulations

	PNTP-TEG	PNTP-V0	PNTP-U0
Bloodmeal	100	100	100
Water	40	60	40
TEG	20	0	20
Urea	10	10	0
SDS	3	3	3
SS	3	3	3

EXPERIMENTAL

Materials and Sample Preparation

Pre-extruded NTP (PNTP) was prepared as described previously[20] using agricultural grade bloodmeal (Wallace Corporation, Hamilton, New Zealand), agricultural grade urea (Ballance Agrinutrients, Kapuni, New Zealand), distilled water, TEG for synthesis (Merck), technical grade sodium dodecyl sulphate (SDS) (Merck), and technical grade sodium sulphite (SS) (Merck) (Table I).

After mixing, the product (PNTP-TEG) was equilibrated overnight below 4°C in sealed plastic bags. Additional formulations containing no TEG (PNTP-V0) and no urea (PNTP-U0) were also prepared for thermal analysis (Table I).

PNTP-TEG was extruded (ENTP), granulated and injection moulded (INTP), and conditioned (CNTP) using previously described parameters.[20] Samples from each processing step were dried over two nights in a Freezone® 2.5 Litre bench-top freeze dryer (Labconco Corporation, Kansas City) set to auto mode (Collector temperature −50°C, vacuum <11 Pa.) before transport to the Australian synchrotron.

Analysis

Synchrotron FT-IR Microscopy. FT-IR experiments were conducted on the infrared micro-spectroscopy beamline at the Australian Synchrotron, Victoria, Australia. For thermal experiments, particles of PNTP-TEG were flattened between two diamond cells then transferred to a barium fluoride slide for analysis in a Linkham FTIR 600 (Linkham Scientific Instruments) heated stage. Sections of ENTP, INTP, and CNTP 2 μm thick were cut using stainless steel blades (TBS™) on a TBS Cut 4060 RE microtome (TBS™) lit by a microlight 150 (Fibreobtic Lightguides, Australia). The microtomed ribbons were then flattened between two diamond cells, then the top cell removed for analysis. Spectra were collected using Bruker Hyperion 3000 equipped with an MCT collector and motorized XY stage and using Opus 6.5 software (Bruker Optik GmbH 2009). For each sample, video images were first captured using Opus 6.5, then grids of points to be scanned chosen. Thirty-two spectra were collected and averaged for each grid point with a resolution of 4 cm^{-1} between 3900 and 700 cm^{-1}.

Three types of experiments were performed on PNTP-TEG to determine the effect of thermal treatment on the pre-extruded material, each with freshly mounted samples:

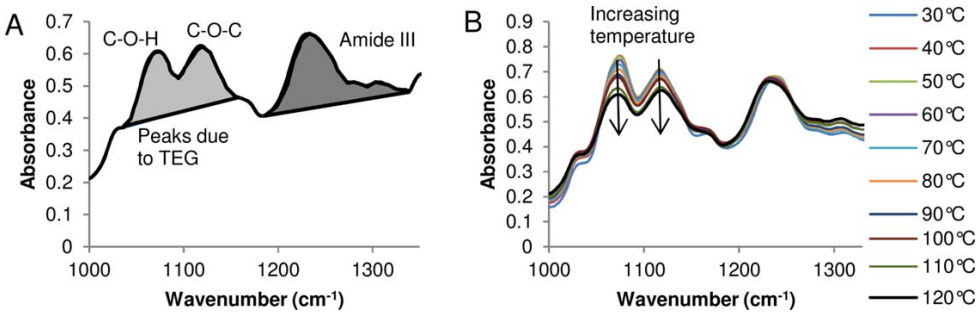

Figure 1. (A) Peaks in FT-IR spectra because of amide III region and those attributed to functional groups in TEG. (B) Changes in peak height as a function of temperature. [Color figure can be viewed in the online issue, which is available at wileyonlinelibrary.com.]

- A 50 × 50 μm spot was chosen to average out spatial variations and spectra were collected at 30-second intervals during a constant heating ramp from −120°C to 120°C at 2°C /min.
- Representative grids with a 10 × 10 μm spot size were mapped in *x–y* coordinates on four separate particles. After spectra collection for each point in the grids, the mounted samples were heated to 120°C, held isothermally for 2 min then returned to room temperature. Spectra were then collected for grids with the same *x–y* coordinates as originally scanned.
- Smaller representative grids, also with a 10 × 10 μm spot size were mapped on three separate particles at room temperature. These samples were then heated to 50°C. Grids with the same *x–y* co-ordinates were mapped again after a 10-min isothermal soak time. This process was repeated at 70°C, 90°C, 110°C, and 130°C.

Microtomed sections of processed (extruded, extruded then injection moulded, extruded then injection moulded, and conditioned) plastic were also examined for spatial distribution but not subjected to additional thermal treatments.

Data Analysis. FT-IR spectra for each point were used to prepare spatial maps of integrated peak ratios using OPUS 6.5. Opus type B integrals were calculated from 1040 to 1150 cm^{-1} (C-O-C and C-O-H functional groups in TEG) and from 1180 to 1330 cm^{-1} (amide III region of proteins), along with the ratio of the first peak over the second. These ratios were used to compare TEG distribution relative to protein in spatial maps. Using peak area ratios has the advantage of eliminating effects of variation in thickness across samples.[21] The ratio between the areas corresponding to each of the two functional groups of TEG (1040–1095 cm^{-1} for C-O-H and 1095–1150 cm^{-1} for C-O-C) was also calculated and examined. Mean, standard deviation, median, upper quartile, and lower quartiles were calculated for the mapped ratios. Data were filtered for a minimum area under the amide III region to exclude points mapped outside particles from statistical analysis.

Thermogravimetic Analysis. Thermogravimetic analysis (TGA) was performed in a Texas Instruments SDT 2960 analyzer using approximately 10 mg of sample in dry air. Freeze dried PNTP-TEG and PNTP-V0 were heated at a constant rate of 10°C/min from room temperature to 700°C. Samples of PNTP-TEG, PNTP-V0 and PNTP-U0 were also analyzed by heating at a constant rate of 10°C/min from room temperature to 120°C and holding at 120°C 3 h.

RESULTS AND DISCUSSION

Thermally Resolved FT-IR

Temperature-Resolved Changes. Bloodmeal-based thermoplastics containing 20 pph_{BM} TEG showed two similar sized peak regions between 1000 and 1350 cm^{-1} attributed to the amide III region (1180–1330 cm^{-1}) and TEG (1040–1150 cm^{-1}) [Figure 1(A)]. Two peaks were observed between 1040 to 1095 cm^{-1} and 1095 to 1150 cm^{-1}. These correspond to expected locations for primary alcohols and aliphatic ethers, respectively, both functional groups present in TEG. Neither peak was apparent in samples that did not contain TEG, therefore it is reasonable to conclude these correspond to vibrations of the C-O bond in the C-O-H and C-O-C functional groups of TEG [Figure 1(A)].

The peaks corresponding to C-O bonding in TEG significantly decreased in intensity when heated from room temperature to 120°C [Figure 1(B)]. A small change in shape was also observed in the amide III region, with a slight shifting of the convoluted peak centered around 1240 cm^{-1} to a lower wavenumber. This shape change was taken to be indicative of increasing β-sheets at the expense of random coils.[5,20]

The alcohol peak intensity (C-O-H, Figure 1) decreased more than the ether group (C-O-C), which suggests a reduction in OH groups. Looking at higher wavenumbers, where stretches of X-H bonds are found (Figure 2), there was also a change in shape and intensity over the same temperature range, with a

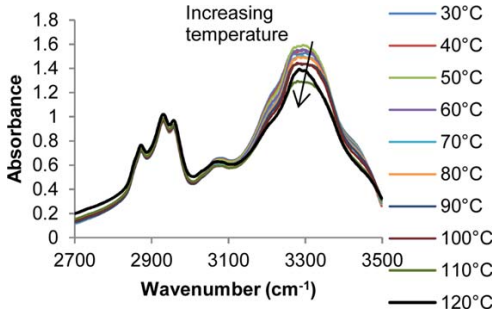

Figure 2. Change in spectral region corresponding to X-H bond vibrations. [Color figure can be viewed in the online issue, which is available at wileyonlinelibrary.com.]

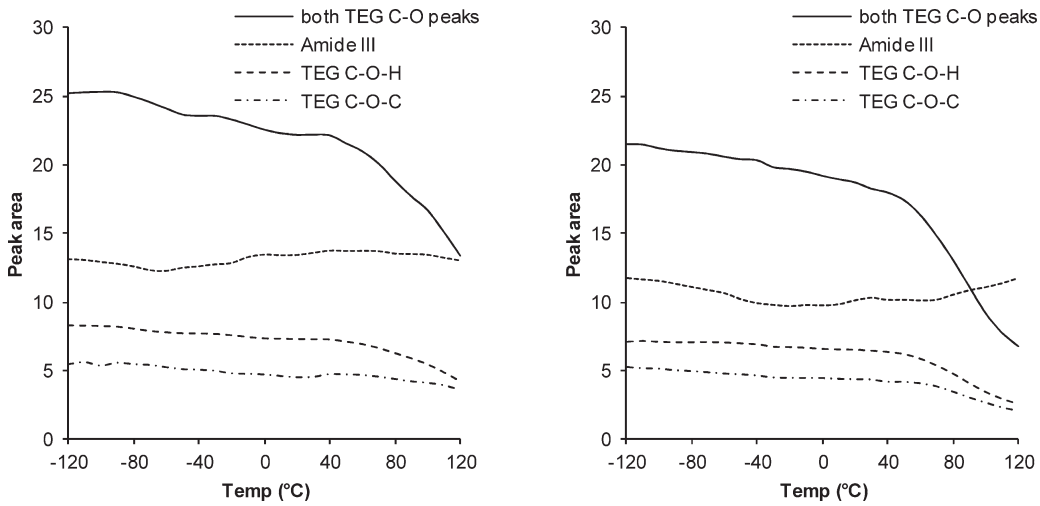

Figure 3. Integrated peaks versus temperature during heating at 2°C/min for 50 x 50 μm spots on two separate PNTP-TEG particles.

decrease and a shift from higher wave number to lower wavenumber. O-H stretching can spread throughout this region (from 3000 to 3500 cm^{-1} and beyond), but N-H stretching would typically be in the lower end of this region. This change in shape would therefore be consistent with a reduction in amount of OH groups present when the plastic is heated. C-H stretches also absorb in this region, but further interpretation from this spectral region is complicated by potential contributions from the large amount of functional groups in different environments possible in protein side groups, the protein backbone and those in TEG.

There was little discernable change in peaks at 2920 and 2850 cm^{-1} when the plastic was heated from room temperature to 120°C (Figure 2). These peaks correspond, respectively, to asymmetric and symmetric stretches in CH_2 aliphatic regions. Reduction of these peak heights is typically indicative of side chain degradation in proteins (such as keratin[22,23]). For NTP, analysis of this region is complicated by CH_2 groups in both protein side chains and in TEG.

To ensure that the trends seen were repeatable, another particle was tested in the same fashion, and peak area versus temperature was plotted for both (Figure 3). In both cases a gradual decrease in area corresponding to TEG's C-O peaks was seen during heating up to 40°C, with a sharper drop beyond this. There was some fluctuation in the size of the amide III, but little discernable trend. Within TEG's C-O peaks, the C-O-H peak showed a greater drop in area than the C-O-C peak in both cases. Although both particles show the same trends, there is some difference in the initial areas of each group, suggesting different sample thicknesses, and potentially different initial TEG concentrations between the two particles.

The decrease in functional groups would indicate either some TEG is lost during heating or that the interaction between protein chains and TEG is changing thereby masking the presence of TEG. If TEG evaporates, it would cause the material to be more brittle. It was thought that more insight could be obtained by not only examining how the peaks changed relative to each other on heating, but also if there was any spatial variation within samples.

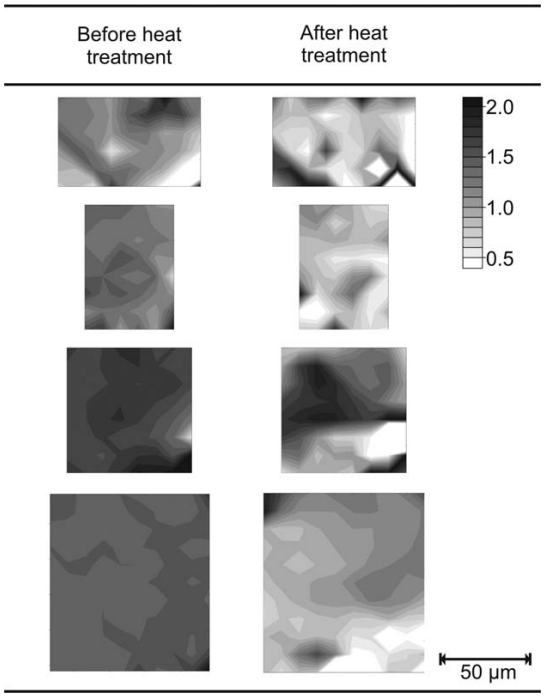

Figure 4. Spatial maps of ratio between peak integrals representing TEG (1040–1150 cm^{-1}) and the amide III region (1180–1330 cm^{-1}) as the same four grids (10 x 10 μm spot size) on four separate FD PNTP-TEG particles were scanned before and after 2-min isothermal heat treatment at 120°C. Darker shading indicates higher relative TEG content.

Table II. Summary Statistics for Grids Mapped on PNTP-TEG Particles Before and After Thermal Treatment at 120°C for 2 min

	Before heating		After heating	
	TEG/amide III	COH/COC	TEG/amide III	COH/COC
Mean	1.53	1.62	1.05	1.60
Standard deviation	0.30	0.22	0.40	0.93
Lower quartile	1.38	1.49	0.79	1.37
Median	1.62	1.54	0.98	1.46
Upper quartile	1.71	1.69	1.23	1.62

Filtered for a minimum integrated area of 5 under the amide III region and excluding negative ratios to exclude points outside particles.

Spatial Distribution Before and After a Heat Treatment. Freeze dried PNTP-TEG showed a heterogeneous distribution of TEG throughout the particles (Figure 4). There was some variation between separate particles, with some particles showing regions with up to twice the area for the peaks corresponding to TEG to that of the amide III, and some regions with only half the amide III area. For the most part, however, the approximate area ratio was 1–1.5 to 1. It is important to note that this does not imply equal or higher TEG concentration in the plastic than protein, as TEG will absorb differently to protein. The area ratio, however, will show if there is change in the relative concentration of TEG across a map, as is the case here.

After a 2-min isothermal period at 120°C (simulating the residence time of an extruder), spatial maps of the same *x*–*y* coordinates of the same FD-PNTP particles were noticeably different (Figure 4). The spatial maps became even more heterogeneous, with some regions darkening and others lightening when drawn on the same intensity scale. This suggests migration of TEG within the plastic as molecular mobility was increased with increasing temperature. As well as an overall decrease in the average TEG/amide III peak ratio, an increase was seen in the standard deviation and the difference between the upper and lower quartile values (Table II). The C-O-H/C-O-C peak ratio was approximately the same on average across the maps, but the standard deviation increased (Table II).

Spatial Distribution at Elevated Temperatures. Freshly mounted samples of PNTP-TEG were examined at 23°C, then the same regions remapped at progressively higher temperatures. TEG content increased towards the edge of the mapped grids, closer to the edges of particles with increasing temperature (Figure 5) and then was partially removed at higher temperatures. While short isothermal treatments led to more heterogeneous distributions, increasing homogeneity was seen after equilibrating samples for 10 min at each temperature before scanning. This was evident from a decreasing standard deviation for the average TEG/ amide III peak area ratio across the maps, along with smaller difference between the lower and upper quartiles (Table III). The C-O-H to C-O-C peak ratio also decreased. This could either mean the strength of the absorbance with concentration varied for the two different functional groups, or it could suggest some plasticizer migration or interaction between protein and TEG interfering with end groups on the TEG molecules.

It has previously been reported that bloodmeal particles are more amorphous in the center, with a higher concentration of β-sheets at the edges, and α-helices scattered throughout. After processing there is a more homogenous distribution, with an overall increase in β-sheets. Samples with 20 pph_{BM} TEG show reduced β-sheets compared with samples without TEG at each processing step.[20] Both α-helices and β-sheets are stabilized by strong hydrogen bonding interactions involving the NH and C=O groups of the polypeptide backbone. In randomly coiled structures, these groups may be hydrogen bonded to solvent or plasticizer instead of each other. The observed conformational change from random coils to β-sheets would require bound plasticizer to transition to free plasticizer as protein–protein hydrogen bonding interactions replace hydrogen bonding interactions with TEG. This free plasticizer is then free to migrate through the material. When soy protein sheets were heated, kinetic studies showed the rate of conformational change was

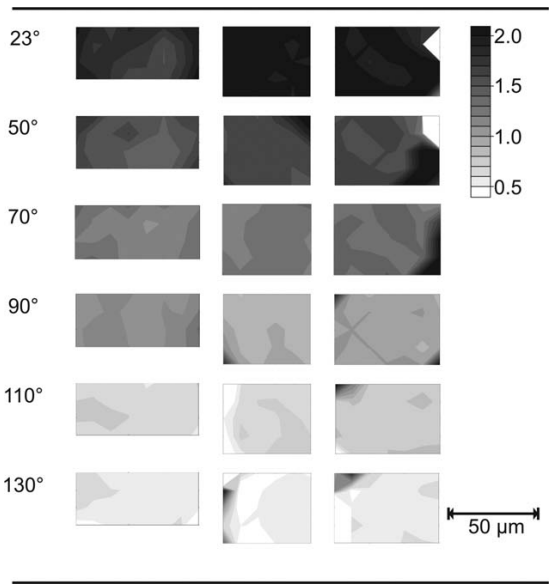

Figure 5. Spatial maps of ratio between peak integrals representing TEG (1040–1150 cm^{-1}) and the amide III region (1180–1330 cm^{-1}) as the same three grids on separate FD PNTP-TEG particles were scanned at progressively higher temperatures. Darker shading indicates higher relative TEG content.

Table III. Summary Statistics for Grids Mapped on PNTP-TEG Particles at Progressively Higher Temperature

	TEG/amide III						COH/COC					
Temperature (°C)	23	50	70	90	110	130	23	50	70	90	110	130
Mean	1.96	1.62	1.34	1.02	0.74	0.55	1.60	1.63	1.55	1.45	1.30	1.26
Standard deviation	0.15	0.12	0.09	0.06	0.08	0.06	0.10	0.11	0.11	0.11	0.17	0.16
Lower quartile	1.88	1.56	1.28	0.97	0.71	0.53	1.52	1.53	1.46	1.35	1.22	1.18
Median	2.00	1.62	1.34	1.02	0.74	0.56	1.61	1.65	1.55	1.47	1.33	1.28
Upper quartile	2.05	1.66	1.39	1.07	0.78	0.58	1.68	1.70	1.61	1.52	1.38	1.34

Filtered for a minimum integrated area of 5 under the amide III region to exclude points outside particles.

too fast to be explained by evaporation of water alone.[24] This would suggest that structural rearrangement is the driver for plasticizer migration, rather than the other way around.

Processing

The ratio of the peak area corresponding to the C-O-H group of TEG to the amide III region was previously used to get an impression of the change in TEG distribution induced by processing.[20] Considering the TEG peaks discussed in this article, similar trends were seen (Figure 5). After extrusion, there was a more homogeneous distribution than in the pre-extruded powders, but still some localized phase separation. Injection moulding smoothed out local variations, but when the full C-O-X region was used to evaluate TEG relative to protein, it could be seen that some larger range phase separation was occurring, giving a broader statistical distribution (Table IV). After conditioning, more localized concentrated spots appeared again (Figure 6).

Comparing the TEG/amide III ratio spatial distribution for the processed plastics with the C-O-H/C-O-C peak ratios provides an interesting contrast to the thermal experiments. The C-O-H peak decreased relative to the C-O-C peak and both decreased in size relative to the amide III in the thermal experiments. From Figure 6, however, it appears that regions with higher TEG content tend to also have a lower C-O-H to C-O-C absorbance ratio. If the difference in thermal response seen were because of different absorbance sensitivities to concentration in the two different functional groups the opposite would be seen. This supports the hypothesis that some of the OH groups in TEG are interacting with other species and this seems to be more prominent in TEG-rich phases in the processed material.

Table IV. Summary Statistics for Grids Mapped on Consolidated Plastics

	TEG/amide III			C-O-H/C-O-C		
	ENTP	INTP	CNTP	ENTP	INTP	CNTP
Mean	1.56	1.37	1.59	1.88	1.76	1.71
Standard deviation	0.08	0.14	0.11	0.07	0.09	0.13
Lower quartile	1.50	1.25	1.51	1.83	1.71	1.63
Median	1.56	1.37	1.60	1.87	1.75	1.70
Upper quartile	1.61	1.51	1.67	1.93	1.80	1.77

Filtered for a minimum integrated area of 1 under the amide III region to exclude points outside microtomed ribbons.

It is interesting to note that the average TEG to amide III ratio in the processed materials (Table IV) is above that of the pre-extruded material after even a 2-min heat treatment (Table II), and well above that of the more slowly treated material tested at incremental temperatures (Table III). This would suggest that even if TEG is being driven off during thermal experiments for FT-IR, it is not significantly removed by processing. The overall reduction in peak intensity, relative to the amide III region could initially suggest that TEG is being driven off by evaporation. This, however, was thought to be unlikely as the boiling point of TEG is around 288°C. The boiling point of TEG water mixtures does drop below this, down to 125°C with 10% water to below 120°C with greater than 20% water.[25] However, in such mixtures it would typically be the more volatile species that would evaporate off first.

TGA

Constant Rate. To confirm whether or not mass loss attributable to evaporation of TEG was occurring at the temperatures tested in the FT-IR thermal analysis, samples were examined by TGA. Samples of freeze dried-PNTP showed very little mass loss below 120°C. The small amount that did occur would be better attributed to the last amount of moisture being removed. The larger mass loss event occurring between 150°C and 250°C could correspond to TEG evaporating. This mass loss was associated with an endothermic event, consistent with volatilization (Figure 7). Furthermore, the event was not seen in bloodmeal alone or in FD-PNTP-V0 (without TEG), though some mass loss occurred in FD PNTP-V0 at the higher end of this range (Figure 8). This demonstrated that TEG evaporated from the material above 150°C, not below 120°C, in a typical TGA experiment.

It should be noted that the typical sample mass used in the TGA experiments of 10 mg is considerably larger than the individual particles tested in the synchrotron FT-IR experiments. Furthermore, the sample holder is a small crucible, and the typical sample ends up in a layer about 1–2 mm thick in the bottom of this. In the spatial maps of TEG distribution discussed above, migration of TEG into rich and poor zones in single particles was seen after even a brief heat treatment (Figure 4), indicating some amount of diffusion through the particle. The surface area to volume ratio for a single particle on a barium

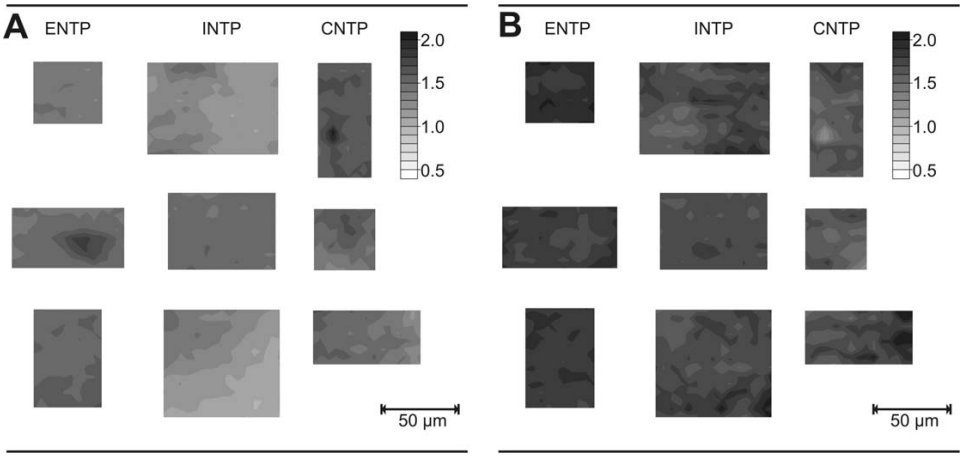

Figure 6. Spatial maps for microtomed sections of bloodmeal-based plastics after extrusion, injection moulding and conditioning. (A) Ratio between peak integrals representing TEG (1040–1150 cm^{-1}) and the amide III region (1180–1330 cm^{-1}); darker shading indicates higher relative TEG content. (B) Ratio between peak integrals representing C-O-H bonds in TEG (1040–1095 cm^{-1}) and C-O-C bonds in TEG (1095–1150 cm^{-1}); darker shading indicates larger relative C-O-H absorbance. Three separate grids are shown for each processing step.

fluoride slide is much greater than for what is effectively a packed column (albeit a small one in TGA). The sample size is deliberately kept small to minimize the effect of diffusion rates on mass loss temperatures, but TEG has been shown to have a strong interaction with proteins which may slow the diffusion rate to where it is significant in TGA.

Isothermal. Isothermal (120°C) TGA experiments on PNTP-V0 and PNTP-TEG found a mass loss greater than the amount of water added to the formulation (Table V). A small mass loss would be expected, as the moisture content of bloodmeal itself is approximately 5 wt % (determined from TGA of bloodmeal alone), corresponding to about 4 wt % of the blended NTP formulation. For PNTP, the amount corresponds to bound water in bloodmeal used in the formulation, but for PNTP-TEG, this additional mass loss exceeds that. It was thought that this may be the result of urea degradation, as TEG was more tightly bound to the protein. However, with no urea present, a similar mass loss was seen (Table V). In all three formulations, the mass loss to 100°C corresponded with the mass of water added in the sample. Only 0–1% of the total starting mass came off between 100°C and 120°C, but both of the formulations with TEG had the extra mass loss, whether urea was included or not. This would then confirm that TEG can be volatilized given enough time.

TEG volatilization during thermoplastic processing is not a great concern as the residence time in the extruder and injection moulder at 120°C is short relative to the experimental times reported in Table V. Nevertheless, it does suggest that as increased folding into β-sheets occurs, TEG is displaced and will migrate out of particles over time at elevated temperatures.

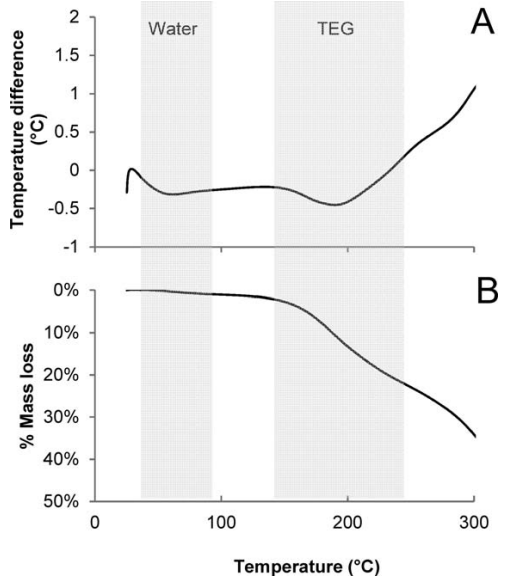

Figure 7. TGA thermograms of (A) temperature difference, and (B) mass loss for FD PNTP-TEG.

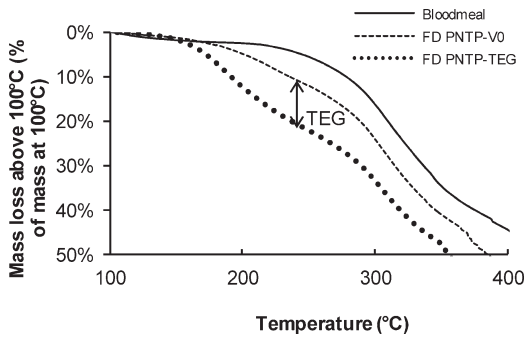

Figure 8. TGA thermograms of mass loss between 100°C and 400°C for bloodmeal, and FD PNTP with and without TEG.

Table V. Percentage Plasticizer and Mass Loss During Isothermal TGA Experiments

		PNTP-TEG (%)	PNTP-V0 (%)	PNTP-U0 (%)
Percentage plasticisers (wet basis)	Added water	23	34	24
	Assumed water in bloodmeal	4	4	4
	Total water	27	38	28
	Percentage urea	9	9	0
	Percentage TEG	11	0	12
Percentage mass loss during heating to	100°C	23	34	24
	120°C	23	35	25
Percentage mass loss during heating to 120°C followed by isothermal hold time of	60 min	30	36	30
	120 min	31	37	32
	180 min	32	37	32
Difference between mass loss at 3 h and added water (% of total starting mass)		9	3	8

The glass transition (T_g) of freeze dried PNTP-V0, determined by DMA in a material pocket is approximately 154°C in contrast to 64°C for freeze dried PNTP-TEG.[20] After removing water, material without TEG is below its T_g at 120°C, whereas material with TEG is still above its T_g. Immobilized, tightly packed protein chains have barrier properties that will restrict the passing of small molecules. With TEG, conformational mobility at 120°C will still allow both the motion of TEG and of other small molecules in the material, enabling both TEG and any degradation products to diffuse out over time.

CONCLUSIONS

TEG present in NTP accumulates in discrete areas then migrates towards the periphery and evaporates upon heating. These happen in parallel to an increase in β-sheet structures. Given TEG bonding to NTP and β-sheet formation involve hydrogen bonding, it suggests that on heating, β-sheet formation is favored, pushing TEG out of NTP. This plasticizer migration and evaporation occurs very slowly, therefore NTP is largely unaffected by it during the thermal processes in extrusion and injection moulding. However, it does mean that NTP should not be exposed to high temperatures for prolonged periods.

ACKNOWLEDGMENTS

This research was undertaken on the infrared microspectroscopy beamline at the Australian Synchrotron, Victoria, Australia. Proposal numbers AS113/IRMFI/4267 and AS122/IRMFI/4951 and The authors would especially like to acknowledge the technical assistance of Dr. Mark Tobin and Dr Danielle Martin. Travel funding support was received from the New Zealand Synchrotron Group Ltd.

REFERENCES

1. Verbeek, C. J. R.; Viljoen, C.; Pickering, K. L.; van den Berg, L. E. Plastic Material. NZ Patent NZ551531, **2007**.
2. Verbeek, C. J. R.; van den Berg, L. E. *J. Polym. Environ.* *1*, **2010**.
3. Verbeek, C. J. R.; van den Berg, L. E. *Macromol. Mater. Eng.* **2010**, *295*, 10.
4. Verbeek, C. J. R.; van den Berg, L. E. *Macromol. Mater. Eng.* **2011**, *296*, 524.
5. Bier, J.; Verbeek, C. J. R.; Lay, M. C. *Macromol. Mater. Eng.* *10*.1002/mame.2012004602013.
6. Pommet, M.; Redl, A.; Guilbert, S.; Morel, M. -H. *J. Cereal Sci.* **2005**, *42*, 81.
7. Mo, X.; Sun, X. *J. Polym. Environ.* **2003**, *11*, 15.
8. di Gioia, L.; Guilbert, S. *J. Agric. Food Chem.* **1999**, *47*, 1254.
9. Rahman, M.; Brazel, C. S. *Prog. Polym. Sci.* **2004**, *29*, 1223.
10. Petersen, J. H.; Breindahl, T. *Food Addit. Contam.* **2000**, *17*, 133.
11. Vieira, M. G. A.; da Silva, M. A.; dos Santos, L. O.; Beppu, M. M. *Eur. Polym. J.* **2011**, *47*, 254.
12. Orliac, O.; Rouilly, A.; Silvestre, F.; Rigal, L. *Ind. Crops Prod.* **2003**, *18*, 91.
13. Chen, P.; Zhang, L. *Macromol. Biosci.* **2005**, *5*, 237.
14. Kunanopparat, T.; Menut, P.; Morel, M. H.; Guilbert, S. *Compos. Part A: Appl. Sci. Manuf.* **2008**, *39*, 777.
15. Olabarrieta, I.; Cho, S. W.; Gallstedt, M.; Sarasu, J. R.; Johansson, E.; Hedenqvist, M. S. *Biomacromolecules* **2006**, *7*, 1657.
16. Wan, V. C. H.; Kim, M. S.; Lee, S. Y. *J. Food Sci.* **2005**, *70*, E387.
17. Thomazine, M.; Carvalho, R. A.; Sobral, P. I. A. *J. Food Sci.* **2005**, *70*, E172.
18. Guerrero, P.; Retegi, A.; Gabilondo, N.; de la Caba, K. *J. Food Eng.* **2010**, *100*, 145.
19. Chen, P.; Tian, H.; Zhang, L.; Chang, P. R. *Ind. Eng. Chem. Res.* **2008**, *47*, 9389.

20. Bier, J. M.; Verbeek, C. J. R.; Lay, M. C. *J. Appl. Polym. Sci.* **2013**, *130*, 359.
21. Yu, P. Q.; McKinnon, J. J.; Christensen, C. R.; Christensen, D. A. *J. Agric. Food Chem.* **2004**, *52*, 7353.
22. Selling, G. W. *Polym. Degrad. Stabil.* **2010**, *95*, 2241.
23. Barone, J. R.; Arikan, O. *Polym. Degrad. Stabil.* **2007**, *92*, 859.
24. Tian, K.; Porter, D.; Yao, J.; Shao, Z.; Chen, X. *Polymer* **2010**, *51*, 2410.
25. Dow Chemical Company. **2007**.

10

The Thermoplastic Nature of Novatein™

A concluding discussion

The Thermoplastic Nature of Novatein™

The aim of this thesis was to develop a fundamental understanding of the interdependent relationship between structure, properties and processing in Novatein™ thermoplastic protein (NTP), using concepts from classical polymer physics. Dynamic mechanical thermal analysis (DMA) and differential scanning calorimetry (DSC) were used to investigate thermal transitions and chain relaxation, accompanied by synchrotron based Fourier transform infrared spectroscopy (FT-IR) to investigate chain architecture and structural changes. Extrusion, injection moulding and mechanical testing were used to investigate macroscopic properties, such as processability and mechanical properties.

Even though denatured, protein secondary structures are present in bloodmeal and NTP, affecting properties and processibility in a manner resembling crystalline regions in synthetic semi-crystalline polymers. Furthermore, it was demonstrated that after extrusion, NTP is a consolidated thermoplastic, which exhibits typical viscoelastic behaviour.

Spatially resolved FT-IR analysis showed bloodmeal particles consist of an amorphous core and β-sheet rich edges, with α-helices evenly distributed throughout. α-helices and β-sheets resemble ordered crystalline regions in other thermoplastics and can improve overall mechanical properties, such as strength and toughness. TEG, urea, sodium sulphite (SS) and sodium dodecyl sulphate (SDS) increased β-sheets, most likely by breaking side chain interactions between protein chains, which then allows conformational rearrangement favouring main chain hydrogen-bonding. Overall β-sheet content increased after extrusion, and a small amount after injection moulding. Heating during processing increases chain mobility, which allows chains to unravel and rearrange into more stable structures on cooling from the melt.

Regions rich in β-sheets were also observed in the extruded and injection moulded NTP, however these were more homogenously distributed than in bloodmeal prior to extrusion. This suggests that processing bloodmeal into a thermoplastic allows the β-sheet rich edges of particles to unravel, disperse and intertwine into a consolidated material. This makes NTP analogous to other thermoplastics with a

semi-crystalline structure, and a similar effect of crystallites on mechanical behaviour can be expected. β-sheets have stronger interchain interactions than α-helices or random coils, resulting in a more brittle material. This restricts current applications of NTP to solid objects, such as injection moulded shapes. If flexible films were required, conditions that favour α-helix formation would have to be explored. Both α-helices and β-sheets are stabilised by hydrogen-bonding interactions, within or between protein chains. Plasticisation with tri-ethylene glycol (TEG) reduced β-sheet formation compared with samples not containing TEG. This is because TEG competes with protein groups for hydrogen bonding sites. This effect, as well a possible free volume effects from incorporating a less volatile plasticiser than water, resulted in a tougher, more ductile conditioned plastic than that produced without TEG.

Bloodmeal has a glass transition temperature (T_g) of 220 °C, which also corresponds to the onset of significant mass loss due to protein degradation when investigated using thermogravimetric analysis (TGA). The T_g is too high for processing without excessive thermal degradation. Water, TEG, urea, SS and SDS reduced the T_g to below 0 °C when tested prior to extrusion, or about 70 °C when dried, but plasticised with TEG. DMA showed multiple thermal transitions indicating there were multiple phases in the plastic. This was confirmed using FT-IR, which found regions rich in TEG and other regions rich in β-sheets. Ideally, a truly homogenous material should have a uniform TEG distribution, however regions with increased plasticiser may resemble toughening phases in other plastics.

Thermal treatments of pre-extruded NTP on a heated FT-IR stage showed β-sheets increased at the expense of random coils. A small increase in α-helices was also seen, but not to the extent of β-sheets, suggesting the proteins favoured the β-sheet conformation. TEG content also decreased on heating, with migration towards particle edges. This was possibly due to aligned hydrogen bonding in β-sheets being favoured over continued protein-TEG hydrogen bonding. It was thought that conformational rearrangement was the driver for TEG migration, rather than the other way around. However, further investigation using FT-IR might reveal this with more clarity if time resolved kinetic studies are done isothermally at multiple temperatures. Ideally, for consistent and predictable material properties, TEG should be evenly distributed throughout the material and

loss of plasticiser during heating kept to a minimum. Loss of TEG during TGA experiments appeared to be slow. It was thought that the small particle sizes of samples examined under FT-IR allowed for increased diffusion and evaporation of TEG due to the greater surface area to volume ratio compared to large injection moulded samples. Consequently, loss of TEG and associated conformational change should not be as significant during processing compared to that observed in thermally resolved FT-IR. FT-IR of extruded, injection moulded and conditioned NTP confirmed TEG had remained in the material throughout these processes. Structural rearrangement towards β-sheets in thermally resolved FT-IR was more severe than that observed between extrusion and injection moulding of the same formulation. This suggested that physical forces such as shear and pressure encountered during extrusion and injection moulding may play a role in restricting β-sheet formation.

Creep, recovery and stress relaxation experiments showed that conditioned NTP exhibited viscoelastic behaviour consistent with a consolidated thermoplastic. NTP is therefore not a compressed powder with flow only enabled by excessive plasticisation. After creep, some of the extension was recovered almost instantaneously when the load was removed, whilst some remained unrecovered after allowing the same time for recovery as for the initial creep portion of the experiment. This suggests creep in NTP was a combination of protein chains stretching (some instantaneously, and some in a restricted time dependent manner) and some of interactions between chains breaking and reforming. Extension due to stretching is recoverable, while extension due to bonds breaking and reforming is not. This behaviour was successfully modelled using a modified four element Burgers model, although parameters obtained for creep could not be applied to recovery behaviour. Recovery occurred much faster than was predicted using the parameters obtained for creep, suggesting that placing NTP under load forces chain rearrangements that allow for rapid recovery when the load is removed. Increased SS content and increased melt temperature during injection moulding increased extension and recovery respectively, due to covalent bonds being broken, allowing greater movement between chains. Increasing either of these factors also reduced strength and stiffness in pull to break tests. Therefore, the properties of NTP are a compromise between having sufficient covalent bonds for good mechanical strength, while maintaining ductility.

Finally, material pocket DMA was validated for NTP by comparing data obtained from solid samples mounted directly in the instrument with powders mounted in the material pockets. This demonstrated the technique could be used to determine thermo-mechanical transition temperatures of protein-based plastics prior to consolidation into a moulded object. Furthermore, the material pocket gave greater resolution of transitions at higher temperatures allowing identification of multiple phases in the plastic. Activation energy for transitions could readily be obtained using an Arrhenius equation and DMA frequency. The observed behaviour resembled that of a semi-crystalline polymer in which structural relaxations in the free amorphous phase, in amorphous regions constrained by crystallites and in the crystalline phase (for example crystal slippage) all contribute to thermal transitions. This is consistent with the hypothesis that protein secondary structures behave like crystallites in other thermoplastics.

Typically, semi-crystalline thermoplastics would be processed above both the amorphous T_g and the melting point of crystalline regions. Whereas T_g is readily detected in DMA, melting is more usually examined in DSC. Although an endothermic event was observed near the glass transition for freeze dried NTP, structural studies over the same temperature range revealed that this was not melting of secondary structures. Rather, above the T_g, random coils fold into β-sheets. This finding suggests β-sheets may persist in the polymer melt. Shear mixing during processing maintains homogeneity and disperses β-sheet aggregates and TEG throughout the material, contributing to the observed properties.

Recommendations for future work

Any future improvements or modifications to NTP need to account for its underlying semi-crystalline nature. To successfully produce flexible thin films, β-sheet formation would need to be reduced and conditions that favour α-helix formation or increased random coils would need to be developed. This could potentially be done using solvents or alternative plasticisers that induce helical conformations, or through investigating alternate shear rates which limit β-sheet formation. Of further relevance for films, the presence of β-sheet aggregates may improve barrier properties, by increasing the path length for diffusion of small molecules through the material.

Both TEG migration and β-sheet formation could be investigated further by synchrotron based FT-IR. In particular, TEG migration kinetics may be modelled using data from time resolved studies at elevated temperatures.

Further development of the modified four element model used to describe viscoelastic behaviour could be carried out to better predict NTP creep, recovery and relaxation using a single set of parameters. These could then potentially be related more directly to the extent of crosslinking by examining the rate of chain rearrangements at various temperatures. To assist with this, structural studies by X-ray scattering could be done during in-situ creep and relaxation experiments. Such experiments would be possible using an appropriate synchrotron beamline.

The amount of water in the TEG plasticised formulation used in this work may be more than is actually necessary for processing and does not remain in the material after conditioning. If the amount of processing water was reduced, it may allow for parts that have properties similar to the conditioned materials here, but with less time needed for conditioning.

Finally, future work could include attempting a model that predicts overall mechanical properties of protein-based thermoplastics based on knowledge about protein size (chain length/molecular weight), amino acid content, crystallinity (including accounting for fractions of both α-helices and β-sheets), covalent cross link, as well as additives such as urea, SS, SDS and plasticisers. This could be done using a thermodynamic model to estimate chain mobility and average bond strengths by summing protein-protein interactions. Validating such a model, however, would require plastics prepared from a variety of different proteins to control for the contribution from different variables, and is a major undertaking, beyond the scope of this thesis.

Appendix: Copyright Information for Published Chapters

Chapter 2

Synthesis and Characterization of Thermoplastic Agro-polymers, previously published in RSC Green Chemistry No. 12. A Handbook of Applied Biopolymer Technology: Synthesis, Degradation and Applications Edited by Sanjay K. Sharma and Ackmez Mudhoo.

Chapter 3

Thermal Transitions and Structural Relaxations in Protein-Based Thermoplastics, previously published in Macromolecular Materials & Engineering.

Chapter 4

Thermal and Mechanical Properties of Bloodmeal-Based Thermoplastics Plasticized with Tri(ethylene glycol), previously published in Macromolecular Materials & Engineering.

Chapter 5

Identifying Transition Temperatures in Bloodmeal-Based Thermoplastics Using Material Pocket DMTA, Previously Published in Journal of Thermal Analysis and Calorimetry.

Chapter 7

Using Synchrotron FTIR Spectroscopy to Determine Secondary Structure Changes and Distribution in Thermoplastic Protein, Previously Published in Journal of Applied Polymer Science.

Chapter 8

Thermally Resolved Synchrotron FT-IR Microscopy of Structural Changes in Bloodmeal-Based Thermoplastics, Previously Published in Journal of Thermal Analysis and Calorimetry. © 2013 Akade´miai Kiado´, Budapest, Hungary. Used with permission. Rightslink License number 3264390690148.

Chapter 9

Plasticizer Migration in Bloodmeal-Based Thermoplastics, Previously Published in Journal of Applied Polymer Science. © 2013 Wiley Periodicals, Inc. Used with permission. Rightslink License number 3264390875685.